ADULT NEUROGENESIS AND NEUROGENIC PLASTICITY IN THE ZEBRAFISH BRAIN

by

Benjamin Wellington Lindsey

A thesis submitted in conformity with the requirements
for the degree of Doctor of Philosophy

Department of Cell & Systems Biology
University of Toronto

Adult Neurogenesis and Neurogenic Plasticity in the Zebrafish Brain

Benjamin Wellington Lindsey

Doctor of Philosophy

Department of Cell & Systems Biology
University of Toronto

2014

Abstract

Adult neurogenesis is a conserved feature of the central nervous system across the animal kingdom. This process takes place in restricted neurogenic niches of the brain, where active populations of adult stem/progenitor cells are capable of producing newborn neurons. The niche is tightly controlled by intrinsic signals within the microenvironment and from stimuli arising from the external world, which together determine the cellular behaviour of the niche and neuronal output. Currently, our understanding of the biological properties of adult neurogenesis rests mainly on two niches of the vertebrate forebrain. To broaden our view of the diversity of this trait comparative models and new niches must be explored. Here, I have taken advantage of the robust neurogenic capacity of the adult zebrafish brain to examine differences in forebrain and sensory neurogenic niches in regards to cytoarchitectural organization, neurogenic plasticity, and regulation. Five principle findings emerge: (1) up to six morphologically distinct cell types compose forebrain and sensory niches, and are devoid of ependymal cells; (2) heterogeniety in the phenotype of the stem/progenitor cell exists across niches; some having radial glial characteristics; (3) active populations of proliferating stem/progenitor cells reside within primary sensory structures of the adult brain, forming a “sensory neurogenic niche”; different from other

models of adult neurogenesis; (4) changes in the social environment induce neurogenic plasticity in sensory niches more readily than integrative niches of the forebrain, and occur independently of cortisol levels; (5) modality-specific stimulation influences stages of adult neurogenesis exclusively in corresponding primary sensory niches as a result of sensory-dependent neurogenic plasticity. Additionally, I have shown that Fibroblast Growth Factor signalling may not be involved in maintaining cell proliferation in sensory niches. These studies showcase the diverse properties of forebrain and sensory neurogenic niches and provide a new perspective concerning the functional role of adult neurogenesis.

Acknowledgments

I owe my sincerest gratitude to Dr. Vincent Tropepe. Your enthusiasm for research in the field of adult neurogenesis captivated me before I even joined your lab. Your supervisory style has allowed me the freedom to develop my research interests and skills, and the confidence to thrive in my field and future career. I have immense respect for how you treat your graduate students, and the level of professionalism to which you hold yourself personally and scientifically. I consider you a great colleague and friend and look forward to continuing to collaborate together in the years to come.

I would also like to thank members of my supervisor committee, Dr. Paul Frankland and Dr. Bryan Stewart. Your invaluable guidance, suggestions, and questions during committee meetings over the last 6 years have helped shape my critical thinking and ensured that the quality of my research was nothing short of the highest standard.

This section would be incomplete without additionally thanking the following colleagues and friends that have been a major part of my graduate education in the Department of Cell & Systems Biology at the University of Toronto. In particular, Dr. Ashley Bruce for everything you have taught me about zebrafish husbandry and for being a sounding board as I planned the next stage in my career. Sincere thanks to Henry Hong and Audrey Darabie of the Imaging Facility not only for your friendships but the countless hours training me on confocal and electron microscopy, and assisting me in the design and execution of experiments. Finally, thank you to members of the Tropepe lab, and Kamilia Miri and Graham MacLeod, for our many scientific and non-scientific discussions, and for your friendships over these past years.

To my parents, Brian and Fiorine Lindsey. Since I was young, you have always encouraged me to follow my passion and do my best. You have instilled in me the importance of a strong work ethic and dedication to the goal at hand. Dad, you have taught me that the best way to learn is to always ask questions. Mom, you have reminded me to always remain humble in my achievements. It is with great pride that I can say that I have had such admiral role models in my life. I love you both.

I owe my deepest thanks to my lovely wife, Lyndsay. You have stood by my side through this academic journey, and I would not be here without your enduring love and support. I know that at times these years of graduate school were more than you had bargained for, but I thank you for seeing me through and keeping me balanced along the way. You are the single most important person in my world, and I thank you for all the sacrifices you have made; they have not gone unnoticed.

I dedicate this thesis to my beautiful wife Lyndsay, and our daughter, Maryn.

I would also like to acknowledge the following scholarship/fellowship programs for financial support during my graduate training: The National Science and Engineering Research Council of Canada (NSERC), and the Ontario Graduate Scholarship (OGS) program.

Contributions

The body of work included in my thesis would not have been possible without the time commitment and intellectual discourse of many. The following contributions of those individual's is formally acknowledged below.

Dr. Vincent Tropepe (Supervisor and Thesis Committee Member) – mentorship; laboratory resources; guidance and assistance in planning experiments, analysis, and interpretation of results; assistance in manuscript and thesis preparation

Dr. Paul Frankland (Thesis Committee Member) – mentorship; guidance in interpretation of results

Dr. Bryan Stewart (Thesis Committee Member) – mentorship; guidance in interpretation of results; assistance with data analysis of cell cycle kinetics in Chapter 2

Ms. Audrey Darabie and Mr. Robert Temkin (CSB Imaging Facility) – assistance with sample preparation, embedding, sectioning, staining, immunohistochemistry, and imaging of brain tissue for transmission electron microscopy in Chapter 2 and Chapter 4

Mr. Henry Hong (CSB Imaging Facility) – assistance with confocal imaging and scanning electron microscopy in Chapter 2

Dr. Helen Rodd – use of Visual elastomer tags in Chapter 3

Dr. Leslie Buck – use of plate reader for cortisol samples in Chapter 3

Dr. Aneil Agrawal – use of Ethovision 3.0 analysis software in Chapter 4

Dr. Marc Ekker and Dr. Ian Scott – use of transgenic lines in Chapter 2

Dr. Nicolas Vesprini – assistance with experiments in Chapter 4

Sabrina Hossain and Bonnie Chu – assistance with experiments in Chapter 2

Charmaine Fong, Sabrina Didonato, Hyein Kim, and Mohsen Javam
– assistance with experiments in Chapter 4

Table of Contents

CHAPTER 2

CHAPTER 4

List of Tables

List of Figures

List of Abbreviations

General abbreviations

BDNF	Brain-derived neurotrophic factor
BMP	Bone morphogenic protein
BrdU	5'bromo-2'-deoxyuridine
CNS	Central nervous system
CORT	Hydrocortisone
Dpf	Days post fertilization
eGFP	Enhanced green fluorescent protein
ETOH	Ethanol
FGF	Fibroblast growth factor
FGFR-1	Fibroblast growth factor receptor 1
GABA	Gamma-amino butyric acid
GF	Growth fraction
GFAP	Glia fibrillary acidic protein
GFP	Green fluorescent protein
GLU	Gluteraldehyde
GR	Glucocorticoid receptor
GS	Glutamine synthetase
HC	Hippocampal complex
HCl	Hydrochloric acid
HMDS	Hexamethyldisilizane
HPI axis	Hypothalamus-pituitary-interrenal axis
HS	Heatshock
HuCD	Anti-human neuronal protein HuC/HuD
HVC	Higher vocal center
IFG1/2	Insulin-like growth factor 1/2
IHC	Immunohistochemistry
MR	Mineralocorticoid receptor
OB	Olfactory bulb
PFA	Paraformaldehyde
PSA-NCAM	Polysialic acid neural cell adhesion molecule
PBS	Phosphate-buffered saline
RMS	Rostral migratory stream
SEM	Scanning electron microscopy
SEZ	Subependymal zone
SGZ	Subgranular zone
Shh	Sonic hedgehog
SOX2	Sex-determining region Y-box 2 transcription factor
TEM	Transmission electron microscopy
TGFα	Transforming growth factor-α
TGFβ1	Transforming growth factor β-1
VEGF	Vascular endothelial growth factor

Zebrafish-specific abbreviations for neuroanatomical terminology

Cce	Corpus cerebelli
Ctec	Commissura tecti
D	Dorsal telencephalic area
Dc	Central zone of D
Dd	Dorsal zone of D
DEL	Dorsal ependymal lining
DiV	Diencephalic ventricle
Dl	Lateral zone of D
Dm	Medial zone of D
Dp	Posterior zone of D
EG	Eminentia granularis
GL	Glomerular layer of olfactory bulb
ECL	External cellular layer of olfactory bulb including mitral cells
ICL	Internal cellular layer of olfactory bulb
IRF	inferior reticular formation
LAT	Lateral olfactory tract
LX	Vagal lobe
MOT	Medial olfactory tract
NXm	Vagal motor nucleus
OB	Olfactory bulb
PGZ	Periventricular grey zone
Ppa	Parvocellular preoptic nucleus, anterior part
PVZ	Periventricular zone
RV	Rhombencephalic ventricle
TelV	Telencephalic ventricle
TeO	Tectum opticum
TeV	Tectal ventricle
TL	Torus longitudinalis
V	Ventral telencephalic area
Vd	Dorsal nucleus of V
Vp	postcommisural nucleus of V
Vs	supracommisural nucleus of V
Vv	Ventral nucleus of V

CHAPTER 1
GENERAL INTRODUCTION

1.1 Foreword

While assembling my thesis it has been my intention to maintain a comparative theme. Having a background in Zoology and Neuroscience pondering adult neurogenesis from the perspective of species diversity or niche-niche variation has developed my appreciation for this field, and in particular, what different animal models of adult neurogenesis can teach us about this biological trait. Many of the questions I have addressed over the last 6 years were designed and tested with a comparative context in mind. Moreover, a number of the experiments I have performed have sought to examine fundamental questions, and fill in obvious gaps in the literature, in an attempt to align the zebrafish as a practical vertebrate model of adult neurogenesis alongside well established mammalian and avian species. What I have discovered across multiple niches of the adult zebrafish brain in the context of cell biology and neurogenic plasticity has laid the groundwork for next investigating more directed questions concerning the molecular programs and genetic regulation of these processes. Most importantly, in my discoveries I have been able to stay true to my research interests and in doing so have enjoyed great personal fulfillment from these accomplishments.

1.2 Thesis Organization

I begin my thesis with a general introduction (**Chapter 1**) aimed at providing the reader with an overview of the field of adult neurogenesis, including a brief history of the field, hallmark features of this biological process, and comparative models that have been examined. Some elements of my introduction have been modified and updated from a review paper published in *Progress in Neurobiology* (Lindsey and Tropepe, 2006). I conclude my introduction by highlighting the zebrafish as a tractable model of adult neurogenesis followed by a statement of my thesis objective and aims. Subsequent data chapters (2-5) are organized in a *multiple paper format*, and have been adjusted for consistency of formatting within the body of my thesis. **Chapter 2** is a reformatted version of a paper published in *The Journal of Comparative Neurology* (Lindsey et al., 2012), examining the cellular properties and ultrastructural organization of adult forebrain neurogenic niches in the zebrafish. **Chapter 3** consists of a manuscript recently submitted to *Developmental Neurobiology*, and which is currently under peer review, focusing on how changes in the social environment can regulate adult neurogenesis within sensory and integrative neurogenic niches of the adult zebrafish brain. **Chapter 4** is a manuscript in preparation for submission that includes a number of completed experiments, as well as some preliminary data. In this last data chapter I investigate the composition, modality-specific neurogenic plasticity, and regulation by Fibroblast Growth Factor of adult neurogenesis within primary sensory neurogenic niches. **Chapter 5** acts to complement and build upon discussion sections provided in each data chapter and to propose futures directions that arise from this body of work.

1.3 The Birth of a New Field of Neuroscience

The central nervous system (CNS) is one of the most fascinating and most complex structures to understand in the body. The importance of the CNS is paramount to every action, memory, thought, evaluation, and behaviour an animal performs. It is not surprising then that every year millions of dollars are spent and researchers in every corner of the world dedicate much of their lives to discovering how this structure develops from birth to adulthood, ages, is altered by disease or injury, and how it can be repaired. Within the last 25 years, these studies have led to the birth of a new field of Neuroscience that has challenged classical ways of thinking about the brain, but of which holds great potential for its future application – the field of Adult Neurogenesis.

For nearly 100 years, neuroanatomical evidence concerning mammalian brain development and growth pointed towards a brain endowed with a finite number of neurons and glia that arose at birth. No new neurons were added, but as the ageing process ran its course, neurons began to die. This theory was put forth by leading neuroanatomists at the time, including Cajal, His, and Koelliker (reviewed in Gross, 2000). Although occasional reports of postnatal neurogenesis surfaced during studies in rodents (Levi, 1898; Hamilton, 1901) and comparative work from teleosts to humans (Schaper, 1897) in the first half of the 20th century, techniques to conclusively show that mitotic cells indeed took on a differentiated glial or neuronal morphology were absent.

With the introduction of tritiated thymidine in the 1960s, Joseph Altman performed a series of experiments in rats suggesting that new neurons were born in the cortex, dentate gyrus, and olfactory bulbs (Altman, 1962; 1963; Altman and Das, 1965; Altman, 1966; 1969). These studies were later followed up by combining tritiated thymidine with electron microscopy to examine the ultrastructural characteristics of dividing cells over time and the presence of neuronal phenotypes (Kaplan and Hinds, 1977; Kaplan, 1983; 1984; 1985). Around this same time, Fernando Nottebohm and colleagues presented convincing data to demonstrate that fluctuations in the size of the higher vocal center (HVC) of the songbird were a direct result of changes in hormone levels and season leading to the birth and recruitment of hundreds of newborn neurons, and that *de novo* neurons had electrophysiological characteristics of neurons that responded to sound (Goldman and Nottebohm, 1983; Nottebohm, 1985). However, such claims were quickly dismissed by authoritative figures in the primate field (Rakic, 1985), since the presence of a

stable population of neurons in adulthood appeared essential to encode learned behaviours over time, while findings outside of the mammalian field were viewed as irrelevant exceptions.

The development of immunohistochemistry along with antibodies designed to label cell-specific phenotypes may have been the single-most important event in the acceptance of the field of adult neurogenesis in the early 1990s. One of the first laboratories to take advantage of these techniques was that of Samuel Weiss at the University of Calgary. By examining the effect of epidermal growth factor (EGF) *in vitro* in populations of cells isolated from the striata of 3 to-18 month old adult mice, and labeling with immunohistochemical markers for dividing stem cells (nestin) and differentiated glia (GFAP) and neurons (GABA, Substance P), they revealed that cells from the adult mouse striatum have the capacity to differentiate into both neurons and astrocytes (Reynolds and Weiss, 1992). At the same time the introduction of the synthetic thymidine analogue bromodeoxyuridine (BrdU), a non-radioactive alternative to tritiated thymidine that labels all dividing cells present in the S-phase of the cell cycle at the time of administration, permitted researchers to definitively label populations of proliferative cells *in vivo* (Nowakowski and Hayes, 2001; Gould and Gross, 2002). Depending on the species, BrdU can be incorporated into the body via drinking water, intraperitoneal injections, or by bath application, and has minimal toxicity to species at low doses (Kee et al., 2002; Taupin, 2007A; 2007B). This allowed some of the first researchers to apply this technique *in vivo,* such as Fred Gage, to identify adult populations of cycling cells in the mature dentate gyrus of the hippocampus of rodents and assess how many of these cells produced a mature neuronal phenotype, by double-labeling with the neuronal marker NeuN (Kuhn et al., 1996). Currently, thymidine analogs, such as BrdU, continue to be most commonly used for labeling proliferating stem/progenitor cells during studies of adult neurogenesis. In Chapters 2-4, I also employ BrdU as my primary proliferative marker and commonly refer to BrdU as labeling the stem/progenitor population within the niche. In doing so, I make the underlying assumption that BrdU is labeling populations of both stem and progenitor cells. However, I remain cognizant that this marker alone cannot distinguish between the two phenotypes unless paired with an additional stem- or progenitor-specific antibody.

Today, we are at a point in the adult neurogenesis field far beyond proving the existing of this biological trait, but rather how it can be harnessed for therapeutic and possibly even regenerative applications in humans. Still, this field remains rooted in three fundamental questions: (1) Where

does adult neurogenesis occur and what is the composition of the niche? (2) How do intrinsic and external factors mediate changes in physiological levels of adult neurogenesis, and what are the molecular mechanisms responsible? (3) What is the functional or adaptive significance of adult neurogenesis in the brain and why does it persist to a greater degree in some groups of animals than others? We have made great strides in advancing our knowledge of these questions in mammals, though from a more global stance we still know very little about how adult neurogenesis is regulated outside of the subependymal (SEZ) and subgranular (SGZ) zones. Comparative models are useful in this regard, as they offer homologous structures to those investigated in mammals, or novel neurogenic niches that may reflect different mechanisms of control, leading to new ways of interpreting the biological principles of adult neurogenesis.

1.4 Characterizing Adult Neurogenesis

The presence of adult neurogenesis in the CNS and its functional implications have forced us to re-evaluate the process of brain development into maturity and the influence of the environment in shaping this structure not only during early sensitive periods, but also later in life. In conceptualizing a dynamic brain that can continue to turn over new neurons into adulthood, the inevitable question that arises is why does this trait persist? Furthermore, why does adult neurogenesis persist within only a small number of brain regions in most species? It is commonly accepted that the presence of adult neural stem cells is a remnant of development (Alverez-Buylla et al., 2001). And although the functional significance of this trait is well understood in some regions of the brain such as the hippocampus (Koehl and Abrous, 2011), in other regions there are competing views as to the significance of this trait: Does it serve and adaptive role to allow animals to thrive in their natural environment or is it a basic necessity for continuous growth? Since the inception of adult neurogenesis it has traditionally been thought that having active pools of adult stem cells in the brain should incur some benefit to an individual, though today the notion that adding new neurons to existing circuitry is advantageous may be shifting as researchers begin to consider the instability accompanied by this process (Frankland et al., 2013). There is yet to be a consensus as to why constitutive rates of adult neurogenesis exist across all species studied to date and it’s certainly possible that there never will since this trait may have evolved differently across major groups of animals. In our attempts

to apply an overarching purpose and origin to adult neurogenesis, a broader scope of this trait may be required than our current vantage point affords, one that incorporates both shared and derived features of this process across a diversity of animal models.

Model organisms have revealed two characteristic features of adult neurogenesis that remain uncontested. First, and most importantly, adult neurogenesis is a process of consecutive stages that gives rise to the birth of new neurons under physiological conditions in the mature brain of animals. This is in contrast to inductive (reactive or compensatory) neurogenesis, where quiescent populations of stem/progenitor cells are activated with stimulation or following injury within a non-neurogenic region (Kaslin et al., 2008; Kizil et al., 2012). This process takes place in restricted neuroanatomical regions of the brain, known as neurogenic niches, which under constitutive conditions are tightly controlled by molecular cues, growth factors, and cell-to-cell communication. The process of adult neurogensis is initiated by populations of adult neural stem cells (ANSCs), capable of self-renewal and producing a continuous supply of daughter cell (i.e. asymmetric division) that may differentiate into neurons, oligodendrocytes, or glia (Brand and Livesley, 2011). Similar to development, studies in mammals have demonstrated that ANSCs have clear glial characteristics (Doetsch, 2003A; Kriegstein and Alvarez-Buylla, 2009). In adulthood, it has been confirmed that the phenotype of ANSCs is an astrocyte (SEZ of mammals), radial astrocyte (SGZ of mammals), or radial glia-like cell (reptiles, birds, fish, invertebrates), however in non-mammalian species the lineage descendents of stem cells are still poorly characterized. In all cases, adult stem/progenitor cells proceed through one or more intermediate, committed cell types before differentiating into their final neuronal phynotype (Kriegstein and Alverez-Buylla, 2009). To date, this cellular transition from an ANSC to a differentiated neuron *in vivo* has been best characterized within the SEZ of mammals, where Type B cells (ANSC astrocytes) produce actively dividing Type C cells (transit amplifying progenitors), that lead to Type A cells (immature neuroblast) that migrate along the rostral migratory stream (RMS) into the olfactory bulbs where they mature and differentiate into interneurons (Ponti et al., 2013). Electron microscopy studies have shown that each cell type in this process is endowed with distinct ultrastructural profiles (Doetsch et al., 1997), while immunohistochemical studies have revealed that each cell type expresses a different set of markers (reviewed in Zhao et al., 2008; Ming and Song, 2011).

A second hallmark feature of adult neurogenesis is its degree of neurogenic plasticity. It is well accepted that the cellular populations making up different stages in this process can be modulated (i.e. increased or decreased) as a result of an array of external stimuli or changes in physiological levels of intrinsic factors, such as circulating hormones. Most studies have shown this to be true at one or more levels, including stem/progenitor cell proliferation, their survival as post-mitotic cells, neuronal differentiation, or the long-term survival of neurons within the niche (Gould et al., 2000; Lu et al., 2003; Cayre et al., 2007; Lieberwirth and Wang, 2012). Therefore, when thinking about neurogenesis one must envision a dynamic process that, under physiological conditions and within a predictable environment, is kept within a narrow range of fluctuations, but with exposure to extreme change, as often performed under laboratory settings, will result in severe shifts in the composition of these cellular populations. For this reason, during investigations of adult neurogenesis one must be mindful that our interpretations are merely based on a snapshot of the properties of the niche at a given moment; this being most important when assessing rates of adult neurogenesis in wild populations. This form of structural plasticity can lead to remodelling of the neurogenic niche in a much more extreme manner than following synaptic plasticity that is known to mediate functional plasticity of neural circuitry. However, outside of commonly studied niches of rodents and songbirds, how the external environment can impinge on rates of adult neurogenesis, and in doing so, further modify internal regulatory signals required for niche homeostasis remains a black box. This is especially true for neurogenic niches residing in primary sensory structures of the brain observed in teleost fishes (Lindsey and Tropepe, 2006). By beginning to uncover the properties of these niches, we may begin to ask whether their modulation correlates with the function of the sensory processing structure and how responsive sensory niches may be to changes in environmental stimuli compared with better understood forebrain compartments. These interactions between external and intrinsic cues highlight the complexity of stimuli controlling the adult neurogenic niche, and ultimately neuronal output.

1.5 Defining the Neurogenic Niche

The adult neurogenic niche can be defined as a permissive microenvironment within the mature brain that is tightly controlled by a host of regulatory factors and that is strictly delineated by

distinct cellular populations residing in a subregion of specific neuroanatomical structures. The composition and behaviour of cells localized to the niche are responsible for generating new neurons throughout the life of an animal. Understanding the relationship between the cell types comprising the niche is fundamental in order to investigate how the niche is re-organized with exposure to stimuli or its functional significance. Many of the cells within the niche serve a functional role in the process of adult neurogenesis, and have phenotypes of ANSCs or intermediate progenitors (Kriegstein and Alverez-buylla, 2009). Alternatively, some serve a more supportive and/or instructional role, such as ependymal cells. A reoccurring theme in the identification of adult niches is that the neuroanatomical position of the niche is commonly situated adjacent brain ventricles. For this reason, embryonic brain development plays a direct role in the future position of adult niches. For instance, by comparing telencephalic development via the process of evagination in mammals and eversion in teleosts, one can begin to appreciate how putatively homologous structures, such as the hippocampus, can be patterned along the medial (i.e. mammals) or lateral (i.e.teleosts) telencephalon (Broglio et al., 2005; Wullimann, 2009), but in both cases still reside at the luminal surface. Mitogens present within the cerebrospinal fluid of ventricles are believed to impose instructional cues to cells within the niche, in particular the stem/progenitor pool, of which Type B cells in mammals extend a single cilium into the ventricle (Doetsch, 2003B; Sawamoto et al., 2006; Mirzadeh et al., 2008; 2010).

In conceptualizing the adult niche and the properties that define it, it is useful to consider the alternative – a non-neurogenic zone devoid of the ability to produce newborn neurons under homeostasis. By contrasting the two, one begins to appreciate the importance of key structural elements that characterize an active adult niche, across all metazoans. Most importantly is the presence of an active population of ANSCs. Quiescent populations of stem cells define non-neurogenic compartments of the brain, but also make up a large percentage of the stem cells in neurogenic niches. However, persistent populations of slowly cycling ANSCs remain present in neurogenic zones, and are essential to give rise to progenitor cells. The cell cycle kinetics of progenitor cells, and the proportion of these that survive, is intimately linked with the percentage of newborn neurons arising from the niche. The role of intrinsic cell cycle components on neuronal progenitor cells within the niche, including the cyclin-dependent kinases and cyclins, are only beginning to be uncovered in some of the most intensely studied niches, and it still remains unclear whether their developmental function is recapitulated within adult neurogenic

zones (Beukalaers et al., 2011). An additionally feature of the niche contributing to its dynamic environment, is the migratory behaviour of differentiating cells. The daughter cells of ANSCs typically migrate towards their target destination from their place of birth, as they become fate committed to a neuronal phenotype. In mammals, long-distance migration of progenitors occurs in ANSCs born in the SEZ and of which migrate out of the niche along the rostral migratory stream (RMS) into the rostral-most olfactory bulbs (Lois and Alvarez-Buylla, 1994; Lois et al., 1996). By contrast, stem/progenitor cells in the ventricular zone of the zebrafish forebrain for example, migrate only a short distance laterally into the parenchyma as they take on a neuronal phenotype (Zupanc et al., 2005; Grandel et al., 2006). Similar to during development, molecular cues present within the niche, as well as from the target destination of newborn neurons act to guide differentiating progenitors as they emigrate from their place of origin (Hagg, 2005; Metin et al., 2008; Kaneko et al., 2010). Despite the importance of guidance molecules for instructing the fate of differentiating neurons, we are far from a comprehensive understanding of their specialized role across most niches.

A more recent feature of the niche which we have only begun to appreciate in the last decade is the presence of vasculature. Studies in songbirds were of the first to show a strong correlation between angiogenesis and adult neurogenesis, demonstrating that testosterone-induced angiogenesis can lead to upregulation of new neurons produced in the song control nucleus (Louissaint et al., 2002). In the SGZ of mammals, irradiation of vessels and endothelial cells confirmed the importance of a well vascularised niche, as once ablated the niche was no longer able to produce newborn neurons (Monje et al., 2002). Blood vessels provide an efficient route for the circulation of hormones such as cortisol, prolactin, estrogen, and testosterone, all of which are known to be potent regulators of adult neurogenesis (Doetsch, 2003B; Bordey, 2006). This means that even remote factors can impact the behaviour of cells within the niche in an antagonistic or agonistic manner, by passing through the blood-brain-barrier or by indirect effects through endothelial cells. As levels fluctuate with stress or estrous cycles for instance, one observes a direct effect on elements of the niche and neurogenic output (Smith et al., 2001; Schoenfeld and Gould, 2012; 2013). In the SEZ of mammals, a specialized pattern of vasculature has been reported where stem cells and their daughter cells are coupled with blood vessels (Tavazoie et al., 2008), and as a result receive signals from diffusible factors arising from vessels or endothelial cells. This work showed that Type C transit-amplifying cells and Type B

astrocytes lie adjacent to blood vessels, with Type A neuroblasts positioned more distally. A complementary study examining the organization of vasculature in relation with the phenotype of SEZ cells within the niche further revealed a unique pinwheel appearance at the ventricular surface consisting of a central apical ending of a Type B1 astrocyte surrounded by ependyma (Mirzadeh et al., 2008). More recent studies characterizing adult neurogenic compartments in crustaceans have further illustrated the importance of an extensive vascular supply in close proximity to the stem/progenitor cells of the niche (Chaves da Silva et al., 2012). In Chapter 2, by characterizing forebrain neurogenic niches (periventricular zones) in the adult zebrafish, I show that vascularisation of the niche indeed appears to also be a common feature of teleost forebrain niches.

In discussing the characteristics of the niche, a most conspicuous features that today still remains unclear, is the variation in the number of neurogenic niches between species. Evidence suggests that the location of the niche, and the number of niches within a species, appears to be a Class-specific property across vertebrates and invertebrates alike (reviewed in Lindsey and Tropepe, 2006). It would appear that with the transition from water to land, there was an associated reduction in the number of neurogenic niches retained in the adult brains of dominant vertebrate groups. Interestingly, this also parallels the regenerative properties of vertebrates, with teleosts housing the greatest number of adult neurogenic niches and capacity for CNS tissue regeneration, and mammals having the least (Kaslin et al., 2008). The current notion is that phylogenetically more ancient species maintain widespread neurogenesis (i.e. teleosts), and thus a greater number of neurogenic zones along the rostrocaudal axis of the brain, whereas modern vertebrates have limited sites of adult neurogenesis housing active pools of ANSCs. However, an important distinction among vertebrates is the number of neurogenic niches where ANSCs reside compared to the number of target structures their neuronal progeny populate in the CNS. From a comparative perspective, it remains a difficult task to find common themes across the stem cell niche, due both to the complexity of regulatory cues, as well as the limited data for some species. A recent review of adult neural stem cell activity across vertebrate niches has illustrated that despite common findings at some levels of investigation, in a number of cases adult neurogenesis and the behaviour of the niche may serve different purposes even for species within the same taxonomic class (Grandel and Brand, 2013). With the genesis of adult-born neurons intimately coupled with the dynamic state of the niche, in the following two sections I

provide a brief overview of the intrinsic factors that regulate the niche, and how the external environment modulates the niche via adult neurogenic plasticity.

1.6 Maintenance and Regulation of the Adult Niche

The ability to maintain constitutively active ANSCs in niches of the mature brain is controlled by a number of endogenous factors. In many cases, these factors recapitulate their developmental role during embryonic neurogenesis (Fuentealba et al., 2012). Within the local environment of the niche, cell-to-cell communication between junctional complexes as well as cues from the adjacent ventricular lumen, some of which are constantly modulated or changing by ventricular flow of cerebrospinal fluid, play a central role in determining the neurogenic capacity of the niche. More distal factors that influence the regulation of the niche arrive by way of the circulatory system into blood vessels interspersed throughout this permissive environment. Collectively, these factors provide signals to the niche as a whole, or drive the cellular behaviour of individual cell types, that ultimately determine the state of the niche and population size of cells at each stage of adult neurogenesis under homeostasis. It is also likely that the abundance of factors controlling the niche undergo interactions in a competitive or agonistic manner, though at present we have little understanding of this. The list of factors that control the niche continues to expand, and further is beginning to encompass a collection of genes required for maintaining neurogenic versus non-neurogenic zones (Overall et al., 2012; Miller et al., 2013). Below I limit this section to some of the best studied examples across the literature within each major category, including the role of growth factors, signalling pathways, neurotransmitters, hormones, and the effect of senescence.

Growth factors play a pivotal role in providing signals within the neurogenic niche. Two of the primary trophic factors involved in maintaining stages of adult neurogenesis are epidermal growth factor (EGF) and fibroblast growth factor (FGF), while the function of insulin-like growth factor 1 and 2 (IFG1/2), vascular endothelial growth factor (VEGF), and brain-derived neurotrophic factor (BDNF) are less clear (Doetsch, 2003B; Fuentealba et al., 2012). In mammals, *in vivo* studies show that EGF and FGF differentially regulate stages of adult neurogenesis. While both growth factors are capable of expanding the initial progenitor

population within the SEZ (Craig et al., 1996; Kuhn et al., 1997), EGF is intimately linked with proliferation, survival and migration of precursor cells (Craig et al., 1996), while FGF-2 acts to increase the number of newborn neurons in the olfactory bulb (Kuhn et al., 1997; Zhao et al., 2008). Studies examining the role of transforming growth factor-α (TGFα) have also shown that it plays a similar role to EGF (Tropepe et al., 1997). In the SEZ, more recently experiments have shown that FGF-2 is expressed in GFAP-positive cells but is otherwise absent in progenitors which express FGFR-1 and FGFR-2 mRNA (Mudo et al., 2009). Contrary to the role of EGF and FGF in the SEZ, within the SGZ of the hippocampus, neither factor promotes cell proliferation of progenitors, though EGF acts to suppress the number of newborn neurons (Kuhn et al., 1997). In the telencephalic ventricles of the adult zebrafish, FGFR-1 signalling has recently been found to be involved in maintaining proliferation rates of $BrdU^{+}$ cells in the ventral glial-domain of the telencephalic subpallium while having little effect on the dorsal pallial niche (Ganz et al., 2010). In a separate study, examination of FGFR1-4/p-ERK expression showed that although present in the ventricular niche, FGF-signalling does not correlate with proliferative progenitors (Topp et al., 2008). The requirement of FGF and its receptor subtypes in regulating different stages of adult neurogenesis is still not fully understood. In fact, few studies have dissected the role of FGF on neuronal differentiation and neuronal survival. In order to expand our understanding of the function of FGF, in Chapter 4 of my thesis, the role of FGFR-1 in maintaining constitutive levels of cell proliferation is investigated in sensory niches of the adult zebrafish brain.

Several signalling pathways critical during early development have, in recent years, become intensity studied in niches of the adult brain (Inestrosa and Aneras, 2010; Ables et al., 2011). These include Notch, Wnt, Sonic Hedghog (Shh), Bone morphogenetic protein (BMP), and Ephrin signalling, although the role of Notch and Wnt (to a lesser degree) signalling has been best characterized to date. Studies of the Notch signalling pathway show opposing roles in the maintenance of the active or quiescent state of ANSCs in mammals compared with zebrafish. It has been reported that Notch signaling is highly expressed in Type B astrocytes in the SEZ and within Type-I cells of the SGZ (Imayoshi and Kagayama, 2011). In the SEZ of mammals, Notch signalling is required to maintain ANSCs in an active, rather than quiescent state (Basak et al., 2012). In adult zebrafish telencephalic neurogenic zones that are located periventricularly, changes in levels of Notch activity toggle ANSCs between an active or quiescent state. Here, Notch induction drives progenitors into a quiescent state whereas reductions in Notch transition

progenitors back into an active state (Chapouton et al., 2010). Recently, is has been shown that Notch receptor expression is heterogeneous among different neurogenic zones in the adult zebrafish, including the telencephalon, optic tectum, and cerebellum (de Oliveira-Carlos et al., 2013). Besides the role of Notch in the cycling state of progenitors, it is becoming clear that Notch may additionally be critical to later stages of adult neurogenesis, including cell migration and neuronal differentiation (Ables et al, 2011).

The role of Wnt signalling in the adult niche is also emerging as an important regulator (Seib et al., 2013; Wu and Hen, 2013), though our understanding of this pathway is limited. Work in the adult mammalian hippocampus has shown that Wnt ligands derived from hippocampal astrocytes bind receptors expressed in progenitors to control levels of neurogenesis (Lie et al., 2005). With a diversity of roles, including CNS development, cell-to-cell communication, stem cell activation, and modulation of synaptic plasticity, and the presence of Wnt expression within the adult niche (Nusse, 2008; Inestrosa and Arenas, 2010; Wu and Hen, 2013), the notion is that Wnt and/or β-catenin signalling is likely to have a functional role in the regulation of the niche, however future studies are needed to prove this claim.

One of the newest mediators of adult neurogenesis is the action of neurotransmitters. Once thought to function solely to modulate synaptic activity between neurons, a role in regulating adult neurogenesis is being unveiled. Reports from rodent models have now shown that GABA, glutamate, dopamine, acetylcholine, nitric oxide, neuropeptide Y, noreadrenaline, and serotonin can indeed inhibit or activate multiple stages of adult neurogenesis, and that several neurotransmitters are themselves released from progenitors in this process (reviewed in Berg et al., 2013). For example, within developing dentate granule cells of the SGZ, GABA acts as a trophic factor for immature neurons and progenitor cells via chloride-mediated depolarization (Dieni et. al., 2013). With $GABA_A$ receptors present on progenitor cells, GABAergic stimulation is correlated with decreases in the rate of proliferation (Waterhouse et al., 2012). In the SEZ, among a number of effects, local GABA signalling within the niche controls the proliferation of Type B astrocytes, and provides feedback concerning the size of the neuroblast pool (Bordey et al., 2006). Conversely, Type A neuroblasts expressing glutamate receptors in the SEZ of rodents demonstrate increased survival and proliferation with elevated levels of glutamate in slice preparations (Brazel et al., 2005; Platel et al., 2008). Earlier studies have additionally implicated serotonin as a regulator of cell genesis in the adult hippocampus, since the dentate gyrus is

enriched with 5HT1A receptors (Gould, 1999). Recently, studies investigating mechanisms linking physical activity with rates of cell proliferation in the adult hippocampus, have illustrated the necessity of serotonin for activity-dependent hippocampal neurogenesis in young-adult and aged mice (Klempin et al., 2013). The widespread action of neurotransmitters within the CNS and their presence within the local environment of the adult niche allows new avenues of inquiry concerning the relationship between neurotransmitter levels, adult neurogenesis, and disorders of the nervous system or neurodegenerative diseases, where neurotransmitters are known to be under non-physiological levels.

Hormones play a central role in species behaviour, and physiological levels are critical for mood regulation in humans. In the context of adult neurogenesis, hormones are clearly a potent regulator. Changes in hormone levels can be triggered by internal physiological events such as ageing (i.e. adolescence, menopause), estrous, reproduction, and postpartum (Smith et al., 2001; Pawluski and Galea, 2007; Galea et al, 2013). Alternatively, endogenous levels of hormone can fluctuate in response to external influences including acute and chronic forms of stress (Gould et al., 1992; Cameron and Gould, 1994; Gould et al., 1998; Westenbroek et al., 2004; Stranahan et al., 2006; Leasure and Deaker, 2009; Spritzer et al., 2011), social interactions with prey or mates (Lieberwirth and Wang, 2012; Glasper and Gould, 2013), and odor discrimination and pheromones (Smith et al., 2001; Tanapat et al., 2001; Mak et al., 2007; Mak and Weiss, 2010). In the SEZ and SGZ of mammals, hormones released from the ovaries (i.e. prolactin, estrogen) and adrenal glands (i.e. glucocorticoids) under different contexts affect neurogenesis (Bordey, 2006). To date, this has been most extensively investigated in the SGZ. Sex differences have been reported in how gonadal hormones influence cell proliferation and differentiation in the hippocampus of adult rodents (Galea, 2008). For instance, release of estrogen from the ovaries exerts a stimulatory effect on adult neurogenesis and is involved in hippocampal-dependent learning and memory. Additionally, increased levels of androgens (i.e. testosterone) have recently been shown to increase survival of adult-born neurons in the dentate gyrus of male rats (Hamson et al., 2013). In songbirds, the addition of new neurons to the song control nucleus is mediated by seasonal surges in testosterone (Chen and Goldman, 2013). Opposite the above, experiments in adult male and female treefrogs show that socially modulated cell proliferation occurs independently of gonadal hormone levels (Almli and Wilczynsky, 2012), exemplifying

that both the contextual environment and individual species physiology dictate whether perturbations in neurogenesis ensue with changes in hormone levels.

Most intensely studied has been the relationship between cortisol levels and adult neurogenesis (Schoenfeld and Gould, 2012; 2013). The difficulty here is that what is stressful to one species may not be to the next. The general notion derived from mammalian literature is that increases in glucocorticoid levels from the adrenal gland act to suppress neurogenesis within the hippocampus. Thus, elevated cortisol levels continue to be viewed as a negative inhibitor of stages of this process, including stem/progenitor proliferation, neuronal differentiation, and survival. However, in recent years accumulating evidence has begun to suggest a possible protective role of stress under certain conditions (reviewed in Schoenfeld and Gould, 2012; 2013). In line with this, rewarding experiences such as running enhance levels of adult neurogenesis, at least in the hippocampus, despite elevated levels of stress hormones (van Praag et al., 1999A; 1999B; Stranahan et al., 2006). In most vertebrates, the hormones cortisol (or corticosterone) and aldosterone are present and activated by their respective glucocorticoid receptor (GR) and mineralocorticoid receptor (MR) (Takahashi and Sakamoto, 2013). In mammals, glucocorticoids are released from the hypothalamic-pituitary adrenal axis and bind to both GRs and MRs expressed on granule cells of the dentate gyrus and olfactory bulb (Morimoto et al., 1996). However, GRs rather than MRs are primarily activated during stress-induced elevations in circulating glucocorticoids in the hippocampus. The stress-coping style and how activation of the stress axis is coupled, if at all, to changes in adult neurogenesis in non-mammalian species remains poorly characterized (Overli et al., 2007). In teleost fish for instance, cortisol appears to be the predominant stress hormone, performing both glucocorticoid and mineralocorticoid actions (Takahashi and Sakamoto, 2013). In Chapter 3, I present evidence that the social context of adult zebrafish is central to the cortisol response of these species, and that unlike the situation in mammals this hormone does not appear to regulate stem/progenitor cell proliferation in neurogenic zones.

This section would not be complete without last discussing the implications of the ageing process itself on physiological rates of neurogenesis. Senescence is a naturally occurring process across all species that begins after embryogenesis is complete and continues until the death of an organism, generally as a result of the inability of cells to undergo self-repair. The current notion is that upon reaching sexual maturity, as animals' progress through young-, middle-, and old

stages of adulthood, neurogenesis declines in parallel within adult niches (Hamilton et al., 2013). Nonetheless, differences in the timing of sexual maturity, the aging process, and the lifespan of species greatly complicate the picture, and further depend on a host of factors, including the genetic background, gender, type of environment (i.e. wild or captive), artificial selection on laboratory populations, and the experimental condition to which the animal is exposed (Rakic, 2002; Abrous et al., 2005; Ricklefs, 2006). Individual invertebrate and vertebrate animals age at different rates, but the biological basis of this variation is poorly understood (Finch, 1990). In mammals the midpoint of the average lifespan for rodents is approximately 1 year, while across species of primates this ranges from 10-25 years, and in humans is now closer to 45 years (Finch and Austad, 2012; Hamilton et al., 2013). However, more ancient vertebrate lineages, such as fish and reptiles, demonstrate three distinct types of senescence. For example, different reptiles can exhibit rapid senescence, gradual senescence (comparable to the majority of vertebrates), or slow/negligible senescence, which can be observed in turtles, tortoises and crocodiles who continue to grow throughout life and may live for more than a century (Patnaik, 1994). In invertebrates, such life-long continuous growth has also been recorded in decapod crustaceans (Schmidt and Harzsch, 1999; Schmidt, 2001). Short-lived species of amphibians show gradual senescence as in laboratory mammals, whereas long-lived animals, like fishes and reptiles, show slow senescence (Kara, 1994).

Only in the last 15 years has senescence been considered in the same light as adult neurogenesis, implicating reductions in neuronal birth with age-related diseases and mental disorders. Mammalian studies of adult neurogenesis have already ascertained that different stages of adulthood are paralleled with different levels of cell proliferation, neuronal differentiation, and survival across neurogenic niches (Altman and Das, 1965; Kaplan et al., 1985; Seki and Arai, 1995; Kuhn et al., 1996; Tropepe et al., 1997; Jin et al., 2003; Amrein et al., 2004B; Bondolfi et al., 2004; Enwere et al., 2004; Heine et al., 2004; Driscoll et al., 2006; Luo et al., 2006; Hamilton et al., 2010; Martinez-Canabal et al., 2012). An elegant review of aging and its effects on adult forebrain neurogenesis recently brought to light that most deficits in neurogenesis are established by middle-age in mammals, and as such, may be linked with the onset of neurodegenerative diseases (Hamilton et al., 2013). Coupling senescence with adult neurogenesis indeed gives rise to many intriguing questions. For example, do all neurogenic compartments age at a similar rate, what role does species variation play in this regard, and what are the underlying mechanisms?

Considering the variation in the types of senescence across animals, differences in the aging process across many non-mammalian species is likely to produce effects on adult neurogenesis.

What mechanisms might be responsible for the observed age-related differences in adult neurogenesis? It would appear that several endogenous regulators of the adult niche are also altered with age. A study of young adult and aged rat brains showed that astrocytic populations in the mammalian SEZ and SGZ express high levels of FGF-receptor-2 (FGFR-2) protein, and that FGF signaling could be involved in maintaining neurogenesis at later stages of adulthood (Chadashvili and Peterson, 2006). These authors observed an age-related decline in FGFR-2 in the olfactory bulb and hippocampus, which may indicate that expression of this receptor at the target destination of developing neurons' could be required for proper differentiation into mature and functional neurons. In a separate study, increases in transforming growth factor-beta 1 (TGFβ1), a cell cycle regulator that increases after injury and with age, and which is secreted from astrocytes, was also shown to strongly inhibit hippocampal neurogenesis in aged transgenic mice (Buckwalter et al., 2006). Aside from growth factors, several hormones and neurotransmitters, including glucocorticoids, corticosterone and glutamate have been associated with age-related reductions in cell proliferation in the hippocampus of rats (Lupien and McEwen, 1997; Nacher et al., 2003; Abrous et al., 2005). Studies have also implicated the importance of environmental enrichment on rescuing age-related declines in cell proliferation and the production of adult-born neurons (Kempermann et al., 1998). This study showed that by switching 6 and 18 month old mice from standard housing to an enriched environment, with opportunities for social and physical interaction, and exploration, survival of $BrdU^+$ cells increased by 68% in 6-month-old mice and 32% in 18-month-old mice in the dentate gyrus. As a corollary to this, sexual experience has most recently been shown to restore age-related declines in adult neurogenesis and hippocampal function (Glasper and Gould, 2013).

The regulatory factors described above are only a small sampling of the most pronounced examples reported to be necessary in maintaining the neurogenic niche into adulthood. As discussed, this intricate regulation of the niche can vary tremendously between niches of the same species, and more broadly between major groups of animals. How widely conserved these regulator factors are and whether they recapitulate their developmental roles rests on future comparative studies. However, one thing is for certain. Endogenous levels of growth hormones, stress hormones, and signalling pathways can be modulated by the outside world of individual

animals (Ming and Song, 2005), adding yet another layer of complexity to how the adult neurogenic niche is controlled.

1.7 Adult Neurogenic Plasticity

One of the most intriguing features of adult neurogenesis is the inherent plasticity of the niche. As mentioned above, the proliferative microenvironment of the niche is maintained in adulthood owing to a number of finely tuned molecular factors, signalling pathways, and hormones. But this is not the entire story. The external surroundings of an animal, both environmental and social, further acts upon the niche to modulate levels of endogenous regulatory factors (Gheusi et al., 2009; Lieberwirth and Wang, 2012), leading to dynamic shifts in the number of cells at different stages of this process as a result of adult neurogenic plasticity. Adult neurogenic plasticity can be defined as changes at the "population level" of cells from constitutive levels of neurogenesis, exerting downstream effects on the ratio of cell types and neurogenic capacity of the niche. This more extreme form of "whole cell" structural plasticity greatly contrasts synaptic plasticity at the morphological level, but common to both is that they are modified by internal and external stimuli. The intrinsic ability of synapses to undergo rapid activity-dependent refinement of their microstructure is crucial for the formation of neural circuitry during embryogenesis (Hensch, 2005). Microstructural changes in the mature brain, and in particular changes in synaptic morphology, also occur in response to sensory stimuli and are required for learning and memory formation (e.g. Feldman and Brecht, 2005). Accordingly, it is clear that the addition and survival of new neurons is critical for novel information processing and learning in the hippocampus of mammals throughout life (Shors et al., 2008), and likely within other niches as well. Thus, the formation, modification and elimination of synapses or entire neurons in the adult brain can play a fundamental role in the ability to encode information within regions of the CNS. Thus, modern neuroscientists are confronted with a brain endowed with vastly different properties than once thought, one that demonstrates plasticity at multiple levels of the neuron (or progenitor) throughout life. This expanded view of neural plasticity, one that includes cell loss, addition or replacement, is only now receiving more attention given the interest in the field of adult neurogenesis.

Exploring the effects of environmental influences, animal behavior, and social interactions on adult neurogenesis has become a major initiative in the field. Even though many of these studies have taken place under simplified laboratory conditions, they have been instrumental in identifying a variety of natural mechanisms influencing the rate of adult neurogenesis in animals. These factors can be categorized as having a direct (i.e. more exposure leads to elevated neurogenesis; vice-versa) or indirect (i.e. more exposure leads to reduced neurogenesis; vice-versa) correlation with adult neurogenesis. Those exhibiting a direct effect include environmental and sensory enrichment (Kempermann et al., 1997; 1998; Sandeman and Sandeman, 2000; Scotto-Lomassese et al., 2000; Hansen and Schmidt, 2001; Scotto-Lamassese et al, 2002; Brown et al., 2003; Bruel-Jungerman et al., 2005; Segovia et al., 2006; Bovetti et al., 2009; Ayub et al., 2011; Dunlap and Chung, 2013), physical activity (Bernocchi et al., 1990; van Praag et al., 1999A, 1999B; Brown et al., 2003; Bednarczyk et al., 2011), mating pheromones and sexual activity (Tanapat et al., 2001; Smith et al., 2001; Mak et al., 2007; Mak and Weiss, 2010; Portillo et al., 2012; Glasper and Gould, 2013), dominant social status (Kozorovitskiy and Gould, 2004; Maruska et al., 2012; 2013), learning and memory (Gould et al., 1999A; Kee et al., 2007; Mouret et al., 2009; Shors et al., 2008; Garthe et al., 2009; Nottebohm and Liu, 2010; Stone et al., 2010; Mandairin et al., 2011; Martinez-Canabal et al., 2012), and sleep (Mirescu et al., 2006; Guzman-Marin et al., 2007; Meerlo et al., 2009; Gibson et al., 2010; Junek et al., 2010; Sportiche et al., 2010). Conversely, factors having an indirect effect include predator odors (Tanapat et al., 2001), stressful experiences (Gould et al., 1992; Cameron and Gould, 1994; Gould et al., 1997, 1998; Tanapat et al., 2001; Bain et al., 2004; Westenbroek et al., 2004; Mirescu and Gould, 2006; Stranahan et al., 2006; Leasure and Decker, 2009; Spritzer et al., 2011), social isolation and sensory deprivation (Barnea et al., 2006; Mandairon et al., 2006; Ibi et al., 2008; Spritzer et al., 2011; Lieberwirth et al., 2012), impoverished environment (Scotto-Lomassese et al., 2000; Sandeman and Sandeman, 2000; von Krogh et al., 2010), subordination (Maruska et al., 2012; 2013), and anxiety (Sah et al., 2012). Additionally, temperature and photoperiod (Ramirez et al., 1997; Peñafiel et al., 2001; Walton et al., 2012) and seasonal variation (Barnea and Nottebohm, 1994; Alverez-Buylla and Lois, 1995; Clayton, 1998; Dawley et al., 2000; Nottebohm, 2002A, 2002B; Hansen and Schmidt, 2004; Hoshooley and Sherry, 2004) have been shown to either activate or inhibit stages of adult neurogenesis. Taken together these data suggest that from insects to mammals, both the daily behavior and immediate environment of animals are intimately related with the addition of new neurons throughout adulthood.

Experiments studying plasticity in adult niches have also highlighted that animals exposed to combinations of direct and indirect correlates often lead to situations where one factor is overriden by the other. For example, social isolation has been shown to delay the positive effects of physical activity in the rat hippocampus, (Stranahan et al., 2006; Leasure and Decker, 2009), whereas reductions in proliferation as a result of short-term restraint stress can be rescued by exposure to environmental enrichment (Veena et al., 2009). A common finding across the literature has also been that exposure to single or multiple environmental factors impacts upon one or more stages of adult neurogenesis in a unidirectional manner, leading to increases or decreases in the cellular population at each stage. Additionally, mammalian studies have shown that a given stimulant may only affect a single niche, rather than exert the same effect on both. One example of this is social isolation. Nearly all studies demonstrate that social isolation during adulthood decreases rates of stem/progenitor proliferation and/or the number of newly differentiated neurons within the SGZ, but not in the SEZ (Brown et al., 2003). However, the limited number of studies examining neurogenic plasticity outside of mammalian models makes it difficult to discern how robust or specific subsets of external modulating factors may be across different vertebrate niches. In Chapters 3 and 4, I provide insight into these questions by investigating how social change or modality-specific sensory stimulation in multiple niches of the zebrafish can perturb baseline rates of cell proliferation and neuronal differentiation, as well as their direction of change.

An important consideration when addressing questions of adult neurogenic plasticity in the laboratory is how representative findings are to the true degree of plasticity that would occur in the natural environment of the animal without restraints. Laboratory-bred animals generally lack the complete assortment of stimuli during development leading up to adulthood, which would otherwise be available under natural conditions. Additionally, it is unlikely that a simulated "enriched laboratory environment", parallels that of the natural habitat of the animal. For instance, interactions that persist in the natural environment of a species, including predation, competition for mates and territory, and environmental stochasticity cannot be recreated under artificial laboratory conditions with laboratory-bred animals (Boonstra et al., 2001). The possibility that laboratory-bred or captive animals may display differences in their rate of adult neurogenesis compared with free-ranging animals first arose during studies of black-capped chickadees by Barnea & Nottebohm (1994). These investigators discovered a nearly 2-fold

decrease in cell labeling in the hippocampus of captive birds compared with wild birds. Hansen & Schmidt (2004) reported a similar trend in adult shore crabs. Since this initial finding, a number of invertebrate and vertebrate papers studying animals under impoverished and enriched living conditions have been put forth (Kempermann et al., 1997; 1998; Sandeman and Sandeman, 2000; Scotto-Lammassese et al., 2000; von Krogh et al., 2010; Ayub et al., 2011). These experiments did not compare free-ranging and laboratory animals, but the experimental designs employed proved that animals living in enriched environments display enhanced rates of adult neurogenesis since neurogenic plasticity was promoted under these conditions.

Thus far only a handful of studies have examined free-living animals (Barnea & Nottebohm, 1994; Lavenex et al., 2000; Amrein et al., 2004A, 2004B; Hansen & Schmidt, 2004; Hoshooley and Sherry, 2004; Barker et al., 2005; Epp et al., 2009; Cavegn et al., 2013; Slomianka et al., 2013). Tracking studies have been proposed to compare laboratory findings of neuronal plasticity and recruitment with those in the natural habitat of the animals (Nottebohm, 2002B). For example, capture-release-recapture experiments can be designed, in which a sample of individuals is captured, injected with a cell birth date marker, released, and then recaptured following a pre-determined time period. As an extension of this, I recommend additional detailed observations of activity patterns, social interactions, foraging mode, and environmental conditions both leading up to, and following injection with the cell proliferation marker. This may be accomplished by either field observations or by implanting a microchip able to record specific species-related or environmental data within the animal. Conversely, the importance of environmental influence on adult neurogenesis and plasticity may be confirmed by altering the natural environment of the animal. Animals could either be reared to adulthood in the novel environment, or transferred to such an environment at a specific developmental stage, with birth-date labeling performed accordingly. Comparisons between the typical environment of the individual and the novel environment could then be assessed. One ongoing caveat of natural population studies however, is the difficulty in pinpointing individual factors that modulate stages of adult neurogenesis, something much simpler to accomplish under laboratory settings.

The fact that populations of ANSCs and neurons themselves can change in number by exposure to environment cues, even in humans, seems closer to science fiction than reality. Certainly this is what Santiago Ramon Y Cayal thought some 100 years ago. However, the existence of innate plasticity in adult neurogenic niches is not met without contending views of its function and

necessity. As one moves along the vertebrate lineage from fishes to mammals, fewer neurogenic niches persist in adulthood, leading to fewer constitutively active zones of adult neurogenic plasticity (Lindsey and Tropepe, 2006; Kaslin et al., 2008). So why is adult neurogenic plasticity maintained at these sites? It has been proposed that neurogenic plasticity in the hippocampus of mammals may have been selected for over evolution to provide mammals with a particular advantage in adapting to their surrounding environment (Kempermann, 2012). Nevertheless, the adaptive value of adult neurogenesis could equally be argued for neurogenic niches housed within primary sensory structures of the brains of zebrafish, a species that greatly relies on chemosensory and visual cues in the wild (Wullimann et al., 1996). Of course the counter argument is that teleost fishes continue to add new neurons to regions of the brain because they continue to growth throughout life (Kaslin et al., 2008). Recent theories based on remodelling of established neuronal circuits with the addition of newborn neurons in the dentate gyrus of mammals have presented the notion that continuous adult neurogenesis may induce forgetting (Frankland et al., 2013). There is no question that the degree of instability that adult neurogenic plasticity brings to the CNS may have more far-reaching, deleterious effects than currently thought, though this remains to be determined. Extending our understanding of neurogenic plasticity to new models of adult neurogenesis, and within new niches, may indeed be required to more robustly acknowledge why evolution has maintained selective zones of neurogenic plasticity in the CNS while others remain incapable of such feats.

1.8 Comparative Models of Adult Neurogenesis

The adult neurogenesis field has progressed over the years in large part by studying mammalian models. Most popular have been rodent models, although some work in primates has also been explored. There is good reason for this. Most importantly, by studying mammals, by essence, we are learning how this trait behaves in humans. By learning how to harness the potential of ANSCs under homeostasis and with stimulation, the promise of aiding human neurodegenerative diseases is grand (Doetsch and Scharff, 2001; Lie et al., 2004; Emsley et al., 2005). In line with this, a number of debilitating neurodegenerative diseases present within forebrain, olfactory bulbs, and hippocampal structures, sites of constitutively active levels of neurogenesis (Eriksson et al., 1998; Hamilton et al., 2010; Curtis et al., 2012; Marxreiter et al., 2013). Moreover, rodent

models were among the first to show potential evidence of this trait during Altman's work in the 1960s, and these animals were among those in which adult neurogenesis was finally proven in the 1990s. Mammalian models have been paramount in teaching us about the fundamental properties of adult neurogenesis in the forebrain, and have a rich future for what they can offer, especially from a therapeutic perspective. However, it would be narrow-minded to think that all niches are constructed, regulated, and modulated the same as what mammalian studies have revealed. Thus, in order to expand our biological understanding of the potential diversity of this trait, different model systems and novel neurogenic compartments must be inspected.

The animal kingdom consists of approximately 1.5 million known species. These species have taken up or evolved within nearly every ecological niche known to man, and have developed a formidable array of behavioural specializations. We thus have at our disposal the best tool afforded to any researcher interested in uncovering how a biological trait has emerged and functions - species diversity. Undoubtedly this could be achieved with only a subset of representative species. What is concerning is that at present our understanding of adult neurogenesis rests on studies of no more than a few dozen species worldwide (Fig. 1-1A-C). Moreover, with the large majority of adult neurogenesis labs examining this process in mammals, we have subconsciously come to expect that how neurogenesis precedes in a rodent model for instance, characterizes this biological trait. The fact is that at present, we don't know how it occurs in many other species. Thus, the extent of shared and/or divergent characteristics of adult neurogenesis among animals still remains largely unexplored. The purpose of this section is to provide a synopsis of invertebrate and vertebrate species that have been examined for the presence of adult neurogenesis within the brain, the location of their niches, and what they have taught us to date.

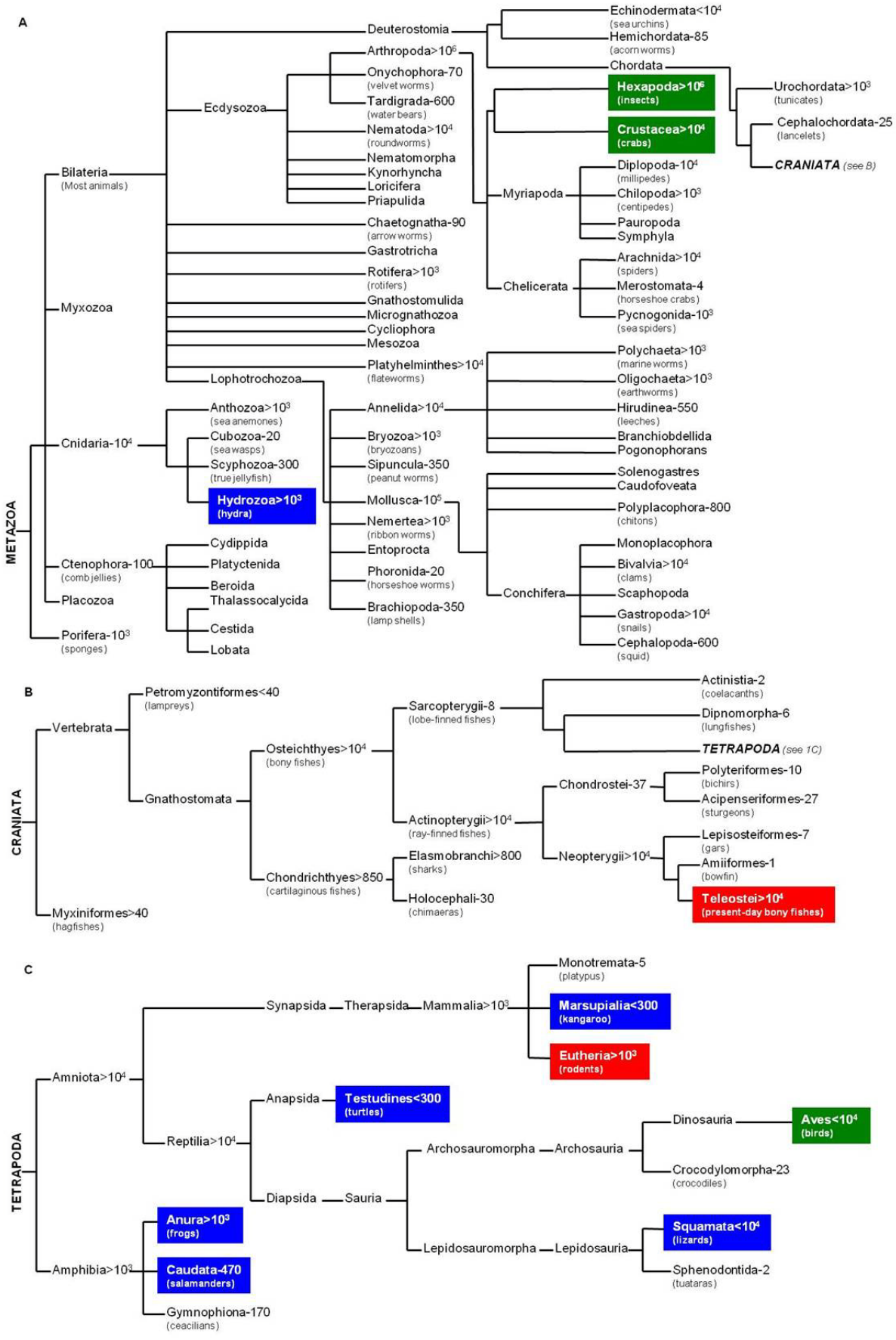
A
METAZOA
Bilateria
(Most animals)
Myxozoa
Cnidaria-10^4
Ctenophora-100
(comb jellies)
Placozoa
Porifera-10^3
(sponges)
Deuterostomia
Ecdysozoa
Lophotrochozoa
Echinodermata<10^4
(sea urchins)
Hemichordata-85
(acorn worms)
Chordata
Urochordata>10^3
(tunicates)
Cephalochordata-25
(lancelets)
CRANIATA (see B)
Arthropoda>10^6
Onychophora-70
(velvet worms)
Tardigrada-600
(water bears)
Nematoda>10^4
(roundworms)
Nematomorpha
Kynorhyncha
Loricifera
Priapulida
Chaetognatha-90
(arrow worms)
Gastrotricha
Rotifera>10^3
(rotifers)
Gnathostomulida
Micrognathozoa
Cycliophora
Mesozoa
Platyhelminthes>10^4
(flatworms)
Hexapoda>10^6
(insects)
Crustacea>10^4
(crabs)
Myriapoda
Diplopoda-10^4
(millipedes)
Chilopoda>10^3
(centipedes)
Pauropoda
Symphyla
Chelicerata
Arachnida>10^4
(spiders)
Merostomata-4
(horseshoe crabs)
Pycnogonida-10^3
(sea spiders)
Anthozoa>10^3
(sea anemones)
Cubozoa-20
(sea wasps)
Scyphozoa-300
(true jellyfish)
Hydrozoa>10^3
(hydra)
Cydippida
Platyctenida
Beroida
Thalassocalycida
Cestida
Lobata
Annelida>10^4
Bryozoa>10^3
(bryozoans)
Sipuncula-350
(peanut worms)
Mollusca-10^5
Nemertea>10^3
(ribbon worms)
Entoprocta
Phoronida-20
(horseshoe worms)
Brachiopoda-350
(lamp shells)
Polychaeta>10^3
(marine worms)
Oligochaeta>10^3
(earthworms)
Hirudinea-550
(leeches)
Branchiobdellida
Pogonophorans
Solenogastres
Caudofoveata
Polyplacophora-800
(chitons)
Conchifera
Monoplacophora
Bivalvia>10^4
(clams)
Scaphopoda
Gastropoda>10^4
(snails)
Cephalopoda-600
(squid)
B
CRANIATA
Vertebrata
Myxiniformes>40
(hagfishes)
Petromyzontiformes<40
(lampreys)
Gnathostomata
Osteichthyes>10^4
(bony fishes)
Chondrichthyes>850
(cartilaginous fishes)
Sarcopterygii-8
(lobe-finned fishes)
Actinopterygii>10^4
(ray-finned fishes)
Elasmobranchi>800
(sharks)
Holocephali-30
(chimaeras)
Actinistia-2
(coelacanths)
Dipnomorpha-6
(lungfishes)
TETRAPODA (see 1C)
Chondrostei-37
Neopterygii>10^4
Polyteriformes-10
(bichirs)
Acipenseriformes-27
(sturgeons)
Lepisosteiformes-7
(gars)
Amiiformes-1
(bowfin)
Teleostei>10^4
(present-day bony fishes)
C
TETRAPODA
Amniota>10^4
Amphibia>10^3
Synapsida
Therapsida
Mammalia>10^3
Monotremata-5
(platypus)
Marsupialia<300
(kangaroo)
Eutheria>10^3
(rodents)
Reptilia>10^4
Anapsida
Testudines<300
(turtles)
Diapsida
Sauria
Archosauromorpha
Archosauria
Dinosauria
Aves<10^4
(birds)
Crocodylomorpha-23
(crocodiles)
Lepidosauromorpha
Lepidosauria
Squamata<10^4
(lizards)
Sphenodontida-2
(tuataras)
Anura>10^3
(frogs)
Caudata-470
(salamanders)
Gymnophiona-170
(ceacilians)

Figure 1-1. Cladogram showing the phylogenetic relationship among Metazoans (A), Craniates (B) and Tetrapods (C) and the taxonomic groups in which adult neurogenesis has been confirmed. Blue 1 to 5 species; Green 6-10 species; Red: > 10 species. The approximate number of species and common names are identified for the dominant groups. Note that the majority of investigations examining the presence of adult neurogenesis have taken place in tetrapode vertebrates (**C**) with the exception of teleost fishes (**B**), while invertebrates (**A**) remain largely unexplored. Cladistic lineages were constructed based on information from *The Tree of Life web project* (1995-2004). Species numbers were compiled from Ruppert and Barnes (1996), Burnie and Wilson (2001), Moyle and Cech (2004), and Pechenik (2005).

1.8.1 Neurogenesis in Adult Invertebrates

Invertebrates have received little attention with respect to adult neurogenesis in comparison to their vertebrate counterparts. Our understanding of this biological trait stems primarily from two major invertebrate groups: insects and crustaceans. Crickets have long been the leading insect model (Cayre et al., 1994, 1996; Scotto-Lomassese et al., 2000, 2002; 2003; Malaterre et al., 2002; Cayre et al., 2005; 2007; Ghosal et al., 2009), although a small number of other insect species have been examined (Nordlander and Edwards, 1970; Technau, 1984; Ito and Hotta, 1992; Fahrbach et al., 1995; Booker et al., 1996; Cayre et al., 1996; Dufour and Gadenne, 2006); Lin et al., 2013). Laboratory studies of adult neurogenesis in crustraceans have for the most part, been limited to a variety of species of crab (Harzsch and Dawirs, 1996; Schmidt, 1997; Schmidt and Harzsch, 1999; Hansen and Schmidt, 2001, 2004; Sullivan and Beltz, 2005; Schmidt, 2007B), crayfish (Sullivan and Beltz, 2005; Sullivan et al., 2007; Song et al., 2007; 2009; Zhang et al., 2009; Ayub et al., 2011; Beltz et al. , 2011; Sintoni et al., 2012; Chaves da Silva et al., 2012; 2013) and lobster (Harzsch et al., 1999; Schmidt, 2001; 2007A; 2007B; Schmidt and Derby, 2011). Convincing evidence of continuous neurogenesis in adult hydrozoans (Phylum: Cnidaria) has also been presented (Sakaguchi et al., 1996; Miljkovic-Licina et al., 2004), but little work has followed this up since. To this end, reviews on the common properties of neurogenesis in the adult brain of invertebrates and vertebrates (Cayre et al., 2002; Lindsey and Tropepe, 2006; Brand and Livesey, 2011; Sandman et al., 2011) are less represented compared to reviews that focus solely on adult neurogenesis in vertebrates (Alverez-Buylla and Lois, 1995; Scharff, 2000; Doetsch and Scharff, 2001; Zupanc, 2001A; Alvarez-Buylla et al., 2002; García-Verdugo et al., 2002; Mackowiak et al., 2004; Abrous et al., 2005; Chapouton et al., 2007; Kaslin et al., 2008; Grandel and Brand, 2013).

Cnidarians have commonly gone unnoticed during comparative studies of adult neurogenesis; however, this organism may be among the first to possess this trait as a mechanism for neuronal replacement (Sakaguchi et al., 1996). Considering that the phylum Cnidaria is believed to possess the first organized CNS, the identification of neurogenic compartments in such an ancestral system provides an ideal starting point for elucidating the evolutionary origin of this trait (Holland, 2003; Miljkovic-Licina et al., 2004). The gastric region has been reported as the primary neurogenic niche in the adult hydra (Class: Hydrozoa). Here, large interstitial stem cells

become committed to a neuronal fate following cell division (Sakaguchi et al., 1996). Although the size of adult animals remains constant, during adulthood neurons and epithelial cells are lost to the extremities by sloughing off or to developing buds. Thus, it is crucial that a system of continuous neurogenesis is present in the hydra to replace those neurons lost and to maintain functionality in the gastric region. However, beyond preliminary characterizations of this neurogenic zone in adult hydra, we still have no information concerning how it is intrinsically regulated or whether environmental modulation is possible.

More species of insects have been examined for the presence of neurogenic niches than any other group of invertebrates (Nordlander and Edwards, 1970; Technau, 1984; Ito and Hotta, 1992; Cayre et al., 1994, 1996; Fahrbach et al., 1995; Booker et al., 1996; Scotto-Lomassese et al., 2000, 2002; 2003; Malaterre et al., 2002; 2003; Cayre et al., 2005; 2007; Dufour and Gadenne, 2006; Ghosal et al., 2009; Lin et al., 2013). These studies have established that the mushroom bodies (corpora pedunculata) are the major neurogenic niche in adults (Fig. 1-2; insect). Mushroom bodies are present in the phylum Annelida, and all arthropod groups with the exception of crustaceans (Strausfeld et al., 1998). Mushroom bodies are considered the dominant integrative centre for multimodal inputs from the antennae, the eyes, and the palpae, and are comprised of Kenyon cells and differentiated neuropils (Cayre et al., 1996, 2002; Malaterre et al., 2002). Therefore, multiple forms of external stimuli can impose structural changes in the adult mushroom bodies. Studies have shown sensory enrichment or deprivation in the form of olfactory or visual stimuli can regulate adult neural stem cell proliferation (Scotto-Lomassese et al., 2000; 2002). Additionally, sensory impairment has been shown to shorten the cell cycle, whereas juvenile hormone promotes quiescent neuroblasts to re-enter the cell cycle (Cayre et al., 2005). More recently, social status and agonistic behaviour have also been implicated in enhanced survival of newborn neurons in the mushroom bodies of crickets (Ghosal et al., 2009). Support for a potential role in learning and memory has also led to the comparison of the mushroom bodies with the hippocampus of mammals (Strausfeld et al., 1998). Indeed studies have shown that suppression of adult neurogenesis impedes olfactory learning and memory in the cricket (Scotto-Lomassese et al., 2003). The studies mentioned above portray that many of the same types of internal and external modulators of adult neurogenesis in vertebrate models also affect stages of adult neurogenesis in the niche of insect mushroom bodies.

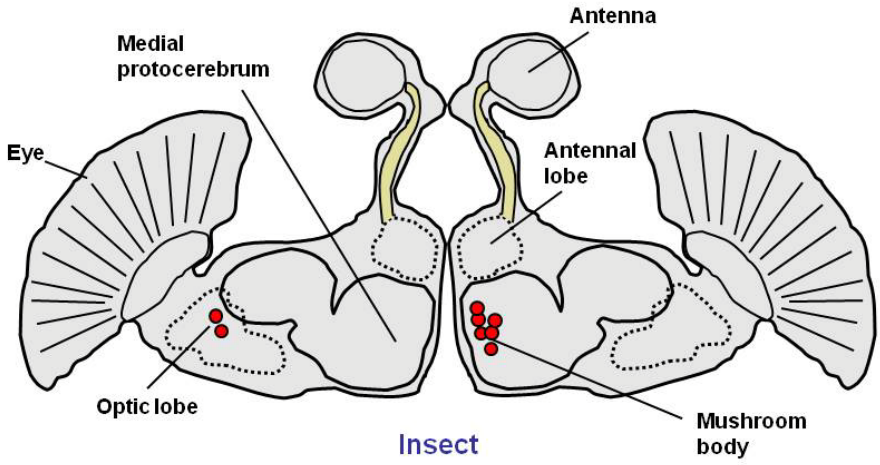
Antenna
Medial protocerebrum
Eye
Antennal lobe
Optic lobe
Mushroom body

Insect

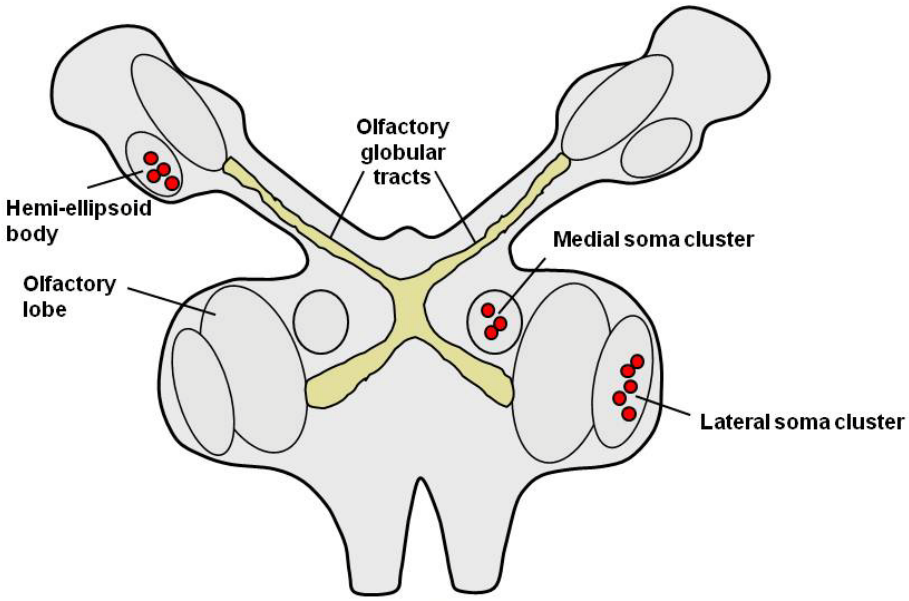
Olfactory globular tracts
Hemi-ellipsoid body
Medial soma cluster
Olfactory lobe
Lateral soma cluster

Crab

Figure 1-2. Schematic representation of neurogenic niches in two representative invertebrate models. Relative positions of neurogenic zones are demarcated by red dots. Overall brain size, size of brain subregions and size of neurogenic zones are not drawn to scale. Schematics are adapted from Sullivan and Beltz (2005), and Cayre et al. (2002).

In adult decapod crustaceans, neurogenesis is a continuous process occurring within the optic lobes (Schmidt, 1997; Sullivan and Beltz, 2005) and cell types of the central olfactory pathway (Schmidt and Harzsch, 1999; Schmidt, 2001; Schmidt, 2002). However, among the approximately nine different species examined to date, evidence for adult neurogenesis in the central olfactory pathway has been most consistently observed (Fig. 1-2; crab), although the specific soma clusters in which constitutive neurogenesis occurs varies among taxa (Beltz et al., 2005; Schmidt, 2007). Adult-born neurons take on phenotypes of both local and projection interneurons that innervate the olfactory and accessory lobes (Chaves da Silva et al., 2012). Since most decapod crustaceans continue to grow throughout adult life, an overall net increase in olfactory sensory neurons persists over adulthood, which is paralleled by a life-long addition of neurons in the central olfactory pathway (Schmidt, 1997; Sandeman et al., 1998). Additionally, in the adult shore crab active progenitor populations have been identified in the soma clusters of the hemi-ellipsoid bodies in the adult shore crab (Hansen and Schmidt, 2001; Schmidt, 2001); with this structure suggested to be homologous to the insect mushroom bodies, acting as the multimodal integration centre in crustaceans (Strausfeld et al., 1998).

Work in crayfish has shown that the stem cell niche of crustaceans is not a closed system, and that the source of adult stem cells do not reside within the niche itself, but is replenished from the hematopoeitic system (Beltz et al., 2011; Noonin et al., 2012; Chaves da Silva et al., 2013). Here, neuronal stem cells appear to be encapsulated by a number of stereotypical, small, glial-like cells (Schmidt, 2007). Following division, these cells give rise to local precursor cells within each soma cluster that reside within a proliferation zone. Ultrastructural characterization of first-generation precursors located on the ventral surface of the brain of the central olfactory pathway has shown that similar to vertebrates, a heterogeneous mixture of cells types are present (Types I-IV), and that similar to studies in mammals, the niche is highly vascularised (Chaves da Silva et al., 2012). Moreover, detailed electron microscopy examination of the cytoarchitecture of the niche of the spiny lobster has further revealed the composition of the neurogenic complex, including both the proliferation zone and the neural stem cell clump which houses a single adult neuroblast (Schmidt and Derby, 2011). At the level of cellular modulation, physiological rates of neurogenesis can undergo changes in response to age, season, captivity and the social environment (Sandeman and Sandeman, 2000; Hansen and Schmidt, 2004; Song et al., 2006; 2007), similar to most other models of adult neurogenesis.

Studies of adult neurogenesis in insect (i.e. crickets) and crustacean (i.e. crayfish, crab, lobster) models have made significant progress over the last decade. In fact, the number of studies examining these models has likely exceeded studies of neurogenesis in amphibian or reptile species. In both invertebrate groups, many properties displayed in vertebrate models of adult neurogenesis have been elucidated, including components of cellular composition of the niche and how environmental enrichment is able to modulate stages of neurogenesis in the niche. Where data is lacking in these models are questions investigating the internal regulation of the niche and the functional significance of newborn neurons. However, outside of these popularized invertebrate models, major gaps continue to exist in the literature. As a consequence, we are presented with a fragmented picture of the extent of neurogenic niches, their regulation, and function across these species. This is surprising since the biology of neural stem cells is not that different between invertebrate and vertebrate animals (Brand and Livesey, 2011), and with this in mind, one would expect more laboratories to pursue questions of adult neurogenesis and plasticity in a wider range of invertebrate species than has occurred. In particular, little work has focused on echinoderms, molluscs, and protochordates. These latter two groups exemplify more highly evolved nervous systems, with protochordates leading to present-day vertebrates. Given their taxonomic position, the identification of neurogenic zones in the vertebrate-like nervous system of transitional forms, such as cephalochordates, is crucial to understanding the phylogenetics underlying this trait.

1.8.2 Neurogenesis in Adult Vertebrates

Research on traditional vertebrate models continues to dominate the literature, comprised foremost of detailed studies of rodents (Altman and Das, 1965; 1966; Altman, 1963; 1966; 1969; Kaplan and Hinds, 1977; Bayer et al., 1982; Corotto et al., 1993; 1994; Seki and Arai, 1995; Kuhn et al., 1996; 1997; Rietze et al., 2000; Liu and Martin, 2003; Maslov et al., 2004; Bain et al., 2004; Baeur et al., 2005; Segovia et al., 2006; Mak et al., 2007; Ibi et al., 2008; Leasure and Decker, 2009; Kannangara et al., 2009; Oboti et al., 2009; Oomen et al., 2009; Veena et al., 2009; Epp et al., 2009; Mak and Weiss, 2010; Clark et al., 2010; Brummelte and Galea, 2010; Stone et al., 2010; McCormick et al., 2011; Spritzer et al., 2011; Portillo et al., 2012; Walton et al., 2012; Hamson et al., 2013; Glasper and Gould, 2013), and songbirds (Goldman and

Nottebohm, 1983; Nottebohm, 1985; Alverez-Buylla and Nottebohm, 1988; Alverez-Buylla et al., 1990; Nottebohm and Alverez-Buylla, 1993; Barnea and Nottebohm, 1994; Nottebohm, 2002A, 2002B; Margotta and Caronti, 2005; Barnea, 2009; Thompson and Brenowitz, 2009; Barnea and Pravosudov, 2011; Thompson et al., 2012). Mammalian research has also been extended to the brains of New and Old World primates (McDermott & Lantos, 1990; Gould et al., 1998; 1999B; Kornack and Rakic, 1999, 2001; Bernier et al., 2002; Koketsu et al., 2003; Ngwenya et al., 2006; Perera et al., 2012; Allen et al., 2013; Miller et al., 2013) and postmortem humans (Eriksson et al., 1998; Kukekov et al., 1999; Bédard and Parent, 2004; Sierra et al., 2011; Wang et al., 2012; Marxreiter et al., 2013). In the last 15 years, adult neurogenesis in the brain of select reptilian species has also been investigated (García-Verdugo et al., 1989; Perez-Sanchez et al., 1989; Pérez-Cañellas and García-Verdugo, 1996; Pérez-Cañellas et al, 1997; Font et al., 2001; Marchioro et al., 2005; Delgado-Gonzales et al., 2011; Font et al., 2012). Conversely, despite early experiments describing the localization of adult neurogenic niches in frogs and salamanders dating back to 1968, contemporary publications on amphibian adult neurogenesis continue to be intermittent (Minelli and Quaglia, 1968; Graziadei and Metcalf, 1971; Richter and Kranz, 1981; Mackay-Sim and Patel, 1984; Bernocchi et al., 1990; Polenov and Chetverukhin, 1993; Dawley et al., 2000; 2006; Simmons et al., 2008; Berg et al., 2011; Almli and Wilczynski, 2012). More than any other vertebrate group, the number of studies on teleostean fishes has steadily increased over the past 10 years, with species such as the zebrafish, and more recently cichlids, emerging as prominent models, renowned for their robust neurogenic and regenerative capacity throughout the adult nervous system (Zupanc and Zupanc, 1992; Zupanc and Horschke, 1995; Byrd and Brunjes, 1995; 1998, 2001; Zupanc et al., 1996; Marcus et al., 1999; Maeyama and Nakayasu, 2000; Zikopoulos et al., 2000; Ekström et al., 2001; Zupanc, 2001B; Zupanc et al., 2005; Adolf et al., 2006; Grandel et al., 2006; Zupanc, 2006; Ampatzis and Dermon, 2007; Hinsch and Zupanc, 2007; Pelligrini et al., 2007; Topp et al., 2008; Kaslin et al., 2009; Lam et al., 2009; Zupanc et al., 2009; Alunni et al., 2010; Kuroyanagi et al., 2010; Ito et al., 2010; Ganz et al., 2010; von Krogh et al., 2010; Strobl-Mazzulla et al., 2010; Chapouton et al., 2010; 2011; Marz et al., 2010; 2011; Rothenaigner et al., 2011; Kroehne et al., 2011; Kishimoto et al., 2011; 2012; Lindsey et al., 2012; Ampatzis et al., 2012; Kizil et al., 2012A, 2012B; Maruska et al., 2012; 2013; Schmidt et al., 2013; Kaslin et al., 2013).

Neurogenesis in the adult mammalian forebrain continues to lead the field in terms of the volume of publications and the breadth of questions studied. These studies are based on two well defined neurogenic niches: the subependymal zone (SEZ), a layer of cells surrounding the ependymal lining of the lateral ventricles, and the subgranular zone (SGZ) in the dentate gyrus of the hippocampus (Fig. 1-3; rodent). Constitutive neurogenesis within the SEZ and SGZ provides new granule-type neurons to the olfactory bulb via the rostral migratory stream (RMS) and to the dentate gyrus, respectively, which mature primarily into GABAergic inhibitory neurons (Zhao et al., 2008). Pioneering work depicting the detailed ultrastructural characterization of these niches has showcased that both neurogenic compartments are composed of a heterogeneous population of cells, many of which are identifiable lineage descendents of adult neural stem cells (Type B, SEZ; Type I, SGZ; Doetsch et al., 1997; Seri et al., 2004; Kriegstein and Alverez-Buylla, 2009). Though rodent models are most pronounced in the literature, studies of non-human primates and post mortem humans have been performed, and at the level of the cellular organization of the niche revealed some notable differences (Doetsch et al., 1997; Gil-Perotin et al., 2009; Kam et al., 2009; Sawamoto et al., 2011).

Both the SEZ and SGZ have undergone detailed marker analysis depicting the timeline of cellular migration and the phenotype of progenitor cells as they take on a committed neuronal fate (reviewed in Ming and Song, 2005; Zhao et al., 2008). Likewise, the influence of the external environment and social interactions has been well documented. At the functional level, neuronal addition or replacement in the SGZ is intimately linked with a role in learning and memory (Gould et al., 1999A; van Praag et al., 1999B; Koehl and Abrous, 2011). However, recent examination of the hippocampus of ceteceans (e.g. whales, dolphins, and porpuses) reveal a relatively small structure lacking adult hippocampal neurogenesis in this group of mammals, implying that this trait may not be as widespread as once believed (Patzke et al., 2013). By contrast, the role of newly differentiated neurons incorporated into the olfactory bulbs from the SEZ is less obvious, but in rodents appears to be related to relevant forms of olfactory behaviors and learning (Alonso et al., 2006; Mak et al., 2007; Mouret et al., 2008; Mak and Weiss, 2010). Additionally, debate continues concerning the presence of an adult RMS in humans by which chain migration of progenitor cells born in the SEZ arrive in the olfactory bulb (Sanai et al., 2004; Curtis et al., 2007; Kam et al., 2009; Sanai et al., 2011; Wang et al., 2011; Brus et al., 2013). We are now entering an era where questions directed towards the genetic and molecular

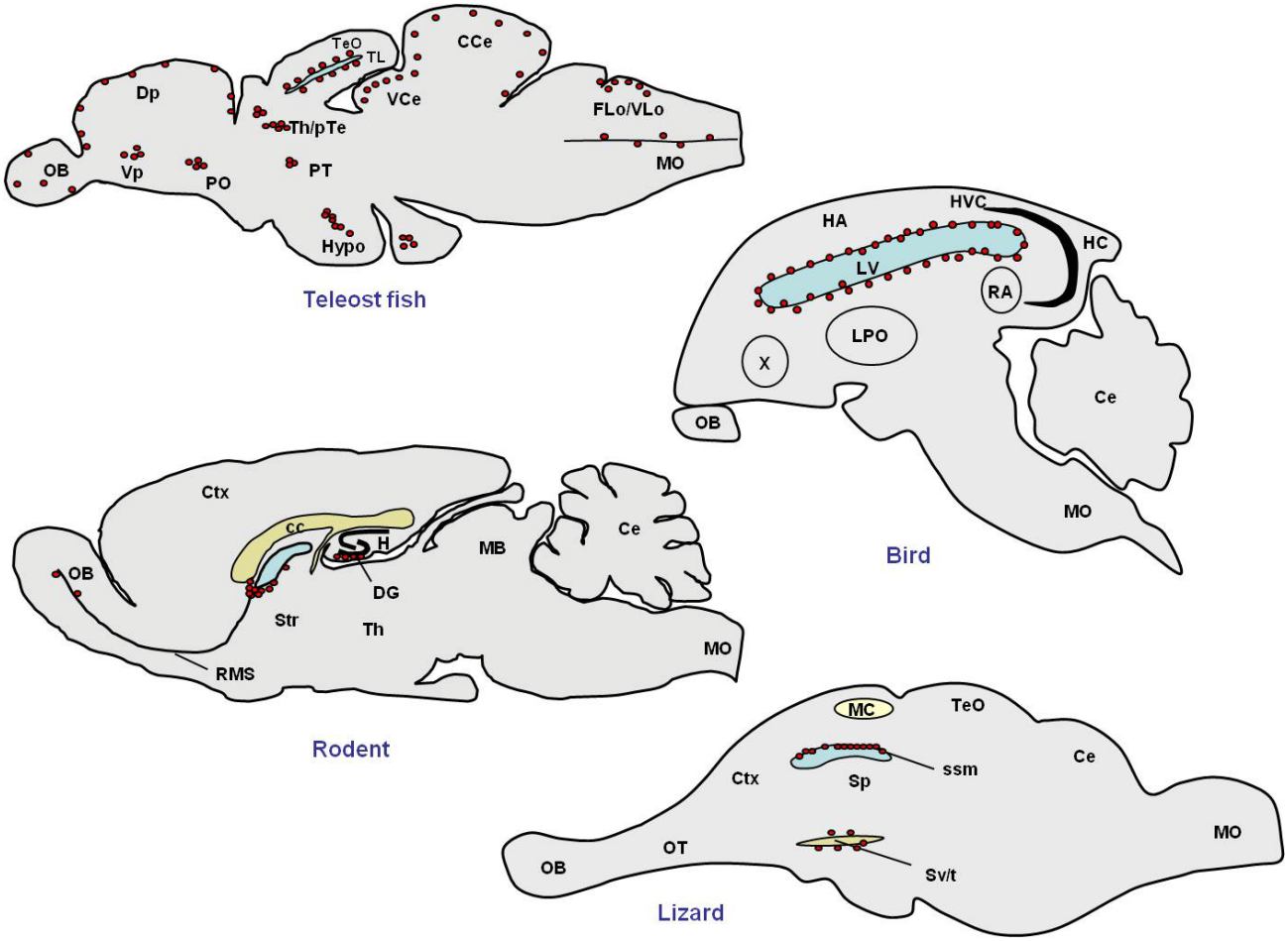
TeO
TL
CCe
Dp
VCe
FLo/VLo
Th/pTe
OB
Vp
PO
PT
MO
Hypo
Teleost fish
HVC
HA
HC
LV
RA
LPO
X
Ce
OB
MO
Bird
Ctx
cc
H
MB
Ce
OB
DG
Str
Th
MO
RMS
Rodent
MC
TeO
Ce
Ctx
Sp
ssm
MO
OT
OB
Sv/t
Lizard

Figure 1-3. Schematic representation of neurogenic niches in four representative vertebrate models. Relative positions of neurogenic zones are demarcated by red dots. Overall brain size, size of brain subregions and size of neurogenic zones are not drawn to scale. Schematics are adapted from Font et al. (2001), Doetsch and Scharff (2001), and Wullimann (1998). Abbreviations: ***Teleost fish***; OB, olfactory bulb; Vp, ventral pallium; Dp, dorsal pallium; PO, preoptic area; Hypo, hypothalamus; PT, posterior tuberculum; Th/pTe, thalamus/pre-tectum; TeO, optic tectum; TL, torus longitudinalis; VCe, valvula cerebelli; CCe, corpus cerebelli; FLo/VLo, facial lobe/vagal lobe; MO, medulla oblongata. ***Lizard***; OB, olfactory bulb; OT, olfactory tract; Ctx, isocortex; MC, medial cortex; Sp, subpallium; ssm, sulcus septomedialis; Sv/t, sulcus ventralis/terminalis; TeO, optic tectum; Ce, cerebellum; MO, medulla oblongata. ***Bird***; OB, olfactory bulb; X, area X; LPO, lobus parolfactorius; LV, lateral ventricle; RA, robust nucleus of the archistriatum; HVC, high vocal center; HC, hippocampal complex; HA, hiperpallium accessorium; MO, medulla oblongata; Ce, cerebellum. ***Rodent***; OB, olfactory bulb; Ctx, isocortex; RMS, rostral migratory stream; Str, striatum; cc, corpus callosum; Th, thalamus; DG, dentate gyrus; HC, hippocampal complex; MB, midbrain; Ce, cerebellum; MO, medulla oblongata.

control of these niches are being uncovered (Overall et al., 2012; Miller et al., 2013). Addressing the genetic regulation of the niche and how to manipulate it will be critical for future therapeutic applications of ANSCs.

In addition to mammals, songbirds have played a pivotal role in our understanding of adult neurogenesis, sparked initially by the work of Fernando Nottebohm in the 1980s (Goldman, 1998). Detailed investigations of adult neurogenesis in the avian CNS have principally focused on canaries and zebra finches as models for studying the song control system (Nottebohm et al., 1982; Paton and Nottebohm, 1984; Scharff and Nottebohm, 1991; Scharff et al., 2000; Nottebohm, 2002B; Nottebohm, 2005; Andalman anf Fee, 2009; Nottebohm and Liu, 2010), though the black-capped chickadee has gained popularity for investigating hippocampal-dependent spatial memory during food caching (Sherry and Vaccarino, 1989; Sherry et al., 1989; Barnea and Nottebohm, 1994; Clayton, 1998; Hoshooley and Sherry, 2004; Hoshooley et al., 2007; Sherry and Hoshooley, 2009; Barnea and Pravosudov, 2011). Across avian models a single neurogenic niche has been observed residing in the ventricular ependyma lining the lateral ventricles of the forebrain (Fig. 1-3; bird; Goldman and Nottebohm, 1983; Nottebohm, 1985, 2002A; Alvarez-Buylla and Nottebohm, 1988; Alverez-Buylla et al., 1990; Nottebohm and Alvarez-Buylla, 1993; Barnea and Nottebohm, 1994; Rousselot et al., 1997; Goldman, 1998; Chen and Goldman, 2013). From different geographical positions along the ventricular ependyma, ANSCs of radial morphology give rise to migrating neuroblasts destined for the higher vocal center (HVC), the mammalian hippocampal homologue, the hippocampal complex (HC), as well as other target structures (Alvarez-Buylla and Nottebohm, 1988; Alvarez-Buylla et al., 1990; Barnea and Pravosudov, 2013).

Within the stem cell niche the greatest activity of ANSCs occurs in the ventral aspect of the ventrolateral wall and, to a lesser extent, in the dorsolateral tip of the wall (García-Verdugo et al., 2002). The HVC is linked to the anterior forebrain pathway responsible for song learning and the motor pathway, responsible for song production (Nottebohm et al., 1982; Scharff and Nottebohm, 1991; Scharff et al., 2000; Nottebohm, 2005; Andalman and Fee, 2009). Mature neurons that survive in the HVC, become anatomically and functionally integrated into the song control system (Paton and Nottebohm, 1984). In songbirds, physiological rates of adult neurogenesis are induced by seasonal changes in systemic testosterone levels, with increases in

this hormone leading to the expansion of the HVC as a consequence of upregulation of neuronal birth and recruitment. Since only males produce new songs during the breading season to attract potential mates, conspicuous sexual dimorphism in the size of the HVC between male and female songbirds is observed at this time of year (Nottebohm and Arnold, 1976). Recently, by examining seasonal changes in gene expression between the HVC and RA (i.e. an associated song control nucleus), researchers have been able to define different molecular programs that regulate seasonal changes in both structures (Thompson et al., 2012). Seasonal changes also promote neurogenic plasticity in the HC (Clayton, 1998). Studies show that during the season when food storing is most abundant, this structure is considerably enlarged do to the recruitment of newborn neurons to function for later retrieval (Smulders et al., 1995; Hoshooley and Sherry, 2007). The same trend is seen in species of migratory birds, which utilize the HC for spatial memory (LaDage et al., 2011). Finally, similar to most other models of adult neurogenesis studied to date, the social environment of birds also plays a direct role in neuronal addition to multiple brain regions (Lipkind et al., 2002; Barnea et al., 2006).

Similar to their avian relatives, reptiles contain only one primary neurogenic niche during adulthood housing actively dividing stem/progenitor cells. Proliferation in the adult reptilian brain follows a pattern similar to embryonic brain development with the niche localized adjacent the lateral ventricular walls (Fig. 1-3; lizard; García-Verdugo et al., 1989; Perez-Sanchez et al., 1989; Pérez-Cañellas and García-Verdugo, 1996; Pérez-Cañellas et al., 1997; Font et al., 2001; Peñafiel et al., 2001; Marchioro et al., 2005; Delgado-Gonzales et al., 2011). Within this region, the greatest intensity of neuronal proliferation exists in the medial cortex of the telencephalon, believed to be homologous to the dentate gyrus in the hippocampus of mammals (Alverez-Buylla and Lois, 1995; Cayre et al., 2002; García-Verdugo et al., 2002; Nacher et al., 2002; Marchioro et al., 2005). Inside the medial cortex, the sulcus septomedialis has been compared with the ‘hot spot’ in the ventricular walls of birds (Font et al., 2001; García-Verdugo et al., 2002). Within the medial cortex, nearly 14% of all new neurons are generated in the medial cortex periventricular zone of the lacertid lizard (Font et al., 2001).

In one of the few studies examining the common garter snake, neurogenic niches have also been observed in the adult vomeronasal epithelium, as seen in the red-backed salamander (Wang and Halpern, 1988; Dawley et al., 2000). The vomeronasal system in these animals is highly specialized for the chemosensory detection of molecules, such as prey chemicals and

pheromones (Halpern and Martinez-Marcos, 2003). To date the most detailed studies of reptilian adult neurogenesis have been limited to lacertid lizards and a single species of turtle (García-Verdugo et al., 1989; Perez-Sanchez et al., 1989; Pérez-Cañellas and García-Verdugo, 1996; Pérez-Cañellas et al., 1997; Font et al., 2001; Font et al., 2012). Studies in the turtle have shown that the majority of cells born at the ventricular lining migrate rostrally to populate the olfactory bulbs, and recently it has been proposed that this may be linked with olfactory mediated behaviours of lizards in general (Font et al., 2011). Moreover, studies of natural populations of lizards showed that rates of cell proliferation occurring at the ventricular wall and the migration of differentiating progeny varied with season, particularly in regions related to olfaction (Delgado-Gonzales et al., 2011). A stunning finding of this study was that newborn neurons were not detected until 90-days post BrdU injection, raising the question of why the differentiation process is slowed in this species compared to most other vertebrate where newborn neurons are already identifiable in less than a week.

Of all major groups of vertebrates, amphibians are least understood in the context of adult neurogenesis. Investigations of amphibian models have established that select neurogenic niches do exist in species of salamanders, axolotls and frogs in the main olfactory epithelium, preoptic area, and forebrain periventricular zone, with clear species-specific differences (Graziadei and Metcalf, 1971; Richter and Kranz, 1981; Mackay-Sim and Patel, 1984; Bernocchi et al., 1990; Polenov and Chetverukhin, 1993; Dawley et al., 2000; 2006; Simmons et al., 2008; Almli and Wilczynski, 2012). Less common have been reports of neuronal generation in the vomeronasal epithelium and optic tectum of some species of salamanders and newts (Minelli and Quaglia, 1968; Dawley et al., 2000; 2006). A recent detailed analysis of cell proliferation and neuronal differentiation in the adult bullfrog, showed that $BrdU^+$ cells were located adjacent the ventricles throughout the neuroaxis, with dominant niches including domains surrounding the telencephalic ventricle, within the dorsal and ventral hypothalamus, preoptic area, optic tectum, and torus semicircularis (Simmons et al., 2008). A subpopulation of proliferating $BrdU^+$ cells across structures were shown capable of both gliogenesis and neurogenesis. Though few studies have begun to probe questions concerning the functional regulation and plasticity of these niches, work in frogs have highlighted that changes in proliferation rates in the preoptic nucleus of females can be induced with exposure to males independently of gonadal steroid levels (Almli and Wilczynski, 2012), while proliferative activity within the hypothalamus may be important in

mediating reproductive behaviours (Simmons et al., 2008). With the discovery that some amphibian species harbour generally widespread proliferation zones throughout the brain, as in the case of the bullfrog, developing our knowledge of adult neurogenesis in these species for comparisons with other vertebrates with robust neurogenic capacities (i.e. teleosts), would allow us to address whether similar molecular programs and cellular phenotypes are present between homologous niches.

Teleost fishes are renowned for housing the greatest number of neurogenic niches within the CNS of any vertebrate Class, with many of these bordering the brain ventricles (Fig. 1-3; teleost fish; Zupanc and Zupanc, 1992; Zupanc and Horschke, 1995; Zupanc et al., 2005; Lindsey and Tropepe, 2006; Adolf et al., 2006; Grandel et al., 2006; Zupanc, 2006; Chapouton et al., 2007; Kaslin et al., 2008; Lindsey et al., 2012; Maruska et al., 2012). The most frequently cited explanation for the occurrence of this trait is that bony fishes have indeterminate growth, and therefore the majority of brain and sensory structures continue to enlarge by the addition of newborn neurons with senescence (Zupanc, 1999; 2006; Kaslin et al., 2008). However, this argument is not without flaws. First, in general indeterminate growth of the brain, or at least brain subregions, is not an exclusive property of teleosts. Some species of rodents have been shown to have an increasing number of granule cell neurons in the hippocampus with age (Amrein et al., 2004A), meaning that new neurons are not simply functioning to replace others. Second, not all fish species exhibit indeterminate growth, especially with regards to increasing muscle mass with age, which is a hallmark feature of indeterminate growth. For example, two species of the cyprinid genus *Danio*, the zebrafish (*Danio rerio*) and the giant danio (*Danio aequipinnatus*), exhibit distinct larval and adult muscle growth patterns. Whereas the giant danio exhibits indeterminate muscle growth and maintain responsiveness to growth promoting hormones as adults, adult zebrafish reach a growth plateau as they mature (Biga and Goetz, 2006). Therefore, while neurogenesis may have a positive allometric relationship to continued brain growth in some teleosts, the relative contribution of adult neurogenesis to adult brain growth in those animals remains to be confirmed. With numerous niches situated in higher-order brain structures of the forebrain as well as within primary sensory processing regions, there is good reason to postulate that pools of actively dividing progenitors have been maintained in teleosts to contribute a biologically functional role besides only passive growth.

Neurogenic niches have been identified in nearly all brain regions of teleosts examined using detailed mapping studies. One of the earliest reports came from experiments using the brown ghost knifefish (*Apteronotus leptorhynchus*), and revealed proliferating cells in over 100 different brain regions with over 100 000 new cells produced in any given 2-hour period (Zupanc and Zupanc, 1992; Zupanc and Horschke, 1995). Since then, this finding has been further validated by in depth analyses of at least seven additional species reporting adult cycling populations capable of giving rise to differentiated neurons in all major subdivisions of the CNS (integrative and sensory structures), most notably in the zebrafish, three-spinned stickleback, medaka, and more recently in species of cichlids (Kirsche, 1967; Zupanc and Horschke, 1995; Zupanc et al., 1996, 2005; Maeyama and Nakayasu, 2000; Byrd and Brunjes, 1998, 2001; Ekström et al., 2001; Adolf et al., 2006; Grandel et al., 2006; Zupanc, 2006; Kuroyanagi et al., 2010; Lindsey et al., 2012; Maruska et al., 2012). Though proliferative populations span the entire rostrocaudal axis of the brain, major sites of adult neurogenesis have been delineated in the cerebellum, where approximately 75% of all newborn cells are generated (Zupanc and Horschke, 1995; Zupanc et al., 1996, 2005; Zupanc, 1999, 2001B; Ekström et al., 2001; Kaslin et al., 2009; 2013), as well as in the telencephalic pallium and subpallium, and within the caudal optic tectum (Kirsche, 1967; Alonso et al., 1989; Zupanc and Zupanc, 1992; Zupanc and Horschke, 1995; Nguyen et al., 1999; Zikopoulos et al., 2000; Ekström et al., 2001; Zupanc, 2005, 2006; Adolf et al., 2006; Grandel et al., 2006; Chapouton et al., 2007; Kaslin et al., 2008; Alunni et al, 2010; Ito et al., 2010; Lindsey et al., 2012; Grandel and Brand, 2013).

With the rise of teleost fishes in the adult neurogenesis field, we have begun to uncover how this biological trait progresses across a number of different adult niches. However, most intensely studied have been the periventricular neurogenic niches of the adult telencephalon, likely as a result of putative homologies between these niches and the pallial and subpallial niches of mammals (Broglio et al., 2005; Wullimann, 2009). These studies have revealed that radial glial cells are the most likely stem/progenitor candidate in several of these neurogenic zones (Ganz et al., 2010; Marz et al., 2010), but at present there has yet to be a detailed ultrastructural study examining the composition of niches bordering the forebrain ventricles, or any other niche for that matter. Likewise, with the exception of a small number of studies examining the effect of social status on rates of cell proliferation in cichlids (Maruska et al., 2012; 2013), how environmental enrichment, sensory stimulation, or the absence of these modulates forebrain and

sensory neurogenic niches is unknown. This is in direct contrast to the vast number of studies examining these same questions in alternative vertebrate models, as well as with insects and crustaceans. Moreover, our understanding of the intrinsic regulation of adult neurogenesis by circulating hormones, growth factors, and signalling pathways has only recently begun to develop (Adolf et al., 2006; Topp et al., 2008; Chapouton et al., 2010; 2011; Ganz et al., 2010; de Oliveira-Carlos et al., 2013; Hochmann et al., 2013). In the proceeding chapters of my thesis (Chapters 2-4), I shed light on several of these questions, by examining the cellular composition of forebrain and sensory neurogenic niches, how stages of adult neurogenesis are modulated by sensory enrichment or deprivation, and how signalling pathways such as Fibroblast Growth Factor (FGF) signalling may be involved in mediating constitutive levels of adult neurogenesis in the zebrafish brain.

1.9 The Zebrafish as a Model of Adult Neurogenesis

Over the last 10 years, the adult zebrafish has emerged as a tractable vertebrate for the study of adult neurogenesis and an excellent complement to more established mammalian and avian models. There are four compelling reasons for this. First, zebrafish maintain greater than 50 neurogenic niches along the entire rostrocaudal axis capable of producing newly differentiated neurons (Zupanc et al., 2005; Hinsch and Zupanc, 2007). These niches are present in a wide variety of anatomical structures, including numerous forebrain regions as well as within primary sensory processing structures of the brain. Additionally, several telencephalic niches in the zebrafish have been proposed to be homologous to structures in the mammalian brain (Salas et al., 2006; Wullimann, 2009; Lau et al., 2011), opening the door for comparative studies of how the adult neurogenic niche may be differentially regulated between species. These include the lateral zone of the dorsal telencephalon (i.e. hippocampus); the medial zone of the dorsal telencephalon (i.e. amygdala); and the dorsal and ventral zones of the telencephalon (i.e. striatum). Neurogenic niches residing within primary sensory structures in the olfactory bulbs, the optic tectum, and the vagal and facial lobes also provide a unique opportunity to exam how the process of adult neurogenesis within sensory structures beyond the olfactory bulbs of mammals are controlled. Second, in recent years, many molecular tools and transgenesis techniques have become available in the zebrafish that are no longer only limited to early

development. Such tools allow for the identification and lineage tracing of adult stem/progenitor populations (Solek and Ekker, 2012), heatshock inducible (and conditional) lines allowing inhibition or activation of signalling pathways or temporal regulation of specific cell types (Lee et al., 2005; Hans et al., 2009; 2011), and cerebroventricular microinjection assisted knockdown using morpholino oligonucleotides to examine loss- of-function or for site-specific infusion of growth factors (Kizil and Brand, 2011).

A third reason zebrafish have become a popular model of adult neurogenesis, is that they exhibit a number of complex social behaviours similar to amniotes (Gerlach et al., 2008; Saverino and Gerlai, 2008; Spence et al., 2008; Miller and Gerlai, 2011). For this reason, the effects of changes in the social environment as well as learning paradigms can be assessed in the context of adult neurogenesis. To this end, reports have shown that zebrafish can undergo olfactory conditioning in respond to L-type amino acids (Braubach et al., 2009) as well as visual discriminatory learning (Coldwill et al., 2005). Lastly, zebrafish are easily maintained and produce a large number of externally fertilized embryos with a single mating (~200), with fish rapidly reaching maturity by 3-4 months (Lawrence, 2007; Nasiadka and Clark, 2012). The precocial nature of zebrafish allow animals to be raised in complete isolation following fertilization, unlike the situation in mammals, and thus how developmental isolation may impinge on neurogenesis compared with exposure at adulthood can be directly compared across a variety of neurogenic niches. These species-specific traits, along with many recently developed molecular tools positions the zebrafish as an invaluable model of adult neurogenesis.

1.10 Thesis Objective and Aims

The objective of my PhD research was to comparatively investigate how the process of adult neurogenesis between forebrain and sensory niches of the mature zebrafish (*Danio rerio*) brain are composed at the cellular level and modulated by external environmental changes and internal mechanisms. My research consisted of three aims.

I. To characterize specific forebrain and sensory neurogenic niches under physiological conditions by examining cellular phenotypes, cell cycle kinetics, cellular ultrastructure, and rates of neuronal differentiation.

II. To investigate how different forms of environmental enrichment or deprivation can regulate constitutive levels of adult neurogenesis by studying environmental changes and modality-specific sensory stimulation.

III. To examine the role of the hormone cortisol and Fibroblast Growth Factor (FGF) signalling in regulating stages of adult neurogenesis under constitutive and experimental conditions.

CHAPTER 2

THE CELLULAR COMPOSITION OF NEUROGENIC PERIVENTRICULAR ZONES IN THE ADULT ZEBRAFISH FOREBRAIN

2.1 Abstract

A central goal of adult neurogenesis research is to characterize the cellular constituents of a neurogenic niche and to understand how these cells regulate the production of new neurons. Since the generation of adult-born neurons may be tightly coupled to their functional requirement, the organization and output of neurogenic niches may vary across different regions of the brain or between animals. Here, I have undertaken a comparative study between six (*D, Vd, Vv, Dm, Dl, Ppa*) periventricular zones (PVZ) harbouring proliferative cells present in the adult forebrain of the zebrafish (*Danio rerio*); a species known to possess widespread neurogenesis throughout life. Using electron microscopy I have documented for the first time the detailed cytoarchitecture of these zones, and propose a model of the cellular composition of pallial and subpallial PVZs, and a classification scheme for identifying morphologically distinct cell types. Immunolabeling of resin embedded tissue confirmed the phenotype of three constitutively proliferating ($BrdU^+$) cell populations, including an $S100\beta^+/GS^+$ radial glial-like (Type IIa) cell. Moreover, my data revealed rostrocaudal differences in the density of distinct proliferative populations and cumulative labeling studies suggested that the cell cycle kinetics of these populations are non-uniform between PVZs. While common among most PVZs the peak numbers of differentiated neurons were generated after ~2 weeks, the number of newborn neurons declined in some regions after 4 weeks time. My data suggest that the cytoarchitecture of neurogenic niches and the tempo of neuronal production are regionally distinct in the adult zebrafish forebrain.

2.2 Introduction

Adult neurogenesis occurs in well circumscribed regions of the mature vertebrate brain. This process is initiated by the proliferation of stem and/or progenitor cells, which over time generate new neurons and glia. Adult neurogenesis is regulated, in part, through the interaction between neurogenic cells and neighbouring cells that are present within their immediate microenvironment, or niche. Moreover, the niche itself may be largely unique in terms of its cellular composition, degree of plasticity, and the molecular factors maintaining it as an active site of adult neurogenesis in different regions of the brain or at different times during development. For instance, studies in the adult rodent brain show differences in the time course of neuronal differentiation, and the neuronal subtypes that arise from the subependymal zone (SEZ) of the forebrain lateral ventricles or the subgranular zone (SGZ) of the hippocampal dentate gyrus (reviewed in Zhao et al., 2008). These findings support the notion of niche-specific regulation at the cellular and molecular levels. Despite significant advances using rodent models, many non-mammalian vertebrates offer the opportunity to explore the regulation and composition of the neurogenic niche in both homologous structures as well as within novel neuroanatomical loci where this trait is absent in mammals (Zupanc, 2001A). Understanding how adult neurogenic niches are differentially regulated across vertebrate species will be an essential step in gaining a fundamental understanding of the functional significance of this conserved trait (Lindsey and Tropepe, 2006).

Studies of the mouse SEZ and SGZ niches have been seminal in constructing a detailed model of the cellular organization of the adult neurogenic niche and continue to serve as a basis for comparison as the stem cell niche of additional animals are described (Doetsch et al., 1997; Seri et al., 2004). Serial reconstructions of the SEZ using electron microscopy have demonstrated the presence of five main cell type within this niche: GFAP expressing neural stem cells (Type B1), astrocytes (Type B2), transiently amplifying progenitor cells likely committed to a neuronal fate (Type C), and migrating neuroblasts (Type A), all of which reside beneath a continuous layer of ependymal cells (Type E) that lines the ventricle (Doetsch et al., 1997). Subsequent experiments confirmed that Type B1 astrocytic cells were the resident adult neural stem cell within the SEZ niche (Doetsch et al., 1999). Functional evidence supporting this view has come from studies using transgenic mice expressing herpes-simplex virus thymidine kinase (tk) from the glial

fibrillary acidic protein (GFAP) promoter that were exposed to the antiviral agent ganciclovir, resulting in the selective ablation of dividing tk expressing cells (Sofroniew and Vinters, 2010). *In vitro* analysis of the cell lineage progression from Type B cells to Type A following ablation of GFAP expressing cells showed the loss of stem cell derived neurospheres, revealing the relationship and sequential dependence of the cell types within the niche upon one another (Morshead et al., 2003). The cellular composition of the hippocampal SGZ has similarly been described, demonstrating a lineage originating from radial glia-like stem cells through an intermediate proliferative stage (Type D1) giving rise to committed neuronal progenitors (Type D2) that over time differentiate into immature granule interneurons (Type D3; Seri et al., 2001; 2004; Steiner et al., 2006). More recently, the importance of the proximity of vasculature to cell types within the niche for trophic support has been highlighted (Tavazoie et al., 2008); in particular for Type B1 cells that have been shown to extend a process onto centrally localized blood vessels (Mirzadeh et al., 2008).

It has become clear that pronounced differences exists in the organization of the SEZ niche of vertebrates. This is true even among mammalian species arising from different Orders. The SEZ of macaques, marmosets, and humans all possess a structurally distinct three-layer organization, comprising a continuous ependymal lining adjacent the lateral ventricles, a middle hypocellular GAP layer, and a lateral-most astrocyte-ribbon layer (Gil-Perotin et al., 2009; Kam et al., 2009; Sawamoto et al., 2011). The hypocellular layer is absent in rodents however, and thus far appears to be restricted to primates, although the significance of this layer remains unknown. Variations in cell types have also been observed. For instance, unlike the SEZ of most mammalian species studied, no type C cells were detected in the macaque SEZ (Gil-Perotin et al., 2009), a finding more closely related to the proliferative ventricular zone of reptiles and birds. Moreover, tanycytes present in neurogenic niches have only been reported in rodents (Doetsch et al., 1997). Studies of the periventricular zone of reptiles and birds have revealed that despite the fact that anatomically homologous cell types comprise the wall of the lateral ventricle, these non-mammalian neurogenic niches lack Type C cells and are generally characterized by the absence of a continuous layer of ependymal cells in contrast to mammals (Perez-Sanchez et al., 1989; Perez-Canalles et al., 1997; Font et al., 2001; Garcia-Verdugo et al., 2002). Furthermore, both humans and all other mammalian species studied share an SEZ and possibly a rostral migratory stream (Kam et al., 2009), while thus far this appears to be absent in birds and reptiles. Given the

differences identified between the SEZ of mammalian and non-mammalian animals to date, it is likely that niche organization and the cell-cell interactions that together determine its neurogenic capacity demonstrate significant variation among species.

Within the last decade the zebrafish (*Danio rerio*) has gained popularity as a model for adult neurogenesis owing to its robust neurogenic capacity throughout the mature brain. Early work revealed that numerous different neuroanatomical regions across the CNS harbour mitotic cell populations (Zupanc et al., 2005), and more recently that nearly 50% of these cells differentiate to give rise to newborn adult neurons (Hinsch and Zupanc, 2007). A number of these proliferative niches are localized within distinct neuroanatomical regions adjacent to the brain ventricles (periventricular zone) similar to rodents, birds, and reptiles (Garcia-Verdugo et al., 2002). Within the forebrain, two regions surrounding the telencephalic ventricle have been suggested to be homologues to the hippocampus and amygdala of the mammalian forebrain (Wullimann and Rink, 2002; Salas et al., 2006), making the zebrafish an attractive model from a comparative standpoint.

The periventricular zone (PVZ) of the adult zebrafish includes several of the most active sites of neurogenesis throughout the forebrain. Separate studies have highlighted a strong dichotomy between the pallial and subpallial division of the rostral half of the adult forebrain in both glial phenotypes and the expression of various transcription factors of developmental importance. These studies have revealed that the PVZ is endowed with both slow and fast cycling cell populations, arising from a radial glia-like adult neural stem/progenitor cell (Adolf et al., 2006). Most recently, a classification scheme based on detailed immunohistochemical (Marz et al., 2010) and clonal analysis (Rothenaigner et al., 2011) has presented three types of cycling progenitor cells, Types II, IIIa and IIIb, as well as a non-dividing glial Type I cell (Marz et al., 2010). Moreover, the pallial-subpallial divisions of rostral forebrain PVZs has illustrated that progenitors express, and may be regulated by, different transcription and growth factors such as fibroblast growth factors (Adolf et al., 2006; Ganz et al., 2008; Topp et al., 2010). Nevertheless, despite a growing number of studies examining adult zebrafish telencephalic forebrain PVZs, we are still far from understanding some of the most fundamental questions, including the anatomical boundaries of these neurogenic compartments, their ultrastructural composition and how this cellular organization might differ between distinct pallial and subpallial PVZs within the same species. The many sites of continuous neurogenesis in the zebrafish brain offer the

opportunity to consider whether the composition and maintenance of the niche is governed by a set of similar cellular components or whether niche-specific environmental differences play a role in the neurogenic output of the niche.

The present study investigates the cellular composition of six distinct neurogenic PVZs in the adult zebrafish forebrain. Using a combination of immunohistochemistry, scanning and transmission electron microscopy, I reveal the detailed cellular organization of these zones. Additionally, I examine differences in the cell cycle kinetics of niche-specific proliferative populations and compare the timeline of neuronal differentiation for each. The results reported here are compared with recent immunohistochemical studies documenting the putative progenitor cells within the adult zebrafish forebrain in order to broaden our understanding of the phenotype of cells composing these neurogenic PVZs. My results provide a foundation for comparative studies of the cellular regulation between different neurogenic niches.

2.3 Methodology

2.3.1 Animals

Adult wildtype (AB) zebrafish (*Danio rerio*) of both sexes were obtained from our laboratory population and housed in a recirculation system (Aquaneering Inc.) under a 14:10 light-dark cycle at 28˚C. All water chemistry parameters (pH, conductivity, nitrate, ammonia) were monitored daily. Fish were between 9-12 months old and fed a diet of granular food (ZM Medium; ZM Ltd.) and brine shrimp. Zebrafish were sacrificed using an overdose of 0.4% Tricaine methanesulfonate until all movement and respiration ceased. Immediately thereafter, the sex, total length (mm) and weight (g) of each fish was determined. Measurements from ~ 200 zebrafish yielded an average total length of 33.92 ± 2.56 mm and an average weight of 0.413 ± 0.136 g. Handling procedures were done in accordance with the policies set forth by the University of Toronto and the Canadian Council for Animal Care (CCAC).

2.3.2 BrdU Administration

Animals were anaesthetized in a solution of 0.04% Tricaine diluted in facility water until movement and respiration slowed, then injected intraperitoneally with a 10 mM bolus of bromodeoxyuridine (BrdU; Sigma) diluted in 1X-Phosphate Buffered Saline (PBS) at a volume of 50 μL/g body weight fish (Zupanc et al., 2005) to detect proliferating cells in the S-phase of the cell cycle. Following injection, fish were monitored in a recovery tank until respiration and swimming returned to normal, then transferred back to their housing tank until sacrifice.

2.3.3 Brain Perfusion and Fixation

Following sacrifice, animals were transcardially perfused through the ventricle of the heart to clear blood from brain vasculature and improve tissue fixation. For immunohistochemistry (IHC) on cryosectioned tissue, ice-cold 1X-PBS was perfused using a Model II Plus Syringe Pump (Harvard Apparatus, MS, USA) until all effluent was clear, followed by 10 mL of ice-cold 4% paraformaldehyde (PFA) diluted in PBS. For transmission (TEM) and scanning (SEM) electron

microscopy, ice-cold 0.1 M Sorenson's phosphate buffer (pH = 7.4) was perfused followed by 10 mL of either 3% gluteraldehyde (GLUT) for ultrastructural analysis, or 0.1% GLUT/4% PFA for immuno-TEM labeling (EM grade, Electron Microscopy Science). Thereafter, the braincase was removed and tissue placed in fresh fixative for 3 hours at 4˚C, after which time the brain was excised and placed in fresh fixative overnight at 4˚C. For all electron microscopy analyses the forebrain was separated from midbrain at the level of the rostral optic tectum before being placed in fixative. For SEM analysis, forebrain hemispheres were additionally separated along the midline for visualization of the medial ventricular surface.

2.3.4 Cryosectioning

Brain tissue was cryoprotected in ascending sucrose solutions before being placed in 30% sucrose overnight at 4˚C. Tissue was infiltrated with a 2:1 solution of 30% sucrose: O.C.T. Compound (Tissue-Tek, Sakura, USA) for 30 min at room temperature, before being cryo-embedded *en bloc* at -20˚C. Brains were serially sectioned at 20 μm intervals using a Leica Cryostat (Model CM3050), and sections collected onto Superfrost Plus slides (VWR), and stored at -80˚C until IHC labeling.

2.3.5 Immunohistochemistry

Cryosections were briefly post-fixed in 4% PFA, blocked for 1 hour and incubated in primary antibody overnight at 4˚C (Table 2-1). For BrdU labeling, antigen retrieval was performed by immersing sections in 10 mM sodium citrate buffer for 30 min at 65˚C and incubating in 1 M hydrochloric acid for 1 hour at 37˚C to denature the double-stranded DNA. For HuCD and γ-tubulin labeling, antigen retrieval was carried out by incubating sections in 50 mM Tris Buffer (pH 8.0) for 30 min at 65˚C. The next day, sections were incubated in one of the following Alexa Fluor conjugated secondary antibody (Jackson ImmunoResearch) for 2 hours at 37˚C: Goat-anti-rat, goat-anti-mouse, goat-anti-rabbit Cy3 (1:400) or Cy2 (1:200). Nuclear staining was performed using a 1% solution of Hoechst 33258 applied to sections for 15-20 min. All double-labeling protocols were performed sequentially and brain sections mounted in 100% glycerol for imaging.

2.3.6 Primary Antibody Characterization

2.3.6.1 Anti-BrdU

The mouse (Roche Diagnostics) and rat (Serotec) monoclonal anti-BrdU antibodies label the nucleus of cells in the S-phase of the cell cycle, by recognizing BrdU incorporated into single-stranded DNA, attached to a protein carrier, or free BrdU (manufacturer's technical information; Wang et al., 2006; Silvestroff et al., 2010). Both antibodies have been shown to successfully label the nuclear profile of $BrdU^+$ mitotic cells in the adult zebrafish brain (Adolf et al., 2006; Grandel et al., 2006; Ganz et al, 2010). Rat anti-BrdU does not cross-react with thymidine but does react weakly with chlorodeoxyuridine, while mouse anti-BrdU shows minimal cross-reactivity with iodouridine (manufacturer's technical information). Positive labeling of both antibodies was originally tested in zebrafish gut tissue, an area shown to be highly proliferative (Crosnier et al., 2005), before pursuing IHC labeling in the adult forebrain. Negative controls using non-BrdU-injected zebrafish or by omitting the primary antibody, showed no $BrdU^+$ labeling in the brain. Based on the above, I was confident that anti-BrdU only labeled nuclei incorporating BrdU into newly synthesized, single-stranded DNA.

2.3.6.2 Anti-HuCD

The anti-human neuronal protein HuC/HuD (HuC/D) monoclonal antibody was raised against the human HuD peptide QAQRFRLDNLLN (Marusich et al., 1994). The Hu antigen is an RNA-binding protein of the embryonic lethal abnormal visual (Elav) family, that is specific to neuronal proteins of the Elav family members HuC, HuD, and Hel-N1 and is expressed most intensely in the perikaryal region of neurons but can also be detected in neuronal nuclei (Yang et al., 2010; Marusich et al., 1994; manufacturer's technical information). Numerous studies of the zebrafish brain have employed this marker to identify resident and newly derived populations of neuronal cells (Zupanc et al., 2005; Grandel et al., 2006; Pelligrini et al., 2007; Topp et al., 2008; Zupanc et al., 2009; Rothenaigner et al., 2011).

Table 2-1. Primary antibodies used for immunohistochemical labelling

Name	Immunogen	Manufacturer (cat. #)	Host	Type	Dilution	Target Phenotype
Bromodeoxyuridine (BrdU)	BU1/75 (ICR1) - clone	Serotec (MCA2060)	Rat	Monoclonal (IgG2a)	1:1000	All dividing cells in S-phase
Bromodeoxyuridine (BrdU)	BMC 9318 - clone	Roche (11170376001)	Mouse	Monoclonal (IgG_1)	1:100	All dividing cells in S-phase
Anti-Human Neuronal Protein HuC/HuD (HuC/D)	Aa 240-251 of human HuD	Molecular Probes (16A11)	Mouse	Monoclonal ($IgG_{2b,k}$)	1:400	All neurons
Polysialic Acid Neural Cell Adhesion Molecule (PSA-NCAM)	Viable Meningococcus group B (strain 355)	Millipore (MAB5324)	Mouse	Monoclonal (IgM)	1:800	Newly differentiated migrating neurons
Glutamine Synthetase (GS)	Glutamine synthetase purified from sheep brain	Millipore (MAB302)	Mouse	Monoclonal (IgG_{2a})	1:800	Astrocytes/radial glia
S100β	S100 isolated from cow brain	Dako Cytomation (Z 0311)	Rabbit	Polyclonal	1:800	General glia, including ependyma
Calbindin D-28k	Purified rat calbindin D-28	SWANT (CB-38a)	Rabbit	Monoclonal	1:600	Calbindin containing neurons
Tyrosine Hydroxylase (TH)	Tyrosine hydroxylase purified from PC12 cells	Millipore (MAB318)	Mouse	Monoclonal ($IgG1_k$)	1:400	Adrenergic neurons
Pax-6	Peptide (QVPGSEPDMSQYWPRLQ) derived from the C-terminus of the mouse Pax-6 protein	Covance (PRB-278P)	Rabbit	Polyclonal	1:100	Stem/ progenitor cells
SOX-2	Synthetic peptide corresponding to amino acids 113-127 of human, mouse and rat SOX-2	StemCell Technologies (01438)	Rabbit	Polyclonal	1:400	Stem/progenitor cells
γ-tubulin (tubg1)	Recombinant protein fragment containing a sequence corresponding to a region within amino acids 3-154 of tubg1	GeneTex (GTX124352)	Rabbit	Polyclonal	1:500	Ciliary basal bodies

2.3.6.3 Anti-PSA-NCAM

The anti-polysialic acid-neural cell adhesion molecule (PSA-NCAM) monoclonal antibody detects a single band of 180 kDA (Rougon et al., 1986). PSA is a long, linear homopolymer that is attached to NCAM, and displays the greatest level of expression in precursor cells during early development and is known to promote their migration following cell division (manufacturer's technical information). PSA-NCAM has been shown to be a reliable marker for the detection of young, migrating neurons in the post-natal and adult brain of mammals (Seki and Arai, 1995; Doetsch et al., 1999), and more recently the mature forebrain of zebrafish (Adolf et al., 2006; Chapoutin et al., 2010; Marz et al., 2010).

2.3.6.4 Anti-GS

The anti-GS (glutamine synthetase) monoclonal antibody was purified from sheep brain and its enzymatic activity makes it an ideal marker of astrocytes (manufacturer's technical information). Additionally, glutamine synthetase is considered an important enzyme in the recycling of the neurotransmitter glutamate (manufacturer's technical information). Recently, glutamine synthetase has been documented in the periventricular zone of the adult zebrafish brain as a marker of radial glial cells (Grupp et al., 2010).

2.3.6.5 Anti-S100β

The anti-S100β polyclonal antibody labels S100β strongly, with little to no reactivity with other variants of S100 proteins tested based on Western blotting of purified human recombinant S100 proteins (manufacturer's technical information). S100 is a multigene family of low molecular weight calcium-binding proteins, comprising 19 members that are differentially expressed in a large number of cell types, with S100β being most abundant in glial cells of the central and peripheral nervous system (manufacturer's technical information). Anti-S100β has been used as a general glial marker (Wainwright et al., 2004) in the proliferation zones of the adult zebrafish brains, and I obtain a similar pattern of labeling as shown previously during *in vivo* and *in vitro* studies (Grandel et al., 2006; Kaslin et al., 2009; Marz et al., 2010; Rothenaigner et al., 2011).

2.3.6.6 Anti-Calbindin

The anti-Calbindin monoclonal antiserum was produced against recombinant rat calbindin D-28k with this calcium binding protein recognized as a single band of approximately 27-28 kDa in immunoblots (manufacturer's technical information). The CB protein has been used as a reliable marker of subpopulations of neurons both in the enteric nervous system (Uyttenbroek et al., 2010) and in the adult brain (Zupanc et al., 2005; Castro et al., 2006) of zebrafish. Presently, only a predicted protein sequence is available for zebrafish calbindin D-28k (XP 001341604; http://www.ncbi.nlm.nih.gov; Uyttenbroek et al., 2010).

2.3.6.7 Anti-TH

The anti-tyrosine hydroxylase (TH) monoclonal antibody specifically recognizes an epitope on the outside of the regulatory N-terminus, and is used to identify neuronal subpopulations having dopaminergic or noradrenergic phenotypes (manufacturer's technical information). The pattern of immunostaining seen in my study is in agreement with previous labeling studies of TH immunoreactive cells in the vertebrate forebrain (Grandel et al., 2006; Dimitrov and Usdin, 2010).

2.3.6.8 Anti-Pax6

The anti-Pax6 polyclonal antibody was generated from the peptide sequence QVPGSEPDMSQYWPRLQ derived from the C-terminus of the mouse Pax6 protein and purified on a peptide affinity column (manufacturer's technical information; Roesch et al., 2008). The peptide sequence is highly conserved among Pax6 of various species, making this a useful marker for studying cell populations in the brain during early and postnatal development (manufacturer's technical information). The *Pax6* gene encodes a transcription factor that contains a paired-domain and a homeodomain, and is involved in peripheral and CNS development and has been shown to be expressed in stem/progenitor cells (Sakurai and Osumi, 2008). Pax6 is required for the multipotent state of retinal progenitor cells (Marquardt et al., 2001) and its expression pattern has been documented in the teleostean forebrain (Wullimann and Rink, 2002).

2.3.6.9 Anti-SOX2

The anti-SOX2 polyclonal antibody was generated using a synthetic peptide sequence corresponding to amino acids 113-127 of human, mouse and rat SOX-2, and is a useful marker for the detection of undifferentiated neural cells in the central nervous system, which have stem cell-like characteristics (manufacturer's technical information). This marker has been previously used to successfully examine populations of neural stem/progenitor markers in the developing and adult mouse brain within the SGZ of the dentate gyrus (Tseng et al., 2010).

2.3.6.10 Anti-γ-tubulin

The anti-tubg1 polyclonal antibody was derived from a recombinant protein fragment containing a sequence corresponding to a region within amino acids 3-154 of γ-tubulin (manufacturer's technical information). Zebrafish neurons and embryos were used as positive control tissue to confirm the expected labeling pattern of this antibody, localized specifically to the basal body of cilia similar to other γ-tubulin antibodies (Mirzadeh et al., 2008; 2010).

2.3.7 Demarcating Periventricular Zones (PVZ)

Many of the proliferative/neurogenic niches in the adult zebrafish forebrain are situated adjacent the telencephalic and diencephalic ventricles, and localized within a subregion of distinct neuroanatomical nuclei that line the lumen. The properties of these neurogenic compartments contain the trademark features of a typical adult neurogenic niche, namely resident proliferating cell populations that harbour the potential to give rise to adult born neurons. Since the zebrafish brain undergoes eversion during telencephalic hemisphere development (Wullimann and Rink, 2002) resulting in many neurogenic niches positioned next to the forebrain ventricles, in this study I will refer to each of the six niches under investigation as periventricular zones (PVZs). For example, a neurogenic niche present within the dorsal telencephalic area (D) would be referred to as the "PVZ of D".

To identify the PVZs in the adult zebrafish forebrain with the greatest density of proliferation, animals (N =10) were sacrificed 2 hours after a 10 mM injection of BrdU. Cryosections of the

forebrain between cross-sectional levels 50-107 of the adult zebrafish brain atlas (Wullimann et al., 1996) were immunostained to visualize BrdU. For each section, all $BrdU^+$ cells were counted within each region of the brain, and the resulting mean calculated by region across all brains. The number of $BrdU^+$ cells per forebrain region was compared statistically to determine regions with the greatest levels of cell proliferation. The localization of $BrdU^+$ cells in these regions in combination with ultrastructural observations of the position of morphologically distinct cell types were next used to demarcate the lateral aspect of PVZs opposite the ventricle, in order to obtain the total surface area of each. Surface area (μm^2) was calculated by tracing along the boundaries of each PVZ in maximum projection confocal images using Leica Application Suite Advance Fluorescence Lite 2.3.0 proprietary software. The mean number of $BrdU^+$ cells per PVZ at each rostrocaudal level was then normalized to the estimated total number of cells calculated in a separate set of age-matched animals ($N = 6$) stained with Hoechst 33258.

2.3.8 Cell Cycle Kinetics

Previous work has demonstrated the presence of both fast and slow proliferating cell populations in distinct neurogenic niches of the pallial and subpallial regions of the adult zebrafish telencephalon (Adolf et al., 2006). Here, a cumulative labeling protocol based on the method of Nowakowski et al. (1989) was used to examine in detail the cell cycle kinetics between anatomically defined neurogenic PVZs. This method has been successfully applied to in the SEZ of the adult mouse brain (Moshead and van der Kooy, 1992), the developing mouse brain (Kim and Shen, 2008), and most recently the zebrafish retina (Wong et al., 2010). By injecting BrdU at regular intervals over time and then using BrdU immunohistochemistry it is possible to determine the maximum labeling index LI_M (or growth fraction; GF), known as the proportion of cells that comprise the proliferating population, in addition to the corresponding time at which the maximum number of $BrdU^+$ cells are labelled (T_M), the length of the cell cycle (T_C), and the length of the DNA-synthesis phase (T_S). Two assumptions are made when using this protocol. First, the proliferative cells within each distinct PVZ are assumed to be a single population, asynchronously distributed across the various stages of the cell cycle. Second, each population is undergoing a steady-state growth phase.

Zebrafish 10 months of age were injected 1-7 times (*N* = 5/group) beginning at 08:00 with a 1 mM bolus of BrdU in 2-hour increments for up to 12 hours, and sacrificed 30 min following the last injection. For each injection group, the total number of $BrdU^+$ cells across 3-4 brain sections within the boundaries of each PVZ were counted and averaged across animals. Mean values at each time point were next plotted for each PVZ using GraphPad Prism 5.04 proprietary software to examine the line of best fit. The notion that after a finite number of BrdU injections all proliferating cells in the population should be labelled, resulting in the GF and the commencement of a plateau at which time no additional cells take up BrdU, suggests that the data should fit a one-phase exponential association model. However, given the toxicity effects of BrdU on cell survival with continuous exposure (Kee et al., 2002; Taupin, 2007A;B), in fitting these data, I considered that following the plateau phase of the curve, cell death may occur. Therefore, the preferred fit of my data to a first (linear) or second (quadratic) order polynomial using regression analysis by least squares fitting was compared for each PVZ using the above software. In cases where the preferred model was a linear regression, the last data point was considered the minimum GF, and this value used to estimate cell cycle parameters. In the event that neither model fit the data with confidence, the possibility of two distinct mitotic populations within the PVZ was investigated by fitting the data to a third order polynomial (cubic). Where a plateau could be observed, the first time point when the slope of the curve approached 0 was taken as the GF and the start of the plateau. All data points prior to and including the GF were then re-plotted to a linear regression to determine cell cycle parameters. Using the equations $slope = GF/T_C$, and $Tm=T_C-T_S$, I could then calculate T_C and T_S. For all graphs the 95% confidence interval bands are shown.

2.3.9 Immunohistochemical Experiments

For all sets of markers the percentage of co-labelled $BrdU^+$ cells to the total mitotic cell population sampled within each PVZ was quantified. A total of 4-6 animals were examined for each set of markers with the exception of qualitative observations made using markers for cilia and vasculature where 2-3 animals were used.

2.3.9.1 Characterization of Periventricular Zones (PVZs)

Immunohistochemistry was used to compare differences in the phenotype of mitotically active cell populations across PVZs, in addition to the presence of ciliated cells and vasculature. The phenotype of mitotic cells was examined 2 hours post-BrdU injection by double-labeling with BrdU and Pax6, S100β, GS, or HuCD antibodies. To identify cells displaying cilia along the ventricular surface, whole-mount preparations of forebrain hemispheres and cross-sectional images were labelled with γ-tubulin and counterstained with Hoechst 33258. A *Tg[flk1:gfp]* transgenic zebrafish line which specifically labels the endothelial cells of the vasculature was used to assess the presence of vessels within niches (A kind gift from Dr. Ian Scott, University of Toronto, Canada).

2.3.9.2 Neuronal and Glial Differentiation and Cell Migration

In order to track the time course of differentiation of $BrdU^+$ cells to mature neuronal or glial phenotypes between PVZs, I injected zebrafish with BrdU and sacrificed animals after 1, 2, or 4 weeks. To investigate the time course of $BrdU^+$ cell differentiation, I first examined the percentage of $BrdU^+$/PSA-$NCAM^+$ cells within PVZs 1 and 2 weeks after BrdU injection. Newly derived populations immunoreactive for BrdU/HuCD were investigated at all three time points (1, 2, and 4 weeks), in addition to a separate set of animals examined 2 hours post-BrdU injection that served as a negative control group. Four weeks post-BrdU injection the differentiated phenotype of $BrdU^+$ cells was assessed by IHC using the following sets of markers: BrdU/GS, BrdU/Calbindin, and BrdU/TH. A separate zebrafish transgenic line *Tg[dlx5a/6aIG:gfp]* ($N = 3$) was examined 10 months following a single pulse of BrdU to detect the presence of $BrdU^+$/dlx5a/6aIG^+ cell populations (A kind gift from Dr. Marc Ekker, University of Ottawa, Canada) The *Tg[dlx5a/6aIG:gfp]* transgene expression has been shown to mark GABAergic neurons within the embryonic and larval brain (MacDonald et al., 2010; Souza et al., 2011).

To next assess the migration of differentiating proliferative cells, the distance of $BrdU^+$ cells from the ventricle in individual PVZs was measured following 2 hour, 4 week, and 10 month chase periods using Leica Application Suite Advance Fluorescence Lite 2.3.0 proprietary

software. For each zone and time point, a minimum of six $BrdU^+$ cells were randomly sampled within each brain. Distance measurements were taken from the center of $BrdU^+$ nuclei to the edge of the ventricle or pial surface (Dl). In the PVZ of D, only $BrdU^+$ cells along the midline were measured.

2.3.10 Cell Counting and Imaging

All imaging of immunostained tissue was performed using a Leica TCS SP5 confocal microscope (Leica, Germany). For BrdU labeling alone, a minimum of every fourth section was examined through the rostrocaudal axis of the forebrain and all $BrdU^+$ cells were counted within each region of the brain. Cell counts for nuclear labeling of Hoechst 33258 and double-labeling experiments were sampled from a single hemisphere on a minimum of two separate cryosections within the boundaries of each PVZ from each biological sample at the respective rostrocaudal level. For all IHC labeling, z-stacks of 0.5-1 μm were created from 20 μm immuno-labelled cryosections at 40x (BrdU, Hoechst 33258) or 100x (double-labeling) magnification. Cell counting was done by counting through the z-stack using the optical dissector principle (West, 1999; Geuna, 2005) with Leica Application Suite Advance Fluorescence Lite 2.3.0 proprietary software. To confirm co-labeling of antibody markers, z-stacks taken at 100x magnification were further examined using orthogonal sectioning. All images shown are maximum projections, with the exception of images of orthogonal views used as evidence for co-labeling, and were adjusted for brightness and contrast using Adobe Photoshop 7.0 software.

2.3.11 Scanning Electron Microscopy

Scanning EM was performed to examine the ventricular wall *en face* for the presence of ciliated cells. Following perfusion and fixation, brain hemispheres ($N = 6$) were rinsed with 0.1 M Sorenson's phosphate buffer then dehydrated through an ascending ethanol series, before being infiltrated in a second ascending series of 100% ethanol and hexamethyldisilizane (HMDS) and placed in fresh HMDS overnight. Specimens were mounted on stubs and sputter coated with gold-palladium for 50 sec (Bal-Tec SCD050), then visualized with a Hitachi S-2500 scanning electron microscope and imaged using Quartz PCI software.

2.3.12 Transmission Electron Microscopy

Transmission EM was used to characterize the ultrastructural composition of PVZs. Following overnight fixation of forebrains (*N* = 7 D, Vd, Vv, Dm, Ppa; *N* = 4 Dl) in 3% GLUT, specimens were rinsed in 0.1 M Sorenson's phosphate buffer and post-fixed for 2 hours with 1% osmium tetroxide. Thereafter, tissue was rinsed and dehydrated through an ascending ethanol (ETOH) series, then infiltrated with an ascending series of 100% ETOH and Spurr's epoxy resin. The next day tissue was infiltrated with fresh Spurr's resin twice over a 6 hour period then flat embedded and polymerized at 65˚C overnight. Using a Leica EM UC6 ultramicrotome, 1 μm semithin sections and 100 nm ultrathin sections were taken at the corresponding rostrocaudal level of each PVZ. At each level semithin sections collected onto glass slides were stained with 0.035%Toluidine Blue/Methylene Blue diluted in methanol, while ultrathin sections where collected onto copper grids for TEM imaging. Ultrathin sections were stained with 3% uranyl acetate in 50% methanol for 45 min, followed by Reynold's lead citrate for 10 min, then dried overnight. Imaging was done using a Hitachi H-7000 transmission electron microscope and AMT Image Capture Engine Software (Version 5.44.599).

To first examine the overall ultrastructural organization of PVZs, low magnification TEM images (2-4K) were taken at rostrocaudal levels 60 (D, Vd, Vv), 85 (Dm), and 98 (Dl, Ppa). These images were used to mark the borders of each PVZ for subsequent analysis of cell types and cell frequencies between niches. For detailed morphological analysis of the different cell types composing PVZs, a minimum of three cells of each type having morphologically unique ultrastructural features, from each PVZ and across all forebrains were sampled. In instances where few cells of a given morphology could be observed within the confines of the PVZ, all cells identified were analyzed. To characterize cell types, the following features were examined: Nucleus - contour, color, chromatin organization, number of nucleoli, length of long and short axis of the nucleus (short axis taken at half the long axis); Cytoplasm - percentage, color, presence of mitochondria, cilia, microvilli, vacuoles, lipid droplets, dense bodies; Localization of cell types; Cell-cell contacts. Using these criteria, the morphological profile and frequency of each cell type within each PVZ and as a percentage of all cells examined was calculated. Based on the morphological features revealed, a model representing the cellular organization of PVZs and a classification scheme of the distinct cell types making up the different niches was established.

2.3.13 TEM Immunohistochemistry

To determine the molecular phenotype of cells identified at the ultrastructural level, two labeling protocols were employed. To identify proliferative cells and those having a glial phenotype, we injected zebrafish (*N* = 2) with a 10 mM bolus of BrdU twice over a 4 hour period, before processing the forebrain for embedding in LR White hydrophilic resin (EMS). In brief, tissue was washed in 0.1 M Sorenson's phosphate buffer following perfusion and fixation then dehydrated in an ascending ethanol series beginning with 70% ETOH at 4˚C and terminating in 100% ETOH at -20˚C. Tissue was next infiltrated in an ascending series of LR White: 100% ETOH over a two day period at -20˚C. Forebrains were then placed in a silicone mold filled with LR White and 0.5% benzoin methyl ether. The mold was covered with Aclar film and placed in a Leica automatic freeze substitution unit. The LR White was polymerized with UV light for 48 hours at -10˚C followed by 24 hours at 20˚C. At the corresponding level of each PVZ, 500 μm semithin sections were collected onto glass slides while 80 nm ultrathin sections were collected onto formvar coated nickel grids for subsequent IHC labeling.

For BrdU labeling, tissue was first pre-treated with 2 M HCl for 20 min to denature the double-stranded DNA. For post-embedding labeling of all antibodies, tissue was rinsed with distilled water and incubated in 1% Bovine Serum Albumin (BSA) for 30 min. Tissue was next incubated in mouse-anti-BrdU (1:20), rabbit-anti-S100 (1:160), or mouse-anti-GS (1:80) primary antibody diluted in incubation buffer for 1 hour. Thereafter, sections were incubated in the appropriate anti-mouse or anti-rabbit IgG secondary antibody conjugated to 10 nm gold diluted in incubation buffer for 2 hours. Tissue was then post-fixed in 2% GLUT for 10 min, stained with 2% aqueous uranyl acetate for 2.5 min, and finally stained with lead citrate for 30 sec. For each antibody, one set of grids was processed without primary antibody as a negative control, while in another set contrast staining was omitted to better visualize gold particles in positively labelled tissue. All imaging was done as described for TEM analysis.

To label neurons at the ultrastructural level, a pre-embedding protocol was used. This protocol was additionally employed to further assess cell types having a glial phenotype. Following fixation, forebrains (*N* = 6) were embedded *en bloc* in a 15% solution of agar. Tissue was cut into 80 μm thick sections through the rostrocaudal axis using a Leica Vibratome (VT12005) and floated onto ice-cold 1X-PBS buffer and stored at 4˚C until staining. Immunohistochemistry was

carried out using a mouse-anti-GS (1:100) or mouse-anti-HuCD (1:400) primary antibody in conjunction with an anti-mouse/rabbit, horseradish peroxidise (HRP)/3,3'-Diaminobenzidine (DAB) detection kit as per the manufacturers protocol (Abcam, ab64264). Labelled sections were then stored in 0.1 M Sorensen's phosphate buffer before processing with Spurr's resin for electron microscopy as described previously. Ultrathin sections were stained only with uranyl acetate for 20 min before TEM imaging.

All cell types positively labelled for specific markers were examined following both labeling protocols. The morphology of these cells was then correlated with my initial classification of the distinct cell types making up the different PVZs under investigation.

2.3.14 Statistical Analysis

All values are expressed as mean ± standard deviation. Differences in pairs of means were assessed using independent-samples t-tests. Multiple mean comparisons were validated using a one-way ANOVA, with Tukey's HSD post hoc tests applied when significance was present. Samples were considered significant at $p \leq 0.05$. All statistical analyses were performed using SPSS Statistics 17.0 and graphs created using SigmaPlot 11.0, Microsoft Excel 2003, or GraphPad Prism 5.04 proprietary software.

2.4 Results

2.4.1 Variation in the Relative Size of the Proliferative Population along the Rostrocaudal Axis Exists Within Distinct PVZs

To initially determine the most proliferative neuroanatomical regions of the adult zebrafish forebrain between rostrocaudal levels 50-107 (Wullimann et al., 1996), BrdU labeling was used to mark cells in the S-phase of the cell cycle following a single 2-hour BrdU injection. By counting dividing cells in 20 μm sections throughout the rostrocaudal axis of 11 different regions, I found six distinct loci having a significantly higher number of $BrdU^+$ cells than all others examined (one-way ANOVA, Tukey's HSD post hoc test), including D, Vd, Vv, Dm, Dl, and Ppa (Fig. 2-1A-C). Among these six regions, D had a significantly higher absolute number of $BrdU^+$ cells compared to other regions, localized within the rostral forebrain. The ventral nucleus of V (Vv) had the second greatest number of $BrdU^+$ cells and was significantly higher than Dm, where the least number of $BrdU^+$ cells were detected. Proliferating cell populations were localized adjacent the telencephalic (D, Vd, Vv, Dm, Dl) or diencephalic (Ppa) ventricles, comprising only a small fraction of each neuroanatomical region (see Fig. 2-1A-B and Fig. 2-3). Very few $BrdU^+$ cells were seen more than 3-4 cell diameters from the ventricle. Given the well circumscribed ventricular position of the proliferating cells within these neuroanatomical regions, I will refer to these highly proliferative regions as periventricular zones.

I next asked whether the relative number of $BrdU^+$ cells varied along the rostrocaudal axis of each PVZ. By normalizing the number of $BrdU^+$ cells to the estimated total cell population within the surface area of each defined region, I was able to quantify the percentage of $BrdU^+$ cells. These experiments yielded three main observations. First, there exists significant variation in the relative number of $BrdU^+$ cells at different rostrocaudal levels in the PVZ of Vd, Vv, Dl, and Ppa, but not D or Dm (Fig. 2-2C, I; one-way ANOVA, Tukey's HSD post hoc test; Fig. 2-2). In Vd and Vv, a drastic decrease in the size of the cycling population occurs caudal to cross-sectional level 60 (Fig. 2-2F), while the opposite trend is seen in Dl and Ppa, resulting in a gradual increase in the size of the $BrdU^+$ population from the rostral- to dorsal-most level (Fig.

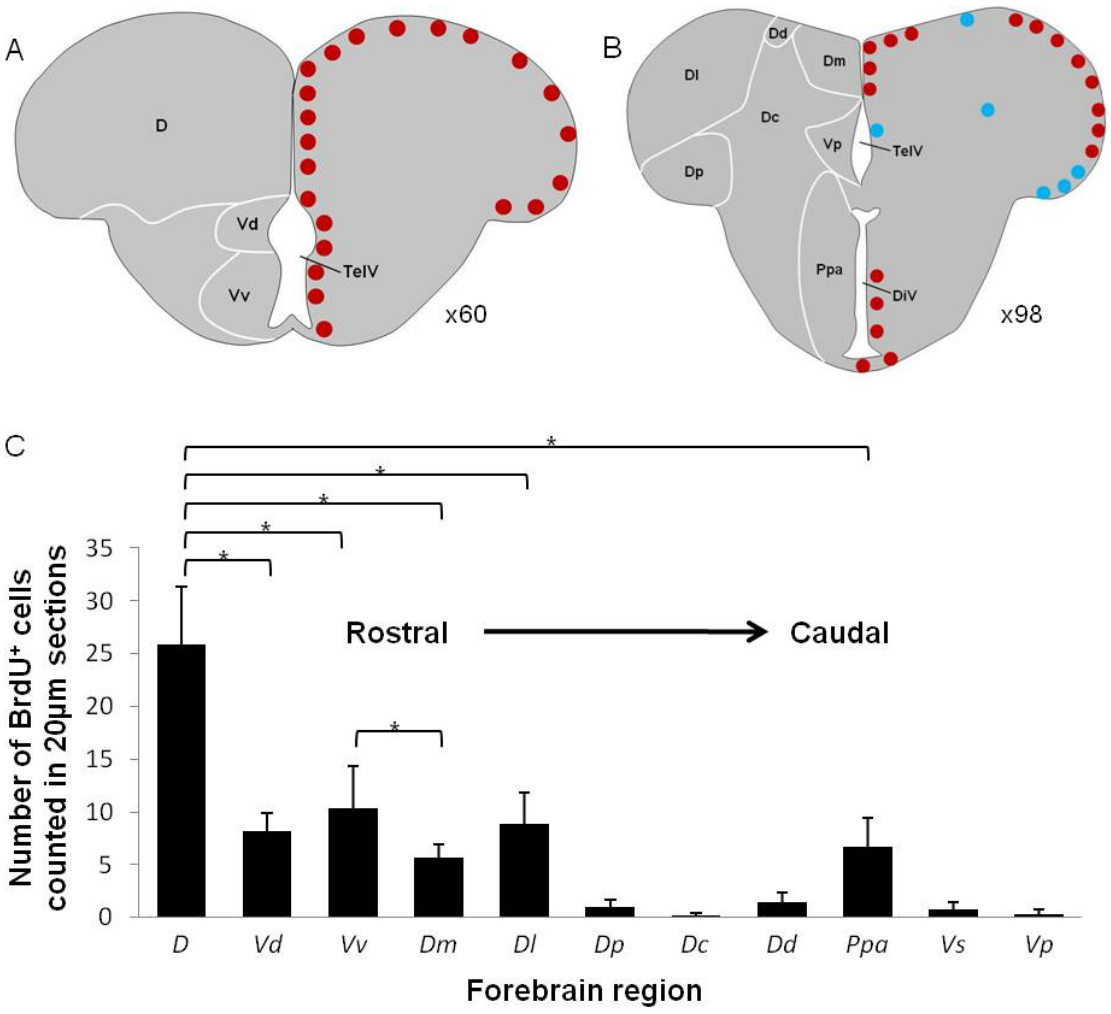
A
D
Vd
Vv
TelV
x60
B
Dd
Dm
Dl
Dc
Vp
TelV
Dp
Ppa
DiV
x98
C
Number of BrdU+ cells counted in 20µm sections
Rostral
Caudal
Forebrain region
D
Vd
Vv
Dm
Dl
Dp
Dc
Dd
Ppa
Vs
Vp

Figure 2-1. BrdU$^+$ labeling across 11 neuroanatomical regions in the adult zebrafish forebrain used to determine major proliferation zones. A, B, Schematics depicting the location of BrdU$^+$ cells along the border of the ventricle at two rostrocaudal levels (x60, x98) that include the specific regions investigated (*Vs* not shown). Red dots indicate regions with significantly higher levels of BrdU$^+$ labeling following a 2 hour pulse-chase compared to regions with blue dots as per the graph in **C**. **C,** Total number of BrdU$^+$ cells counted through the entire rostrocaudal axis for each region in 20 µm cryosections. The number of BrdU$^+$ cells in the proliferation zones of *D*, *Vd*, *Vv*, *Dm*, *Dl*, and *Ppa* were significantly greater than all other zones examined, and thus for clarity no indication of significance is denoted on the graph for these comparisons. Significance (*) was determined using a one-way ANOVA and Tukey's HSD post hoc tests ($p \leq 0.05$). Refer to list of abbreviations for terminology.

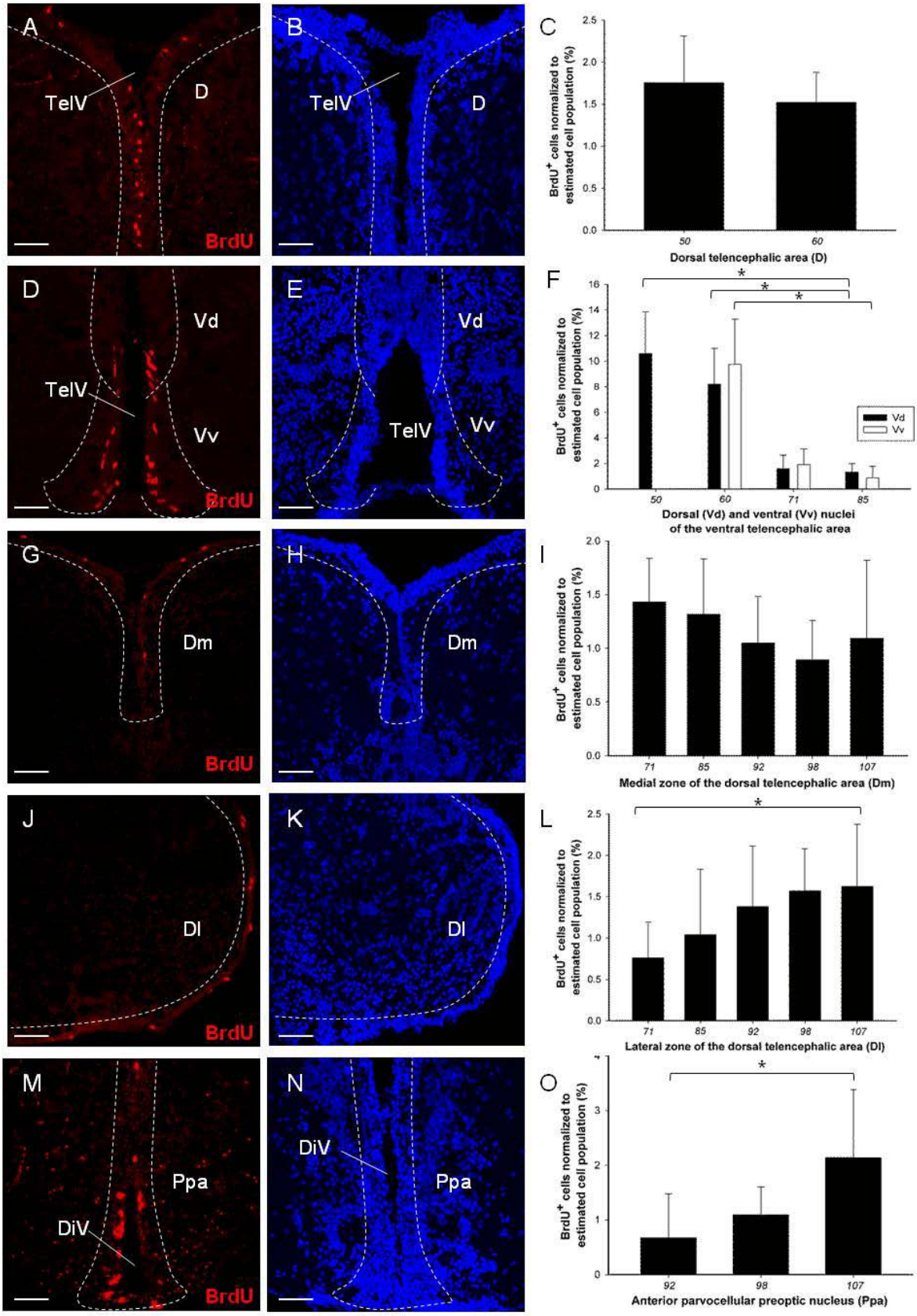
A
TelV
D
BrdU
B
TelV
D
C
BrdU+ cells normalized to estimated cell population (%)
2.5
2.0
1.5
1.0
0.5
0.0
50
60
Dorsal telencephalic area (D)
D
Vd
TelV
Vv
BrdU
E
Vd
TelV
Vv
F
*
*
*
16
14
12
10
8
6
4
2
0
Vd
Vv
50
60
71
85
Dorsal (Vd) and ventral (Vv) nuclei of the ventral telencephalic area
G
Dm
BrdU
H
Dm
I
2.0
1.5
1.0
0.5
0.0
71
85
92
98
107
Medial zone of the dorsal telencephalic area (Dm)
J
Dl
BrdU
K
Dl
L
*
2.5
2.0
1.5
1.0
0.5
0.0
71
85
92
98
107
Lateral zone of the dorsal telencephalic area (Dl)
M
Ppa
DiV
BrdU
N
DiV
Ppa
O
*
3
2
1
0
92
98
107
Anterior parvocellular preoptic nucleus (Ppa)

Figure 2-2. BrdU$^+$ cells normalized to the total cell population at separate rostrocaudal levels across the six proliferation zones having the greatest number of BrdU$^+$ cells (*D, Vd, Vv, Dm, Dl, Ppa*). **A, D, G, J, M,** Location of BrdU$^+$ cells (red) in each zone at the rostrocaudal level where most BrdU$^+$ labeling was observed indicating the level of the PVZ niche. **B, E, H, K, N,** Hoechst 33258 nuclear staining at corresponding levels for each PVZ niche showing the density of the cell population where BrdU$^+$ labeling is observed. **C, F, I, L, O,** Percentage of BrdU$^+$ cells normalized to the estimated total cell population throughout different levels of the rostrocaudal axis of the proliferation zones. The level at which the proliferation zones displayed the greatest number of BrdU$^+$ cells was considered the level of the PVZ niche for that neuroanatomical region, with this rostrocaudal level examined specifically in subsequent experiments. Brackets denote a significant difference in the percentage of BrdU$^+$ cells between rostrocaudal levels within the same proliferation zone. Significance (*) was determined using one-way ANOVA and Tukey's HSD post hoc tests ($p \leq 0.05$). In **F**, for clarity only a subset of significantly different comparisons are shown graphically. However, a significant difference was reported between Vd at crossectional levels 50/60 and levels 71/85, and Vv at crossectional level 60 compared with both 71/85. White, hashed lines demarcate the boundaries of PVZs within each neuroanatomical region, used to estimate the surface area and total population size to normalize BrdU$^+$ cell counts. Refer to list of abbreviations for terminology. See also Table 2-2 for estimates of the total cell population comprising PVZs. In all images dorsal is up. Scale bar: 50 μm.

2-2L, O). Second, my surface area estimates showed widespread variation in the overall size of each of these six PVZs, with the order from largest to smallest being D, Dl, Ppa, Dm, Vv, Vd (Table 2-2). However, there was no correlation between the total surface area and the number of proliferating $BrdU^+$ cells in each PVZ. Third, my normalized data demonstrated that the $BrdU^+$ cell population account for only a small fraction of the total cell population within PVZs (Fig. 2-2C, F, I, L, O); those comprising the largest percentage of the overall cell population were observed in Vd (10.59%, level x50) and Vv (9.74%, level x60), which also had the smallest estimated surface area (Table 2-2). All subsequent experiments were done at the rostrocaudal levels and within the neuroanatomical boundaries of each PVZ where the highest density of $BrdU^+$ cells was reported, as shown schematically in Figure 2-3.

2.4.2 Cell Cycle Parameters Vary Between PVZs

To assess whether the difference in the size of the $BrdU^+$ cell population across different PVZs was related to differences in cell cycle kinetics, I performed a BrdU cumulative labeling experiment. Zebrafish were intraperitoneally injected with a 1 mM bolus of BrdU at 2-hour intervals over a 12 hour period, and separate groups of fish sacrificed every 2 hours, 30 min after the last injection. Preliminary experiments confirmed that my method of injection could be sustained over the 12 hour period, and that the multiple injections of BrdU used for this experiment were not toxic to the animals (data not shown). The cumulative labeling method allowed me to estimate the growth fraction (GF), which is the size of the proliferative population, the maximum length of time for the GF to take up BrdU (T_M), the length of the cell cycle (T_C), and the S-phase (T_S), by comparing the best fit of my data to first-, second-, or third order polynomial equations. Over the injection period, all proliferating cells in the S-phase of the cell cycle will incorporate BrdU, however upon re-entry into the S-phase these cells would not be counted as newly $BrdU^+$ cells. Therefore, assuming the injection period is long enough, at a specific time point, only previously labelled $BrdU^+$ cells would comprise the cell population leading to the GF and plateau phase of the best fit curve. In the event that the 12.5 hour cumulative labeling period used here was insufficient to mark all proliferating cells, I would expect to see a linear regression as the best fit to all data points.

Table 2-2. Estimated surface area and BrdU+ cell population size of periventricular zones (PVZ)

	D		*Vd*		*Vv*	*Dm*		*Dl*		*Ppa*	
Rostro-caudal cross-sectional level studied	x50	x60	x50	x60	x60	x71	x85	x98	x107	x98	x107
Estimated PVZ surface area (μm^2)	44 624	53 693	4807	3244	5848	18 905	11 703	20 447	23 711	18 489	15 675
Mean number of $BrdU^+$ cells 2 hours post injection	26.2	26.05	17.46	10.45	21.54	8.4	4.97	11.41	11.67	5.52	10.35
Estimated cell population of PVZ	1493	1712	165	128	221	587	378	726	720	506	484
$BrdU^+$ cells of total cell population (%)	1.75	1.52	10.59	8.19	9.74	1.43	1.32	1.57	1.62	1.09	2.14

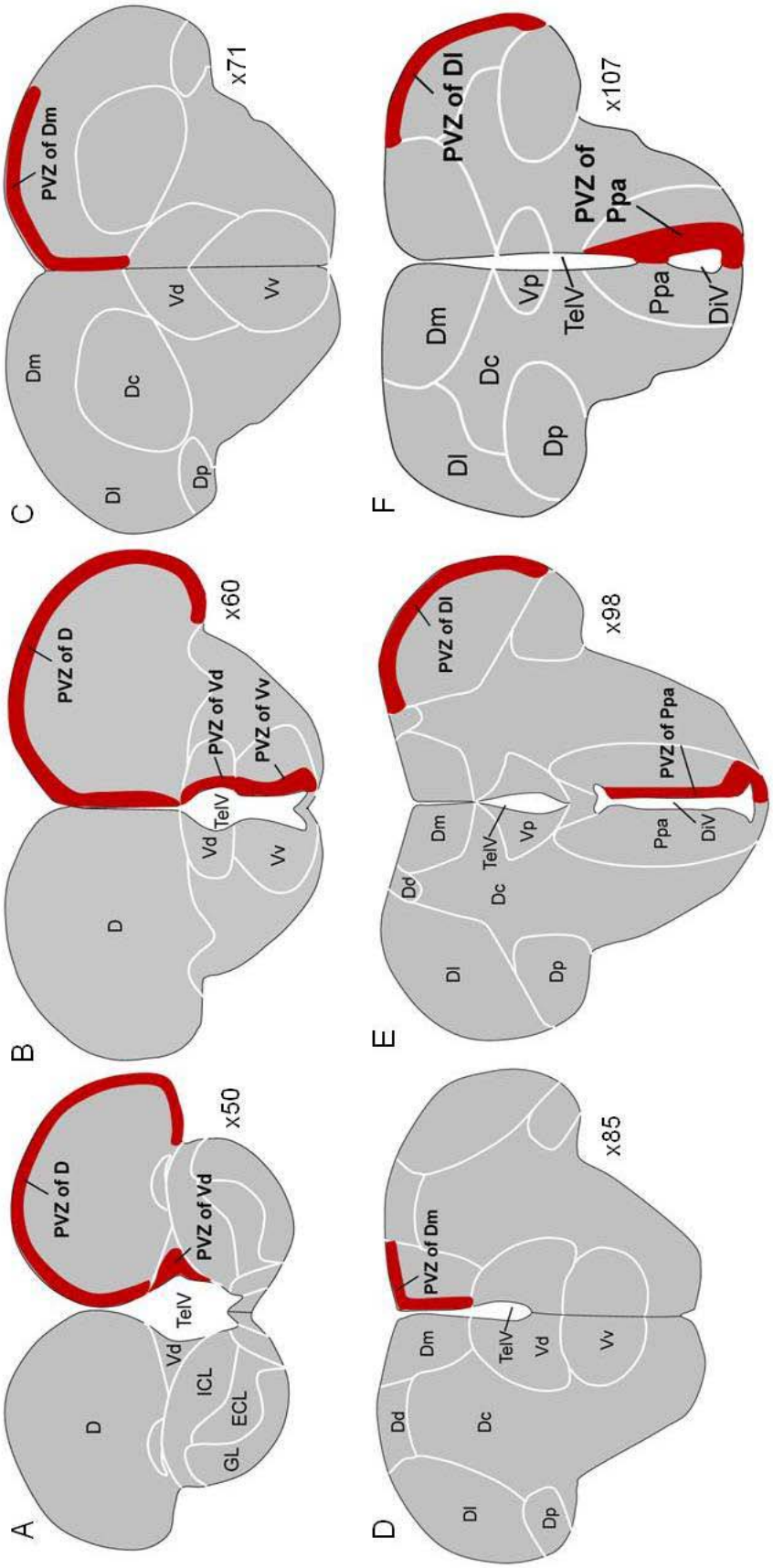
A
PVZ of D
PVZ of Vd
x50
D
TelV
Vd
ICL
ECL
GL
B
PVZ of D
PVZ of Vd
PVZ of Vv
x60
D
Vd
TelV
Vv
C
PVZ of Dm
x71
Dm
Dc
Vd
Vv
Dl
Dp
D
PVZ of Dm
x85
Dm
Dd
Dc
TelV
Vd
Vv
Dl
Dp
E
PVZ of Dl
PVZ of Ppa
x98
Dd
Dm
TelV
Vp
Dc
Ppa
DiV
Dl
Dp
F
PVZ of Dl
PVZ of Ppa
x107
Dm
Vp
TelV
Ppa
DiV
Dc
Dl
Dp

Figure 2-3. Schematic drawings showing the six PVZs in red in relation to the larger neuroanatomical forebrain region in which they are located, at the rostrocaudal levels where BrdU$^+$ cells were most abundant. Note the position of PVZs is consistently localized adjacent the ventricles at all levels, with PVZs differing considerably in size. Some PVZs spanned two rostrocaudal levels, including the PVZ of *D*, *Vd*, *Dm*, and *Dl*. All subsequent experiments were examined only at these rostrocaudal levels, and within the neuroanatomical boundaries shown here. Schematics and nomenclature based on Wullimann et al., 1996. Refer to list of abbreviations for terminology. See also Table 2-2 for surface area estimates of each PVZ.

My results show clearly that the cell cycle parameters differ across regionally distinct PVZs. Representative confocal images of $BrdU^+$ cells 30 min following the first injection and when the percentage of BrdU-labelled cells reached its maximum (i.e., the first time point when the plateau is reached = GF) are shown in Figure 2-4. The results of all cell cycle parameters based on a single population model are stated in Table 2-3. Data from D, Vv, Dm, and Dl were best fit to a linear regression model using the least squares method (Fig. 2-4A, G, J, M), suggesting a single proliferative population, but having yet to reach a plateau. The continuous increase in BrdU- labelled cells beyond the 12 hour cumulative labeling endpoint of this study prevented me from accurately determining the GF and total cell cycle and S-phase lengths. Thus, I reasoned that across these PVZs the last time point assayed at 12.5 hours could be interpreted only as the minimum GF, with the PVZ of D, Dm, and Dl having a minimum GF of between 3.2-4.3% compared with the GF of 28.76% seen in Vv (Table 2-3).

The Ppa and Vd cumulative labeling data were found to best fit quadratic and cubic polynomial regression models, respectively. In the PVZ of Ppa (Fig. 2-4P-R), the beginning of the plateau was observed ~6.5 hours after the first BrdU injection (red dot), resulting in a maximum GF of 4.35%. Using the first four data points that fit a linear model ($R^2=0.4603, y = 1.401 + 0.477x$; Table 2-3), I was able to estimate the total cell cycle length to be 11 hours with an S-phase length of 4.5 hours. Unlike the apparent single population of cells seen in the PVZ of Ppa, Vd showed evidence of two separate mitotic populations (Fig 2-4D-F). The data for this zone conformed most closely to a third order polynomial, with the curve having three distinct phases. Between 0.5-4.5 hours the number of $BrdU^+$ cells can be seen to steadily increase, after which time a plateau could be noted extending until ~8.5 hours after the first BrdU injection. I interpret the time elapsed between 0.5-8.5 hours to represent the first mitotic population within the PVZ of Vd, with 4.5 hours marking the GF (red dot) calculated to be 13.62%. By fitting the first 3 data points to a linear model ($R^2=0.7289, y = 5.624 + 1.820x$), I obtain a total cell cycle length of 7.48 hours and S-phase length of 2.98 hrs for this first population in Vd (Table 2-3). A putative second proliferative population can be seen commencing 8.5 hours after the first BrdU injection and increasing towards our last time point at 12.5 hours, although my cumulative labeling period would need to be extended to definitively assess the kinetics of this putative second

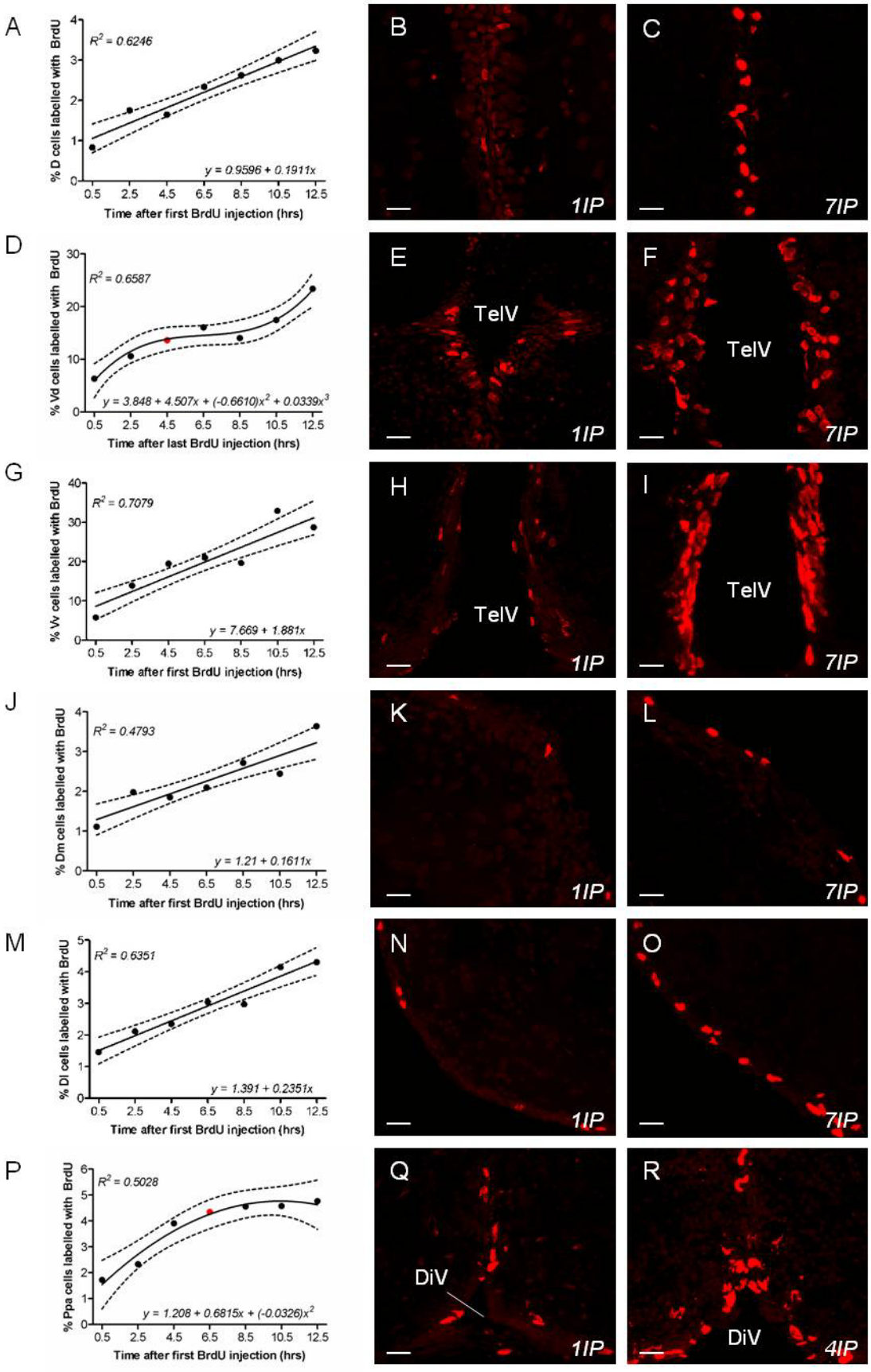
A
R^2 = 0.6246
y = 0.9596 + 0.1911x
% D cells labelled with BrdU
Time after first BrdU injection (hrs)
B
1IP
C
7IP
D
R^2 = 0.6587
y = 3.848 + 4.507x + (-0.6610)x^2 + 0.0339x^3
% Vd cells labelled with BrdU
Time after last BrdU injection (hrs)
E
TelV
1IP
F
TelV
7IP
G
R^2 = 0.7079
y = 7.669 + 1.881x
% Vv cells labelled with BrdU
Time after first BrdU injection (hrs)
H
TelV
1IP
I
TelV
7IP
J
R^2 = 0.4793
y = 1.21 + 0.1611x
% Dm cells labelled with BrdU
Time after first BrdU injection (hrs)
K
1IP
L
7IP
M
R^2 = 0.6351
y = 1.391 + 0.2351x
% Dl cells labelled with BrdU
Time after first BrdU injection (hrs)
N
1IP
O
7IP
P
R^2 = 0.5028
y = 1.208 + 0.6815x + (-0.0326)x^2
% Ppa cells labelled with BrdU
Time after first BrdU injection (hrs)
Q
DiV
1IP
R
DiV
4IP

Figure 2-4. Cumulative BrdU$^+$ labeling over a 12-hour injection period demonstrating variation in the cell cycle kinetics of proliferative populations across the six PVZs. A, D, G, J, M, P, Percentage of BrdU$^+$ labelled cells fitted to the best linear or non-linear (quadratic, cubic) model plotted over the injection period. On all graphs the 95% confidence bands (black, hashed lines) and r-squared value for the best fit model is noted. Red dots denote the commencement of the plateau phase of a single cell population, with all data points from here prior re-plotted to a linear regression and used to calculate the maximum growth fraction of the population (GF_M), in addition to the total length of the cell cycle (T_C) and S-phase (T_S). Where the line of best fit was a linear regression and continued to increase beyond the end of the 12.5 hr injection period (**A, G, J, M**), the GF_M could not be determined, and therefore only the minimal growth fraction for the population could be interpreted from the graph. In *D*, note the presence of two possibly separate proliferative cell populations, the first ranging from 0.5-4.5 hrs and the second beginning at 8.5 hrs. For all graphs the corresponding confocal images of the number of BrdU$^+$ cells for each niche 30 min after the first injection (**B, E, H, K, N, Q**) and at the time point when the estimated maximum or minimum growth fraction (**C, F, I, L,O, R**) was reached are shown. Refer to list of abbreviations for additionaly terminology not described here. See also Table 2-3 for values of cell cycle parameters calculated for each PVZ. In all images dorsal is up. Scale bar: 8 µm.

Table 2-3. Cell cycle parameter estimates following a 12.5 hour BrdU cumulative labelling study

	D	*Vd*	*Vv*	*Dm*	*Dl*	*Ppa*
Growth fraction (%)	3.23*	13.62**	28.76*	3.637*	4.304*	4.348
Time at $BrdU^+$ cell maximum (hrs)	12.5	4.5	12.5	12.5	12.5	6.5
Cell cycle length (hrs)	16.90	7.484	15.29	22.58	18.31	11.00
S-phase length (hrs)	4.402	2.984	2.79	10.08	5.81	4.50

*Indicates that the cell population only reached a minimum growth fraction after 12.5 hours
**Denotes the growth fraction of the first of two putative subpopulation of proliferative cells in Vd

population. Overall, these data clearly indicate that the size of proliferative populations and their cell cycle characteristics are relatively non-uniform between PVZs.

2.4.3 Ciliated Cells and Distinct Populations of BrdU$^+$ Glial Vary by PVZs Between Pallial and Subpallial Regions and are in Proximity to the Surrounding Vasculature

To gain insight into the general features previously shown to be characteristic of other vertebrate niches studied along the ventricular wall (Alvarez-Buylla and Lim, 2004; Morrison and Spradling, 2008; Shen et al., 2008), I used both scanning EM and confocal microscopy to examine the presence of ciliated cell populations, glial phenotypes, and vasculature within PVZs. To first identify the presence of ciliated cells, I separated the forebrain hemispheres and processed the tissue for SEM to look at the ventricular zone *en face* (Fig. 2-5A-C). At the dorsal-most aspect of the forebrain, the dorsal ependymal lining (DEL) can be seen covering the entire rostrocaudal aspect of D and Dm (Fig. 2-5A). From my scanning EM preparations I noted that the DEL does not continue ventrally along the ventricle, but rather bridges the two hemispheres dorsally, as expected. By surveying PVZs along the rostrocaudal axis a small number of ciliated cells were observed, displaying 1-3 cilia extending into the ventricle from the tip of cells or seen individually arising between adjacent cells from a deeper cell layer (Fig. 2-5B-C). Variations in surface topography of cells between PVZs or within different regions of the same zone were also observed, however, this was not examined in detail. The presence of ciliated cell populations observed at the SEM level was further corroborated by whole-mount IHC of the forebrain ventricular surface labelled with the antibody against γ-tubulin. Figure 2-5D shows γ-tubulin$^+$ labeling (red) in discrete regions of the ventricular wall, with several of these regions overlapping with the PVZs of interest. Labeling with γ-tubulin provided additional evidence that ciliated cell populations contained ciliary basal bodies on the apical cell membrane facing the ventricle or localized at the ventricular midline (Fig. 2-5E-F).

To identify the phenotype of cells composing PVZs, zebrafish were injected with BrdU and sacrificed 2-hours later for co-labeling with BrdU and the glial markers S100β or GS, or BrdU

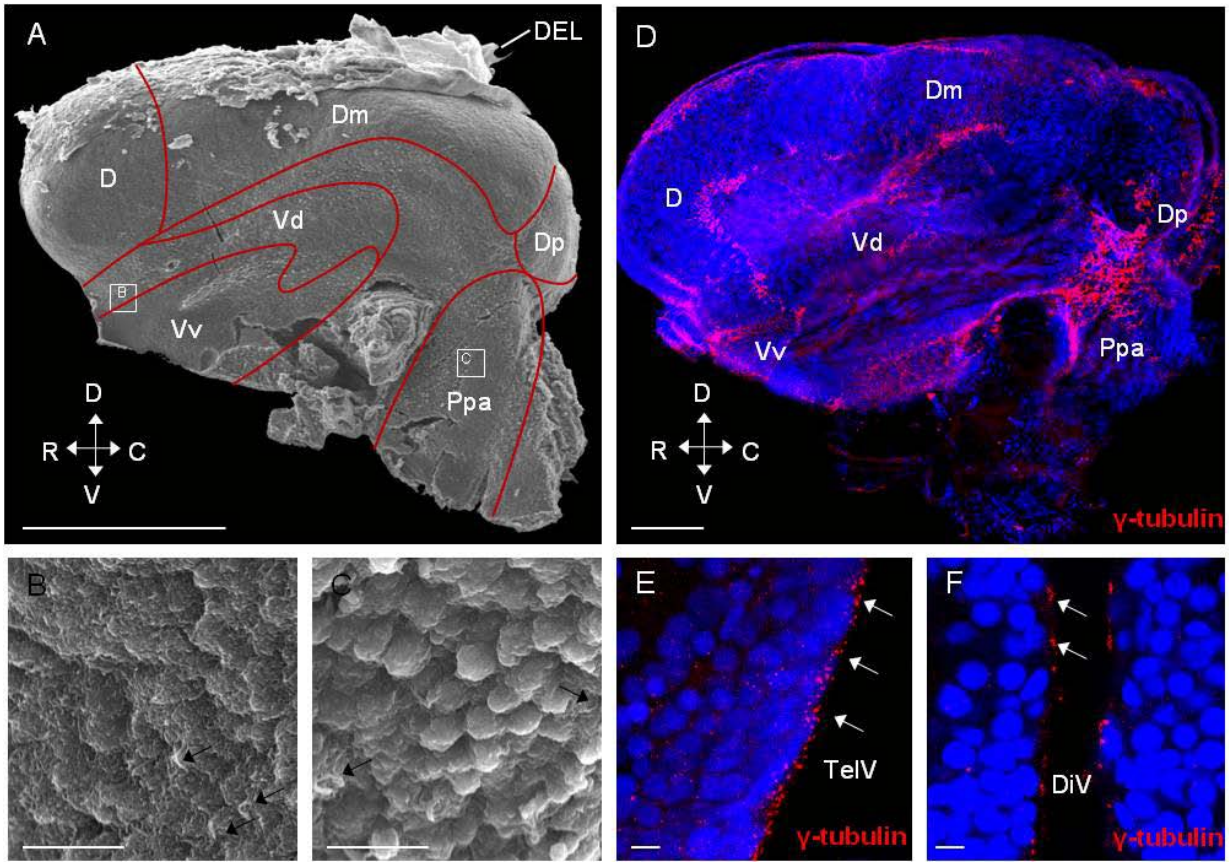
A
DEL
Dm
D
Vd
Dp
B
Vv
C
Ppa
D
R
C
V
D
Dm
D
Dp
Vd
Vv
Ppa
D
R
C
V
γ-tubulin
B
C
E
TelV
γ-tubulin
F
DiV
γ-tubulin

Figure 2-5. Evidence of ciliated cell types along the ventricular surface of the adult zebrafish forebrain. A-C, Scanning electron microscopy showing an *en face* view of the ventricular surface (VS) of a single forebrain hemisphere. Red lines demarcate the general boundaries of the major neuroanatomical regions in which PVZs are situated, seen along the VS. White boxes in **A** correspond to higher magnification images seen in **B-C** displaying evidence of ciliated cells (white) extending from the apical cell surface into the lumen (black arrows). **D,** Whole-mount preparation of a single forebrain hemisphere stained with γ-tubulin (red) to label the basal bodies of cilia and counterstained with Hoechst 33258. The orientation is the same as in **A**. Note the orientation of images in **A** and **D** along the dorsoventral (D-V) and rostrocaudal (R-C) axes. **E-F,** Images showing γ-tubulin^{+} staining (white arrows) similar to **D**, but viewed in cross-section along the surface of the telencephalic (TelV) and diencephalic (DiV). Refer to list of abbreviations for terminology. In all images dorsal is up. Scale bars: **A**, 270 µm; **B-C**, 10.5 µm; **D**, 100 µm; **E-F**, 8 µm.

and the putative stem/progenitor markers Pax6 or SOX2, for comparisons between niches. $BrdU^+/S100\beta^+$ cells made up nearly 10% or more of the cell population sampled in all PVZs (Fig. 2-6A-C). A statistically significant difference in this population was noted between Dm and Ppa (one-way ANOVA; Tukey's HSD post hoc test), with Dm having nearly 40% of cells $BrdU^+/S100\beta^+$. Although $BrdU^+/S100\beta^+$ cell populations were seen in all six PVZs, those having the highest percentage of co-labeled cells were localized in the pallial zones (D, Dm, and Dl). Unlike the consistent finding of $BrdU^+/S100\beta^+$ cells throughout all PVZs, $BrdU^+/GS^+$ cells were absent from both of the subpallial Vv and Ppa (Fig. 2-6D-F). This result is due to the general absence of GS^+ labeling in Vv, as well as within the ventral aspect of Ppa. The lack of GS^+ labeling in Vv helps to demarcate the boundary between Vd (which displays GS^+ labeling) and Vv. Despite an overall statistically significant effect between PVZs (one-way ANOVA), the high degree of variation between samples from a single zone, did not allow for accurate post hoc tests to be performed. From my analysis, I show however, that the PVZ where the greatest population of $BrdU^+/GS^+$ resided was D (25%). The pattern of $BrdU^+/GS^+$ labeling seen here suggests that this cell population resides primarily in the pallial PVZs of the zebrafish forebrain, but also includes the subpallial zone of Vd. By contrast, $Pax6^+$ cells were often localized adjacent the PVZ boundaries of Vd and Vv, while some degree of labeling could additionally be seen within niches of D (mainly along the midline), Dm, Dl, and Ppa (Fig. 2-6G). However, from cell counting of $BrdU^+/Pax6^+$ cells across forebrain PVZs only in rare instances were co-labeled cells observed (Fig. 2-6H). Similarly, few $BrdU^+/SOX2^+$ cells were detected across any of the six PVZs (Fig. 2-6I). This suggests that dividing $Pax6^+$ and $SOX2^+$ periventricular cells are sparse among PVZs, though these markers may be useful to identify putative stem/progenitor cells, which are typically thought to be rare among the population of niche cells.

Finally, to examine the location and degree of vascularisation of PVZs I used a *Tg[flk1:gfp]* transgenic zebrafish line which marks the endothelial cells of the brain vasculature. While the degree to which vasculature infiltrated each zone varied, they were all in close proximity to surrounding vessels. Qualitative observations showed that the PVZs of D, Vd, and Ppa were most highly vascularised compared with Vv, Dm, and Dl (Fig. 2-6J-L). Nevertheless, Dl and Ppa (Fig. 2-6K-L) appeared to possess the greatest density of vessels adjacent the neuroanatomical boundaries of the niche.

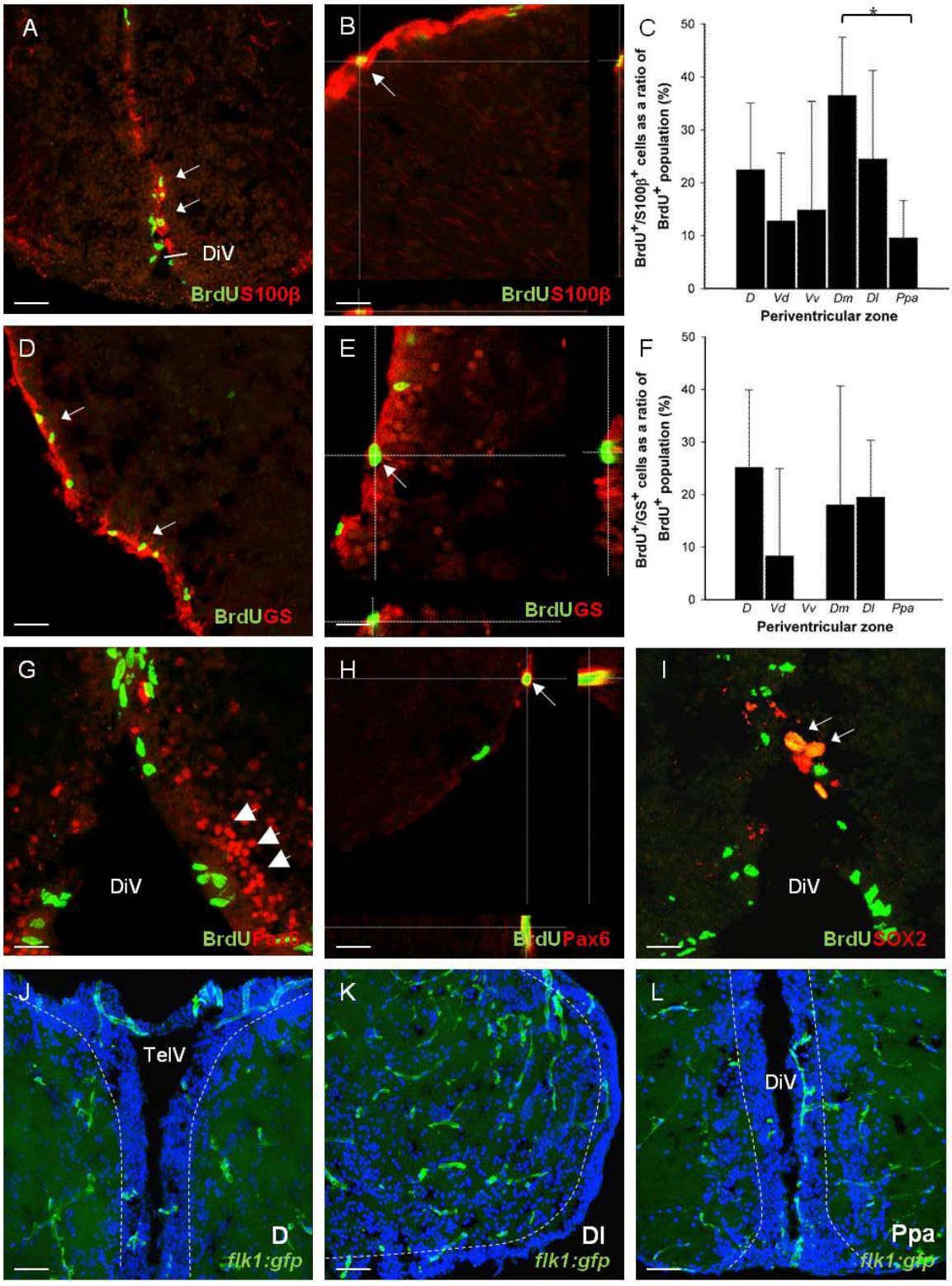
A
DiV
BrdUS100β
B
BrdUS100β
C
BrdU+/S100β+ cells as a ratio of BrdU+ population (%)
50
40
30
20
10
0
*
D
Vd
Vv
Dm
Dl
Ppa
Periventricular zone
D
BrdUGS
E
BrdUGS
F
BrdU+/GS+ cells as a ratio of BrdU+ population (%)
50
40
30
20
10
0
D
Vd
Vv
Dm
Dl
Ppa
Periventricular zone
G
DiV
BrdUPax6
H
BrdUPax6
I
DiV
BrdUSOX2
J
TelV
D
flk1:gfp
K
Dl
flk1:gfp
L
DiV
Ppa
flk1:gfp

Figure 2-6. Characterization of BrdU$^+$ glial populations 2-hours post-BrdU injection and localization of vasculature compared between PVZs. **A-C,** BrdU$^+$/S100β$^+$ co-labeling (**A-B**) quantified (**C**) following a single BrdU injection. In **C**, note the smaller size of this population in the PVZ of *Vd*, *Vv*, and *Ppa*. **D-F,** BrdU$^+$/GS$^+$ co-labeling (**D-E**) quantified (**F**) following a single BrdU injection. In **F**, note the absence of BrdU$^+$/GS$^+$ cells in the PVZ of *Vv* and *Ppa*. Significance (*) was determined using one-way ANOVA and Tukey's HSD post hoc tests ($p \leq 0.05$). **G-H,** BrdU$^+$/Pax6$^-$ (**G**) and BrdU$^+$/Pax6$^+$ cells (**H**) cells detected in PVZs. In most cases Pax6$^+$ cell populations were observed near the border of the PVZ (**G,** white arrowheads), and only rarely were dividing Pax6$^+$ cells observed (**H**). **I,** One of few BrdU$^+$/SOX2$^+$ cells detected across PVZs. In **A-I**, white arrows and cross-hairs in orthogonal views denote examples of positively co-labelled cells. **J-K,** Localization of vasculature (green, *flk1:gfp*) in relation to Hoechst 33258 labeled cells (blue) in PVZs; examples are provided for the PVZ of *D* (**J**), *Dl* (**K**), and *Ppa* (**L**). White, hashed lines demarcate the border of PVZs. Refer to list of abbreviations for terminology. In all images dorsal is up. Scale bars: **A, D, J, K, L,** 40 µm; **B, E, H, I,** 10 µm.

2.4.4 Ultrastructural Characterization of PVZs Reveals Pallial and Subpallial Variation in the Cytoarchitecture and Differences in the Frequency of Distinct Cell Types

I performed a detailed morphological study in order to compare the cytoarchitectural composition of six PVZs in the zebrafish forebrain. All zones bordered the telencephalic (D, Vd, Vv, Dl, Dm) or diencephalic (Ppa) ventricle medially along the dorsoventral axis of the forebrain, and were composed of several distinct cell types. Lateral to the ventricle, the deeper layers of each zone terminated with one or more layers of neurons or in the adjacent parenchyma. The first complete cell layer composed exclusively of neurons was considered the lateral-most boundary of each zone, with this layer not included as part of the PVZ. Varying degrees of vasculature could be seen in the form of venules and arterioles and these were noted when appropriate. Periventricular zones were studied at the following rostrocaudal cross-sectional levels to investigate the ultrastructural organization and cell types composing each niche: D, Vd, Vv (x60), Dm (x85), Dl and Ppa (x98). A summary of the characteristic features of the distinct cell types comprising PVZs is listed in Table 2-4, while the frequency of each cell type across zones is noted in Table 2-5. In cases where multiple cell types shared some, but not all, features, cells were divided into subtypes. Where cell types could not be determined but were present in the niche, they were classified as unknown.

2.4.4.1 Dorsal Telencephalic Area (D)

The PVZ of D encompassed the greatest surface area (see Table 2-2) and ran medially along the dorsoventral axis of the telencephalic ventricle, terminating at Vd, which marked the ventral-most position of the pallial zone. A continuous dorsal ependymal lining (DEL) composed of a single cell layer of classical ependymal cells could be seen spanning the roof of the telencephalic ventricle at the level of the PVZ of D and Dm (Figs. 2-7A; 2-8A; 2-11A-B) and continuing a short distance laterally along both hemispheres (Fig. 2-11C), before being replaced by a thin layer of squamous epithelial cells. The DEL appeared to form an ependymal-like sheath covering

Table 2-4. Morphological features of cell types identified in adult forebrain periventricular zones

	Ependyma	Type IIa	Type IIb	Type III	Type IVa	Type IVb	Type V	Neurons (VI)
Sample Size	n=30	n=113	n=17	n=52	n=88	n=26	n=43	n=51
NUCLEI								
Contour	elliptical; elongate ± some invag.	ovoid; irregular ± shallow invag.	ovoid; irregular	elongate; irregular ± invag.	ovoid; irregular ± invag.	elongate; irregular ± deep invag.	ovoid; irregular	ovoid
Long axis (µm)	4.39 ± 1.39	5.79 ± 1.34	5.15 ± 1.32	5.73 ± 1.96	5.28 ± 1.43	4.37 ± 1.10	3.47 ± 1.22	5.96 ± 0.94
Short axis (µm)	2.04 ± 0.65	3.49 ± 1.03	3.06 ± 0.97	2.66 ± 0.88	2.36 ± 0.79	2.38 ± 0.70	1.88 ± 0.56	4.84 ± 1.01
Chromatin	clumped hetero; evenly distributed	evenly distributed; non-clumped	reticulated; non-clumped	evenly distributed; non-clumped	reticulated; clumped hetero.	reticulated; clumped hetero.	reticulated; hetero. peripheral	mainly dispersed; some clumped
Color	light	light-medium	medium-dark	medium	dark	dark	dark	light-medium
Nucleoli	1-2	1-2	none visible	1-2	1-2; seldom visible	1-2; seldom visible	1; seldom visible	1
CYTOPLASM								
Percentage/ colour	abundant/light	abundant/light	abundant/light	scant/light	scant/medium	scant/medium	scant/dark	intermediate/light
Mitochondria	many	many	few	few	few	few	few	intermediate
Cilia	few to many	none	many	no	no	many	no	no
Microvilli	many; bulbus	few-intermediate	intermediate-many	no	no	intermediate	no	no
Vacuoles	many; large	many; small	few	no	no	no	no	some;small
Lipid droplets	yes	yes	yes	0-1	no	0-1	no	no
Dense bodies	no	yes	yes	no	no	no	no	no
LOCALIZATION	DEL (D & Dm only)	VS	VS (Ppa only)	VS and deeper layers	VS and deeper layers	VS (mainly Ppa)	1+ cell layers deep to VS	1-2 cell layers deep to VS
CELL CONTACTS	Ependymal cells	Types II-VI	Type IIa, Type VI	Types II-VI	Types II-VI	Types II-VI	Types II-VI	Types II-VI

Invag., invagination; hetero., heterochromatin; DEL, dorsal ependymal lining; VS, ventricular surface

Table 2-5. Frequency of cell types in periventricular zones (% total N)

	Ependyma	Type IIa	Type IIb	Type III	Type IVa	Type IVb	Type V	Neurons	Unknown	N cells/ PVZ
D	1.85	32.45	0	0.53	31.93	0.26	1.58	29.29	2.11	379
Vd	0	18.89	0	8.52	40.74	0	2.22	29.63	0	270
Vv	0	0.35	0	20.74	56.38	0	0.53	21.63	0.35	564
Dm	13	29.33	0	2	8.33	0	1.67	44.33	1.33	300
Dl	0	28.70	0	8.70	22.61	0	0.87	31.30	7.83	115
Ppa	0	19.17	3.56	2.57	24.90	5.93	1.38	41.11	1.38	506
%total/ cell type	2.16	18.46	0.84	8.01	34.02	1.45	1.31	32.33	1.41	2134

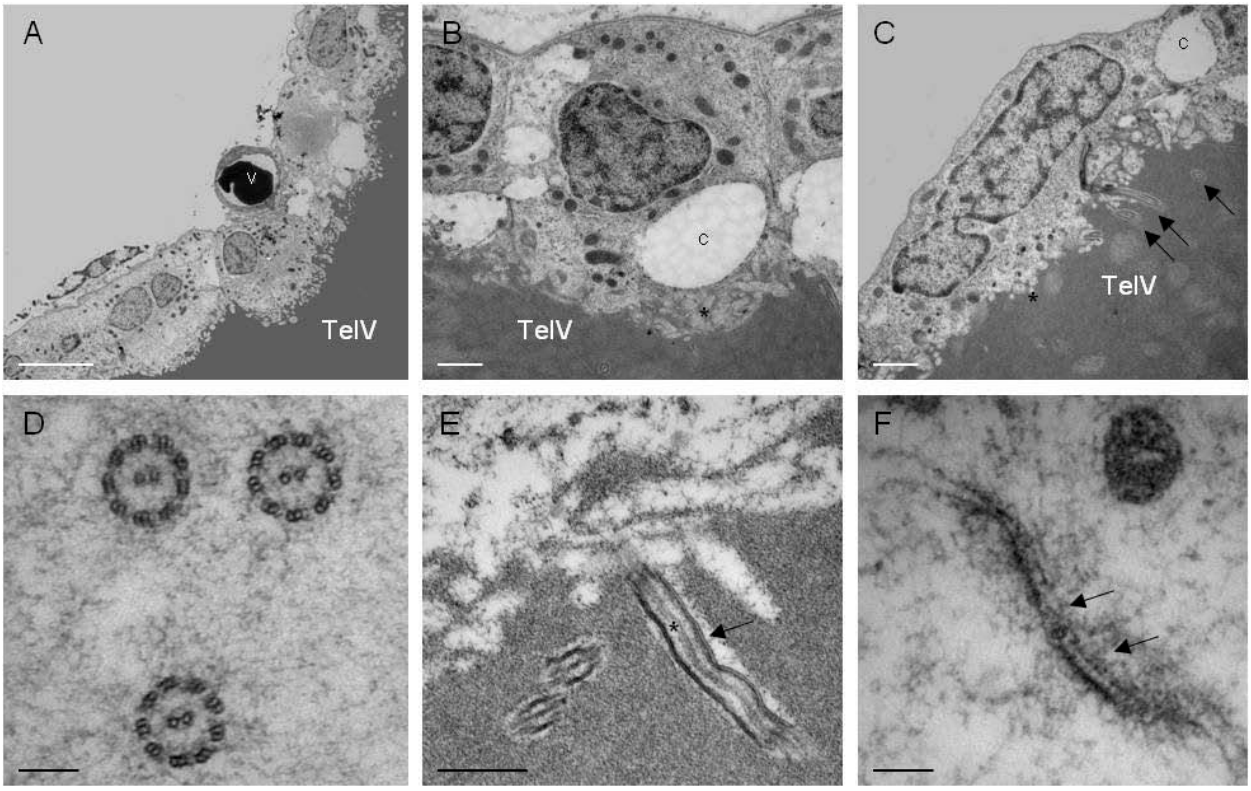
A
V
TelV
B
C
TelV
C
TelV
D
E
*
F

Figure 2-7. Ultrastructural organization of the dorsal ependymal lining (DEL) above the pallial PVZs of *D* and *Dm*. A single row of characteristic ependymal cells (**A**) are seen enclosing the dorsal aspect of the telencephalic ventricle (TelV) and displaying a cuboidal (**B**) to low cuboidal (**C**) conformation. These cells contained clumped heterochromatin, numerous bulbus microvilli (asterisk), and many mitochondria and vacuoles dispersed throughout the cytoplasm. In several cells large capillaries (c) could be seen coursing through the cytoplasm (**B, C**). Cilia can be seen extending from the apical cell surface (**C**, black arrows), having a typically 9+2 microtubule arrangement in cross-sections (**D**). In longitudinal section both the peripheral (black arrow) and central (asterisk) microtubules can be detected (**E**). Adjacent ependymal cells contacted one another via junctional complexes (**F**, black arrow). See also Table 2-4 for additional morphological features of ependymal cells, and Table 2-5 for the frequency of ependymal cells across PVZs. In all images dorsal is up. v, vessel. Scale bars: **A**, 4 µm; **B, C,** 1 µm; **E,** 500 nm; **D, F,** 100 nm.

the entire dorsal surface of the forebrain (see Fig. 2-5A), although in many cases the DEL went undetected since it is lost during specimen preparation. Ependymal cells were typically cuboidal to low cuboidal, displaying clumps of heterochromatin throughout an elliptical to elongated shaped nucleus (Fig. 2-7B-C). Abundant, light staining cytoplasm contained numerous mitochondria with several cilia and bulbus microvilli projecting into the lumen at the apical surface. Cilia were composed of a 9+2 arrangement of microtubules, which were easily recognizable in both cross- and longitudinal sections (Fig. 2-7D-E). Capillaries were often found tightly interspersed among ependymal cells near the apical surface (Fig. 2-7B, C), in addition to the presence of darkly staining lipid droplets within the cytoplasm. Junctional complexes could be seen joining the membrane of adjacent ependymal cells, as shown in Figure 2-7F. These ependymal cells were localized exclusively to the roof of the telencephalic ventricle and were not observed elsewhere across any of the PVZs.

Laterally, the PVZ of D extended around the entire perimeter of the pallium, beneath a thin layer of squamous epithielial cells, ending at the lateral olfactory tract. For ultrastructural analysis, the medial portion of D was studied in most detail, where the greatest heterogeneity of cell types was observed in this niche (Fig. 2-8B-D). At the dorsal-most aspect of the midline of D, this zone often consisted of a single layer of cells having a modified ependymal-like appearance (Fig. 2-8A, Type IIa). Type IIa cells had an ovoid or irregular nuclear contour with mostly evenly distributed, light staining, chromatin, with 1-2 large nucleoli easily identified within the nucleus (Fig 2-8E). At times the long axis of the nucleus could be seen oriented parallel to the midline ventricle (Fig. 2-8F). Similar to ependymal cells, the cytoplasm was abundant and lightly stained and often extended along the luminal surface. In some cases, cytoplasmic processes of Type IIa cells situated at the lumen could be seen extending into the deeper cell layers of the PVZ and terminating in the parenchyma (see Fig. 2-11E), reminiscent of radial glia (Gotz et al., 2002). Cytoplasmic organelles included numerous mitochondria and small vacuoles, lipid droplets and dense bodies. Unlike ependymal cells however, no cilia were seen projecting from the apical cell surface, although often a small number of microvilli were present. Type IIa cells made contacts with all cell types and were abundant across nearly all PVZs, with the exception of Vv, where these cells only contributed to 0.35% of the population (Table 2-5). Both Type IIa and IIb (see PVZ of Ppa) could be seen bound to adjoining cells of similar or different morphologies via tight

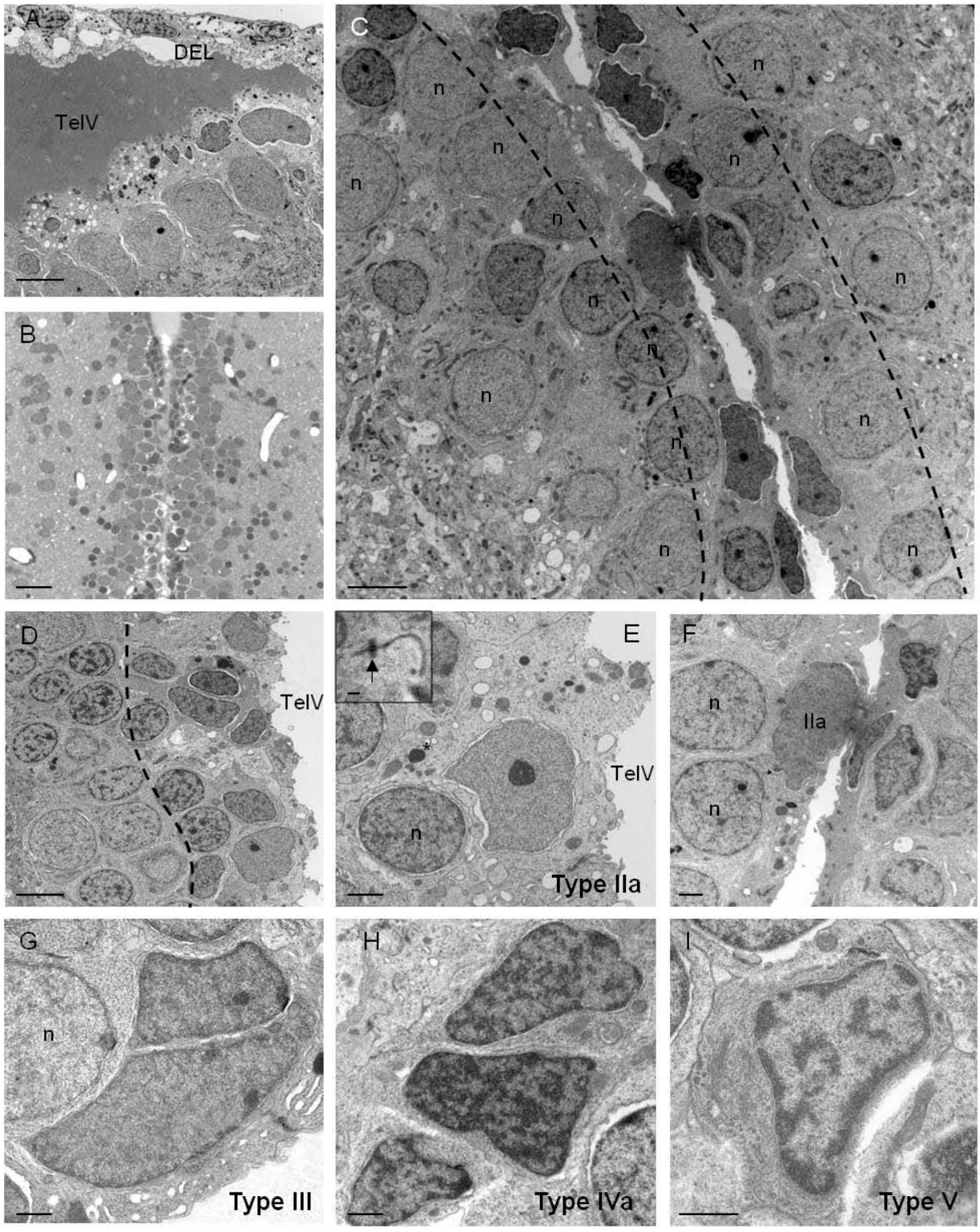
A
DEL
TelV
B
C
n
D
TelV
E
TelV
n
Type IIa
F
n
IIa
n
G
n
Type III
H
Type IVa
I
Type V

Figure 2-8. Ultrastructural organization of the pallial PVZ of *D*. A, Mid-dorsal image showing the dorsal ependymal lining (DEL) enclosing the roof of the telencephalic ventricle (TelV) and the large modified ependymal-like cells lining the lumen. **B-D,** Semithin (**B**) and high (**C, D**) magnification images showing the midline region of the PVZ of *D* that was studied in detail at the ultrastructural level. Note the heterogeneity of cell types forming a 1-3 cell layer deep PVZ (**C, D**) on either side of the TelV with a number of putative neurons at the lateral border of the PVZ. Black hashed lines denote the lateral boundaries of the PVZ. **E,** A single ***Type IIa*** cell distinguished by its abundant, light staining cytoplasm, with numerous vacuoles and mitochondria, dense bodies (asterisk), and evenly distributed chromatin with a single large nucleolus, situated at the ventricular surface. The profile of a putative neuron can be seen at the basal surface of the cuboidal shaped ***Type IIa*** cell. Inset displays a tight junction (desmosome) seen between adjacent ***Type IIa*** cells (black arrow). **F,** ***Type IIa*** cell observed with the long axis of the nucleus orientated parallel to the lumen, with its cytoplasmic dividing adjacent neurons from the ventricular space. **G:** Two adjacent ***Type III*** cells distinguished by their elongated to irregular nucleus with evenly distributed chromatin, 1-2 visible nucleoli, and minimal cytoplasm containing few organelles. A putative neuron can be seen at the basal surface of these cells. **H,** Three adjacent ***Type IVa*** cells characterized by their often irregular nucleus with variable degrees of dark staining, reticulated chromatin, and scant cytoplasm containing few organelles. ***Type IVa*** cells were often seen in clusters. **I,** A single ***Type V*** cell recognized by its small size and medium-darkly staining minimal cytoplasm, with a large proportion of heterochromatin localized to the periphery of the nucleus. These cells were typically located in the deeper layers of the PVZ and were the most infrequent cell type detected. See also Table 2-4 for additional morphological features of ***Type IIa***, ***Type III***, ***Type IVa***, and ***Type V*** cells, and Table 2-5 for the frequency of cell types within the PVZ of *D*. In all images dorsal is up. n, neuron. Scale bars: **A, C, D, F,** 4 µm; **B**, 10 µm; **E, G, H, I,** 1 µm; inset in **E,** 150 nm.

and intermediate junctions, including desmosomes (Fig. 2-8E, inset).

As the PVZ of D extended ventrally adjacent the midline telencephalic ventricle, an increasing number of different cell morphologies were observed (Fig. 2-8C-D). Here, the PVZ expanded to 2-3 cell layers deep and abutted one or more layers of neurons laterally (Fig. 2-8D). In addition to Type IIa cells described previously, three distinct cell morphologies were identified. Type III cells were distinguished by their elongated or irregular nucleus, with shallow to deep invaginations, evenly distributed medium staining chromatin containing 1-2 prominent nucleoli (Fig. 2-8G). These cells contained limited electroluscent cytoplasm with few visible organelles; only a small number of mitochondria or vacuoles were typically observed. Type III cells were least populous in the PVZ of D, comprising only 0.53% of the cell population (Table 2-5). Type IVa cells rather were easily distinguished from Type III cells by their darkly staining, highly reticulated chromatin structure of varying degrees of clumped heterochromatin, and the rare presence of visible nucleoli. The cytoplasm of Type IVa cells was typically darker than Type III and contained very few visible organelles (Fig. 2-8H). The cytoplasm of both Type III and Type IVa cells intimately conformed to the shape of the nucleus, which for Type IVa cells was most highly variable, taking on either an ovoid or irregular shape. Type IVa cells were the most abundant cell type across all PVZs (34.02%) followed by Type IIa (18.46%), both of which could be seen localized at the ventricular surface or within the deeper layers of PVZs.

The final cell type identified in the PVZ of D was classified as Type V. Type V cells were the smallest in size (LA: 3.47 μm ± 1.22; SA: 1.88 μm ± 0.56) and the least frequent of the cell types present throughout PVZs. These cells were primarily characterized by a large percentage of darkly staining heterochromatin localized to the periphery of their nucleus, which had an ovoid to slightly irregular shape (Fig. 2-8I). The color of the cytoplasm of Type V cells was similar or darker than that of Type IVa cells, scant, and often contained only a few mitochondria. Type V cells were never located at the lumen, but rather were observed one or more cell layers deep to the ventricular surface, and were situated adjacent all other cell types.

2.4.4.2 Dorsal Zone of the Ventral Telencephalon (Vd)

The PVZ of Vd comprised the smallest estimated surface area compared with all other niches examined (Table 2-2). The dorsal-most aspect of this zone marked the beginning of the medial subpallial zone where the telencephalic ventricle (TelV) began to enlarge from an initially compressed pallial midline ventricle (Fig. 2-9A). Multiple cell types can be seen 2-3 layers deep forming the dorsal region of this zone, including Type IIa, Type III, and Type IVa (Fig. 2-9B-C). This region of Vd was largely dominated by numerous Type IIa cells, identified by their abundant, lightly staining cytoplasm (Fig. 2-9D). Moving ventrally, the number of cell layers comprising the PVZ expanded to 3-4, in addition to having a greater number of rows of neurons dividing the lateral boundary of this zone from the parenchyma. An increasingly heterogeneous population of cell types were observed as the PVZ extended towards the junction with Vv (Fig. 2-9E-I; see 2-9A for ventral boundary of Vd with Vv). Type IVa cells made up the greatest population of cells (Fig. 2-9H; 40.74%) in this niche, while Type V cells were far less frequent (Fig. 2-9I; 2.2%). The ventral-most aspect of Vd was located where the telencephalic ventricle had reached its greatest width and began to narrow, and an increasing number of darkly stained cells lined the lumen (Type IVa), marking the beginning of the PVZ of Vv (boundary seen in Fig. 2-9A).

2.4.4.3 Ventral Zone of the Ventral Telencephalon (Vv)

The PVZ of Vv extended ventrally from the border of Vd, and along the telencephalic ventricle, ending at the ventral-most corners of the lumen (Fig 2-10A). The floor of the ventricle was not considered part of this niche, since immunostaining experiments revealed the absence $BrdU^{+}$ proliferating cells. The greatest number of cell layers extending laterally into the surrounding parenchyma was located in the PVZ of Vv, typically ranging from 2-5 layers deep (Fig. 2-10B, E). This zone was dominated by Type III (Fig. 10C; 20.74%) and Type IVa (Fig. 2-10D; 56.38%) cells that could be seen intermingled with neurons (Fig. 2-10B), or densely clustered together displaying characteristic irregular nuclear contours towards the ventrolateral edges of this zone (Fig. 2-10E). By contrast, the smallest percentage of Type V cells (0.53%) was

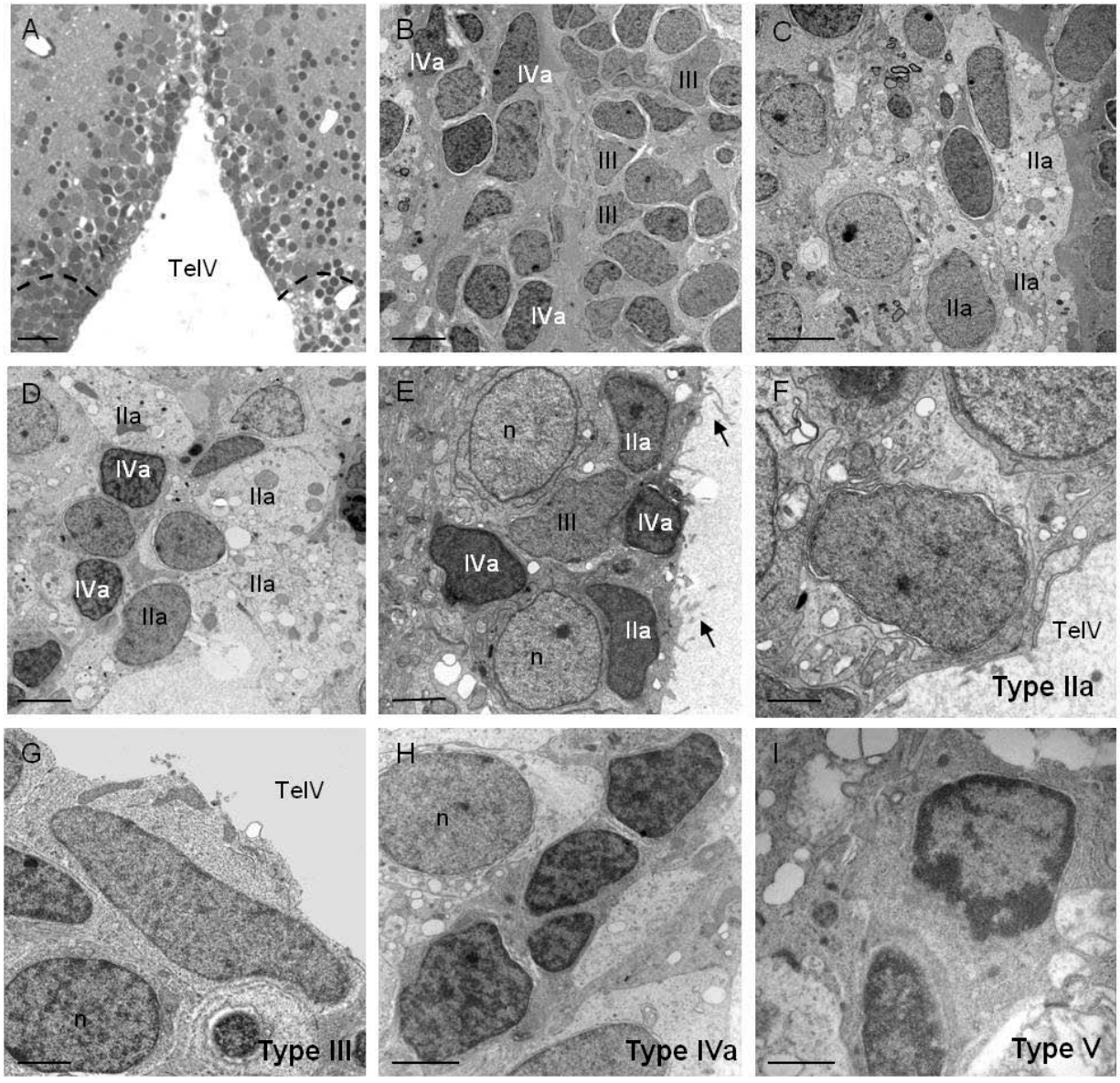
A
TelV
B
IVa
IVa
III
III
III
IVa
C
IIa
IIa
IIa
D
IIa
IVa
IIa
IVa
IIa
IIa
E
n
IIa
III
IVa
IVa
IIa
n
F
TelV
Type IIa
G
TelV
n
Type III
H
n
Type IVa
I
Type V

Figure 2-9. Ultrastructural organization of the subpallial PVZ of *Vd*. A, Semithin image showing the density of cell types composing this PVZ adjacent the large telencephalic ventricle (TelV) and the ventral border (black hashed lines) with the dorsal aspect of the PVZ of *Vv*. **B-C,** A mixture of ***Type IIa***, ***Type III*** and ***Type IVa*** cells are evident beginning at the dorsal-most aspect of the PVZ of *Vd* before the ventricle enlarges. **D,** A greater density of ***Type IIa*** cells were detected as the TelV began to enlarge. **E,** Representative image of the three primary cell types comprising the PVZ of *Vd* adjacent the lumen. Note the presence of microvilli extending from the apical surface of ***Type IIa*** cells (black arrows). **F-I,** Profiles of the morphology of ***Type IIa*** (**F**), ***Type III*** (**G**), ***Type IVa*** (**H**), and ***Type V*** (**I**) cells in the PVZ of *Vd*. See also Table 2-5 for the frequency of cell types within the PVZ of *Vd*. In all images dorsal is up. n, neuron. Scale bars: **A,** 10 µm; **B, C, D, H,** 4 µm; **E, G,** 2 µm; **F, I,** 1 µm.

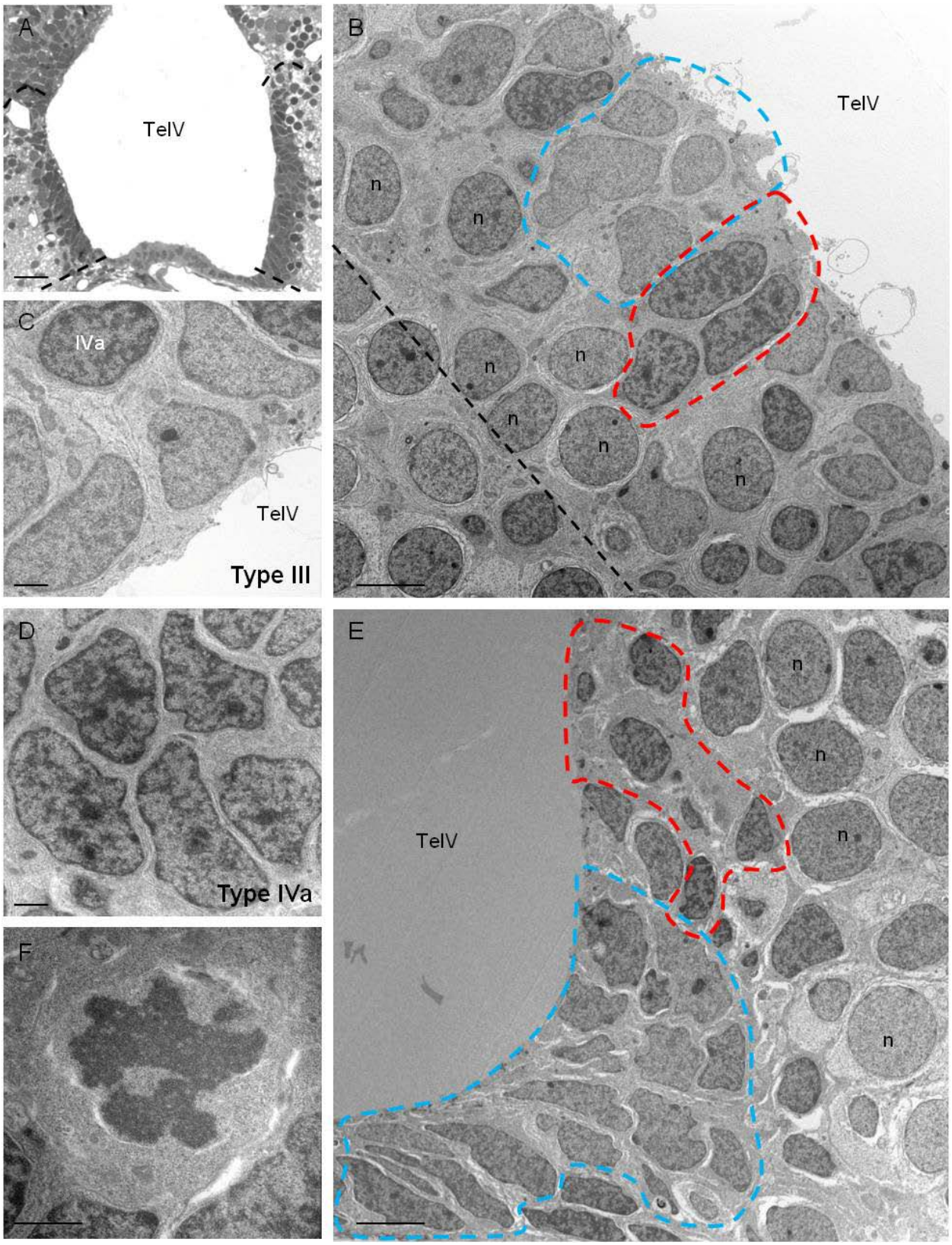
A
TelV
B
TelV
n
n
n
n
n
n
n
C
IVa
TelV
Type III
D
Type IVa
E
TelV
n
n
n
n
F

Figure 2-10. Ultrastructural organization of the subpallial PVZ of *Vv*. A, Semithin image showing the density of cells making up the PVZ of *Vv* along the telencephalic ventricle (TelV) and the dorsal and ventral borders (black hashed lines) of this zone. Note that the floor of the TelV is not considered part of this PVZ. **B,** High magnification image illustrating approximately 4-5 cell layers composing this PVZ along the lateral walls of the TelV and made up primarily of ***Type III*** (blue hashed lines) and ***Type IVa*** (red hashed lines) cells. Black hashed line demarcates the lateral extend of the PVZ. **C-D,** Clusters of ***Type III*** (**C**) and ***Type IVa*** (**D**) displaying their characteristic evenly distributed or reticulated chromatin, respectively. The morphological profiles of these two cell types composed nearly the entire PVZ of *Vv*, in addition to neurons (**E**). Blue and red hashed lines in **E** are the same as **B**. The irregular and elongated nuclear profile of ***Type III*** cells is most evident at the ventrolateral corners of the PVZ of *Vv*. **F,** A mitotic cell detected adjacent the TelV that appears to be in late prophase. See also Table 2-5 for the frequency of cell types within the PVZ of *Vv*. In all images dorsal is up. n, neurons. Scale bars: **A,** 10 µm; **B, E,** 4 µm; **C, D, F,** 1 µm.

detected in this niche. Neurons demarcating the lateral boundary could be readily identified by their large, ovoid nuclei in this zone (Fig. 2-10E). Within the PVZ of Vv, a small number of mitoses were identified, typically localized at or near the ventricular surface (Fig. 2-10F).

2.4.4.4 Medial Zone of the Dorsal Telencephalon (Dm)

The PVZ of Dm was lined dorsally by cuboidal ependymal cells (DEL) that bridged both forebrain hemispheres and continued laterally a short distance (Fig. 2-11A-C), similar to the PVZ of D described above. Along the dorsal aspect of the forebrain, this zone extended laterally beneath the ependymal lining and luminal space, and consisted of only 1-2 cell layers (Fig. 2-11C). Ventrally this niche lined the telencephalic ventricle until it came into contact with the dorsal boundary of Vd. Type IIa cells (Fig. 2-11D-E; 29.33%) and Type IVa cells (Fig. 2-11F; 8.33%), and a small number of Type III and Type V cells (Fig. 2-11G-H) comprised the PVZ of Dm. Figure 2-11E shows an example of the cytoplasm of a Type IIa cell (arrows) as it extends its processes both along the ventricular surface as well as into the deeper cell layers of this zone, while coursing between adjacent neurons. The PVZ of Dm had the greatest percentage of neurons localized within any of the six PVZs examined (44.33%), with 1-3 layers of neurons generally marking the niche boundary (Fig. 2-11I).

2.4.4.5 Lateral Zone of the Dorsal Telencephalon (Dl)

The PVZ of Dl was situated along the dorsal lateral region of the forebrain, beneath a single layer of squamous epithelial cells (Fig. 2-12A-C, arrows). A small amount of luminal space beneath the epithelial cells could be seen in some preparations representing the continuation of the telencephalic ventricle (Fig. 2-12B, asterisk). No ependymal cells were present in this region. The dorsal boundary of Dl was the dorsal zone of D (Dd), while its lateral boundary followed the contour of each hemisphere until the posterior zone of D (Dp) was reached. Typically this PVZ was only 1-2 cell layers deep (Fig. 2-12B-C) similar to that of Dm, although it had the second

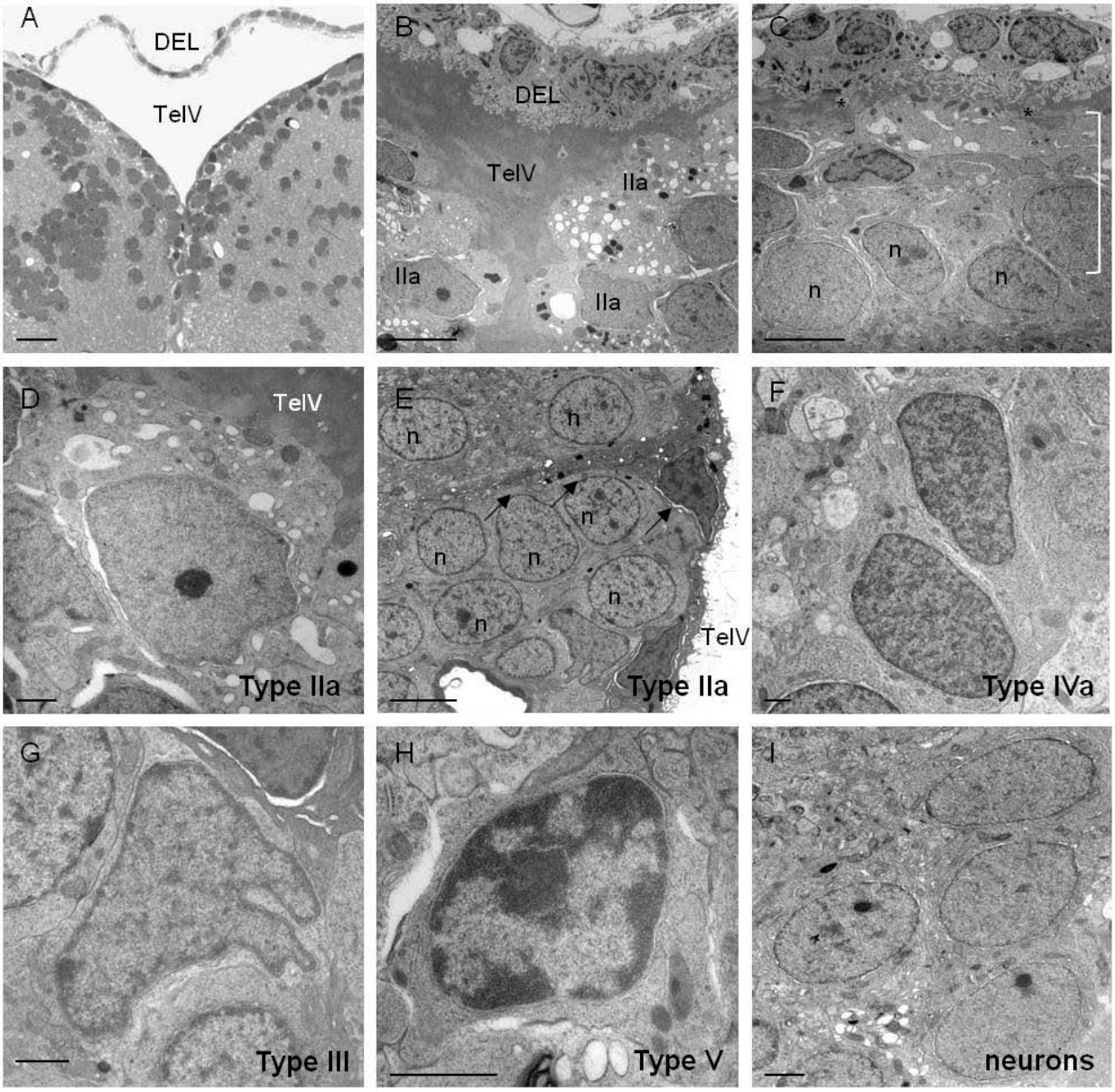
A
DEL
TelV
B
DEL
TelV
IIa
IIa
IIa
C
*
*
n
n
n
D
TelV
Type IIa
E
n
n
n
n
n
n
n
TelV
Type IIa
F
Type IVa
G
Type III
H
Type V
I
neurons

Figure 2-11. Ultrastructural organization of the pallial PVZ of *Dm*. A-B, Semithin (**A**) and high (**B**) magnification images showing the dorsal aspect of the PVZ of *Dm* and the single layer of ependymal cells enclosing the telencephalic ventricle (TelV) and forming the dorsal ependymal lining (DEL). Similar to the PVZ of *D*, ***Type IIa*** cells can be seen lining this zone in **B**. **C,** Dorsolateral zone of the PVZ of *Dm* displaying the DEL extending laterally along one hemisphere and enclosing the remnants of the TelV (*). Only 1-2 cell layers comprise this PVZ beneath the ventricle dorsally (white bracket). **D-E,** Representative ***Type IIa*** cells situated at the lumen. In **E** notice the cytoplasmic processes of a ***Type IIa*** cell extending into the deeper layers of the PVZ (black arrows), interspersed among neurons. **F-I,** Nuclear profiles of the morphology of ***Type IVa*** (**F**), ***Type III*** (**G**), and ***Type V*** (**H**) cells, and neurons (**I**) composing the PVZ of *Dm*. Note the highly invaginated nature of ***Type III*** cells in **G**. See also Table 2-5 for the frequency of cell types within the PVZ of *Dm*. In all images dorsal is up. n, neurons. Scale bars: **A,** 10 µm; **B, C, E,** 4 µm; **D, F, G, H, I,** 1 µm.

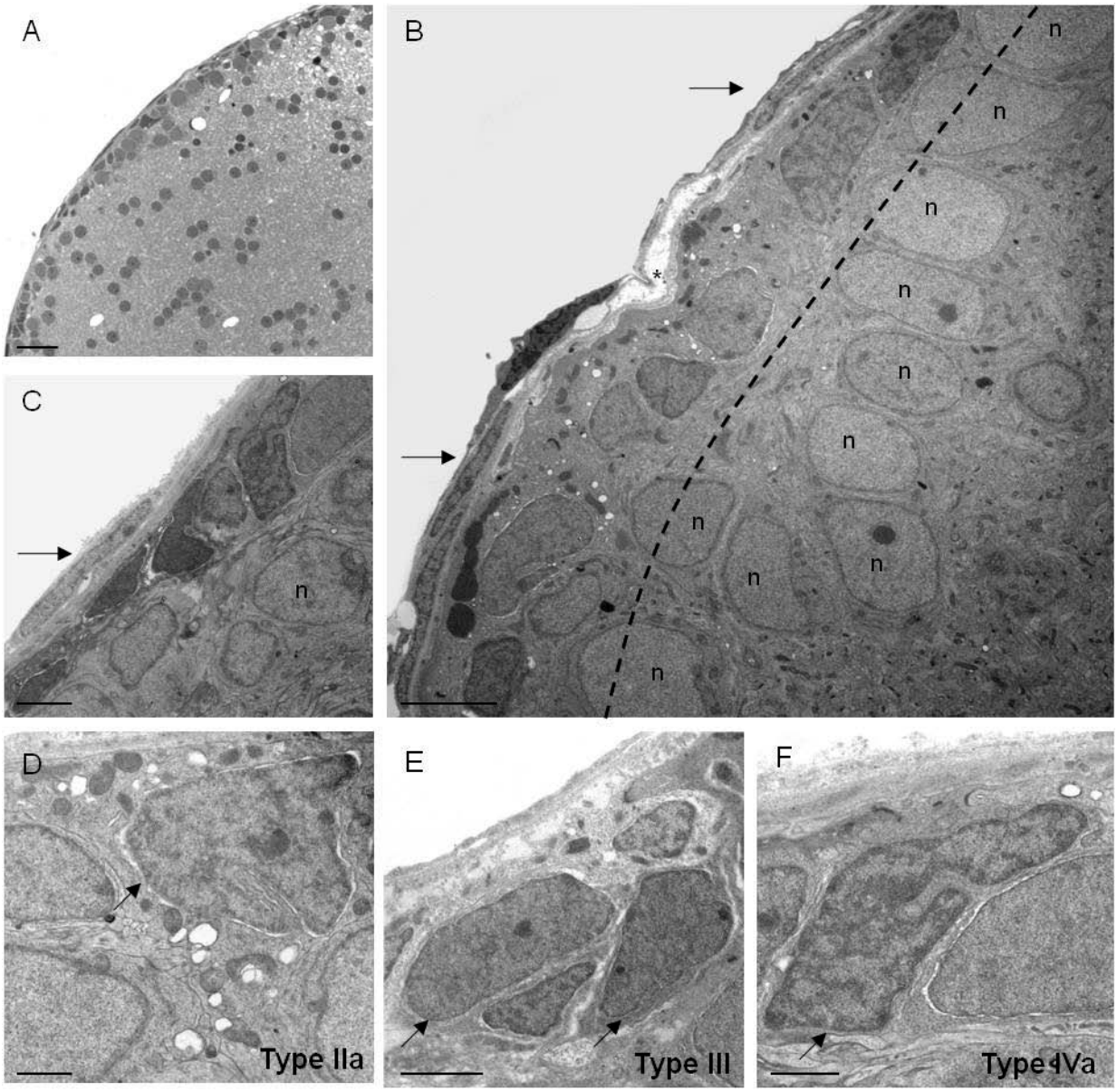
A
B
C
D
E
F
n
n
n
n
n
n
n
n
n
n
n
*
Type IIa
Type III
Type IVa

Figure 2-12. Ultrastructural organization of the pallial PVZ of *Dl*. A-C, Semithin (**A**) and high (**B, C**) magnification images displaying the 1-2 cell layer thick PVZ of *Dl* covered by a thin epithelial lining at the outer surface of the hemisphere (black arrows in **B, C**). Clusters or rows of neurons separating the PVZ from the parenchyma can also be seen. In **B** the lateral extension of the telencephalic ventricle (*) is seen beneath the epithelial lining. Black hashed lines denote the boundary of the PVZ of *Dl*. **D-F,** Morphological profiles of the major cell types composing the niche of *Dl*, including ***Type IIa*** (***D***)***, Type III*** (***E*****),** and ***Type IVa*** (***F***)**.** Black arrows indicate the cell type of interest in each image. See also Table 2-5 for the frequency of cell types within the PVZ of *Dl*. In all images dorsal is up. n, neurons. Scale bars: **A,** 10 µm; **B,** 4 µm; **C, E,** 2 µm; **D, F,** 1 µm.

highest estimated surface area (Table 2-2). However, in contrast to Dm, a more heterogeneous mixture of cell types was present in this niche. These included Type IIa (Fig. 2-12D), Type III (Fig. 2-12E), and Type IVa (Fig. 2-12F), all representing nearly 10% or greater of the total cell population of this zone. Infrequently, Type V cells were found, while a considerable number of neurons made up nearly a third of the cell population of this PVZ.

2.4.4.6 Parvocellular Preoptic Nucleus, Anterior Part (Ppa)

The PVZ of Ppa extended dorso-ventrally along the walls of the diencephalic ventricle within the subpallial zone of the forebrain (Fig. 2-13A). The number of cell layers composing this zone generally increased from 2-4 along the dorsoventral axis, and most resembled the organization described in the subpallial PVZ of Vv (see Fig. 2-10D). However, the PVZ of Ppa encompassed the greatest diversity of distinct cell types, including two additional multiciliated cell types not previously detected in other niches. These ciliated cells were most commonly observed in the dorsal aspect of this niche (Fig. 2-13B), with fewer observed ventrally.

The first of these cell types shared many morphological features with Type IIa cells (Fig. 2-13C), and as a result were classified as Type IIb cells. Type IIb cells were most easily distinguished from Type IIa cells (Fig. 2-13C) by the presence of many cilia (9+2 microtubules) projecting into the lumen from the apical cell surface (Fig. 2-13D-E). Type IIb cells comprised 3.56% of the cell population of the PVZ of Ppa. These cells had ovoid or irregular nuclei, however their chromatin had a significantly darker, and more reticulated appearance compared with Type IIa, and lacked any visible nucleoli. Moreover, despite the abundant cytoplasm of Type IIb cells, it contained fewer mitochondria and vacuoles compared with Type IIa. However, lipid droplets, dense bodies and microvilli were commonly observed. Type IIb cells were localized only at the surface of the diencephalic ventricle and made contacts with adjacent type Type IIa cells and neurons.

The second ciliated cell type identified within the PVZ of Ppa was most closely related in morphological profile to Type IVa cells (Fig. 2-13H), and as such was referred to as Type IVb (Fig. 2-13F-G). Type IVb cells had much the same heterochromatin organization and variation

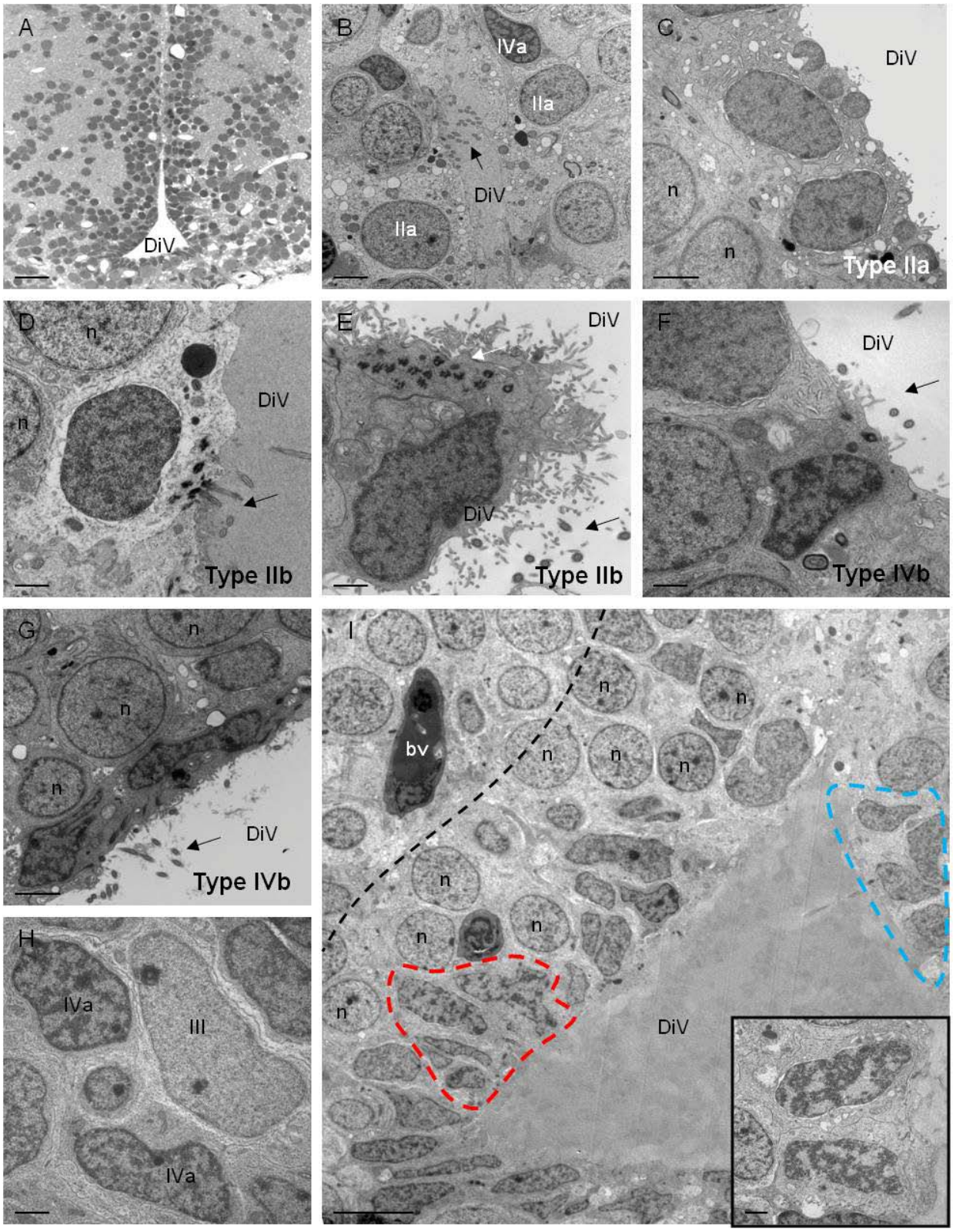
A
DiV
B
IVa
IIa
DiV
IIa
C
DiV
n
n
Type IIa
D
n
n
DiV
Type IIb
E
DiV
DiV
Type IIb
F
DiV
Type IVb
G
n
n
n
DiV
Type IVb
H
IVa
III
IVa
I
bv
n
n
n
n
n
n
n
n
n
DiV

Figure 2-13. Ultrastructural organization of the subpallial PVZ of *Ppa*. A, Semithin image showing the density of cells composing this PVZ situated along the diencephalic ventricle (DiV). **B,** Image showing the rich heterogeneity of cell types within the dorsal zone of the PVZ of Ppa, including two ciliated cell types not previously described in any other PVZs examined. The black arrow shows cilia extending into the ventricle. **C-E, *Type IIa*** (**C**) and ***Type IIb*** cells observed in the PVZ of *Ppa*. ***Type IIb*** cells (**D-E**) had darker and slightly more reticulated chromatin compared with ***Type IIa*** cells, with multiple microvilli and cilia (black arrows) extending into the DiV, and a lesser number of organelles present in the cytoplasm. **F-G,** Multiciliated ***Type IVb*** cells detected in the PVZ of *Ppa*. Compared with ***Type IVa*** cells (**H**), the morphological features of ***Type IVb*** cells included cilia, a slightly greater number of organelles within the cytoplasm, and clumped/reticulated heterochromatin similar to ***Type IVa*** cells. Both multiciliated ***Type IIb*** and ***Type IVb*** cells were predominantly seen in the dorsal zone of the PVZ of *Ppa*, with few detected in the ventral zone of *Ppa*. **H:** Morphological profiles of ***Type III*** and ***Type IVa*** cells that, along with neurons, composed nearly all the ventral zone of the PVZ of *Ppa* as illustrated in **I**. **I,** Overview of the cytoarchitecture of the ventral zone of the PVZ of *Ppa*. The black hashed line denotes the lateral boundary of the PVZ of *Ppa*, while the blue and red hashed lines show clusters of ***Type III*** and ***Type IVa*** cells respectively, composing this ventral zone of *Ppa*. The inset displays two newly divided daughter cells seen at the ventricular surface. See also Table 2-4 for additional morphological features of ***Type IIb*** and ***Type IVb*** cells, and Table 2-5 for the frequency of cell types within the PVZ of *Ppa*. In all images dorsal is up. n, neuron; bv, blood vessel. Scale bars: **A,** 10 µm; **B, C, G,** 2 µm; **D, E, F, H,** 1 µm; **I,** 5 µm, inset in **I**, 1 µm.

in nuclear contour as Type IVa cells, however it generally contained more cytoplasm surrounding the nucleus; although this was still far less than seen in ependymal cells, Type IIa or IIb cells. The distinguishing characteristic of Type IVb cells was its highly ciliated nature, and microvilli extending from the apical surface into the lumen, localized exclusively at the ventricular surface. In the PVZ of Ppa, Type IVb cells consisted of 5.93% of the cell population.

More ventrally along the PVZ of Ppa the number of cell layers composing the niche increased similar to the PVZ of Vv. Few ciliated Type IIb and IVb cells were seen in this region, and rather this ventral region of Ppa was made up of mainly Type III and Type IVa cells, along with neurons (Fig. 2-13I). Thus, it appeared that the dorsal zone of Ppa was composed of a more heterogeneous mixture of cell types, while ventrally, as the lumen enlarged, only two cell types comprised this PVZ. A notable difference between the niche of Ppa and that of Vv, was that the ventral floor of the diecephalic ventricle was proliferative and therefore included as part of the PVZ (Fig. 2-13I). Within the ventral portion of this zone of Ppa several mitotic events were also detected at the luminal surface (Fig. 2-13I, inset).

2.4.5 Immunolabeling of Morphologically Distinct Cell Types Reveals the Phenotype of Three Proliferative Cell Populations within PVZs

To further confirm the phenotype of the different cells composing forebrain PVZs, immunohistochemical labeling experiments were performed on resin embedded tissue (Table 2-6). Positive antibody labeling of cells was visualized using either 10 nm gold particles or by DAB labeling. Where gold particles were used, one or more sections were left unstained for each marker to better visualize positive labeling. Sections encompassing rostral (D, Vd, Vv) and caudal (Dm, Dl, Ppa) PVZs were labelled with antibodies against GS, S100β, and HuCD. GS^+ cytoplasmic labeling appeared to be restricted exclusively to Type IIa cells as evidenced by the density of gold particles within these cells (Fig. 2-14A-B). Type IIa cells could easily be distinguished by their abundant cytoplasm, numerous mitochondria and vacuoles, and position adjacent the lumen (Fig. 2-14C-F). DAB labeling additionally revealed GS^+ cell bodies with

Table 2-6. Immunohistochemical labelling of morphologically distinct cell types							
	Type IIa	Type IIb	Type III	Type IVa	Type IVb	Type V	Neurons
BrdU	+	N.D.	+	+	N.D.	-	-
S100	+	+	+	+	N.D.	-	-
GS	+	N.D.	-	-	N.D.	-	-
HuC/D	-	-	-	-	-	-	+

N.D. indicates that the morphological profile of the cell type was not detected in LR White sections

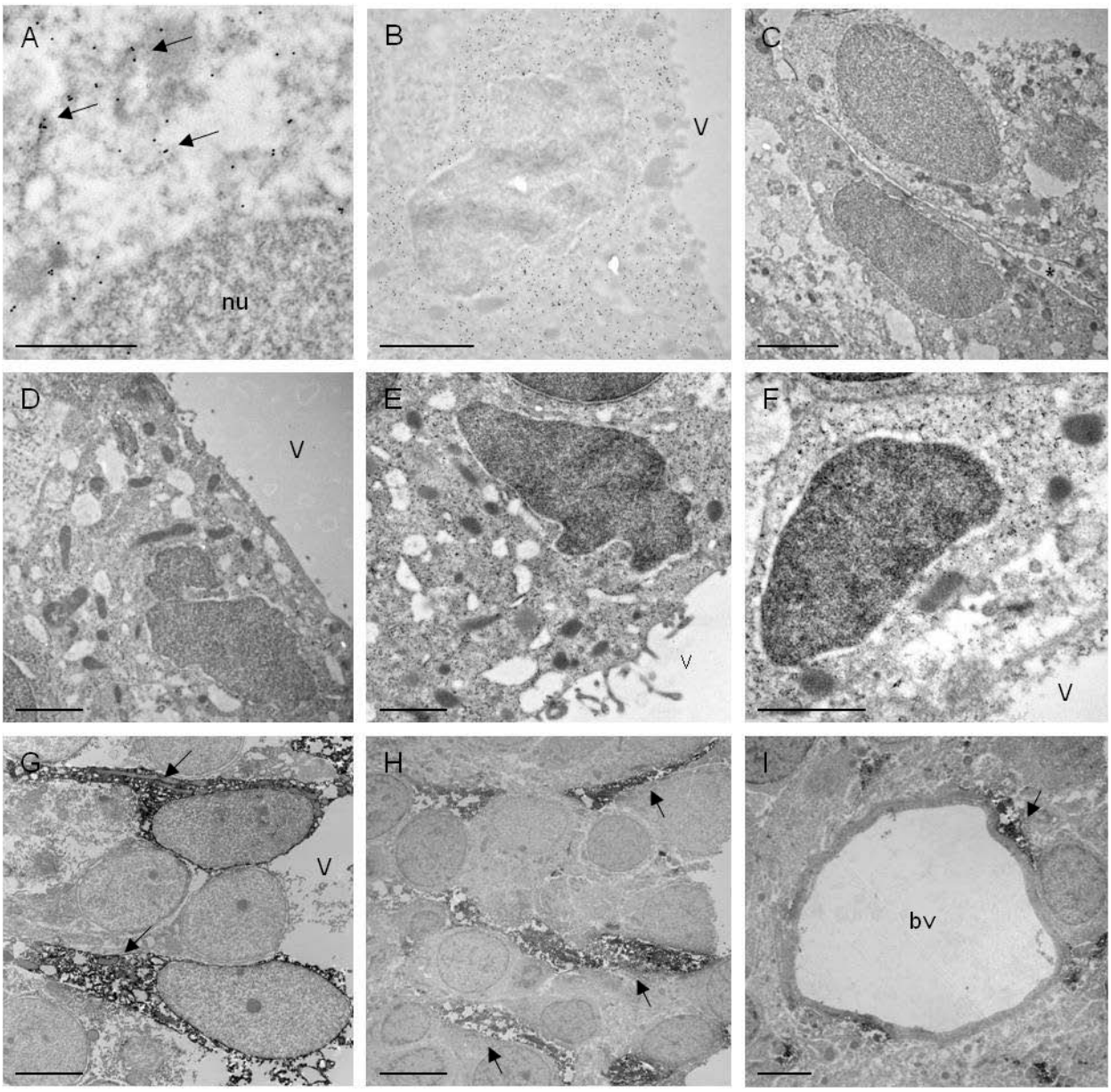
A
nu
B
V
C
*
D
V
E
V
F
V
G
V
H
I
bv

Figure 2-14. Glutamine synthetase-positive (GS^+) immuno-gold labeling of *Type IIa* cells. **A-B,** High (**A**) and low (**B**) magnification image showing the specificity of gold particles to the cytoplasm (black arrow in **A**) of ***Type IIa*** cells in the absence of contrast staining. **C-F,** Examples of GS^+ labeling in subpopulations of ***Type IIa*** cells situated at the ventricular surface distinguished by their large nuclei, abundant cytoplasm containing many mitrochondria and vacuoles, and a small number of microvilli projecting into the lumen. **G-I,** Using DAB labeling, the cytoplasmic processes of ***Type IIa*** cells are seen extending into the deeper cell layers of the PVZ (**G-H**, black arrows), and in some instances these processes (black arrows in **I**) were detected on the walls of surrounding blood vessels. See also Table 2-6 for a summary of immunohistochemical labeling across all cell types. In all images dorsal is up. DAB, 3,3'-Diaminobenzidine; nu, nucleus; bv, blood vessel; V, ventricle. Scale bars: **A,** 500 nm; **B, D, E, F,** 1 µm; **G, H,** 4 µm; **C, I,** 2 µm.

cytoplasmic processes extending from the soma of Type IIa cells into the deeper layers of the PVZ (Fig. 2-14G-H), suggestive of radial glial cells. Moreover, in rare instances, GS^+ staining could also be detected on the walls of proximal blood vessel (Fig. 2-14I). By contrast, as predicted, $S100\beta^+$ labeling appeared more widespread across cell types. A subpopulation of both Type IIa cells (Fig. 2-15B-C) and less frequently ciliated Type IIb cells (Fig. 2-15D) displayed gold labeling in the cytoplasm, with some labeling also seen in nucleus (Fig. 2-15A). A small number of putative Type III and Type IVa cells were also $S100\beta^+$ (Fig. 2-15E-F), however, GS^+ labeling in these cell types was much less frequent than Type IIa. Finally, DAB labeling using the neuronal marker HuCD confirmed the presence of neurons both interspersed within PVZs as well as bordering these zones laterally adjacent the parenchyma (Fig. 2-15G-I).

To next identify which of the above cell types were mitotically active, I used antibodies against BrdU conjugated to 10 nm gold particles to label and visualize cells in the S-phase of the cell cycle. Three morphologically distinct cell types were $BrdU^+$ across PVZs, including subpopulations of Type IIa, Type III, and Type IVa cells (Fig. 2-16). All cell types displayed gold labeling localized specifically to the nucleus (Fig. 2-16A). Type IIa $BrdU^+$ cells were identified mainly at the ventricular surface (Fig. 2-16B-D); their morphological profile confirmed by the extensive cytoplasm surrounding the positively-labelled nucleus. Proliferative Type III (Fig. 2-16E-H) and Type IVa (I-L) cells were observed both at the lumen and deeper cell layers, and appeared to be more frequently labelled within the ventral aspect of the PVZ of Vv. Multiciliated Type IIb and IVb cells could not be detected in the tissue, and thus it remained undetermined whether these cells contribute to the proliferative population. These findings indicate the presence of at least three proliferative cell populations with distinct cell morphologies within forebrain PVZs of the mature zebrafish: $S100\beta^+/GS^+/BrdU^+$ Type IIa cells, $S100\beta^+/BrdU^+$ Type III cells, and $S100\beta^+/BrdU^+$ Type IVa cells.

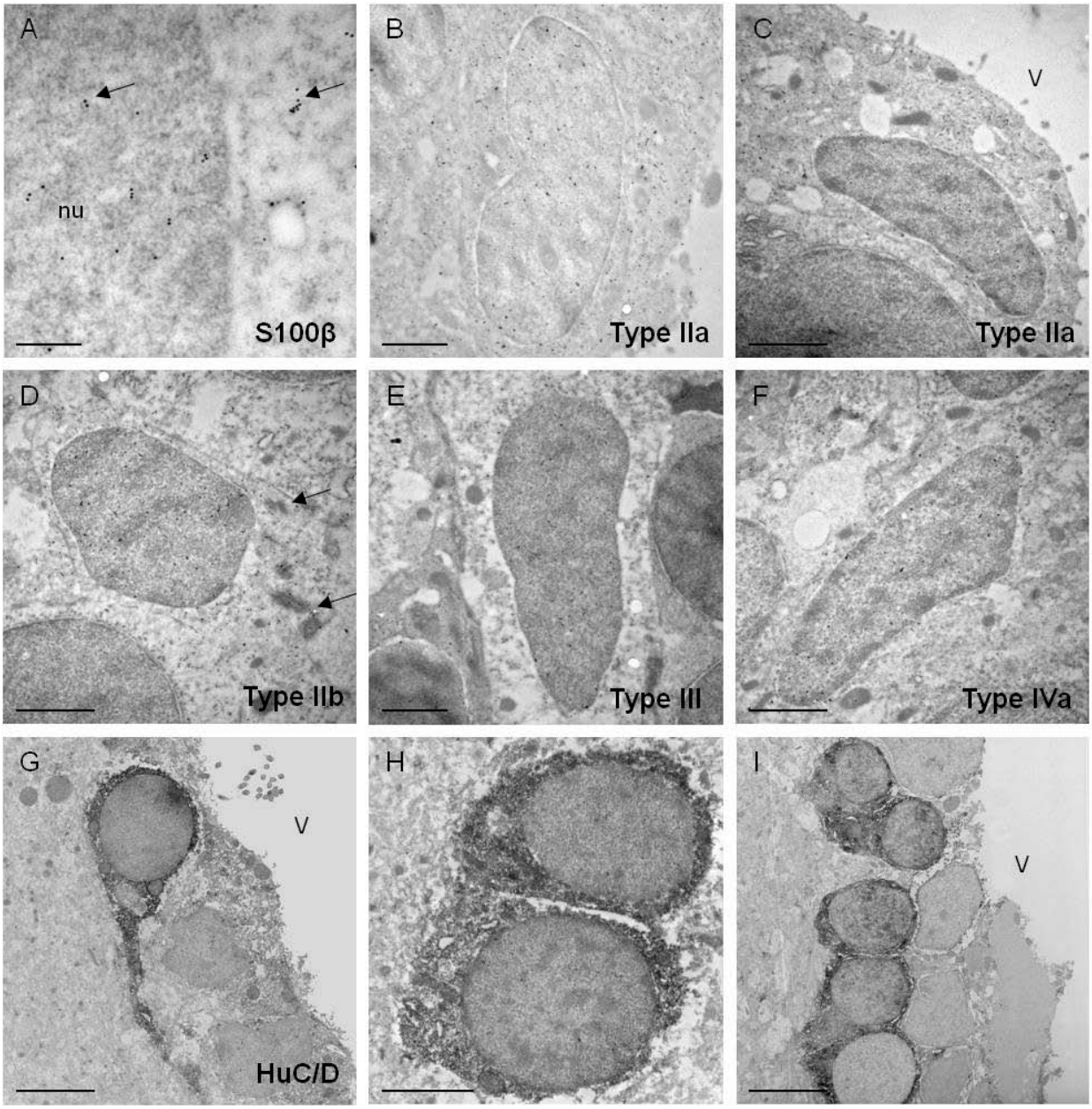
A
nu
S100β
B
Type IIa
C
V
Type IIa
D
Type IIb
E
Type III
F
Type IVa
G
V
HuC/D
H
I
V

Figure 2-15. Immunolabeling of resin-embedded tissue used to identify the morphological profile of cells with a general glial (S100β) or neuronal (HuCD) phenotype. **A-B,** High (**A**) and low (**B**) magnification images showing the localization of immuno-gold labeling of S100β overlapping in both the nucleus and cytoplasm (black arrows in **A**) in ***Type IIa*** cells in the absence of contrast staining. **C-F,** Examples of $S100\beta^{+}$ immuno-gold labeling of subpopulations of ***Type IIa*** (**C**), ***Type IIb*** (**D,** black arrows denote cilia), ***Type III*** (**E**), and ***Type IVa*** (**F**) cell types across different PVZs. **G-I,** Immuno-positive DAB labeling for the mature neuronal marker $HuCD^{+}$ confirming the morphological phenotype of neurons located within PVZs, and typically divided from the ventricular surface by cytoplasmic processes of surrounding cells. Mature neurons could often be easily detected by their large, ovoid nucleus. Note the staining pattern was specifically localized to the cytoplasm and processes of these cells. See also Table 2-6 for a summary of immunohistochemical labeling across all cell types. In all images dorsal is up. nu, nucleus; V, ventricle; DAB, 3,3'-Diaminobenzidine. Scale bars: **A,** 200 nm; **B, D, E, F,** 1 µm; **H,** 2 µm; **G, I,** 4 µm.

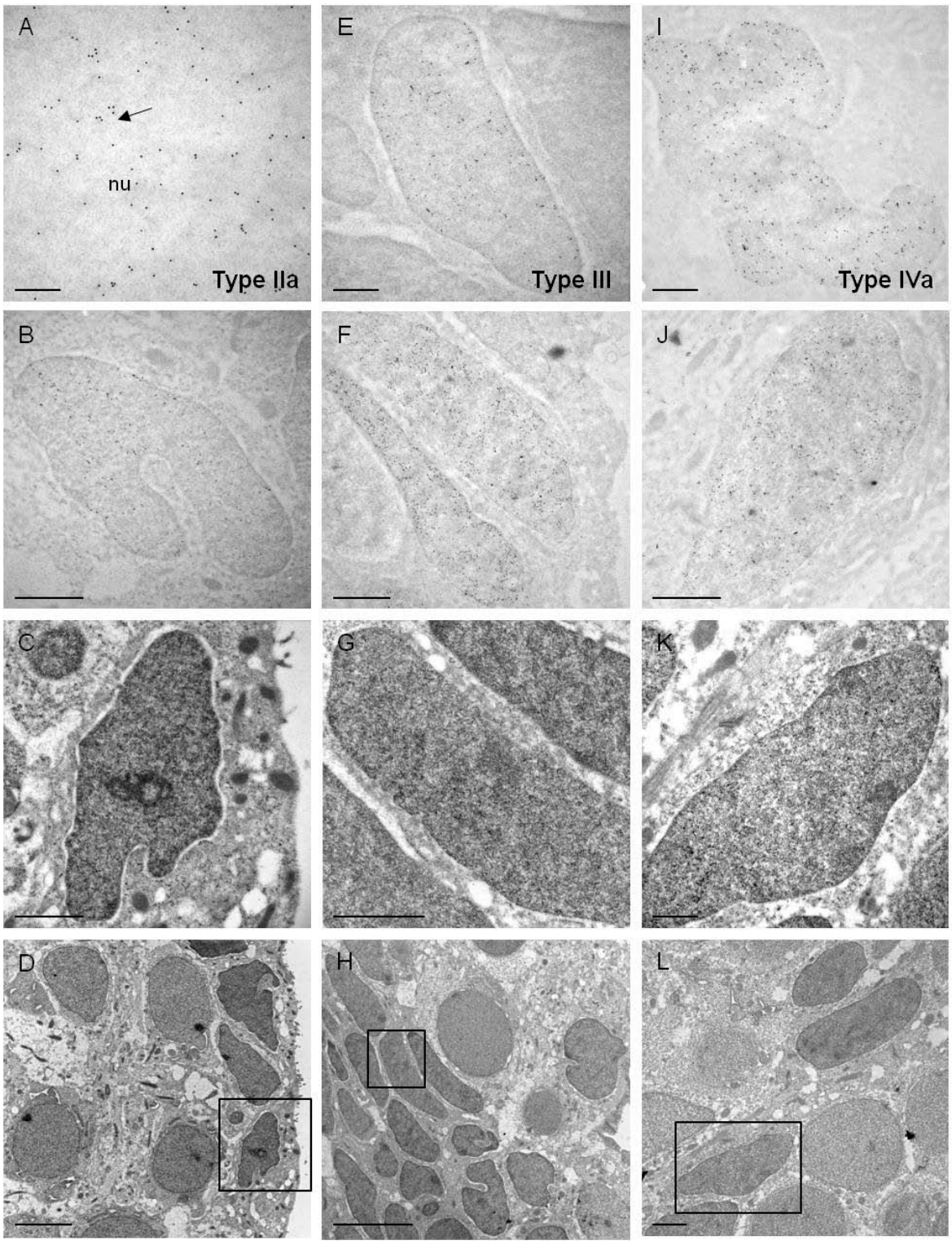
A
nu
Type IIa
E
Type III
I
Type IVa
B
F
J
C
G
K
D
H
L

Figure 2-16. BrdU^{+} immuno-gold labeling in *Type IIa* (A-D), *Type III* (E-H), and *Type IVa* (I-L) cells. A-D, High (**A**) and low (**B**) magnification images showing the specificity of gold particles to the nucleus (black arrow in **A**) in a subpopulation of proliferative ***Type IIa*** cells in the absence of contrast staining. Morphological features of ***Type IIa*** cells observed following contrast staining (**C**) and their position among adjacent cell types in the PVZ (**D**). **E-H,** A subpopulation of proliferative ***Type III*** cells without (**E-F**) and with (**G-H**) contrast staining showing their morphological features and position in the PVZ. **I-L,** A subpopulation of proliferative ***Type IVa*** cells without **(I-J**) and with (**K-L**) contrast staining displaying their characteristic morphological features and position in the PVZ. Black boxes in **D, H, L** indicates the same cell type shown at higher magnification in **C, G,** and **K** respectively. See also Table 2-6 for a summary of immunohistochemical labeling across all cell types. In all images dorsal is up. nu, nucleus. Scale bars: **A,** 200 nm; **B, C, F, G, J, L,** 1 µm; **D, H,** 4 µm; **E, I, K,** 500 nm.

2.4.6 The Number of Newborn Neurons Peaks 2 Weeks after Birth, Accounting for Nearly Half of the BrdU$^+$ Cell Population, But at 4 Weeks Few Neuronal Subtypes are Detected

In order to determine the timeline of neuronal differentiation across PVZs, I next performed an immunohistochemical labeling study where animals were pulsed with BrdU and sacrificed 1, 2, or 4 weeks later. Co-labeling of BrdU with PSA-NCAM to identify newly differentiated, migrating neurons revealed a notable increase in the number of BrdU$^+$/PSA-NCAM$^+$ cells between 1-2 weeks (Fig. 2-17A-B), however a significant difference was reported only for the PVZ of D (independent samples t-test). Four weeks following BrdU injections, BrdU$^+$/GS$^+$ labeling showed that in some niches (Dm, Dl) nearly 35% of BrdU$^+$ cells had given rise to radial glia cells (Fig. 2-17C, E). Considerable variation in the size of the BrdU$^+$/GS$^+$ cell population across PVZs could be seen, mainly between the pallial and subpallial zones (Fig. 2-17E). No BrdU$^+$/GS$^+$ co-labeling was found within the PVZ of Vv (Fig. 2-17D), while Ppa had less than 10% of the population BrdU$^+$/GS$^+$ (Fig. 2-17E). As a result, a significant difference in the percentage of BrdU$^+$/GS$^+$ cells was revealed between the subpallial zone of Vv and the pallial zone of Dm and Dl (one-way ANOVA; post hoc test). Moreover, by tracking the number of BrdU$^+$/HuCD$^+$ cells at multiple time points I was able to assess what percentage of the niche-specific BrdU$^+$ cell population gave rise to *de novo* neurons and when differentiation rates began to vary between PVZs (Fig. 2-17F-G). My data demonstrated a consistent rate of increase in neuronal differentiation across all PVZs from 2 hours to 1 week, after which time zones appeared to either increase (Dm, Ppa) or decrease (Vd, D) the rate of neuronal production, or the rate remained approximately the same (Vv, Dl; Fig. 2-17G). I found that with the exception of Vd, all forebrain PVZs reached the maximum number of newborn neurons by 2 weeks, with the number of BrdU$^+$/HuCD$^+$ cells typically decreasing thereafter.

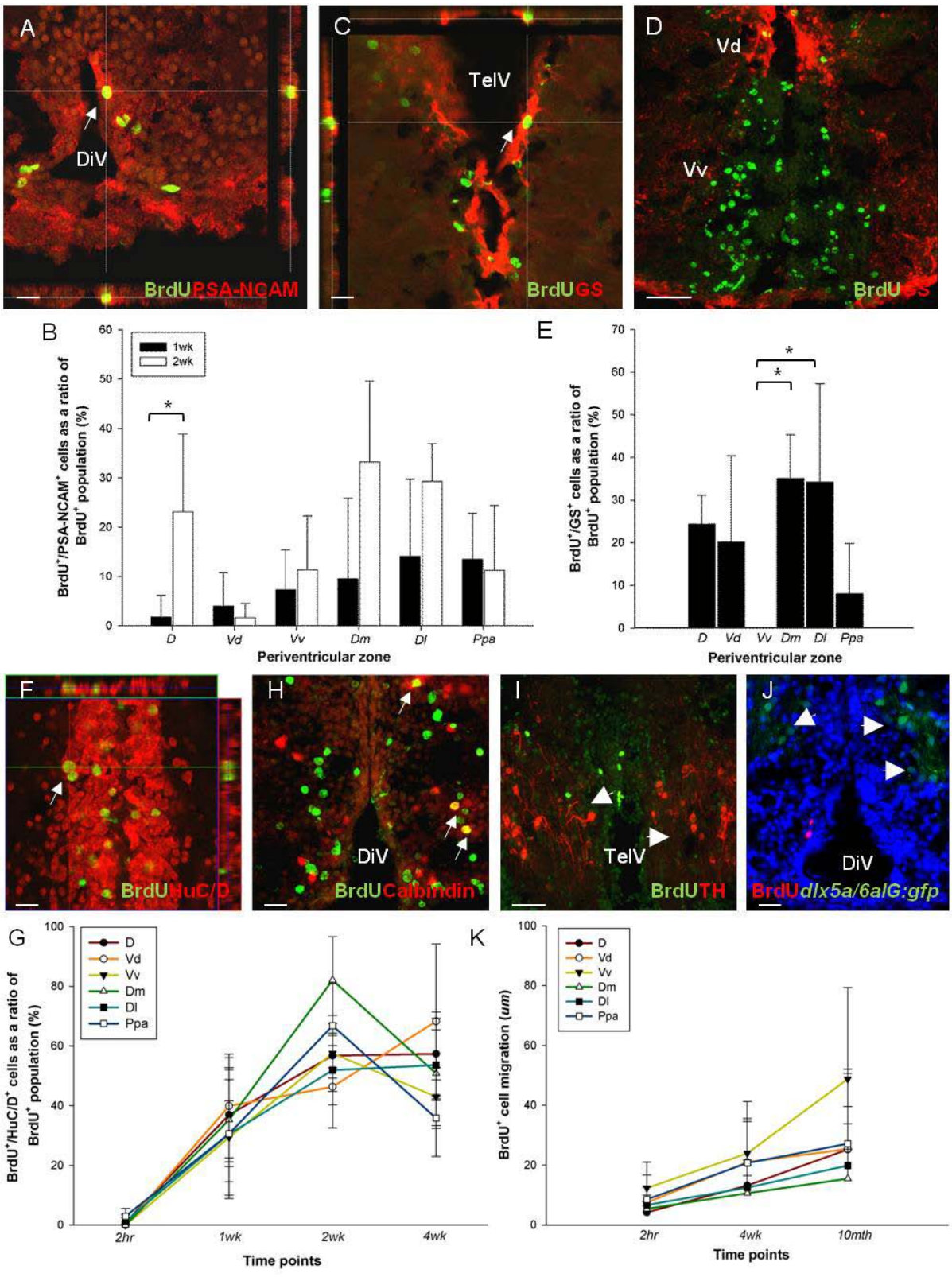
A
DiV
BrdU PSA-NCAM
C
TelV
BrdU GS
D
Vd
Vv
BrdU GS
B
1wk
2wk
BrdU+/PSA-NCAM+ cells as a ratio of BrdU+ population (%)
D
Vd
Vv
Dm
Dl
Ppa
Periventricular zone
E
BrdU+/GS+ cells as a ratio of BrdU+ population (%)
D
Vd
Vv
Dm
Dl
Ppa
Periventricular zone
F
BrdU HuC/D
H
DiV
BrdU Calbindin
I
TelV
BrdU TH
J
DiV
BrdU dlx5a/6aIG:gfp
G
D
Vd
Vv
Dm
Dl
Ppa
BrdU+/HuC/D+ cells as a ratio of BrdU+ population (%)
2hr
1wk
2wk
4wk
Time points
K
D
Vd
Vv
Dm
Dl
Ppa
BrdU+ cell migration (um)
2hr
4wk
10mth
Time points

Figure 2-17. Phenotype of BrdU$^+$ cells and displacement of this population following BrdU pulse-chase experiments compared between PVZs. A-B, BrdU$^+$/PSA-NCAM$^+$ co-labeling (**A**) quantified 1 and 2 weeks post-BrdU injection (**B**). Significance (*) was determined using independent samples t-tests ($p \leq 0.05$). **C-E,** BrdU$^+$/GS$^+$ co-labeling (**C**) quantified 4-weeks post-BrdU injection (**E**). Note that with the exception of the PVZ of *Ppa* and *Vv*, this population comprises nearly 20-30% of the phenotype of BrdU$^+$ cells. The absence of co-labeling detected in the PVZ of *Vv* is a result of little to no GS$^+$ staining within this region (**D**). Significance (*) was determined using a one-way ANOVA and Tukey's HSD post hoc tests ($p \leq 0.05$). **F-G,** BrdU$^+$/HuCD$^+$ co-labeling (**F**) quantified 2 hours, 1, 2, and 4 weeks post-BrdU injection to examine the percentage of newborn BrdU$^+$/HuCD$^+$ cells composing the BrdU+ cell population (**G**). Notice that within all PVZs a steady increase in the number of co-labelled cells is seen from 2 hours to 1 week, and that this trend continues until 2 weeks when the number of BrdU$^+$/HuCD$^+$ cells reaches a maximum, with the exception of the niche of *Vd*. The number of newborn neurons between PVZs was most variable between the chase period of 2-4 weeks, where this cell population could be seen to decrease (*Dm, Ppa, Vv*), plateau (*D, Dl*), or continue to increase (*Vd*). **H,** BrdU$^+$/Calbindin$^+$ staining observe in the PVZ of *Ppa* 4-weeks following birth. This population was only detected in *Ppa*, and consisted of less than 2% of the BrdU$^+$ cells. **I,** BrdU$^+$/TH$^-$ labeling in the PVZ of *Vv* after 4 weeks. In most PVZs the TH$^+$ cells could be seen near the lateral boundary (white arrowheads), but no co-labeling was observed. **J:** Dlx5a/6aIG/gfp+ labeling of a subpopulation of GABAergic cells detected within and bordering (white arrowheads) the different PVZs. No co-labeling of this cell population with BrdU$^+$ cells was observed. Nuclear counterstaining was done using Hoechst 33258 (blue). **K,** Migration of BrdU$^+$ cells from their original position within the boundaries of the PVZs at 2 hours, and examined following 4-week and 10-month BrdU chase periods. All PVZs demonstrated radial displacement ranging from 15-20 µm after 10 months relative to their original, with the exception of the PVZ of *Vv* which showed a considerably higher rate of migration over time. Refer to list of abbreviations for terminology. In all images dorsal is up. Scale bars: **A, C, F, H, J,** 8 µm; **D, I,** 50 µm.

To assess the phenotype of newborn neurons across PVZs, a series of labeling experiments using neuronal subtype-specific markers were further executed over the same 4 week pulse-chase timeline as above. Co-labeling with BrdU and the calcium binding protein, calbindin, or the dopaminergic marker tyrosine hydroxylase (TH) revealed a near absence of co-labeled populations following the 4 week differentiation period. Less than 2% of $BrdU^+$ cells were also positively labeled for calbindin in the PVZ of Ppa (Fig. 2-17H). $Calbindin^+$ labeling was observed in all other PVZs, however, no co-labeling was detected. No co-labeling of $BrdU^+/TH^+$ cells was observed across any of the PVZs investigated, with TH^+ cells typically localized to the lateral aspect of most niches (Fig. 2-17I). Similarly, positive co-labeling of BrdU and expression of GFP from the transgene *Tg[dlx5a/6aIG:gfp]*, which marks a large fraction of GABAergic neurons during late embryonic and early larval development, could not be detected in any PVZs, despite the presence of a relatively high number of GFP^+ cells within and surrounding some PVZs (Fig. 2-17J).

Finally, to obtain positional data related to the migration pattern of differentiating $BrdU^+$ cells arising from within the PVZ over the long term, I examined the position of $BrdU^+$ cell populations after 2 hours, 4 weeks, and 10 months (Fig. 2-17K). The displacement of $BrdU^+$ cells was determined by measuring the cell from the center of the nucleus to the edge of the ventricle at each time point. The movement of $BrdU^+$ cells shows that across all PVZs this population migrated away from the ventricle over the first 4 weeks, albeit at different rates. After only 4 weeks many of the $BrdU^+$ cells sampled were positioned outside of the lateral borders of the PVZ. With the exception of Vv, it appeared that 10 months post-BrdU injection cells had displaced between 10-20 μm from their original position within the boundaries of the niche at 2 hours; some resembling a near plateau. In contrast, $BrdU^+$ cells within the PVZ of Vv displayed a marked increase in cell migration between 4 weeks and 10 months, with the curve suggesting migratory behaviour of these cells well beyond the maximum 10 month time point used here. These findings suggest that at least one common mode of cell migration of newborn neurons is to exit the boundaries of the PVZ over time by radial migration towards the parenchyma. I did not evaluate the possibility of tangential migration in these experiments. However, whether the rate of migration and position of newborn neurons over time can indicate the phenotypic fate of these cells remains to be tested.

2.5 Discussion

Studies of the adult neurogenic niche of vertebrate (Garcia-Verdugo et al., 2002) and invertebrate (Schmidt and Derby, 2011) species have reported a range of different cellular organizations since the composition of the mammalian SEZ niche was first proposed over a decade ago (Doetsch et al., 1997). To advance our understanding of niche-specific differences across vertebrates, the present study has documented the cytoarchitectural organization of six distinct forebrain neurogenic niches (periventricular zones; PVZs) in a model teleost species, the zebrafish, by comparing the cellular composition between niches. Based on this work I present a novel classification scheme of the niche-specific cell types and propose a model of the organization of these cells between pallial and subpallial zones of the adult zebrafish forebrain. I further complemented these morphological studies with comparisons of the density of proliferative cells, the cell cycle kinetics, the phenotype of proliferative cells, and the rate of neuronal differentiation between PVZs to gain insight towards the fundamental cellular properties regulating neuronal production in the adult brain.

2.5.1 Model of the Ultrastructural Composition of Adult Zebrafish Forebrain Neurogenic Niches

A central aim of the present study was to provide a detailed account of the ultrastructural composition of the major forebrain PVZs in the adult zebrafish. Here, I propose two cytoarchitectural models summarizing my descriptive analysis of six distinct neurogenic PVZs (Fig. 2-18). Detailed transmission EM across PVZs revealed seven morphologically distinct cell types, all of which display varying frequencies between zones. Of these cell types only two were multiciliated (Type IIb, Type IVb), while four non-ciliated cell profiles were observed in addition to neurons. Figure 2-18A shows the common cellular composition of the PVZs of D, Vd, Dm, Dl, and the dorsal zone of Ppa, with Type IIb and IVb cells exclusive to the niche of Ppa. Type IIa cells with extensive cytoplasmic processes, along with neurons, were typically

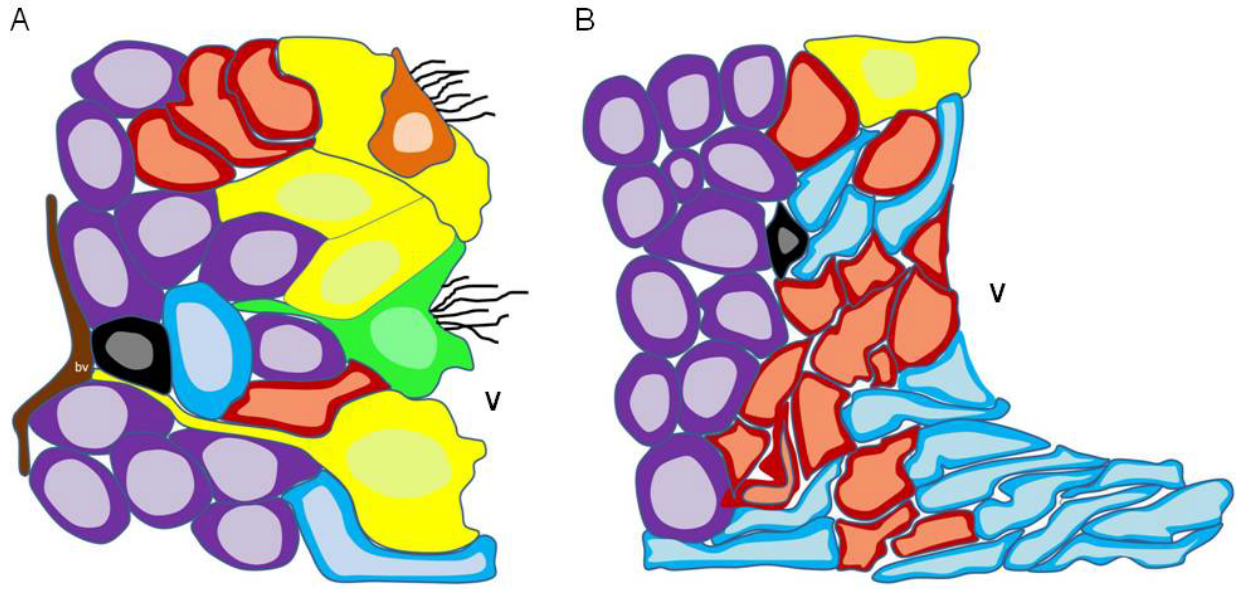

Type IIa
- Frequent
- Non-ciliated
- Subpopulation BrdU+
- Subpopulation GS+
- S100β+

Type IIb
- Infrequent
- Multiciliated
- Subpopulation S100β+

Type III
- Frequent
- Non-ciliated
- Subpopulation BrdU+
- Subpopulation S100β+

Type IVa
- Frequent
- Non-ciliated
- Subpopulation BrdU+
- Subpopulation S100β+

Type IVb
- Infrequent
- Multiciliated
- No labelling detected

Type V
- Infrequent
- Non-ciliated
- No labelling detected

Neurons
- Frequent
- HuC/D+

Figure 2-18. Model of the ultrastructural organization and cell types composing the six neurogenic PVZ niches described in this study. A, Schematic representation of the cellular composition of the PVZ of *D, Vd, Dm, Dl*, and the dorsal zone of *Ppa*. Note that multiciliated ***Type IIb*** and ***IVb*** cells were only observed in the dorsal zone of the PVZ of *Ppa*, while all other cell types were commonly observed across PVZs. The processes of ***Type IIa*** cells could be observed extending into the deeper layers of the PVZ and at times contacting proximal blood vessels (bv). Note that the subpallial PVZ of Vd and the dorsal zone of Ppa appear to contain a cytoarchitectural organization more closely resembling pallial PVZs. **B,** Schematic representation of the cellular composition of the PVZ of *Vv* and the ventral zone of the PVZ of *Ppa*. These two ventrally located niches consisted almost exclusively of a density of ***Type III*** and ***Type IVa*** cells, with a number of neurons forming the deeper layers of the niche. The main features of each cell type are denoted in the legend. v, ventricle. Refer to list of abbreviations for additional terminology.

most abundant in these niches, with a lesser number of Type III, IVa, and V cells observed. By contrast, the subpallial ventral zone of Ppa and the PVZ of Vv shared a similar composition, comprised primarily by Type III and Type IVa cells, and neurons (Fig. 2-18B). These findings reveal that the subpallial located niche of Vd and dorsal zone of Ppa more closely resemble the ultrastructural organization of pallial PVZs. This may imply that a similar set of cellular and non-cellular cues regulating the pallial niches overlap within the niche of Vd and the dorsal zone of Ppa. Immunolabeling of resin embedded tissue exposed three proliferative cell types, including subpopulations of $S100\beta^+/GS^+/BrdU^+$ Type IIa cells, $S100\beta^+/BrdU^+$ Type III cells, and $S100\beta^+/BrdU^+$ Type IVa cells. These findings suggest a dichotomy not only between the cellular makeup of pallial and subpallial PVZs, but additionally the proliferative phenotypes of cells, with pallial PVZs (including the dorsal zone of Ppa) containing three different mitotic populations, compared with only two in the subpallial PVZs of Vv and Ppa (ventral zone).

2.5.2 Forebrain Neurogenic Niches in the Adult Zebrafish Share Intermediate Features with the Ultrastructural Composition of the Ventricular Niche of their Vertebrate Relatives

The number of neurogenic niches in teleosts out-numbers those described in mammals, though the mechanisms regulating this difference are still not well understood. Few studies have examined the cellular composition of neurogenic niches of telost fishes or amphibians, two anamniotic vertebrate classes distinguished for both their regenerative and neurogenic capacities throughout life (reviewed in Lindsey and Tropepe, 2006). Uncovering the constituent cell types composing the neurogenic microenvironment remains an essential starting point to elucidate the manner by which active proliferation and neurogenesis are maintained throughout maturity in these species. Given the phylogenetic position of teleost fishes, the notion that the ultrastructural features of niches may more closely resemble those of their non-mammalian relatives might be expected compared with mammals, however, from my studies I find that these niches demonstrate intermediate cellular features of both groups. I show that the composition of periventricular niches in the adult zebrafish forebrain are made up of a complexity of cell morphologies creating distinct neurogenic compartments, similar to the numerous cell types present in the SEZ of mammals. The occurrence of the seven cell types described in these

compartments show both niche-specific pallial and subpallial differences, in addition to regionally specific variation in cell types within a single niche (i.e., PVZ of Ppa). A key finding of this work was the paucity of classical ependymal cells within any of the niches examined (Fig. 2-7), unlike the continuous ependymal lining observed along the ventricular surface of the SEZ of mammals (Doetsch et al., 1997; Gil- Kam et al, 2009; Perotin et al., 2009; Sawamoto et al., 2011) or the fragmented ependymal lining seen in the neurogenic niches of reptiles and birds (reviewed in Garcia-Verdugo et al, 2002). Ependymal cells were exclusively observed forming the roof of the telencephalic ventricle and covering the forebrain hemispheres a short distance dorsolaterally in the pallial niches of D and Dm.

Within the neurogenic PVZs themselves, GS^+ radial glial-like Type IIa cells seem to resemble Type B1 astrocytes previously described in mammals (Doetsch et al., 1997) and the homologous Type B radial glia of birds and reptiles (Garcia-Verdugo et al., 2002). The apparent absence of a single cilium in Type IIa cells described in my study may indicate a modified form of radial glia or that these went undetected during my analysis. A small number of cilia could often be seen in the ventricle adjacent all PVZs, however, unless cilia could be reliably traced back to the corresponding cell type, cells were classified as lacking cilia.

Based on the occurrence of cell types between niches, a clear dichotomy in the cellular composition between select pallial and subpallial niches was apparent. The subpallial rostral niche of Vv and the ventral zone of the caudal niche of Ppa surrounding the diencephalic ventricle were composed almost exclusively of a number of tightly packed Type III and Type IVa cells. The ultrastructural features and $BrdU^+$ labeling of Type III and Type IVa cells are reminiscent of morphological profile of Type A and Type C cells in mammals (Garcia-Verdugo et al., 2002), respectively. However, in the forebrain niches of the adult zebrafish these cell types are seen both at the ventricular surface in addition to the deeper layers of the niche, in contrast to the position of Type A cells in mammals, birds, and reptiles, and Type C cells in mammals, which are divided from the luminal surface by Type B cells. Furthermore, Type III cells in zebrafish express S100β, which is not expressed in the Type A neuronal progenitors in the mammalian forebrain.

In one of the first studies investigating the proliferative ventricular zone of a teleost, Zupanc and Zupanc (1992) revealed a density of cells with medium to darkly staining nuclei,

elongate/irregular nuclear contours and lightly staining cytoplasm within the central posterior pre-pacemaker nucleus situated in the third ventricle of the weakly electric knifefish (*Eigenmannia* sp.). Similar to the localization of Type III and IVa cells in this study, the elongated cells with lighter staining nuclei were more often situated at the lumen, while the darkly staining cells which appeared to have more irregular nuclear contours were located 1-2 layers. This earlier study also showed evidence of multiciliated subpopulations of cells intermingled with the above cell types along the third ventricle, which is in line with the multiciliated Type IIb and Type IVb cells detected specifically in the PVZ of Ppa here. The restricted localization of Type IIb and IVb cell types to the niche of Ppa was a surprising finding, given the proposed role of cilia for cerebrospinal fluid flow to provide directional migration of differentiating neurons (Mirzadeh et al., 2010; Amador-Arjona et al., 2011). Whether these multiciliated cell types present only in the subpallial niche of Ppa surrounding the diencephalic ventricle have developed specialized functions or serve as the ependymal-like cells of this ventricle to provide fluid flow in the absence of an ependymal lining, as seen in the roof of the telencephalic ventricle, remains to be determined.

More recently, studies in the adult zebrafish forebrain have revealed the compact cellular nature of the subpallial neurogenic compartment of Vv. Work by Ganz et al., (2010) used resin embedded semithin sections to display the general composition of this niche and the presence of mitotic profiles at the ventricular surface, similar to the location of mitoses seen in the niche of Vv and Ppa here. In line with this, I have confirmed the proliferative nature of subpopulations of Type III and Type IVa cells at the ultrastructural level by using immunogold labeling for $BrdU^{+}$ cells. I show that these two cell types which are most prevalent in niches surrounding the ventral telencephalic and diencephalic ventricles are immunopositive for BrdU and the general glial marker S100β. However, in contrast to Type IIa cells discussed above, these two populations did not label with the radial glial/astrocytic marker GS. Interestingly, a recent study examining the putative rostral migratory stream in the adult zebrafish forebrain proposed the presence of three morphologically distinct cell types in the niche of Vv, identified by having either round nuclei, non-elongated nuclei, or elongated nuclei with a single cilium extending into the ventricle, with these authors proposing the elongated cell morphology as the radial glial cell resident in the niche (Kishimoto et al, 2011). The elongated cell morphology described by Kishimoto et al. (2011) is in agreement with the Type III cells based on my classification scheme across PVZs,

however, my data do not support the notion that these cells are radial glia. First, across all PVZs examined I did not convincingly detect cilia projecting from this cell type, nor were these cells immunopositive for GS at the ultrastructural level. Moreover, immunolabeling studies of cryosectioned tissue corroborated these ultrastructural results, showing an almost complete lack of $BrdU^+/GS^+$ co-labeling in cells located in the subpallial niches of Vv and Ppa 2-hours (Fig. 2-6F) and 4-weeks (Fig. 2-17C-E) post-BrdU injections composed mainly of Type III and Type IVa cells. Finally, never did I see radial-glia like processes extending into the deeper layers of the niche while examining Type III cells, whereas this was most commonly detected in Type IIa cells (Fig. 2-11E). I do not dispute that the elongated profile of Type III cells is suggestive of a proliferating progenitor phenotype, although the multiple lines of evidence shown here do not support the view that these cells have a radial glial morphology.

2.5.3 Specifying the Boundaries of the Neurogenic Niche and Evaluating its Proliferative Capacity

A hallmark feature of adult neurogenesis is the existence of an actively dividing proliferative pool of stem/progenitor cells from which *de novo* neurons can be generated over time. The size of the proliferative pool and their associated cell cycle kinetics directly influence the neurogenic output of the niche, and thus defining the niche boundaries where this mitotic population is maximal is crucial to uncovering the phenotype of adult neural stem/progenitor cells. Here, I show that along the rostrocaudal axis of each of the six neurogenic PVZs examined there exists a narrow range in which the density of mitotic cells is greatest, which can be used to more stringently specify the niche boundaries in this plane (Figs. 2-2; 2-3). In defining the rostrocaudal boundaries I found niches could be categorized into three groups: niches showing a fairly even distribution of $BrdU^+$ cells between the rostral- and caudal-most levels (D, Dm); niches displaying significantly denser populations of $BrdU^+$ cells more rostrally (Vd, Vv); and, niches demonstrating a significantly higher density of $BrdU^+$ cells at the caudal-most extent of the neuroanatomical region in which they reside (Dl, Ppa). The density of $BrdU^+$ cells situated rostrally in the PVZ of Vv reported here, agrees well with other studies examining the subpallial niche of Vv as the source of proliferative cells migrating along a putative rostral migratory stream towards the olfactory bulbs (Adolf et al., 2006; Marz et al., 2010; Kishimoto et al, 2011).

The localization of niche boundaries along the rostrocaudal axis of the forebrain nuclei in which they reside appears in most cases to be positively correlated with the size of the forebrain ventricle. For instance, the size of the telencephalic ventricle along the rostrocaudal axis of D and Dm shows little variation, whereas this same ventricle in the subpallium is most prominent at the rostral aspect of Vd and Vv, with the diencephalic ventricle adjacent Ppa showing a more caudal enlargement. This trend may in part be explained by the need for ventricular fluid flow to provide trophic support to the stem/progenitor populations residing in the niche in order to maintain an active state for proliferation (Buddensiek et al., 2010). Additionally, the vascular environment is likely to play a role in the regionalization of neurogenic niches in the zebrafish forebrain as demonstrated in the mammalian SEZ (Tavazoie et al., 2008).

The cell cycle kinetics of proliferative stem/progenitor cells initiate the process of adult neurogenesis within the boundaries of the niche and provide a method of identifying different proliferative populations based on their cell cycle parameters. Earlier studies using cumulative BrdU labeling in the SEZ of mammals have shown that within a single adult niche regional variation exists, demonstrating the greatest growth fraction of $BrdU^+$ cells in the dorsolateral region of the SEZ with a total cell cycle time of 12.7 hours and S-phase length of 4.2 hours (Morshead and van der Kooy, 1992). I found that the number of proliferating $BrdU^+$ cells labeled in the PVZ of D, Vv, Dm, and Dl continued to increase in size (i.e., growth fraction) beyond the endpoint of my study (12.5 hours), with the niche of Vv having the greatest estimated minimum growth fraction (~29%). From the minimum growth fraction estimates of these niches, my findings indicate the presence of relatively slowly cycling cell populations with the total length of the cell cycle ranging from ~15 – 23 hours. By contrast, the niche of Ppa and the first of two potential cellular populations within Vd displayed properties suggestive of relatively fast cycling cells, with cell cycle lengths of ~7.5 hours and 11 hours, respectively.

My results are in partial agreement with one previous study using co-labeling of $BrdU^+/PCNA^+$ cells to detect slow and fast mitotic populations across similar niches as examined here (Adolf et al., 2006). These authors proposed the existence of fast dividing cells within the subpallial niches of Vv and Ppa, with the remaining niches consisting of slow dividing cells and that this latter population continued to increase over 10 days. However, since only the growth fraction was reported from the different niches assessed in the previous study, it is difficult to make direct comparisons with the cell cycle kinetics revealed from my experiments. Furthermore, a

limitation in my analysis is that I cannot precisely identify which cell type is cycling at a given estimated cell cycle time within the different PVZs. Nonetheless, my data suggests that in D, Vv, Dm, and Dl all three proliferative cell types present (Type IIa, III, IVa) are cycling at similar rates, whereas this may not be the case in the niche of Vd which demonstrated possible evidence of two different proliferative populations. Future studies aimed at tracking specific cell type are required to gain a richer understanding of the population kinetics of the niche.

2.5.4 Towards a More Comprehensive View of the Phenotype of Cells Composing Neurogenic Niches and Regulating Neuronal Output in the Adult Zebrafish Forebrain

The ability to classify the cell types within the microenvironment of the niche by phenotype and lineage is critical to permit comparisons with the cellular organization of different animals and to understand differences in the molecular control of these cells. In line with earlier studies (Ganz et al., 2010; Marz et al., 2010), my work has shown the presence of at least two separate glial cell populations within PVZs, including populations immunopositive for BrdU/S100β or BrdU/GS; some demonstrating the presence of cilia. Similar to Ganz and colleagues (2010), I showed a complete absence of the canonical radial glia markers GS in the subpallial niches of Vv and Ppa, and only minimal $BrdU^+/GS^+$ expression in Vd, compared with the pallial niches of D, Dm, and Dl. Moreover, all pallial niches also showed larger $BrdU^+/S100\beta^+$ populations. The above studies align well with my classification scheme based on the morphological cell phenotypes identified at the ultrastructural level across PVZs. First, subpopulations of $BrdU^+/S100\beta^+/GS^+$ Type IIa cells were not present within the niche of Vv, nor the ventral zone of the niche of Ppa, but could be detected in all other niches examined displaying features of radial glial cells. Secondly, populations of Type III and IVa cells, positive for BrdU/S100β almost exclusively composed the niches of Vv and Ppa (ventral zone), but could be observed in all niches. In addition to describing glial populations across PVZs, in this study I also discovered rare proliferative pools of cells immunopositive for BrdU/Pax6 and BrdU/SOX2. Expression of the transcription factor Pax6 is well known to play a critical role during teleostean (Wullimann and Rink, 2002) and mammalian (Sakara and Osumi, 2008) forebrain development. Both SOX2 and Pax6 have been used extensively as stem cell markers, and in the adult zebrafish forebrain SOX2

expression has been associated with defining progenitor cell types within neurogenic zones (Marz et al., 2010). The infrequent detection of cycling $Pax6^+$ (PVZ of Dl) and $SOX2^+$ (PVZ of Ppa) cells make these phenotypes potential candidates of slow cycling stem/progenitor populations.

Marz and colleagues (2010) reported the phenotype of four progenitor cell types within niches lining the telencephalic ventricle, consisting of non-dividing radial glia (Type I), dividing radial glia (Type II), dividing radial glia with PSA-NCAM expression (Type IIIa), and non-glial PSA-$NCAM^+$ progenitors (Type IIIb). With the exception of Type IIIb, all other cell types were seen to exhibit strong $nestin^+$ expression. In fitting my ultrastructural classification with the above progenitor phenotypes, it would appear that my Type IIa cells align most closely with Type II progenitors as evidence both by immunolabeling and the location of these cells in the dorsomedial (Vd, D, Dm) and lateral niches (Dl). These cells were immunopositive for the two glial markers (S100β, GS) as well as the S-phase marker BrdU. Long processes could further be seen radiating into the deeper cell layers in medially located niches and a high occurrence of Type IIa cells could be observed in the PVZs of D, Vd, Dm, Dl and the dorsal zone of Ppa. More challenging is correlating $BrdU^+/S100^+$ Type III and IVa cells with the above progenitor classification given that the location of these cells agree with the subpallial position of progenitor cells in the niche of Vv and Ppa. However, the difficulty in successfully immunolabeling these cell types with multiple markers at the ultrastructural level limits the degree to which I may infer their phenotype. The positive immuno-gold labeling for S100β and BrdU for both Type III and IVa cells seen from my data likely suggests one of these two cell types as candidates for Type IIIa progenitor phenotype proposed by Marz et al. (2010). From the above comparisons between immunolabeling and ultrastructural studies I propose that Type IIa cells, or at least a subpopulation of these, is of a radial glial phenotype. However, the lineage relationship of the cell types identified within the adult forebrain neurogenic niches of the zebrafish still remains an open question that will require further detailed analyses.

Adult-born neurons commonly undergo radial or tangential migration to arrive in locations outside the boundaries of the niche and become committed to a specific neurotransmitter-expressing phenotype. Since my findings showed that approximately 50% or more $BrdU^+$ cells give rise to newborn neurons across PVZs (Fig. 2-17G), by tracking proliferative cells over time I was able to evaluated the displacement of differentiating cells. My data shows that cell

displacement continues up until 8 months, with newborn neurons in most PVZs having migrated radially from their initial position by this time. Whether the rate of displacement by newborn cells is correlated with the time required for a neuronal-specific phenotype to become specified during the process of migration remains unknown. However, only one week post-BrdU injections co-labeling of $BrdU^+/HuCD^+$ cells could be detected in all niches. Adolf et al. (2006) showed that as early as 3 days post-BrdU injection newborn neurons could be detected, with proportions reaching a maximum after 2 weeks time. My experiments investigating the timeline of neuronal differentiation revealed a nearly identical pattern, with PVZs displaying the greatest proportion of differentiated neurons at 2 weeks and consisting of 40-80% of the $BrdU^+$ cell population. By 4 weeks however, a drop in the percentage of newly differentiated neurons was noted across most niches. Further, these data show that the number of differentiated neurons between 2-4 weeks time decreases by approximately 20% in the niches of Dm and Ppa, which may be a result of greater apoptotic activity. To my surprise, at 4 weeks only a small number of $calbindin^+/BrdU^+$ cells were detected in the niche, with no co-labeling of BrdU with TH or a transgenic marker of GABAergic neurons, *Tg[dlx5a/6aIG:gfp]*. Long-term chase experiments of up to 270 days in related proliferative zones have shown a complete absence of $calbindin^+/BrdU^+$ labeling (Zupanc et al., 2005). However, newly differentiated subtypes of TH^+ and $gad67^+$ neurons have been identified 2 months after BrdU injections in the rostral telencephalon (Adolf et al., 2006), and indicate that these neuronal subpopulations require a longer time period than used here, in order to become committed to one of these two subtypes. Aside from the length of the differentiation period, my data suggests that mitotic cells arising from PVZs might instead give rise to alternative neuronal phenotypes than those examined here, such as glutamatergic or cholinergic neurons. Determining the neuronal-specific phenotype of cells generated from neurogenic niches will be an important step in elucidating their functional role in the mature CNS.

2.5.5 Conclusions

I propose a model illustrating differences in the cellular organization of forebrain neurogenesis in zebrafish niches and a novel classification scheme of the seven morphologically distinct cell types composing these niches. Of these cell types my data suggests that cycling Type IIa cells are a likely candidate for the morphological phenotype of radial glial-like stem cells. These studies also revealed that pallial and subpallial niches harbour differences in their cellular organization. Finally, by investigating the cell cycle characteristics and rates of neuronal differentiation between niches, I show that although similar cell types are distributed among forebrain niches, the frequency of these cells and how they are regulated within the niche to give rise to adult-born neurons varies widely. The findings presented here should serve as a foundation for investigating the lineage relationships of cells within these niches as well as the degree to which they undergo neurogenic plasticity.

CHAPTER 3

CHANGES IN THE SOCIAL ENVIRONMENT INDUCE NEUROGENIC PLASTICITY PREDOMINANTLY IN PRIMARY SENSORY NICHES OF THE ZEBRAFISH BRAIN INDEPENDENTLY OF CORTISOL LEVELS

3.1 Abstract

The social environment is known to modulate adult neurogenesis. Studies in mammals and birds have shown a strong correlation between social isolation and decreases in neurogenesis, whereas time spent in an enriched environment has been shown to restore these deficits and enhance neurogenesis. These data suggest that there exists a common adaptive response among neurogenic niches to each extreme of the social environment. I sought to further test this hypothesis in zebrafish, a social species that harbours distinct neurogenic niches within brain regions that function as primary sensory processing centers or integrative centers. By examining stages of adult neurogenesis, including the proliferating stem/progenitor population, their surviving cohort, and the resulting newly differentiated neuronal population, I show that social isolation or novelty are both capable of decreasing the number of proliferating cells while increasing the number of newborn neurons within a single niche, challenging the notion that social deprivation and social enrichment have entirely opposite effects on adult neurogenesis. This was most prevalent in the sensory niche of the optic tectum. Contrary to observations in rodents, I demonstrate that cortisol levels do not negatively regulate changes in adult neurogenesis, but rather are correlated with the social context. Moreover, modulation of cortisol levels appears to be associated with experience from a preceding social environment. I propose that activation or inhibition of adult neurogenesis in the zebrafish brain under different social contexts depends largely on the type of niche (sensory or integrative), and occurs independently of changes in cortisol levels.

3.2 Introduction

The social environment is known to regulate constitutive levels of adult neurogenesis in vertebrates. Predictable social interactions with kin, mates, and predators, as well as environmental factors, are responsible for maintaining adult neurogenesis within a narrow physiological range at each stage of this process, including stem/progenitor cell proliferation, long-term survival of the post-mitotic population, their potential to differentiate into neurons, and their survival and functional integration into existing circuitry (Lindsey and Tropepe, 2006; Kempermann, 2011). By deconstructing the complexity of the social environment however, it is clear that much of the information that an animal encodes encompasses both learned components that are processed in higher-order brain regions, such as the hippocampus, as well as modality-specific sensory components that are processed in corresponding primary sensory structures. What happens then to baseline levels of adult neurogenesis when social animals venture outside of their home range, are separated from their social group, or undergo novel social interactions? How might environmental change activate neurogenic plasticity and alter the composition of the neurogenic niche in the adult vertebrate brain? This raises the question of whether neurogenic niches residing within primary sensory regions of the brain, compared with those localized to higher-order integrative brain structures that receive sensory input, respond differently at the cellular level to deviations from a familiar social context.

Studies in birds and mammals have shown convincing evidence that acute post-embryonic or adult social isolation is strongly correlated with decreases in cell proliferation and/or neuronal differentiation in hippocampal structures (Barnea et al., 2006; Lieberwirth et al., 2012), owing to an increase in the stress-related hormone cortisol (Schoenfeld and Gould, 2011). The negative effect of isolation stress on cell proliferation in the dentate gyrus can also override the positive effects incurred by physical exercise in rats (Stranahan et al., 2006; Leasure and Decker, 2009), while stress-related decreases in hippocampal subgranular zone (SGZ) proliferation can be restored with short-term environmental enrichment (Veena et al., 2009). Interestingly, enrichment paradigms that elicit a structural change in adult hippocampal neurogenesis often have little effect in the subependymal zone (SEZ) of rodents (Brown et al., 2003), implying that niches may be independently modulated by specific environmental cues. Studies show that SEZ neurogenesis can be altered in response to olfactory enrichment (Rochefort et al., 2002), estrous

induction (Smith et al., 2001), and male exposure (Fowler et al., 2002), though it is still unclear whether social isolation can mediate changes in this niche. Few studies have successfully shown examples of parallel neurogenic plasticity in the SEZ and SGZ using the same methodology. Where observed, researchers have probed biologically relevant contexts including offspring recognition and mating pheromones (Mak et al., 2007; Mak and Weiss, 2010).

Besides our understanding of adult neurogenic plasticity within the SEZ of mammals, there is relatively little information available on how alternative sensory structures are modulated in vertebrates in response to changes in the social environment. Even within mammalian models, the primary source of adult neural stem cells destined for the olfactory bulbs reside within the SEZ (Gritti et al., 2002), and not within the olfactory bulb proper. Changes in constitutive levels of adult neurogenesis reported in the olfactory bulb under different environmental conditions are achieved by targeting SEZ stem/progenitor cell populations, and therefore it still remains unclear how changes in social context could modulate a stem/progenitor population localized to the vertebrate olfactory bulbs. Teleost fish, such as the zebrafish, offer a vertebrate model system that maintains proliferative populations within the olfactory bulbs, allowing direct examination of this question.

Earlier studies of natural populations of cichlids in the African Great Lakes have demonstrated a direct relationship between the lifestyle of these individuals within their microhabitat and the size of primary sensory structures (Huber et al., 1997; Kotrschal et al., 1998), highlighting that the composition of sensory structures such as the olfactory bulbs (olfaction), optic tectum (vision), and vagal lobe (gustation), can be shaped by environmental cues. Invertebrate models of adult neurogenesis have also revealed neurogenic plasticity directly within neurogenic niches that process olfactory stimuli (Hansen and Schmidt, 2004), and that such changes can lead to a re-organization of the composition of the niche. Most recently, studies in the *Drosophila* brain have elucidated how both enrichment and experience can differentially modulate cell lineages within the mushroom bodies (olfactory processing) and antennal lobes (parallel processing), and that these changes as a result of plasticity have an adaptive role in line with the ethology of the species (Lin et al., 2013). In the present study, I was interested in whether the notion that neurogenic plasticity in vertebrates is associated with suppressed adult neurogenesis in the presence of environmental deprivation, while enhanced under conditions of enrichment, holds true in alternative vertebrate neurogenic compartments, in particular those that process primary

sensory stimuli.

Here, I sought to test how contrasting social contexts, such as isolation and novelty, can modulate constitutive levels of adult neurogenesis in primary sensory neurogenic niches of the olfactory bulb, optic tectum, and vagal lobe compared with integrative niches of the dorsal (pallium), ventral (subpallium), and lateral (i.e. proposed homologue of mammalian hippocampus) zones of the telencephalon, within the adult zebrafish brain. Additionally, I investigated the role of whole-body cortisol levels under different social contexts as a putative mechanism underscoring changes in the size of the stem/progenitor population. The zebrafish (*Danio rerio*) has become an attractive model for its array of social behaviours (Spence et al., 2008) and robust neurogenic capacity within both sensory and integrative centers (Zupanc et al., 2005). Moreover, the precocial nature of zebrafish allows animals to be reared in chronic isolation, providing the opportunity to further examine how developmental isolation compares with adult isolation. Studying neurogenic plasticity at specific stages of the process of adult neurogenesis in the zebrafish brain will broaden our understanding of the innate plasticity of distinct vertebrate niches in response to changes in the social environment.

3.3 Methodology

3.3.1 Animals

Wildtype zebrafish (AB strain) of both sexes were randomly selected for all experiments and maintained on a 14h light:10h dark photoperiod at 28°C in our fish facility (Aquaneering Inc., San Diego, U.S.A.). Fish were fed a diet of granular food (ZM, Winchester, U.K.) and brine shrimp thrice daily, unless stated otherwise. Zebrafish were a minimum of 6-months old and a maximum of 11-months old before they were examined for changes in adult neurogenesis or cortisol levels in response to social isolation or social novelty. Animals were killed using an overdose of 0.4% Tricaine methanesulfonate diluted in tank water. Thereafter, the total body length (mm), weight (g), and sex of all fish were recorded, while brain length (mm) was additionally measured in animals used to study changes in cell proliferation and differentiation following treatment exposure. These parameters, along with the sample size of animals examined for changes in adult neurogenesis under each treatment condition are listed in Table 3-1. Handling procedures were done in accordance with the policies set forth by the University of Toronto and the Canadian Council for Animal Care (CCAC).

3.3.2 Social Isolation and Social Novelty Treatments

3.3.2.1 Developmental Isolation and Novelty

To examine the effects of being raised in isolation compared with a familiar social environment, fertilized zebrafish embryos were raised in an incubator at 28°C until 5-6 days post fertilization (dpf) when their yolk is substantially depleted. Kin recognition between larvae is not yet established at this stage of development (Gerlach et al., 2008). Larval zebrafish from the same cohort were separated into individual tanks as groups of 6 animals (Gp, control) or isolates (Iso) and dividers placed between tanks to prevent visual cues from adjacent fish. Isolated and grouped zebrafish were fed a diet of rationed ZM granular fish food throughout development to ensure group-raised and isolate-raised fish received the same amount of food per fish. Upon reaching 6-months, half of the isolate-raised fish were tagged (Fig. 3-S1 and see Elastomer

tagging below) and exposed to social novelty (Iso-Nov) for an additional 2-weeks to investigate whether any effects that occurred as a result of social isolation could be restored using this form of social enrichment (Fig. 3-2A). Social novelty consisted of a mixture of six age-matched, unfamiliar adult male and female zebrafish. For all developmental isolation groups (Gp, Iso, Iso-Nov), following treatments animals received a single pulse of bromodeoxyuridine (BrdU; Sigma) and were killed 2-hours or 4-weeks after to examine changes in cell proliferation, the label-retaining $BrdU^+$ population, and neuronal differentiation. Comparisons were made between Gp:Iso and Iso:Iso-Nov. Since the control group (Gp) came from the same cohort of animals bred for all isolation and novelty treatments, it was additionally used as the control group for comparisons below.

3.3.2.2 Adult Isolation

To assess whether periods of adult social isolation could affect adult neurogenesis as commonly observed in the hippocampus of mammals, 6-month adult zebrafish were isolated for 2-weeks (Gp-Iso2wk) or 4-weeks (Gp-Iso4wk) in separate tanks and compared with the group-raised controls (Gp; Fig. 3-4A). Dividers were placed between tanks to prevent visual cues from adjacent fish and animals maintained as above. Following isolation treatments, animals were injected with BrdU and killed after 2-hours or 4-weeks to examine stages of adult neurogenesis. Comparisons were made between Gp:Gp-Iso2wk and Gp:Gp-Iso4wk.

3.3.2.3 Adult Novelty and Isolation

To investigate the effect of adult social novelty in zebrafish raised in a social environment alongside familiar conspecifics, 6-month old animals were tagged and exposed to social novelty for 2-weeks (Gp-Nov) before being pulsed with BrdU and killed for comparison with group-raised controls (Fig. 3-6A). To next determine whether subsequent exposure to social isolation and social novelty, two extremes of the social environment, had a compound effect on rates of cell proliferation, survival, and differentiation, a separate set of 6-month old group-raised animals were isolated for 2-weeks, then exposed to social novelty for 2-weeks (Gp-Iso-Nov). Thereafter, all animals were injected with BrdU and processed after 2-hours or 4-weeks to

examine stages of adult neurogenesis. Comparisons were made between Gp:Gp-Nov and Gp-Nov:Gp-Iso-Nov.

3.3.3 Elastomer Tagging

Non-toxic, Visible Implant Elastomer tags (Northwest Marine Technology, Inc., Washington, U.S.A.) were used to identify zebrafish during introduction into a novel social group of unfamiliar animals. Visible implant elastomer was prepared fresh according to the manufacturers' protocol the morning of tagging and kept on ice until application. Zebrafish were anaesthetized with 0.04% Tricaine diluted in facility water until movement slowed, then tagged with visible implant elastomer dorsolaterally beneath the skin, between black stripes using a 0.3 cc injecting syringe. Tags were approximately 3-5 mm long and easily visible (Fig. 3-S1). Thereafter, animals were briefly placed in a recovery tank and respiration and swimming behaviour monitored. After this time, tagged zebrafish were introduced into novel groups of adult zebrafish according to treatments.

3.3.4 BrdU Administration and Brain Processing

Bromodeoxyuridine (BrdU) administration and tissue processing was performed as described in Lindsey et al. (2012). In brief, a single 10 mM bolus of BrdU (Sigma) was administered intraperitoneally at a volume of 50 µL/g body weight into anaesthetized fish to detect proliferating cells in the S-phase of the cell cycle. Following 2-hour or 4-week BrdU chase periods, animals were killed and transcardially perfused with ice-cold 1X-phosphate buffered saline (PBS; pH 7.4) and 4% paraformaldehyde, brains processed, and cryosectioned at 20 µm

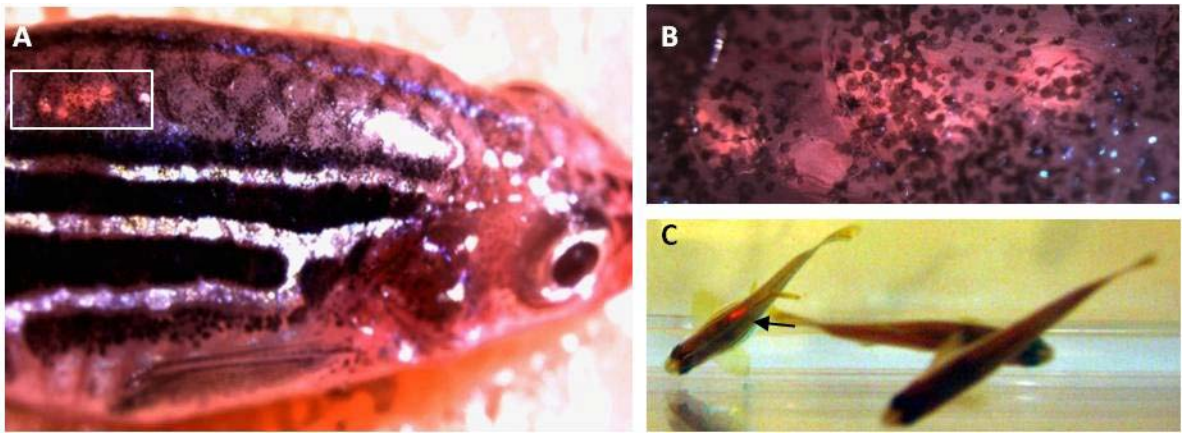
A
B
C

Figure 3-S1. Visible implant elastomer tagging of adult zebrafish for exposure to social novelty. **A**, Image demonstrating the location of elastomer tag injected mid-dorsally, below the surface of the epidermis and rostral to the dorsal fin. White box depicted in **B**. **B**, Enlargement of white box in **A**, showing elastomer tag injected dorsally in lightly-pigmented region. **C**, Image of a group of three adult zebrafish showing the readily visible elastomer tag in a single fish for identification (black arrow).

intervals for immunohistochemistry.

3.3.5 Immunohistochemistry

Immunohistochemistry (IHC) was used to label $BrdU^+$ cells 2-hours and 4-weeks post-BrdU injection within neurogenic niches to identify proliferating populations, and cells that newly differentiated into a neuronal phenotype, respectively. This marker was additionally used to detect changes in the proliferative population in response to different concentrations of hydrocortisone injections. Single-labeling of $BrdU^+$ cells and double-labeling of $BrdU^+$ cells with the neuronal marker HuCD were carried out accordingly to protocols described in Lindsey et al. (2012). For BrdU labeling alone, brain sections were incubated in rat-anti-BrdU polyclonal primary antibody (1:1000; Serotec; MCA2060), followed by goat-anti-rat-Cy3 secondary antibody (1:400; Jackson Immunoresearch Labs). For double-labeling, the above BrdU primary antibody was conjugated to a goat-anti-rat Cy2 secondary antibody (1:200; Jackson Immunoresearch Labs), and tissue next labelled with monoclonal mouse-anti-HuCD (1:400; Molecular Probes; 16A11) conjugated to goat-anti-mouse Cy3 secondary antibody (1:400; Jackson Immunoresearch Labs). A separate cohort of group-raised controls (Gp) and developmentally-raised isolates (Iso) were additionally labelled with Hoechst 33258 nuclear counterstain to compare changes in the density of cells within each of the six neurogenic niches under investigation, to further validate stereological counting methods used here. All brain sections were mounted in 100% glycerol for visualization and imaging.

3.3.6 Cell Counting and Imaging

Imaging was performed using a Leica TCS SP5 confocal microscope. Cell counting was completed in three primary sensory and three telencephalic neurogenic niches within tightly demarcated rostrocaudal boundaries of the adult zebrafish brain (Fig. 3-1A, B, E, H, K, N, Q; red portion of schematics). All neuroanatomical terminology and rostrocaudal boundaries stated are

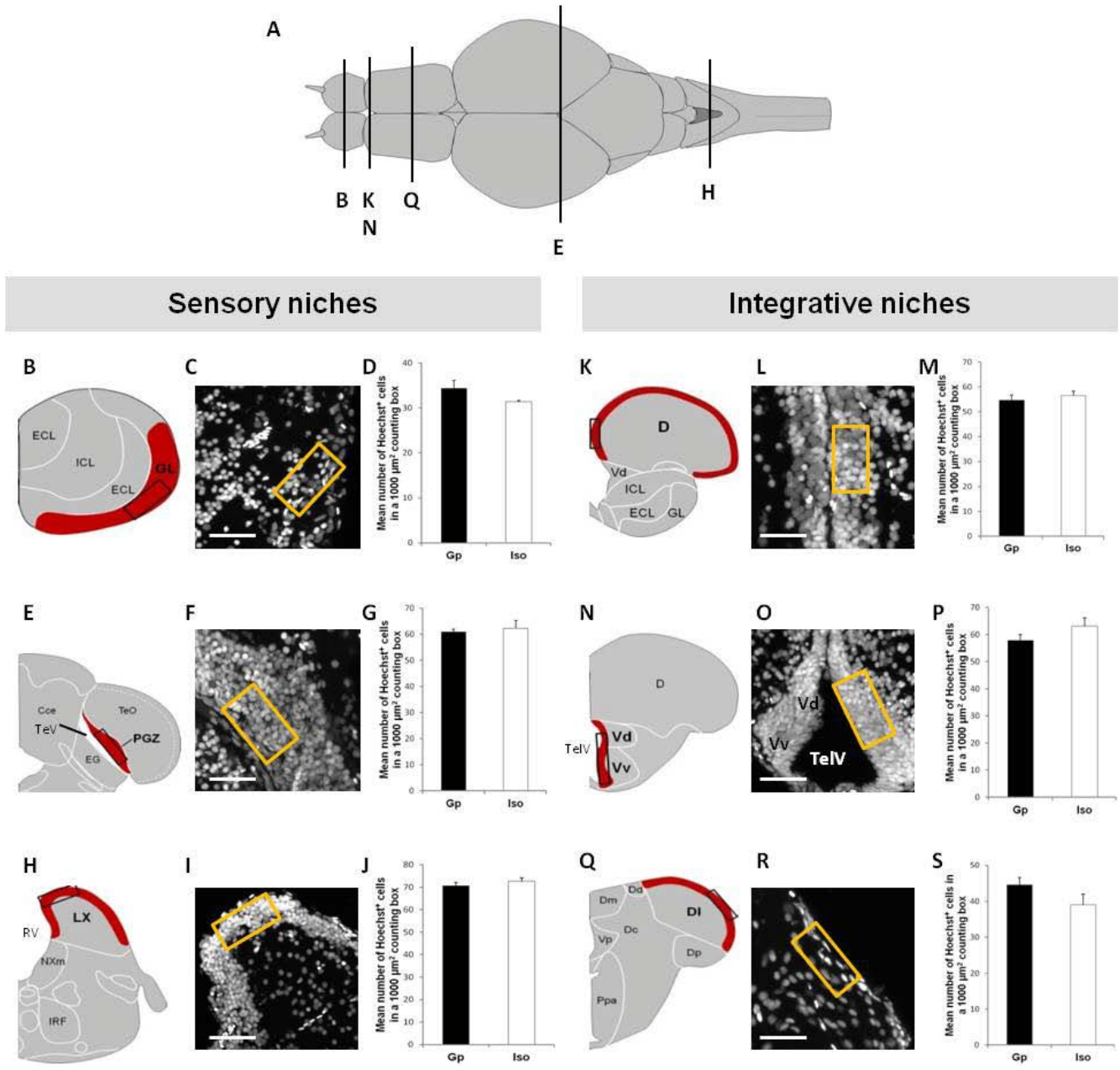
A
B K N Q
E
H
Sensory niches
Integrative niches
B
ECL
ICL
GL
ECL
C
D
Mean number of Hoechst⁺ cells in a 1000 µm² counting box
Gp
Iso
K
D
Vd
ICL
ECL GL
L
M
Mean number of Hoechst⁺ cells in a 1000 µm² counting box
Gp
Iso
E
Cce
TeO
TeV
PGZ
EG
F
G
Mean number of Hoechst⁺ cells in a 1000 µm² counting box
Gp
Iso
N
D
TelV
Vd
Vv
O
Vd
Vv
TelV
P
Mean number of Hoechst⁺ cells in a 1000 µm² counting box
Gp
Iso
H
RV
LX
NXm
IRF
I
J
Mean number of Hoechst⁺ cells in a 1000 µm² counting box
Gp
Iso
Q
Dm
Dd
Dl
Dc
Vp
Dp
Ppa
R
S
Mean number of Hoechst⁺ cells in a 1000 µm² counting box
Gp
Iso

Figure 3-1. Density counts in neurogenic niches compared between group-raised (Gp) and isolate-raised (Iso) treatments. A, Schematic showing the top view of an adult zebrafish brain and the rostrocaudal position of cross-sections where sensory (**B, E, H**) and integrative (**K, N, Q**) niches reside. Notation corresponds to cross-sectional view of neurogenic niches in schematics below. **B, C, D,** Sensory niche of the olfactory bulbs (OB). **B**, Schematics showing cross-sectional view of OB. The niche of OB is primarily located in the glomerular layer (GL; red). ECL, external cellular layer; ICL, internal cellular layer. ***C***, Representative image of Hoechst-labelled cells in GL of OB. **D**, Comparison of the number of $Hoechst^+$ cells between group and isolate-raised zebrafish in OB. **E, F, G,** Sensory niche of the periventricular grey zone (PGZ) of the optic tectum (TeO). ***E***, Schematics showing cross-sectional view of PGZ within the TeO. The niche of the PGZ of the caudal optic tectum (red) is located adjacent the tectal ventricle (TeV). Cce, corpus cerebelli; EG, eminentia granularis. **F**, Representative image of Hoechst-labelled cells in PGZ. **G**, Comparison of the number of $Hoechst^+$ cells between group and isolate-raised zebrafish in PGZ. **H, I, J,** Sensory niche of the vagal lobe (LX) located in the hindbrain. **H,** The niche of LX is restricted to the perimeter of this structure (red), and medially lies adjacent the rhombencephalic ventricle (RV). NXm, vagal motor nucleus; IRF, inferior reticular formation. ***I***, Representative image of Hoechst-labelled cells in LX. **J**, Comparison of the number of $Hoechst^+$ cells between group and isolate-raised zebrafish in LX. **K, L, M,** Integrative niche of the dorsal zone of the telencephalon (D, pallium). **K**, The niche of D surrounds the perimeter of the dorsal telencephalon (red). ***L***, Representative image of Hoechst-labelled cells in D. **M**, Comparison of the number of $Hoechst^+$ cells between group and isolate-raised zebrafish in D. **N, O, P,** Integrative niche of the ventral telencephalon (VdVv, subpallium). **N**, The niche of VdVv is located adjacent the telencephalic ventricle (TelV) and consists of the dorsal (Vd) and ventral (Vv) zones of the ventral telencephalon (red). **O**, Representative image of Hoechst-labelled cells in VdVv. TelV, telencephalic ventricle. **P**, Comparison of the number of $Hoechst^+$ cells between group and isolate-raised zebrafish in VdVv. **Q, R, S,** Integrative niche of the lateral zone of the dorsal telencephalon (Dl). **Q**, The niche of Dl surrounds the perimeter of this structure (red) and is localized between the dorsal zone (Dd) and posterior zone (Dp) of the dorsal telencephalon. **R**, Representative image of Hoechst-labelled cells in Dl. **S**, Comparison of the number of $Hoechst^+$ cells between group and isolate-raised zebrafish in Dl. In **B, E, H, K, N, Q,** black rectangles in schematics represent subregions of each niche examined for the size of the label-retaining population between 2-hours and 4-weeks, and for co-labeling of $BrdU^+/HuCD^+$ cells. In **C, F, I, L, O, R,** Dorsal is up. Orange boxes represent the location of 1000 μm^2 counting boxes within which the total number of $Hoechst^+$ cells where assessed for each niche. Orange counting boxes are located within a subregion of black rectangles shown in schematics. Scale bars = 10 µm. In **D, G, J, M, P, S,** $*p < 0.05$ (independent samples t-tests).

in accordance with Wullimann et al. (1996). Primary sensory niches were defined as neurogenic niches displaying constitutive levels of adult neurogenesis that resided within a neuroanatomical subregion of adult primary sensory processing structures of known function. These included the olfactory bulbs that processes primary sensory input (OB, 23-50x; primarily the glomerular layer, GL; Fig. 3-1B), the caudal aspect of the periventricular grey zone of the optic tectum, responsible for processing visual stimuli including movement, shape, and color (PGZ, 213-223x; Fig. 3-1E), and the vagal lobe situated in the hindbrain that receives primary taste stimuli (LX, 279-303; Fig. 3-1H). Telencephalic niches included three integrative processing regions that receive direct and/or indirect afferent information from the above primary sensory structures, and that have been proposed to be homologues to neuroanatomical regions within the mammalian telencephalon (Salas et al., 2006; Wullimann, 2009): the dorsal telencephalic area (D, 50-60x; Fig. 3-1K) surrounding the perimeter of the pallium, which receives both retinal and olfactory input, the dorsal (Vd) and ventral (Vv) zone of the ventral telencephalon (VdVv, x60; Fig. 3-1N) lining the medial subpallium adjacent the telencephalic ventricle (Lindsey et al., 2012), that processes olfactory input and which are proposed as a homologue to the mammalian striatum (Wullimann, 2009), and the lateral zone of the dorsal telencephalon (Dl, x70-107; Fig. 3-1Q) that receives retinal input from the optic tectum, and presumably other sensory processing structures and is thought to be homologous to the mammalian hippocampus (Salas et al., 2006). Hereafter, I refer to the above three telencephalic niches collectively as ‘integrative niches’.

Quantification of $BrdU^+$ cells was done by counting a minimum of every third section through the rostrocaudal range of each niche at 40x magnification (Fig. 3-1B, E, H, K, N, Q; red region of each niche). Hoechst-labeled cells within each niche were sampled in a 1000 μm^2 counting box and imaged at 63x magnification (Fig. 3-1C, F, I, L, O, R; orange rectangles) between group-raised and developmentally isolated zebrafish. To quantify the number of $BrdU^+/HuCD^+$ cells only a subregion of each niche was analyzed from images taken at 100x magnification from two or more, non-adjacent, sections (Fig. 3-1B, E, H, K, N, Q; black rectangles within red niches). During this analysis, all $BrdU^+$ cells were counted within subregions, and those positively co-labeled with HuCD confirmed using orthogonal view. Cell counting was completed by quantifying the number of cells present in 0.5-1 µm z-stacks using the optical disector principle (West, 1999; Geuna, 2005) with Leica Application Suite Advance Fluorescence Lite 2.3.0 proprietary software. Images shown are maximum projections or orthogonal views where

appropriate and were adjusted for brightness and contrast using Adobe Photoshop 7.0 software.

3.3.7 Population Dynamics of Niche-Residing BrdU$^+$ Cells

To analyze the manner by which the size of the BrdU$^+$ cell population changed (label-retaining population) within individual neurogenic niches at 2-hours (proliferative) compared with 4-weeks (post-mitotic) under different isolation and novelty treatments, I sub-sampled images from both time points to compare. Data from 2-hour BrdU pulse-chase experiments was normalized to the same counting frame and surface area as analyzed for the 4-week chase period used to examine neuronal differentiation (Fig. 3-1B, E, H, K, N, Q; black rectangles within red niches).

3.3.8 Cortisol Assays

To determine whether changes in cortisol levels were correlated with zebrafish exposed to different treatment conditions, I measured whole-body cortisol concentrations (ng/g fish) in separate sets of animals: group-raised (Gp), isolate-raised (Iso), 1-hour adult isolated (Gp-Iso1hr), 2-week adult isolated (Gp-Iso2wk), 4-week adult isolated (Gp-Iso4wk), and group-raised fish exposed to novelty for 2-weeks (Gp-Nov). Cortisol extractions and assays were performed as described by Cachat et al. (2010). In brief, zebrafish heads were removed, body weight measured, and tissue homogenized in 1 mL of ice-cold 1X-PBS. Five milliliters of diethyl ether (Sigma) was next added to glass centrifuge tubes, the tissue vortexed for 1 min and then centrifuged at 7,000 rcf thrice for 15 min. After each spin, the top organic layer containing cortisol (yellow) was removed and placed in a glass vial overnight at room temperature in a fumehood to allow ether to evaporate. Once evaporated, the next day cortisol samples were reconstituted in 1 mL of 1X-PBS overnight at 4°C. Thereafter, whole-body cortisol samples were assayed in triplicate using a Salimetrics Salivary Cortisol Enzyme Immunoassay Kit as per the manufacturers' instructions (Salimetrics, LLC, State College, PA, U.S.A). The optical density of samples was read at 450 nm using a SPECTRAmax PLUS Microplate Spectrophotometer (Molecular Devices, CA, U.S.A). The final concentration of whole-body cortisol (µg/dL) was determined by interpolation using a 4-parameter sigmoid minus curve fit and final cortisol levels normalized to body weight (ng/g).

3.3.9 Cortisol Injections

To directly test the effect of increased cortisol levels on the size of the proliferative population across sensory and integrative niches, I injected hydrocortisone intraperitoneally (Fig. 3-8A). A stock solution of 10 mg/mL hydrocortisone (Sigma) was first made by diluting the solute in a 1:1 solution of 100% ethanol: chloroform. The stock solution was then diluted in 1X-PBS to yield three ascending hydrocortisone concentrations: 50 ng, 175 ng, and 350 ng. These concentrations were chosen since they were all within or above the range of cortisol levels shown to be stressful in zebrafish following exposure to various types of stressors (Pavlidis et al., 2011; Alderman and Vijahan, 2012; Dhanasiri et al., 2013). Controls included 1X-PBS alone, or 5 uL of 100% ethanol diluted in 1X-PBS (ETOH control) to account for possible effects of the diluent on levels of cell proliferation. Zebrafish were fasted 24-hours prior to the first injection, and thereafter injected under anesthetic once a day at 10:00 over three consecutive days with hydrocortisone or vehicle at a volume of 50 µL/g body weight. The following day, animals were injected with a single bolus of 10 mM BrdU and killed 2-hours later. Thereafter, their brains were perfused, fixed and cryosectioned as described above in preparation for BrdU immunohistochemistry.

3.3.10 Statistical Analysis

Values are expressed as mean ± standard error of the mean. Pairs of means were compared using independent samples t-tests. In cases where the same treatment group was used for more than one comparison, I applied the Holm-Sidak corrections for familywise comparisons to reduce my chances of obtaining a Type I error and at the same time maintaining biologically meaningful differences across experiments (Abdi, 2010). In such instances, the corrected *p*-value is listed. For multiple comparisons between treatment groups a one-way ANOVA was used. Samples were considered significant at $p < 0.05$, and statistical analyses completed using SPSS Statistics 17.0 or SigmaPlot 11.0 and graphs made using Microsoft Excel 2003.

3.4 Results

3.4.1 Exposure to Social Isolation and Novelty Treatments do not Alter Growth Parameters in the Adult Zebrafish

Exposing animals to different environmental contexts, in particular during early development, can be associated with changes in body and brain growth as a result of increased stress or changes in physiology. For instance, removal of the social environment during sensitive periods of development has been shown to potentially impact the development of neuronal connections and the speed of signal propagation (Berardi et al., 2000; Hensch, 2004; Makinodan et al., 2012;). Since I examined a number of different social contexts, I first wanted to confirm that time spent by zebrafish in these environments did not produce any morphological changes that might affect downstream analyses. Therefore, upon sacrifice, I recorded the total body length (mm), rostrocaudal brain length using digital calipers (mm), and body weight (g), and performed statistical comparisons for each cohort of animals to be analyzed for changes in cell proliferation or differentiation under each treatment condition (Table 3-1). I found that with the exception of a significant difference in gross morphological changes in the body length (t-test; $p = 0.004$; Holm-Sidak correction) and body weight (t-test; $p= 0.004$; Holm-Sidak correction) between developmentally isolated animals (Iso) and those subjected to novelty following development (Iso-Nov), exposure to the treatment conditions used in my study had little effect on growth parameters. Notably, there was no significant difference (t-tests; $p > 0.05$) across any of the three growth parameters examined between group-raised and isolate-raised animals. In the above groups where a significant difference was observed, these differences in body length and weight could be explained by the ratio of males to females comprising each group (gender was randomly assigned), with females often being larger and typically gravid at the time of sacrifice.

To further validate that different social contexts did not produce changes in the overall density of cells making up neurogenic niches within distinct neuroanatomical structures, I performed density counts following Hoechst nuclear labeling. I compared the total number of Hoechst-labeled cells in a 1000 μm^2 counting box in each of the six neurogenic niches between animals raised in a familiar social environment (Gp; $N = 6$) and those raised in social isolation (Iso; $N =$

Table 3-1. Zebrafish morphometric measurements at adulthood following social isolation and social novelty treatments

	PROLIFERATION				DIFFERENTIATION			
	Sample size (n)	Body length (mm)	Brain length (mm)	Weight (g)	Sample size (n)	Body length (mm)	Brain length (mm)	Weight (g)
Developmental Isolation/Novelty								
Gp	5	27.6 ± 0.87	4.5 ± 0.22	0.23 ± 0.03	7	30.4 ± 0.84	4.6 ± 0.09	0.26 ± 0.02
Iso	5	29.0 ± 0.55	4.5 ± 0.16	0.23 ± 0.01	4	30.3 ± 0.25*	4.6 ± 0.24	0.31 ± 0.02*
Iso-Nov	4	27.3 ± 0.56	4.5 ± 0	0.20 ± 0.01	4	26.5 ± 0.65	5.0 ± 0	0.19 ± 0.002
Acute Adult Isolation								
Gp-Iso2wk	9	29.4 ± 0.60	4.5 ± 0.08	0.30 ± 0.03	7	30.4 ± 1.04	4.36 ± 0.09	0.33 ± 0.03
Gp-Iso4wk	7	29.9 ± 0.51	4.8 ± 0.21	0.27 ± 0.02	7	30.9 ± 0.46	4.8 ± 0.15	0.31 ± 0.02
Adult Novelty/Isolation								
Gp-Nov	6	29.7 ± 0.25	4.6 ± 0.08	0.22 ± 0.002	6	30.5 ± 0.62	5.0 ± 0.13	0.23 ± 0.01
Gp-Iso-Nov	6	30.3 ± 0.56	4.5 ± 0	0.26 ± 0.01	7	29.7 ± 0.42	4.6 ± 0.20	0.26 ± 0.01

Statistical comparisons were performed between the following treatment groups for proliferation and differentiation: Gp:Iso; Iso:Iso-Nov; Gp:Gp-Iso2wk; Gp:Gp-Iso4wk; Gp:Gp-Nov; Gp-Nov:Gp-Iso-Nov.
*Indicates a significant difference ($p < 0.05$) between Iso:Iso-Nov.

5). I reasoned that animals isolated for 6-months over the course of development should display the greatest change in cell density, if any, compared to group-raised controls, given the timing and duration of exposure. My results showed consistent evidence that no significant difference was present in the density of Hoechst-labeled cells across any of the three sensory (Fig. 3-1D, G, J; t-tests: OB, $p = 0.157$; PGZ, $p = 0.708$; LX, $p = 0.373$) or integrative (Fig. 3-1M, P, S; t-tests: D, $p = 0.531$; VdVv, $p = 0.197$; Dl, $p = 0.163$) neurogenic niches between group- and isolate-raised animals. My morphometric measurements indicate that the zebrafish husbandry protocol generally ensured that across treatment groups the animals were similar in size and the brains had comparable cell density, at least in those brain regions under investigation. As such, stereological methods were used for quantification of differences in cell proliferation or differentiation between treatment groups.

3.4.2 Developmental Social Isolation Decreases Proliferation and is Further Exacerbated by Social Novelty in the Neurogenic Niche of the Olfactory Bulbs

Larval zebrafish can be raised successfully in isolation without the need for parental care, therefore I first addressed whether chronic isolation from a social environment over the first 6-months of life causes a long-term effect on neurogenesis in adulthood between group- and isolate-raised zebrafish (Fig. 3-2A; Gp vs. Iso). Within sensory niches, a significant decrease in the proliferative population was detected in isolated fish in OB (Fig. 3-2B-C; t-test; $p = 0.034$) and PGZ (Fig. 3-2H-I; t-test; $p = 0.039$) compared to group-raised controls. By contrast, no significant change in the cycling population was evident in the vagal lobe (LX) of the hindbrain (Fig. 3-S2D; t-test; $p = 0.765$). Thus, developmental isolation is strongly associated with decreased progenitor cell proliferation in a niche-specific manner. Four weeks post BrdU-injection I observed a significant increase in the number of post-mitotic $BrdU^+$ cells in OB compared to the size of the proliferative population at 2-hours in both group- (t-test; $p = 0.015$) and isolated (t-test; $p = 0.0003$) animals (Fig. 3-2D), while a significant decrease was present in PGZ (Fig. 3-2J; t-test; Gp, $p = 0.024$; Iso, $p = 0.001$). By comparison, the $BrdU^+$ population at 2-hours and 4-weeks (Fig. 3-S2E) showed no significant difference in group (t-test; $p = 1.00$) or

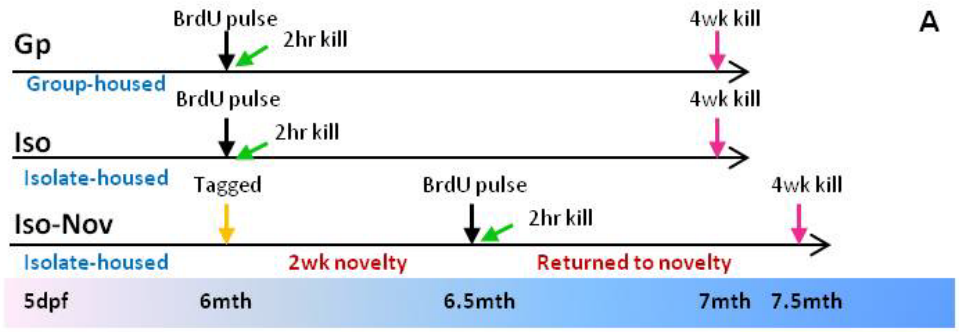

Olfactory Bulbs (OB)

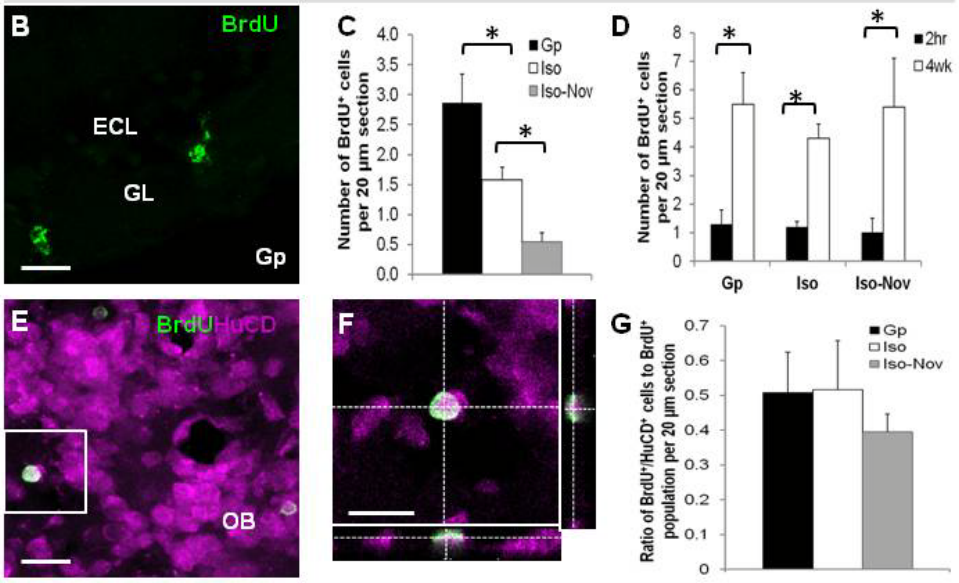

Periventricular Grey Zone (PGZ)

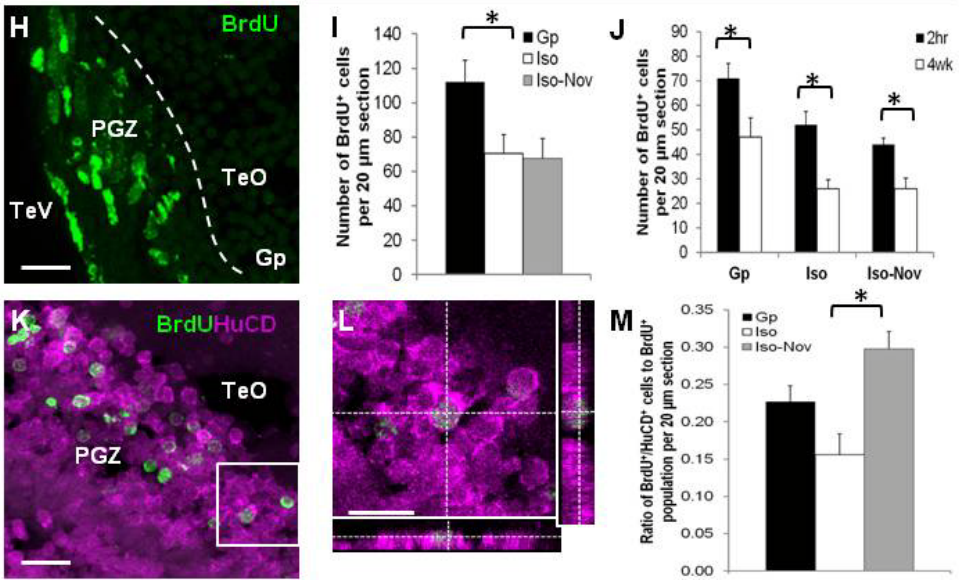

Figure 3-2. Effect of *Developmental Isolation and Novelty* treatments on cell proliferation, population dynamics, and neuronal differentiation in the sensory neurogenic niches of the olfactory bulbs (OB; B-G) and periventricular grey zone (PGZ; H-M) of the optic tectum. A, Experimental design of zebrafish developmental isolation and novelty treatments. *Gp*: Raised in a familiar social group of 6 animals until 6-months. *Iso*: Raised in isolation until 6-months. *Iso-Nov*: Raised in isolation until 6-months then elastomer-tagged and introduced into a novel group of 6 unfamiliar, adult zebrafish for 2-weeks (social novelty). dpf, days post fertilization. Groups of animals to be examined for changes in neuronal differentiation 4-weeks post-BrdU injection were maintained under the treatment condition until processing. **B, H,** Representative images from group-raised animals (*Gp*) showing $BrdU^+$ cells localized primarily to the glomerular layer (GL) of OB (**B**) and within PGZ (**H**) adjacent the tectal ventricle (TeV) and deep to the more superficial layers of the optic tectum proper (TeO). Hashed line on confocal image represents the division between the GL and ECL. Hashed line on confocal image represents the division between the PGZ and TeO. **C, I,** Number of $BrdU^+$ proliferating cells 2-hours post-BrdU injection following *Gp, Iso*, and *Iso-Nov* treatments. **D**, **J**, Niche-residing $BrdU^+$ cycling population at 2-hours and 4-weeks post-BrdU injection following *Gp, Iso*, and *Iso-Nov* treatments. Statistical comparisons were made between the same treatments only. **E**, **K**, Representative images of a $BrdU^+/HuCD^+$ newly differentiated neuron in group-raised animals (*Gp*). White squares depict higher magnification shown in **F** (OB) and **L** (PGZ). **F**, **L**, Orthogonal views confirming co-labeling of $BrdU^+/HuCD^+$ cell in x and y axes. **G**, **M**, Ratio of $BrdU^+/HuCD^+$ cells to the total $BrdU^+$ cell population within OB (***G***) and PGZ (**M**) following *Gp, Iso*, and *Iso-Nov* treatments. In **B, E, F, H, K, L** dorsal is up; scale bars = 10 µm. In **C, G, I, M**, statistical comparisons were performed between *Gp:Iso* and *Iso:Iso-Nov*. $*p < 0.05$ (independent samples t-tests).

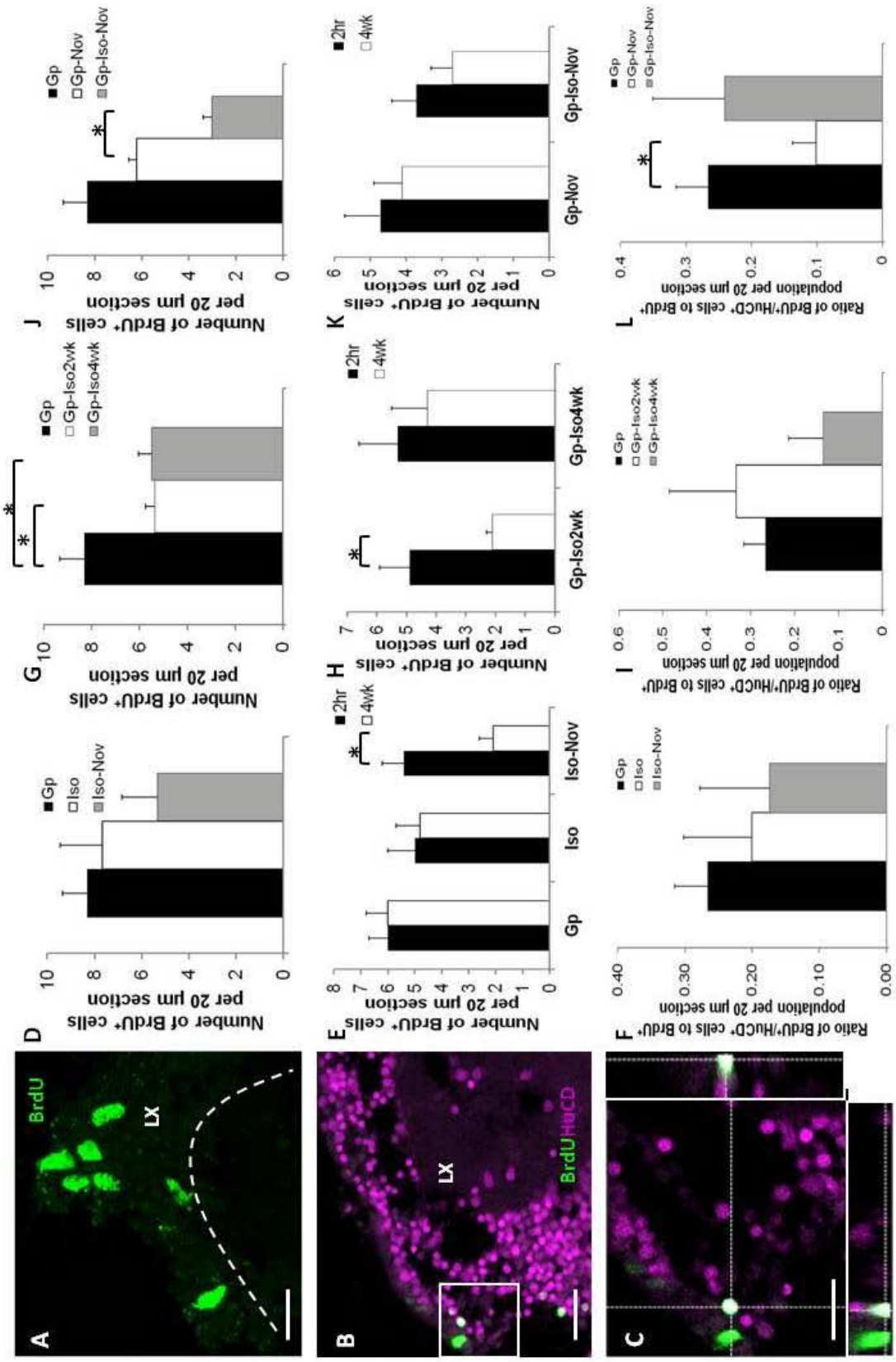
A
BrdU
LX
B
LX
BrdU/HuCD
C
D
Number of BrdU+ cells per 20 μm section
Gp
Iso
Iso-Nov
E
Number of BrdU+ cells per 20 μm section
2hr
4wk
Gp
Iso
Iso-Nov
F
Ratio of BrdU+/HuCD+ cells to BrdU+ population per 20 μm section
Gp
Iso
Iso-Nov
G
Number of BrdU+ cells per 20 μm section
Gp
Gp-Iso2wk
Gp-Iso4wk
H
Number of BrdU+ cells per 20 μm section
2hr
4wk
Gp-Iso2wk
Gp-Iso4wk
I
Ratio of BrdU+/HuCD+ cells to BrdU+ population per 20 μm section
Gp
Gp-Iso2wk
Gp-Iso4wk
J
Number of BrdU+ cells per 20 μm section
Gp
Gp-Nov
Gp-Iso-Nov
K
Number of BrdU+ cells per 20 μm section
2hr
4wk
Gp-Nov
Gp-Iso-Nov
L
Ratio of BrdU+/HuCD+ cells to BrdU+ population per 20 μm section
Gp
Gp-Nov
Gp-Iso-Nov

Figure 3-S2. Effect of *Isolation and Novelty* treatments on cell proliferation, population dynamics, and neuronal differentiation in the sensory neurogenic niche of the vagal lobe (LX). **A**, Representative image of $BrdU^+$ cells localized to LX. Hashed line on confocal image demarcates the ventral border of the niche. **B**, Representative image of a $BrdU^+/HuCD^+$ newly differentiated neurons. White squares depict higher magnification shown in **C**. **C**, Orthogonal view confirming co-labeling of $BrdU^+/HuCD^+$ cells in x and y axes. In **A, B, C** dorsal is up; scale bars = 10 µm. **D, E, F,** Effect of *Developmental Isolation and Novelty* treatments. Refer to Figure 3-2 for experimental design. **D**, Number of $BrdU^+$ proliferating cells 2-hours post-BrdU injection following *Gp, Iso*, and *Iso-Nov* treatments. **E**, Niche-residing $BrdU^+$ cycling population at 2-hours and 4-weeks post-BrdU injection following *Gp, Iso*, and *Iso-Nov* treatments. Statistical comparisons were made between the same treatments only. **F**, Ratio of $BrdU^+/HuCD^+$ cells to the total $BrdU^+$ cell population within LX following *Gp, Iso*, and *Iso-Nov* treatments. In *D* and *F*, statistical comparisons were made between *Gp:Iso* and *Iso:Iso-Nov* only. **G, H, I,** Effect of *Adult Isolation* treatments. Refer to Figure 3-4 for experimental design. **G**, Number of $BrdU^+$ proliferating cells 2-hours post-BrdU injection following *Gp, Gp-Iso2wk*, and *Gp-Iso4wk* treatments. **H**, Niche-residing $BrdU^+$ cycling population at 2-hours and 4-weeks post-BrdU injection following *Gp-Iso2wk* and *Gp-Iso4wk* treatments. Statistical comparisons were made between the same treatments only. **I**, Ratio of $BrdU^+/HuCD^+$ cells to the total $BrdU^+$ cell population within LX following *Gp, Gp-Iso2wk*, and *Gp-Iso4wk* treatments. In **G** and **I**, statistical comparisons were made between *Gp:Gp-Iso2wk* and *Gp:Gp-Iso4wk* only. **J, K, L,** Effect of *Adult Novelty and Isolation* treatments. Refer to Figure 3-6 for experimental design. **J**, Number of $BrdU^+$ proliferating cells 2-hours post-BrdU injection following *Gp, Gp-Nov*, and *Gp-Iso-Nov* treatments. **K**, Niche-residing $BrdU^+$ cycling population at 2-hours and 4-weeks post-BrdU injection following *Gp-Nov* and *Gp-Iso-Nov* treatments. Statistical comparisons were made between the same treatments only. **L**, Ratio of $BrdU^+/HuCD^+$ cells to the total $BrdU^+$ cell population within LX following *Gp,Gp-Nov,* and *Gp-Iso-Nov* treatments. In **J** and **L**, statistical comparisons were made between *Gp:Gp-Nov* and *Gp-Nov:Gp-Iso-Nov* only. $*p < 0.05$ (independent samples t-tests).

developmentally isolated animals in LX (Fig. 3-S2E; t-test; $p = 0.908$). Despite niche-specific differences in the size of the label-retaining population at 4-weeks in a subset of sensory niches, no significant differences in the relative number of newborn neurons in OB (Fig. 3-2E-G; t-test; $p = 0.968$), PGZ (Fig. 3-2K-M; t-test; $p = 0.071$), or LX (Fig. 3-S2F; t-test; $p = 0.526$) were detected between group- and isolated animals. These data suggest that the rate of neuronal differentiation under developmental isolation is unchanged, but that the total number of surviving $BrdU^+$ post-mitotic cells could be either increased or decreased in a sensory modality dependent manner.

To investigate whether I could restore decreases in cell proliferation observed in OB and PGZ following developmental social isolation, I exposed isolated zebrafish to a novel social group of adult zebrafish for 2-weeks (Fig. 3-2A; Iso vs. Iso-Nov). I predicted that exposure to social novelty should be positively correlated with an increase in cell proliferation given that it is a typical component of an enriched environment (Baroncelli et al., 2010). To my surprise, compared to fish isolated alone, isolated animals exposed to social novelty had significantly lower numbers of proliferating cells in OB (Fig. 3-2C; t-test; $p = 0.028$), while the cellular population within PGZ remained unaffected between these same two treatments (Fig. 3-2I; t-test; $p = 0.877$). The same result was observed in LX (Fig. 3-S2D; t-test; $p = 0.365$). This indicated to me that either the duration or type of social novelty was insufficient or that complete lack of social interactions during chronic developmental isolation could impede any positive effects acute social novelty might have on proliferation rates later in life.

The post-mitotic cohort remaining at 4-weeks in the Iso-Nov group revealed a significant increase in OB (Fig. 3-2D; t-test; $p = 0.024$) and corresponding decrease in PGZ (Fig. 3-2J; t-test; $p = 0.002$), in agreement with group- and isolate-raised zebrafish. These data suggest that developmental isolation alone or preceding exposure to a novel group at adulthood has no effect on long-term survival of progenitor cells residing within these two sensory niches, since this population behaved similarly to group-raised animals. In LX, rather, a significant decrease in the $BrdU^+$ population at 4-weeks was observed in the Iso-Nov group (Fig. 3-S2E; t-test; $p = 0.004$), opposite to the trend seen in group- and isolate-raised animals in this niche, indicating a clear effect of novelty on the survival of the post-mitotic population. Exposure of isolated zebrafish to social novelty was, however, correlated with a significant increase in the proportion of newly generated neurons within PGZ compared to isolated animals never introduced into a social

environment (Fig. 3-2K-M; t-test; $p = 0.007$). This effect was absent in OB (Fig. 3-2E-G; t-test; $p = 0.527$) and LX (Fig. 3-S2F; t-test; $p = 0.866$) alike. The relationship between the size of the post-mitotic population and the degree of neuronal output at 4-weeks across niches demonstrates that different social context differentially regulate these stages. For example, data from the PGZ highlights that under conditions of Iso-Nov, a smaller surviving pool of post-mitotic cells is capable of generating a greater proportion of newborn neurons.

3.4.3 Developmental Social Isolation has Little Effect on Cell Proliferation or Differentiation in Pallial and Subpallial Niches of the Telencephalon

Compared to sensory neurogenic niches, developmental social isolation (Fig. 3-2A; Gp vs. Iso) had little effect on constitutive levels of neurogenesis in integrative niches of the telencephalon. No significant difference in the population of cycling cells was noted between group- and isolated fish in D (Fig. 3-3A-B; t-test; $p = 0.957$), VdVv (Fig. 3-3G-H; t-test; $p = 0.296$), or Dl (Fig. 3-S3D; t-test; $p = 0.768$). Within D (Fig. 3-3C; Gp, t-test; $p = 0.463$; Iso, t-test; $p = 0.069$) and Dl (Fig. 3-S3E; Gp; t-test; $p = 0.338$; Iso; t-test; $p = 0.411$), the size of the 2-hour $BrdU^+$ cohort was unaltered after 4-weeks in either treatment. By contrast, a significant decrease in the size of the post-mitotic $BrdU^+$ population was observed between 2-hours and 4-weeks within VdVv (Fig. 3-3I; Gp, t-test; $p = 0.001$; Iso, t-test; $p = 0.00001$). In line with proliferation data, I observed no significant difference in the proportion of differentiated neurons between group- and isolated animals in any of the three integrative niches (Fig. 3-3D-F; D: t-test; $p = 0.981$; Fig. 3-3J-L; VdVv: t-test; $p = 0.588$; Fig. 3-S3F; Dl; t-test; $p = 0.186$), although a modest decrease in the newly differentiated population in Dl could be seen.

Exposure of isolated zebrafish to social novelty for 2-weeks (Fig. 3-2A; Iso vs. Iso-Nov; $N = 4$) also showed no significant niche-specific response in D (Fig. 3-3B; t-test; $p = 0.115$), VdVv (Fig. 3-3H; t-test; $p = 0.149$), or Dl (Fig. 3-S3D; t-test; $p = 0.703$) compared to animals that were chronically isolated over development. Moreover, no significant long-term effect on the $BrdU^+$ population at 4-weeks was observed in animals exposed to social novelty in D (Fig. 3-3C; t-test;

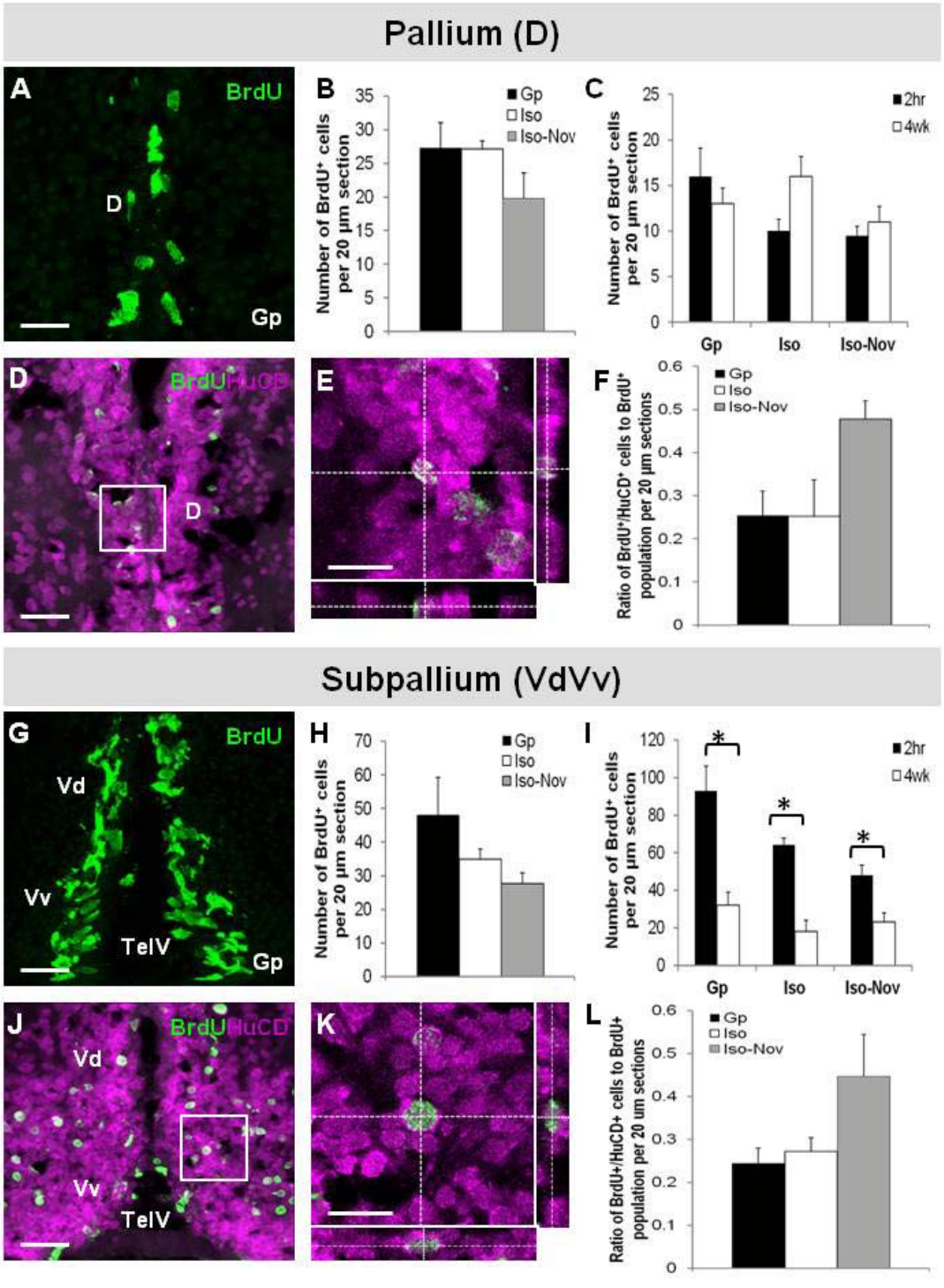
Pallium (D)
A
BrdU
D
Gp
B
Number of BrdU⁺ cells per 20 µm section
Gp
Iso
Iso-Nov
C
Number of BrdU⁺ cells per 20 µm section
2hr
4wk
Gp
Iso
Iso-Nov
D
BrdU HuCD
D
E
F
Ratio of BrdU⁺/HuCD⁺ cells to BrdU⁺ population per 20 µm sections
Gp
Iso
Iso-Nov
Subpallium (VdVv)
G
BrdU
Vd
Vv
TelV
Gp
H
Number of BrdU⁺ cells per 20 µm section
Gp
Iso
Iso-Nov
I
Number of BrdU⁺ cells per 20 µm section
2hr
4wk
Gp
Iso
Iso-Nov
J
BrdU HuCD
Vd
Vv
TelV
K
L
Ratio of BrdU+/HuCD+ cells to BrdU+ population per 20 um sections
Gp
Iso
Iso-Nov

Figure 3-3. Effect of *Developmental Isolation and Novelty* treatments on cell proliferation, population dynamics, and neuronal differentiation in the telencephalic neurogenic niches of the pallium (D; A-F) and subpallium (VdVv; G-L). **A, G**, Representative images from group-raised animals (*Gp*) showing $BrdU^+$ cell localized at the dorsal midline of D (**A**) and within VdVv (**G**) adjacent the telencephalic ventricle (TelV). **B, H**, Number of $BrdU^+$ proliferating cells 2-hours post-BrdU injection following *Gp, Iso*, and *Iso-Nov* treatments. **C, I**, Niche-residing $BrdU^+$ cycling population at 2-hours and 4-weeks post-BrdU injection following *Gp, Iso*, and *Iso-Nov* treatments. Statistical comparisons were made between the same treatments only. **D, J**, Representative images of a $BrdU^+/HuCD^+$ newly differentiated neuron in group-raised animals (Gp). White squares depict higher magnification shown in **E** (D) and **K** (VdVv). **E, K**, Orthogonal views confirming co-labeling of $BrdU^+/HuCD^+$ cell in x and y axes. ***F, L***, Ratio of $BrdU^+/HuCD^+$ cells to the total $BrdU^+$ cell population within D (**F**) and VdVv (**L**) following *Gp, Iso*, and *Iso-Nov* treatments. In **A, D, E, G, J, K** dorsal is up; scale bars = 10 µm. In **B, F, H, L**, statistical comparisons were performed between *Gp:Iso* and *Iso:Iso-Nov*. $*p < 0.05$ (independent samples t-tests).

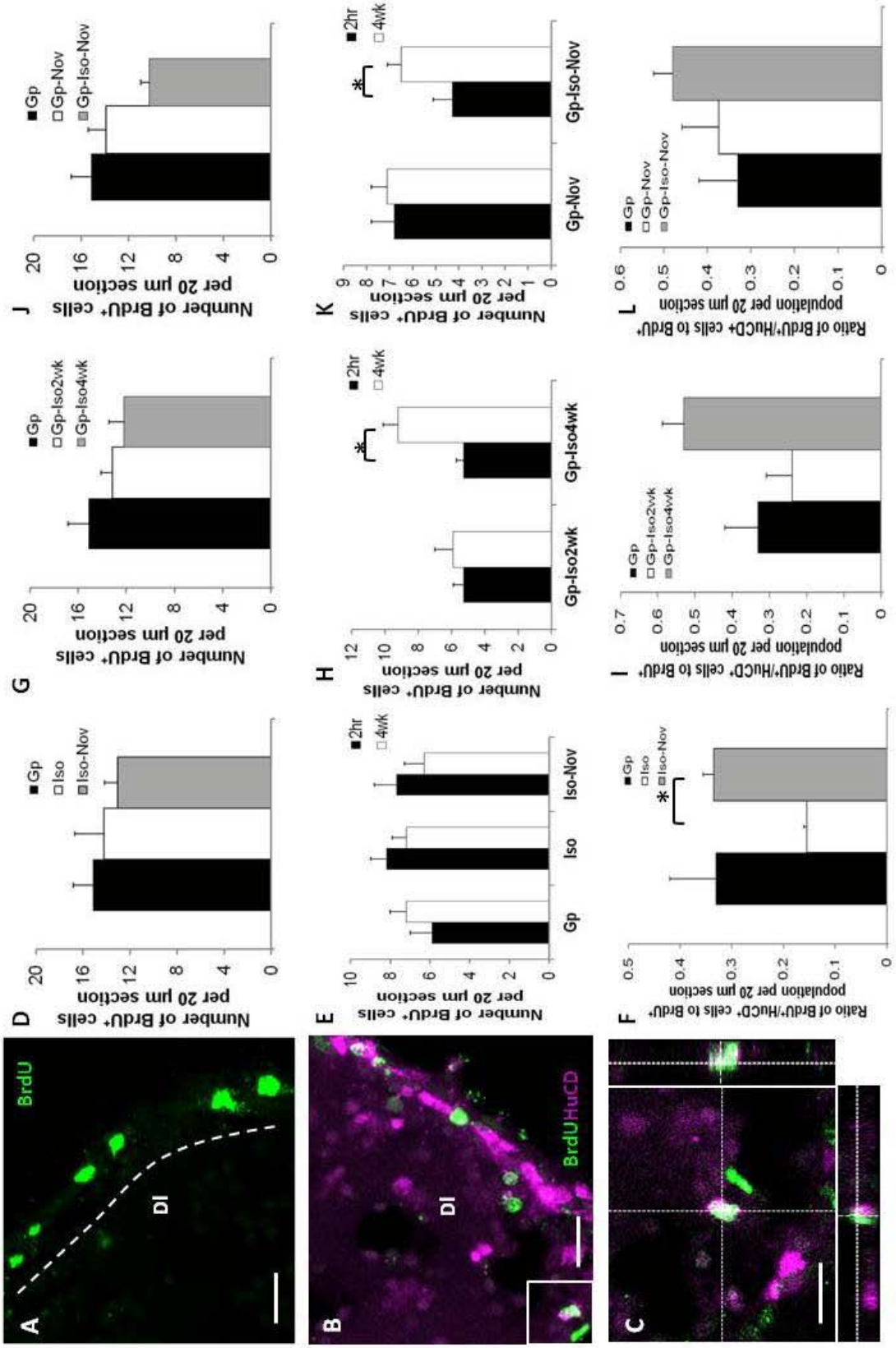
A
BrdU
DI
B
DI
BrdU HuCD
C
D
Number of BrdU+ cells per 20 μm section
Gp
Iso
Iso-Nov
E
Number of BrdU+ cells per 20 μm section
2hr
4wk
Gp
Iso
Iso-Nov
F
Ratio of BrdU+/HuCD+ cells to BrdU+ population per 20 μm section
Gp
Iso
Iso-Nov
*
G
Number of BrdU+ cells per 20 μm section
Gp
Gp-Iso2wk
Gp-Iso4wk
H
Number of BrdU+ cells per 20 μm section
2hr
4wk
*
Gp-Iso2wk
Gp-Iso4wk
I
Ratio of BrdU+/HuCD+ cells to BrdU+ population per 20 μm section
Gp
Gp-Iso2wk
Gp-Iso4wk
J
Number of BrdU+ cells per 20 μm section
Gp
Gp-Nov
Gp-Iso-Nov
K
Number of BrdU+ cells per 20 μm section
2hr
4wk
*
Gp-Nov
Gp-Iso-Nov
L
Ratio of BrdU+/HuCD+ cells to BrdU+ population per 20 μm section
Gp
Gp-Nov
Gp-Iso-Nov

Figure 3-S3. Effect of *Isolation and Novelty* treatments on cell proliferation, population dynamics, and neuronal differentiation in the integrative neurogenic niche of the lateral zone of the dorsal telencephalon (Dl). **A**, Representative image of $BrdU^+$ cells localized to Dl. Hashed line on confocal image demarcates the border of the niche. **B**, Representative image of a $BrdU^+/HuCD^+$ newly differentiated neurons. White squares depict higher magnification shown in **C**. **C**, Orthogonal view confirming co-labeling of $BrdU^+/HuCD^+$ cells in x and y axes. In **A, B, C,** dorsal is up; scale bars = 10 µm. **D, E, F,** Effect of *Developmental Isolation and Novelty* treatments. Refer to Figure 3-2 for experimental design. **D**, Number of $BrdU^+$ proliferating cells 2-hours post-BrdU injection following *Gp, Iso*, and *Iso-Nov* treatments. **E**, Niche-residing $BrdU^+$ cycling population at 2-hours and 4-weeks post-BrdU injection following *Gp, Iso*, and *Iso-Nov* treatments. Statistical comparisons were made between the same treatments only. **F**, Ratio of $BrdU^+/HuCD^+$ cells to the total $BrdU^+$ cell population within Dl following *Gp, Iso*, and *Iso-Nov* treatments. In *D* and *F*, statistical comparisons were made between *Gp:Iso* and *Iso:Iso-Nov* only. **G, H, I,** Effect of *Adult Isolation* treatments. Refer to Figure 3-4 for experimental design. **G**, Number of $BrdU^+$ proliferating cells 2-hours post-BrdU injection following *Gp, Gp-Iso2wk*, and *Gp-Iso4wk* treatments. **H**, Niche-residing $BrdU^+$ cycling population at 2-hours and 4-weeks post-BrdU injection following *Gp-Iso2wk* and *Gp-Iso4wk* treatments. Statistical comparisons were made between the same treatments only. ***I***, Ratio of $BrdU^+/HuCD^+$ cells to the total $BrdU^+$ cell population within Dl following *Gp, Gp-Iso2wk*, and *Gp-Iso4wk* treatments. In **G** and **I**, statistical comparisons were made between *Gp:Gp-Iso2wk* and *Gp:Gp-Iso4wk* only. **J, K, L,** Effect of *Adult Novelty and Isolation* treatments. Refer to Figure 3-6 for experimental design. **J**, Number of $BrdU^+$ proliferating cells 2-hours post-BrdU injection following *Gp, Gp-Nov*, and *Gp-Iso-Nov* treatments. **K**, Niche-residing $BrdU^+$ cycling population at 2-hours and 4-weeks post-BrdU injection following *Gp-Nov* and *Gp-Iso-Nov* treatments. Statistical comparisons were made between the same treatments only. ***L***, Ratio of $BrdU^+/HuCD^+$ cells to the total $BrdU^+$ cell population within Dl following *Gp,Gp-Nov,* and *Gp-Iso-Nov* treatments. In **J** and **L**, statistical comparisons were made between *Gp:Gp-Nov* and *Gp-Nov:Gp-Iso-Nov* only. $*p < 0.05$ (independent samples t-tests).

p = 0.376) or Dl (Fig. 3-S3E; t-test; p = 0.358), though a significant decrease in the post-mitotic population as observed in group- and isolate-raised animals was present in the subpalliual niche of VdVv (Fig. 3-3I; t-test; p = 0.004). These findings corroborate the notion that the consistent pattern of change in cell dynamics of the label-retaining population within individual niches over time is largely regulated by niche-specific properties in response to external manipulations of the environment. Of the remaining proliferating cells in all three integrative niches, a consistent trend towards an increase in the proportion of differentiated neurons was present, although a significant effect was observed only in Dl (Fig. 3-3SF; t-test; p = 0.001; Fig. 3-3F; D: t-test, p = 0.071; Fig. 3-3L; VdVv: t-test; p = 0.136). These results support the hypothesis that changes in the social (complex sensory) environment during development has a predominant effect on neurogenic niches located within primary sensory brain structures, oppose to those located in higher order integrative brain structures in zebrafish.

3.4.4 Adult Social Isolation Affects Neurogenesis in the Sensory Niche of the Periventricular Grey Zone of the Optic Tectum Similar to Developmental Isolation

To uncover how periods of social isolation during adulthood might modify constitutive levels of adult neurogenesis similar to studies performed in mammals, I raised zebrafish in standard social environments until 6-months and then isolated animals for 2- or 4-weeks (Fig. 3-4A; Gp vs. Gp-Iso2wk, Gp vs. Gp-Iso4wk). Compared to group-raised animals, no significant effect of 2-week (t-test; p = 0.673) or 4-week (t-test; p = 0.081; Holm-Sidak correction) isolation was detected in OB (Fig. 3-4B-C), though a trend toward a decrease in the size of the $BrdU^+$ population could be seen after 4-weeks isolation. By contrast, in PGZ a significant decrease in the number of $BrdU^+$ cells was observed after 2-weeks isolation (Fig. 3-4H-I; t-test; p = 0.027), in line with rates of cell proliferation within this niche during developmental social isolation (Fig. 3-2I; Iso). The effect of isolation was not, however, maintained 4-weeks after social isolation in PGZ (Fig. 3-4I; t-test; p = 0.092). In the LX, I noted a significant decrease at both 2-weeks (Fig. 3-S2G; Gp-Iso2wk; t-test; p = 0.021) and 4-weeks (Fig. 3-S2G; Gp-Iso4wk; t-test;

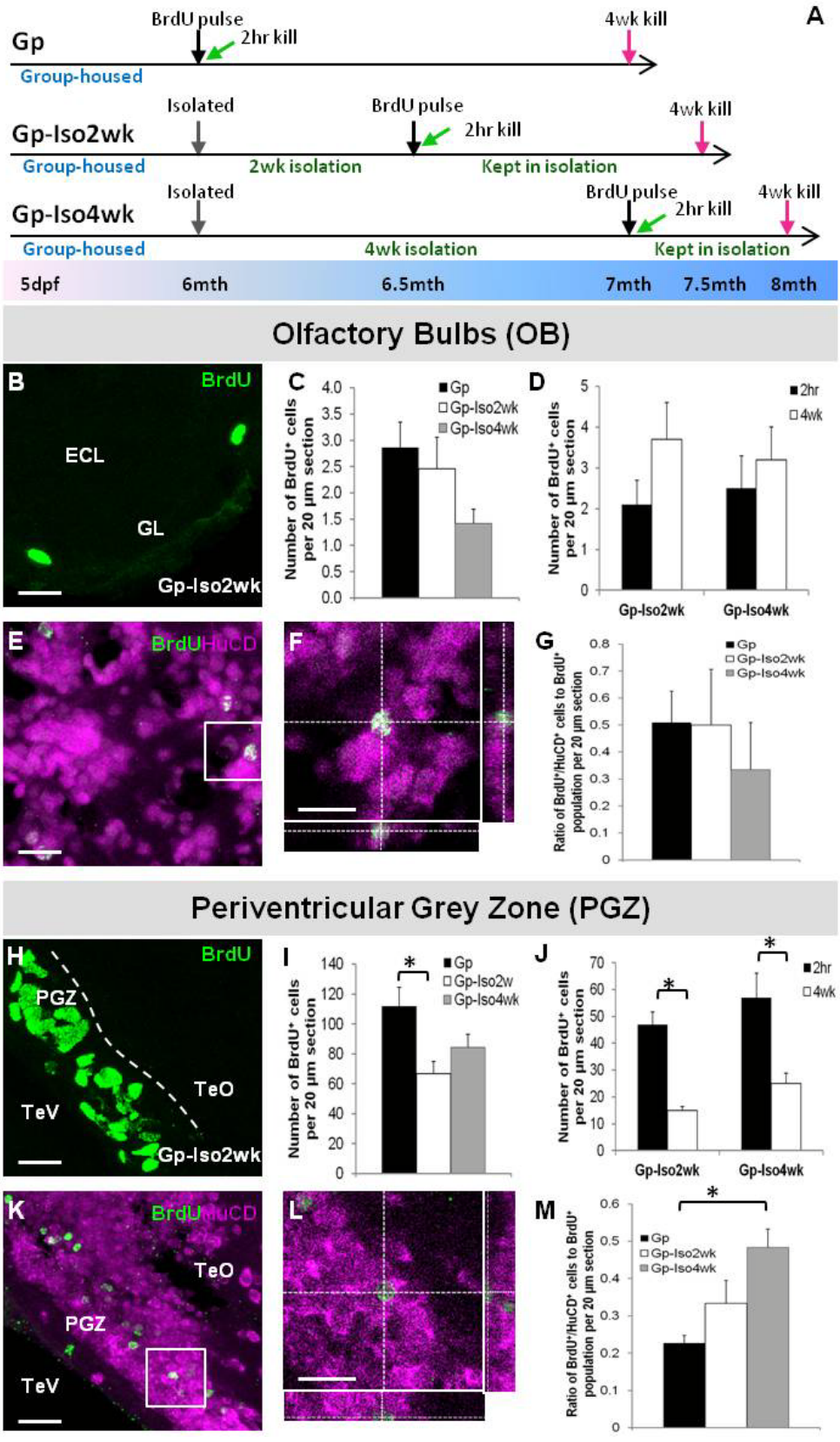
A
Gp
BrdU pulse
2hr kill
4wk kill
Group-housed
Gp-Iso2wk
Isolated
BrdU pulse
2hr kill
4wk kill
Group-housed
2wk isolation
Kept in isolation
Gp-Iso4wk
Isolated
BrdU pulse
2hr kill
4wk kill
Group-housed
4wk isolation
Kept in isolation
5dpf
6mth
6.5mth
7mth
7.5mth
8mth
Olfactory Bulbs (OB)
B
BrdU
ECL
GL
Gp-Iso2wk
C
Number of BrdU+ cells per 20 µm section
Gp
Gp-Iso2wk
Gp-Iso4wk
D
Number of BrdU+ cells per 20 µm section
2hr
4wk
Gp-Iso2wk
Gp-Iso4wk
E
BrdU HuCD
F
G
Ratio of BrdU+/HuCD+ cells to BrdU+ population per 20 µm section
Gp
Gp-Iso2wk
Gp-Iso4wk
Periventricular Grey Zone (PGZ)
H
BrdU
PGZ
TeO
TeV
Gp-Iso2wk
I
Number of BrdU+ cells per 20 µm section
Gp
Gp-Iso2w
Gp-Iso4wk
J
Number of BrdU+ cells per 20 µm section
2hr
4wk
Gp-Iso2wk
Gp-Iso4wk
K
BrdU HuCD
TeO
PGZ
TeV
L
M
Ratio of BrdU+/HuCD+ cells to BrdU+ population per 20 µm section
Gp
Gp-Iso2wk
Gp-Iso4wk

Figure 3-4. Effect of *Adult Isolation* treatments on cell proliferation, population dynamics, and neuronal differentiation in the sensory neurogenic niches of the olfactory bulbs (OB; B-G) and periventricular grey zone (PGZ; H-M) of the optic tectum. A, Experimental design of adult isolation treatments. *Gp*: Raised in a familiar social group of 6 animals until 6-months. *Gp-Iso2wk*: Isolated for 2-weeks beginning at 6-months. *Gp-Iso4wk*: Isolated for 4-weeks beginning at 6-months. dpf, days post fertilization. Groups of animals to be examined for changes in neuronal differentiation 4-weeks post-BrdU injection were maintained under the treatment condition until processing. **B, H,** Representative images from group-raised animals isolated for 2-weeks (*Gp-Iso2wk*) showing $BrdU^+$ cell localized primarily to the glomerular layer (GL) of OB (**B**) and within PGZ (**G**) adjacent the tectal ventricle (TeV) and deep to the more superficial layers of the optic tectum proper (TeO). In **B**, Hashed line represents the division between the GL and ECL. In **H**, Hashed line represents the division between the PGZ and TeO. **C, I**, Number of $BrdU^+$ proliferating cells 2-hours post-BrdU injection following *Gp, Gp-Iso2wk*, and *Gp-Iso4wk* treatments. **D, J**, Niche-residing $BrdU^+$ cycling population at 2-hours and 4-weeks post-BrdU injection following *Gp-Iso2wk* and *Gp-Iso4wk* treatments. Statistical comparisons were made between the same treatments only. **E, K,** Representative images of a $BrdU^+/HuCD^+$ newly differentiated neuron in group-raised animals isolated for 2-weeks (*Gp-Iso2wk*). White squares depict higher magnification shown in **F** (OB) and **L** (PGZ). **F, L**, Orthogonal views confirming co-labeling of $BrdU^+/HuCD^+$ cell in x and y axes. **G, M**, Ratio of $BrdU^+/HuCD^+$ cells to total $BrdU^+$ cell population within OB (**G**) and PGZ (**M**) following *Gp, Gp-Iso2wk*, and *Gp-Iso4wk* treatments. In **B, E, F, H, K, L** dorsal is up; scale bars = 10 µm. In **C, G, I, M**, statistical comparisons were performed between *Gp:Gp-Iso2wk* and *Gp:Gp-Iso4wk*. $*p < 0.05$ (independent samples t-tests).

$p = 0.049$) isolation. These results following 2- and 4-week adult social isolation between OB, PGZ, and LX, further emphasizes how each sensory neurogenic niche requires a different threshold of environmental change to elicit a cellular response in the proliferating stem/progenitor population.

Survival of the label-retaining, post-mitotic population 4-weeks following adult isolation treatments revealed the same overall pattern in OB (increase) and PGZ (decrease) as detected during developmental social isolation (Fig. 3-4D, J). Nonetheless, only in PGZ did adult isolation produce a significant effect (PGZ: Fig. 3-4J; Gp-Iso2wk; t-test; $p = 0.0001$; Gp-Iso4wk; t-test; $p = 0.003$) compared to OB (Fig. 3-4D; Gp-Iso2wk; t-test; $p = 0.168$; Gp-Iso4wk; t-test; $p = 0.057$). In LX, 2-weeks of adult social isolation led to a significant reduction in the resulting $BrdU^+$ post-mitotic population, while this effect was absent with 4-weeks isolation (Fig. 3-S2H; Gp-Iso2wk; t-test; $p = 0.026$; Gp-Iso4wk; t-test; $p = 0.588$). This implies that the duration of social isolation is capable of regulating the proportion of $BrdU^+$ cells that are maintained within the niche to give rise to newborn neurons.

Within the PGZ, a significant increase in the rate of neuronal differentiation was noted after 4-weeks isolation compared with animals raised in a familiar group (Fig. 3-4K-M; Gp-Iso4wk; t-test; $p = 0.004$; Gp-Iso2wk; t-test; $p = 0.090$). As such, the same correlation between the size of the $BrdU^+$ post-mitotic pool at 4-weeks and the proportion of differentiated neurons observed under Iso-Nov (see Fig. 3-2J, M), could be seen here under the context of Gp-Iso4wk. In contrast, no change compared with group-raised controls was seen in the OB (Fig. 3-4E-G; Gp-Iso2wk; t-test; $p = 0.419$; Gp-Iso4wk; t-test; $p = 0.419$) or LX (Fig. 3-S2I; Gp-Iso2wk; t-test; $p = 0.697$; Gp-Iso4wk; t-test; $p = 0.169$), in agreement with my findings during developmental social isolation. These results suggest that neurogenic plasticity in the PGZ may be more responsive to changes in the social context both at stages of cell proliferation and differentiation compared with chemosensory niches such as OB and LX, perhaps as a consequence of the dominant visual-related behaviours used by zebrafish.

3.4.5 Adult Social Isolation Increases Neuronal Differentiation but Not Cell Proliferation Within the Niche of the Dorsal Pallium

Adult social isolation (Fig. 3-4A; Gp vs. Gp-Iso2wk, Gp vs. Gp-Iso4wk) had no significant effect on proliferation rates following 2- or 4-week treatments in D (Fig. 3-5A-B; Gp-Iso2wk; t-test; $p = 0.773$; Gp-Iso4wk; t-test; $p = 0.200$), VdVv (Fig. 3-5G-H; Gp-Iso2wk; t-test; $p = 0.608$; Gp-Iso-4wk; t-test; $p = 0.617$), or Dl (Fig. 3-S3G; Gp-Iso2wk; t-test; $p = 0.293$; Gp-Iso4wk; t-test; $p = 0.177$) compared to group-raised controls. Survival of the post-mitotic population of newborn cells within integrative niches of D and VdVv following adult isolation behaved similarly to developmental isolation (Fig. 3-3C, I), with no significant change in D (Fig. 3-5C; Gp-Iso2wk; t-test; $p = 0.350$; Gp-Iso4wk; t-test; $p = 0.145$), but a significant decline in the number of post-mitotic $BrdU^+$ cells in VdVv after 4-weeks (Fig. 3-5I; Gp-Iso2wk; t-test; $p = 0.002$; Gp-Iso4wk; t-test; $p = 0.000004$). In Dl, a significant difference between the surviving $BrdU^+$ cohort 2-hours and 4-weeks post-injection was observed only following a 4-week adult isolation period (Fig. 3-S3H; Gp-Iso2wk; t-test; $p = 0.645$; Gp-Iso4wk; t-test; $p = 0.002$). Nevertheless, I did observe a significant increase in the number of newly differentiated neurons in D after both 2-weeks and 4-weeks isolation (Fig. 3-5D-F; Gp-Iso2wk; t-test; $p = 0.005$; Gp-Iso4wk; t-test; $p = 0.008$). However, no significant increase in the number of newborn neurons was present within VdVv (Fig. 3-5J-L; Gp-Iso2wk; t-test; $p = 0.873$; Gp-Iso4wk; t-test; $p = 0.093$; Holm-Sidak correction) or Dl (Fig. 3-S3I; Gp-Iso2wk; t-test; $p = 0.448$; Gp-Iso4wk; t-test; $p = 0.091$), although in both of these niches a trend towards an increase in the differentiated population after 4-weeks adult isolation was evident (Gp-Iso4wk; Fig. 3-5L; VdVv; Fig. 3-S3I; Dl). Thus, these findings suggest that adult social isolation appears to act by enhancing neuronal differentiation, but not proliferation, in integrative niches of the telencephalon.

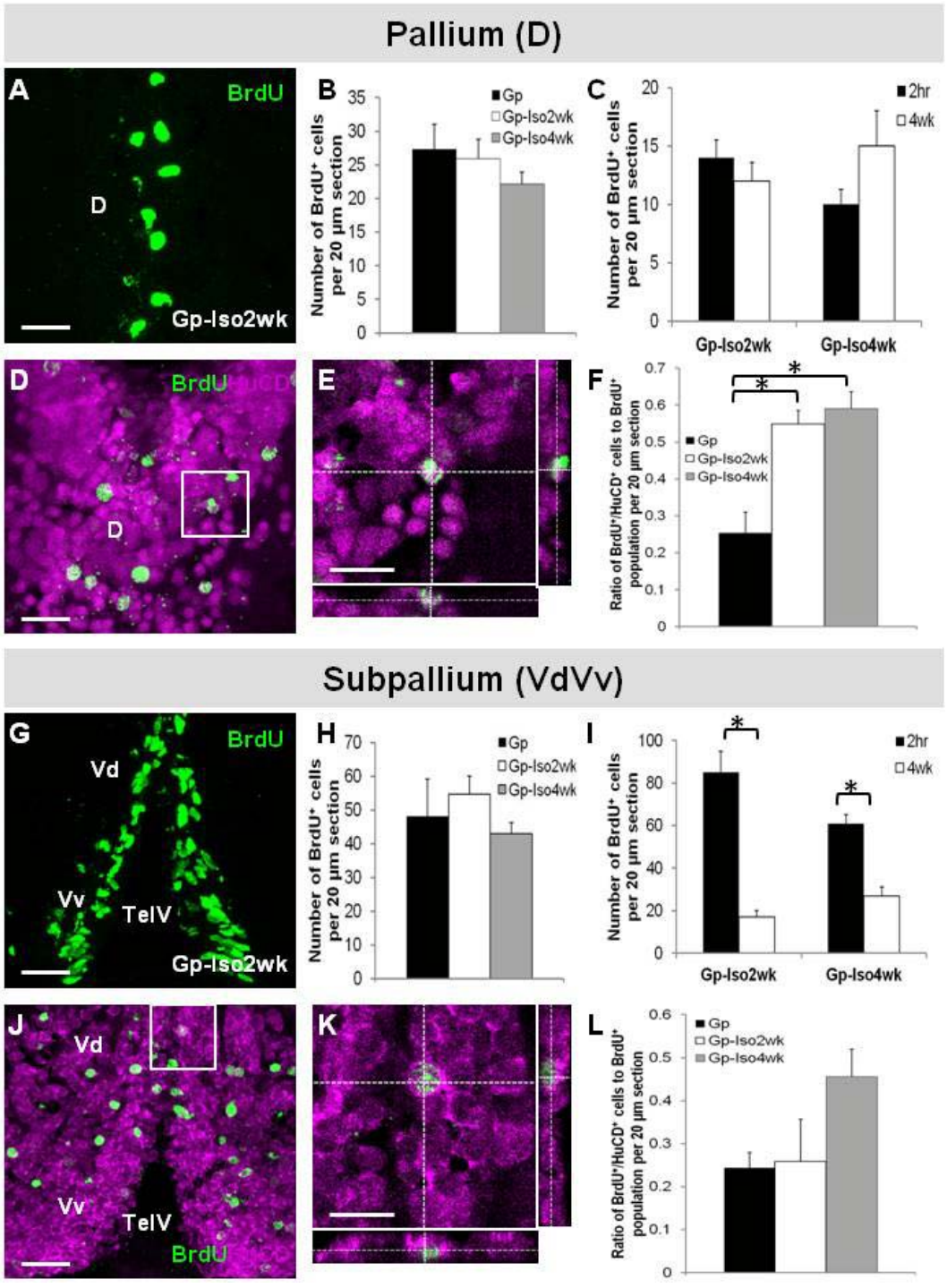
Pallium (D)
A
BrdU
D
Gp-Iso2wk
B
Number of BrdU+ cells per 20 µm section
Gp
Gp-Iso2wk
Gp-Iso4wk
C
Number of BrdU+ cells per 20 µm section
2hr
4wk
Gp-Iso2wk
Gp-Iso4wk
D
BrdU
D
E
F
Ratio of BrdU+/HuCD+ cells to BrdU+ population per 20 µm section
Gp
Gp-Iso2wk
Gp-Iso4wk
Subpallium (VdVv)
G
BrdU
Vd
Vv
TelV
Gp-Iso2wk
H
Number of BrdU+ cells per 20 µm section
Gp
Gp-Iso2wk
Gp-Iso4wk
I
Number of BrdU+ cells per 20 µm section
2hr
4wk
Gp-Iso2wk
Gp-Iso4wk
J
Vd
Vv
TelV
BrdU
K
L
Ratio of BrdU+/HuCD+ cells to BrdU+ population per 20 µm section
Gp
Gp-Iso2wk
Gp-Iso4wk

Figure 3-5. Effect of *Adult Isolation* treatments on cell proliferation, population dynamics, and neuronal differentiation in the telencephalic neurogenic niches of the pallium (D; A-F) and subpallium (VdVv; G-L). **A, G**, Representative images from group-raised animals isolated for 2-weeks (*Gp-Iso2wk*) showing $BrdU^+$ cells localized at the dorsal midline of D (**A**) and within VdVv (**G**) adjacent the telencephalic ventricle (TelV). **B, H**, Number of $BrdU^+$ proliferating cells 2-hours post-BrdU injection following *Gp, Gp-Iso2wk*, and *Gp-Iso4wk* treatments. **C, I**, Niche-residing $BrdU^+$ cycling population at 2-hours and 4-weeks post-BrdU injection following *Gp-Iso2wk* and *Gp-Iso4wk* treatments. Statistical comparisons were made between the same treatments only. **D, J,** Representative images of a $BrdU^+/HuCD^+$ newly differentiated neuron in group-raised animals isolated for 2-weeks (*Gp-Iso2wk*). White squares depict higher magnification shown in **E** (D) and **K** (VdVv). **E, K**, Orthogonal views confirming co-labeling of $BrdU^+/HuCD^+$ cell in x and y axes. **F, L**, Ratio of $BrdU^+/HuCD^+$ cells to total $BrdU^+$ cell population within D (**F**) and VdVv (**L**) following *Gp, Gp-Iso2wk*, and *Gp-Iso4wk* treatments. In **A, D, E, G, J, K** dorsal is up; scale bars = 10 µm. In **B, F, H, L**, statistical comparisons were performed between *Gp:Gp-Iso2wk* and *Gp:Gp-Iso4wk*. $*p < 0.05$ (independent samples t-tests).

3.4.6 Adult Isolation Followed by Social Novelty Produces Opposing Effects in Cell Proliferation and Differentiation in the Niche of the Periventricular Grey Zone

To examine how the presence of a novel social group might modulate adult neurogenic plasticity in adult-raised fish housed with familiar conspecifics (Fig. 3-6A; Gp vs. Gp-Nov), 6-month old group-raised animals were tagged and exposed to social novelty for 2-weeks. Though not significant, a modest decrease in the number of proliferative cells was observed between group controls and animals exposed to social novelty in OB (Fig. 3-6B-C; t-test; $p = 0.089$), PGZ (Fig. 3-6H-I; t-test; $p = 0.061$; Holm-Sidak correction), and LX (Fig. 3-S2J; t-test; $p = 0.091$). This finding is intriguing since it suggests that at least at the level of cell proliferation, 2-week exposure to social novelty following rearing under either developmental social isolation (Fig. 3-2) or a familiar social environment generally gives rise to the same trend in sensory niches compared to group-raised animals. Four weeks post-BrdU injection, a significant increase in the size of surviving label-retaining population was detected in zebrafish exposed to social novelty within OB (Fig. 3-6D; t-test; $p = 0.017$), but not PGZ (Fig. 3-6J; t-test; $p = 0.057$) or LX (Fig. 3-S2K; t-test; $p = 0.685$). By contrast, niches of OB and PGZ revealed no significant difference in the proportion of $BrdU^+$ post-mitotic cells at 4-weeks that differentiated into neurons (OB: Fig. 3-6E-G; t-test; $p = 0.157$; PGZ: Fig. 3-6K-M; t-test; $p = 0.680$), whereas a significant decrease in the newborn neuronal population was detected in LX (Fig. 3-S2L; t-test; $p = 0.046$). These data imply that with the exception of a significant reduction in the proportion of differentiated neurons in LX, exposing group-raised animals to social novelty for 2-weeks has little influence on any of the three stages of adult neurogenesis examined here.

To test how the combination of social novelty and social isolation would act on constitutive levels of adult neurogenesis in zebrafish first raised in a social environment, I designed an experiment where animals were isolated for 2-weeks before being exposed to social novelty for an additional 2-week period (Fig. 3-6A; Gp-Nov vs. Gp-Iso-Nov). My results showed that similar to developmental isolation (Fig. 3-2I), PGZ had a significantly lower number of proliferating cells in animals that received social isolation plus social novelty compared with animals exposed to social novelty alone (Fig. 3-6I; t-test; $p = 0.043$), suggestive of a possible

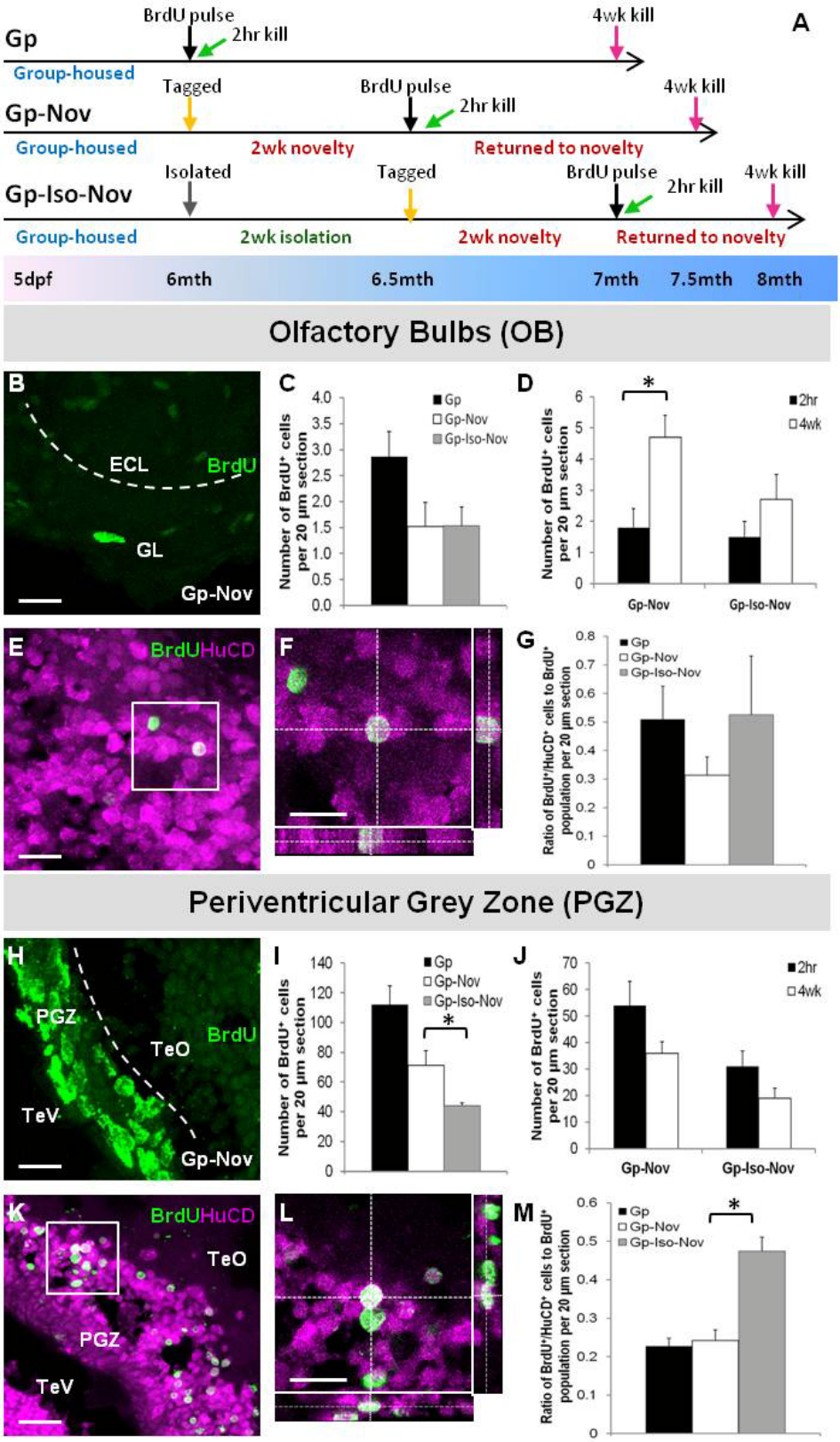
A
Gp
BrdU pulse
2hr kill
4wk kill
Group-housed
Gp-Nov
Tagged
BrdU pulse
2hr kill
4wk kill
Group-housed
2wk novelty
Returned to novelty
Gp-Iso-Nov
Isolated
Tagged
BrdU pulse
2hr kill
4wk kill
Group-housed
2wk isolation
2wk novelty
Returned to novelty
5dpf
6mth
6.5mth
7mth
7.5mth
8mth
Olfactory Bulbs (OB)
B
ECL
BrdU
GL
Gp-Nov
C
Number of BrdU+ cells per 20 µm section
Gp
Gp-Nov
Gp-Iso-Nov
D
Number of BrdU+ cells per 20 µm section
2hr
4wk
Gp-Nov
Gp-Iso-Nov
E
BrdUHuCD
F
G
Ratio of BrdU+/HuCD+ cells to BrdU+ population per 20 µm section
Gp
Gp-Nov
Gp-Iso-Nov
Periventricular Grey Zone (PGZ)
H
PGZ
TeO
BrdU
TeV
Gp-Nov
I
Number of BrdU+ cells per 20 µm section
Gp
Gp-Nov
Gp-Iso-Nov
J
Number of BrdU+ cells per 20 µm section
2hr
4wk
Gp-Nov
Gp-Iso-Nov
K
BrdUHuCD
TeO
PGZ
TeV
L
M
Ratio of BrdU+/HuCD+ cells to BrdU+ population per 20 µm section
Gp
Gp-Nov
Gp-Iso-Nov

Figure 3-6. Effect of *Adult Novelty and Isolation* treatments on cell proliferation, population dynamics, and neuronal differentiation in the sensory neurogenic niches of the olfactory bulbs (OB; B-G) and periventricular grey zone (PGZ; H-M) of the optic tectum. **A**, Experimental design of adult novelty and isolation treatments. *Gp*: Raised in a familiar social group of 6 animals until 6-months. *Gp-Nov***:** Tagged and introduced into a novel group of 6 unfamiliar, adult zebrafish for 2-weeks beginning at 6-months (social novelty). *Gp-Iso-Nov***:** Isolated for 2-weeks beginning at 6-months then tagged and introduced into a novel group of 6 unfamiliar, adult zebrafish for an additional 2-weeks (social novelty). dpf, days post fertilization. Groups of animals to be examined for changes in neuronal differentiation 4-weeks post-BrdU injection were maintained under the treatment condition until processing. **B, H**, Representative images from group-raised animals re-introduced into a novel group for 2-weeks (*Gp-Nov*) showing $BrdU^+$ cell localized primarily to the glomerular layer (GL) of OB (**B**) and PGZ (**H**) adjacent the tectal ventricle (TeV) and deep to the more superficial layers of the optic tectum proper (TeO). In **B**, Hashed line represents the division between the GL and ECL. In **H**, Hashed line represents the division between the PGZ and TeO. ***C, I***, Number of $BrdU^+$ proliferating cells 2-hours post-BrdU injection following *Gp, Gp-Nov*, and *Gp-Iso-Nov* treatments. **D, J**, Niche-residing $BrdU^+$ cycling population at 2-hours and 4-weeks post-BrdU injection following *Gp-Nov* and *Gp-Iso-Nov* treatments. Statistical comparisons were made between the same treatments only. **E, K**, Representative images of a $BrdU^+/HuCD^+$ newly differentiated neuron in group-raised animals re-introduced into a novel group for 2-weeks (*Gp-Nov*). White squares depict higher magnification shown in **F** (OB) and **L** (PGZ). **F, L**, Orthogonal views confirming co-labeling of $BrdU^+/HuCD^+$ cell in x and y axes. **G, M**, Ratio of $BrdU^+/HuCD^+$ cells to total $BrdU^+$ cell population within OB (**G**) and PGZ (**M**) following *Gp, Gp-Nov*, and *Gp-Iso-Nov* treatments. In **B, E, F, H, K, L** dorsal is up; scale bars = 10 µm. In **C, G, I, M**, statistical comparisons were performed between *Gp:Gp-Nov* and *Gp-Nov:Gp-Iso-Nov*. $*p < 0.05$ (independent samples t-tests).

additive effect of isolation plus novelty. This same result was also present in the niche of LX (Fig. 3-S2J; t-test; $p = 0.0001$), while no significant difference in the proliferative population was seen in OB (Fig. 3-6C; t-test; $p = 0.984$). Data examining the size of the $BrdU^+$ post-mitotic population 4-weeks after exposure to the combination of social isolation and novelty in OB (increase: Fig. 3-6D; t-test; $p = 0.229$), PGZ (decrease: Fig. 3-6J; t-test; $p = 0.098$) and LX (decrease: Fig. 3-S2K; t-test; $p = 0.316$), matched patterns observed in earlier treatments. In line with developmental isolation and novelty, in PGZ I detected a significant increase in the population of newly differentiated neurons (Fig. 3-6M; t-test; $p = 0.001$), while a significant difference was absent in OB (Fig. 3-6G; t-test; $p = 0.276$) and LX (Fig. 3-S2L; t-test; $p = 0.313$) in animals exposed to isolation and novelty compared with novelty alone. From these results, I present a unique example of how a single neurogenic niche, here the niche of the PGZ, can be differentially modulated in a bi-directional manner at the stage of cell proliferation (i.e., decrease) and neuronal differentiation (i.e., increase) following exposure to the same environmental perturbation (Gp-Iso-Nov). To the best of my knowledge this is the first report showing evidence that stages of adult neurogenesis can be uncoupled in such a way, while still producing a resulting greater proportion of newly differentiated neurons.

3.4.7 Isolation Followed by Novelty Increases Differentiation Within the Pallial Niche of the Telencephalon but does Not Affect Cell Proliferation Rates

None of the three integrative niches of the telencephalon showed an effect of social novelty on levels of cell proliferation compared with group-raised controls (Fig. 3-6A; Gp vs. Gp-Nov; D: Fig. 3-7A-B; t-test; $p = 0.674$; VdVv: Fig. 3-7G-H; t-test; $p = 0.692$; Dl: Fig. 3-S3J; t-test; $p = 0.588$). However, I did note a significant increase in D (Fig. 3-7C; t-test; $p = 0.034$) and subsequent decrease in VdVv (Fig. 3-7I; t-test; $p = 0.002$) in the proportion of surviving, label-retaining, post-mitotic cells after 4-weeks in animals exposed to novelty, though no change in the relative number of differentiated neurons was observed (D: Fig. 3-7D-F; t-test; $p = 0.107$; VdVv: Fig. 3-7J-L; t-test; $p = 0.531$). In the niche of Dl, no change in the $BrdU^+$ population between 2-

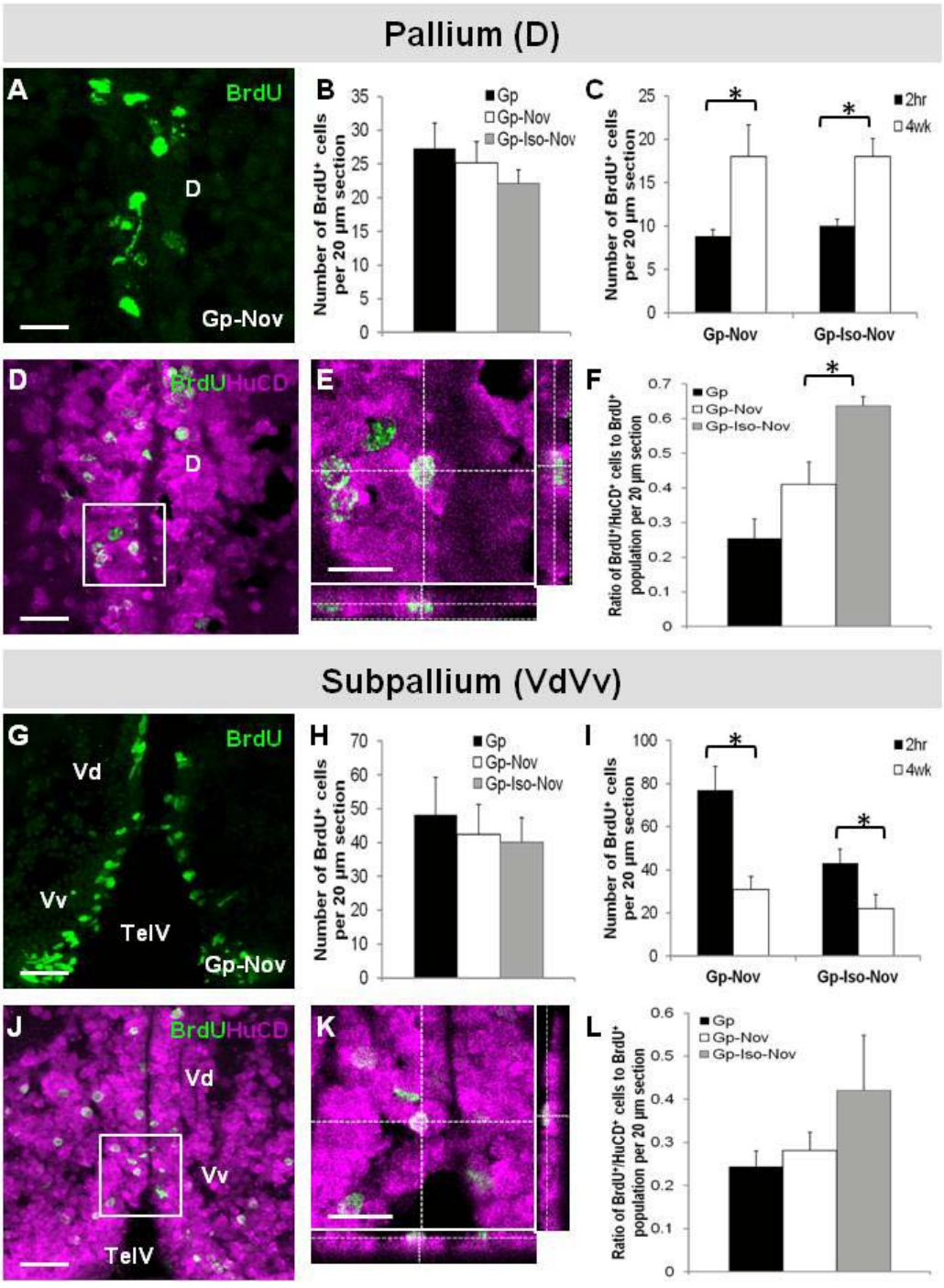
Pallium (D)
A
BrdU
D
Gp-Nov
B
Gp
Gp-Nov
Gp-Iso-Nov
Number of BrdU+ cells per 20 µm section
C
2hr
4wk
Number of BrdU+ cells per 20 µm section
Gp-Nov
Gp-Iso-Nov
D
BrdU HuCD
D
E
F
Gp
Gp-Nov
Gp-Iso-Nov
Ratio of BrdU+/HuCD+ cells to BrdU+ population per 20 µm section
Subpallium (VdVv)
G
BrdU
Vd
Vv
TelV
Gp-Nov
H
Gp
Gp-Nov
Gp-Iso-Nov
Number of BrdU+ cells per 20 µm section
I
2hr
4wk
Number of BrdU+ cells per 20 µm section
Gp-Nov
Gp-Iso-Nov
J
BrdU HuCD
Vd
Vv
TelV
K
L
Gp
Gp-Nov
Gp-Iso-Nov
Ratio of BrdU+/HuCD+ cells to BrdU+ population per 20 µm section

Figure 3-7. Effect of *Adult Novelty and Isolation* treatments on cell proliferation, population dynamics, and neuronal differentiation in the telencephalic neurogenic niches of the pallium (D; A-F) and subpallium (VdVv; G-L). **A, G**, Representative image from group-raised animals re-introduced into a novel group for 2-weeks (*Gp-Nov*) showing $BrdU^+$ cell localized at the dorsal midline of the D (**A**) and within VdVv (**G**) adjacent the telencephalic ventricle (TelV). **B, H**, Number of $BrdU^+$ proliferating cells 2-hours post-BrdU injection following *Gp, Gp-Nov*, and *Gp-Iso-Nov* treatments. **C, I**, Niche-residing $BrdU^+$ cycling population at 2-hours and 4-weeks post-BrdU injection following *Gp-Nov* and *Gp-Iso-Nov* treatments. Statistical comparisons were made between the same treatments only. **D, J**, Representative images of a $BrdU^+/HuCD^+$ newly differentiated neuron in group-raised animals re-introduced into a novel group for 2-weeks (*Gp-Nov*). White squares depict higher magnification shown in **E** (D) and **K** (VdVv). **E, K**, Orthogonal views confirming co-labeling of $BrdU^+/HuCD^+$ cells in x and y axes. **F, L**, Ratio of $BrdU^+/HuCD^+$ cells to total $BrdU^+$ cell population within D (**F**) and VdVv (**L**) following *Gp, Gp-Nov*, and *Gp-Iso-Nov* treatments. In **A, D, E, G, J, K** dorsal is up; scale bars = 10 µm. In **B, F, H, L**, statistical comparisons were performed between *Gp:Gp-Nov* and *Gp-Nov:Gp-Iso-Nov*. $*p < 0.05$ (independent samples t-tests).

hours and 4-weeks was detected in adult animals exposed to novelty conditions (Fig. 3-S3K; t-test; $p = 0.818$), nor was a significant difference seen in the resulting differentiated population of newborn neurons compared with group-raised animals (Fig. 3-S3L; t-test; p = 0.636). Thus, here I show that the proportion of differentiating neurons remains stable despite a change in the size of the surviving pool of new cells.

The combination of social isolation plus social novelty (Fig. 3-6A; Gp-Nov vs. Gp-Iso-Nov) additionally showed no difference in the initial $BrdU^+$ cycling population in any of the three telencephalic niches compared with zebrafish that received novelty alone (D: Fig. 3-7B; t-test; $p = 0.444$; VdVv: Fig. 3-7H; t-test; $p = 0.872$; Dl: Fig. 3-S3J; t-test; $p = 0.062$). Consistent with group-raised animals exposed to social novelty only, fish exposed to the combination of social isolation and novelty showed a significant increase or decrease in the size of the $BrdU^+$ post-mitotic population in D (Fig. 3-7C; t-test; $p = 0.026$) and VdVv (Fig. 3-7I; t-test; $p = 0.046$) at 4-weeks, respectively. This treatment condition also led to a significant increase in the size of the $BrdU^+$ post-mitotic population at 4-weeks in Dl (Fig. 3-S3K; t-test; $p = 0.047$). Here, I exhibit a case where a distinct neurogenic niche, the pallial niche of the telencephalon (D), gives rise to a larger pool of surviving post-mitotic cells between 2-hours and 4-weeks exclusively under the conditions of social novelty alone or in combination with social isolation compared with exposure to all other treatments in our study where no change in this population was detected. A significant increase in the proportion of $BrdU^+/HuCD^+$ cells in D was also detected (Fig. 3-7F; t-test; $p = 0.021$), whereas this was absent in VdVv (Fig. 3-7L; t-test; $p = 0.219$) and Dl (Fig. 3-S3L; t-test; $p = 0.253$) in animals exposed to social isolation and novelty. This final set of experiments contributes to my consistent finding that in contrast to sensory neurogenic niches, neurogenesis in integrative telencephalic niches of the adult zebrafish brain are relatively less sensitive to perturbations in the social environment. Under treatments where I detected significant differences at stages of adult neurogenesis in integrative niches, these changes were restricted to the surviving post-mitotic population and the resulting proportion of newly differentiated neurons.

3.4.8 Baseline Cortisol Levels are Elevated in Animals Raised Developmentally in a Familiar Social Group or in Isolation but are Decreased by Social Isolation and Novelty in Adulthood

Numerous studies have implicated higher cortisol levels as a mechanism responsible for decreases in levels of adult neurogenesis with isolation in mammals (Schoenfeld and Gould, 2011; Lieberwirth et al., 2012). However, the manner by which cortisol levels regulate stages of neurogenesis under different social contexts in mammals or other vertebrate models of neurogenesis remain poorly understood. To explore whether elevated cortisol levels could account for the trend in lower rates of cell proliferation in sensory niches of OB, PGZ, and LX with developmental and adult isolation, and novelty, I assayed whole-body cortisol levels. Strikingly, I found that zebrafish reared in a familiar group environment (N = 8, Gp) alongside conspecifics or isolated for 6-months developmentally (N = 8, Iso) showed nearly identical cortisol levels (Fig. 3-8A; t-test; p = 0.942). However, animals first raised to adulthood before being exposed to 1-hour (Fig. 3-8B; N = 12; t-test; p = 0.048) and 2-week (N = 10, Gp-Iso2wk; t-test; p = 0.004) adult isolation (but not 4-week; N = 8, Gp-Iso4wk; t-test; p = 0.078), or introduced into a novel social group for a duration of 2-weeks (Fig. 3-8C; N = 8, Gp-Nov; t-test; p = 0.04) displayed significantly lower levels of cortisol compared to group-raised controls. These data show that the timing of social isolation (i.e., long-term over development vs. short-term during adulthood) can differentially alter cortisol levels in adult zebrafish, and that reductions in the proliferative population in animals subjected to isolation (and novelty) treatments during either period are not accounted for by increases in physiological levels of cortisol, in contrast to studies in mammals.

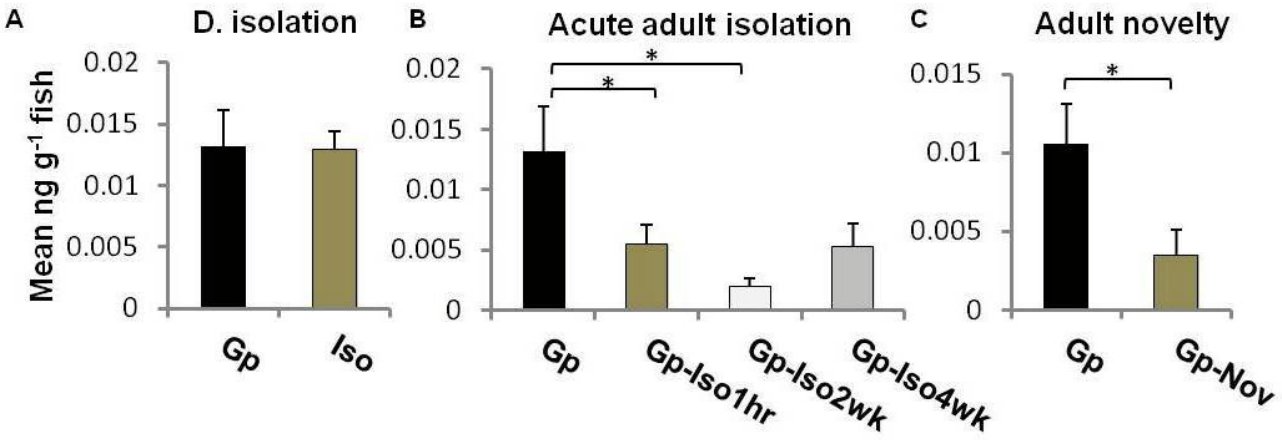
A
D. isolation
Mean ng g-1 fish
0.02
0.015
0.01
0.005
0
Gp
Iso
B
Acute adult isolation
*
*
Gp
Gp-Iso1hr
Gp-Iso2wk
Gp-Iso4wk
C
Adult novelty
*
Gp
Gp-Nov

Figure 3-8. Results of whole-body cortisol assays in adult zebrafish following exposure to different social contexts. **A**, Cortisol levels measured between 6-month group-raised (*Gp*) and 6-month isolate-raised (*Iso*) fish. D. isolation, Developmental isolation **B**, Cortisol levels measured in animals raised to adulthood in a group environment (*Gp*), or raised to adulthood in a group and exposed to 1-hour (*Gp-Iso1hr*), 2-week (*Gp-Iso2wk*), or 4-week (*Gp-Iso4wk*) social isolation. Statistically comparisons were performed between *Gp:Gp-Iso1hr*, *Gp:Gp-Iso2wk*, and *Gp:Gp-Iso4wk* only. **C**, Cortisol levels measured in zebrafish raised in a group environment (*Gp*) or group-raised followed by exposure to a novel group of adult fish for a duration of 2-weeks (*Gp-Nov*). All cortisol values are normalized to the averaged body weight of animals and represented in ng/g. *$p < 0.05$ (independent samples t-tests).

3.4.9 Changes in the Size of the Proliferative Population Occur Independently of Cortisol Levels

To more directly test the relationship between cortisol levels and cell proliferation within neurogenic niches I injected zebrafish with three different concentrations of hydrocortisone (CORT: 50 ng; 175 ng; 350 ng) or vehicle and counted the number of $BrdU^+$ cells after a 2-hour chase period (Fig. 3-9A). Since there was no significant difference in the number of $BrdU^+$ cells across all six neurogenic niches under investigation between fish exposed to my 1X-PBS control and ETOH control (B.W.L and V.T., data not shown), these data were merged ($N = 9$) for comparisons with treatment groups. For treatment groups, the resulting total concentrations of hydrocortisone per gram fish were ~13 ng/g ($N = 8$), ~50 ng/g ($N = 8$), and ~100 ng/g ($N = 8$), all well above physiological baseline levels of endogenous cortisol reported for zebrafish (Alderman and Vijahan, 2012; Dhanasiri et al., 2013). Contrary to my hypothesis, no significant between-group effect was detected within sensory niches of OB (Fig. 3-9B-C; one-way ANOVA; $p = 0.217$; df = 3; $F = 1.634$) and PGZ (Fig. 3-9D-E; one-way ANOVA; $p = 0.742$; df = 3; $F = 0.991$), nor within integrative niches of D (Fig. 3-9F-G; one-way ANOVA; $p = 0.972$; df = 3; $F = 0.077$) and VdVv (Fig. 3-9H-I; one-way ANOVA; $p = 0.823$; df = 3; F = 0.303). Similar results were obtained in LX (PBS: 3.65 ± 0.79; CORT 50 ng: 2.41 ± 0.65; CORT 175 ng: 3.26 ± 0.75; CORT 350 ng: 4.55 ± 1.07; one-way ANOVA; $p = 0.413$; df = 3; F = 0.991) and Dl (PBS: 10.38 ± 1.4; CORT 50 ng: 7.95 ± 0.71; CORT 175 ng: 9.14 ± 1.4; CORT 350 ng: 7.67 ± 0.66; one-way ANOVA; $p = 0.464$; df = 3; F = 0.894). This led me to consider whether the already heightened levels of endogenously circulating cortisol present in the group-raised fish used for the analyses were masking any effect on cell proliferation following hydrocortisone injections.

To address this, I used the 2-week adult isolation paradigm in conjunction with hydrocortisone injections of 350 ng/mL (or 1X-PBS control) to investigate whether the social context played a role in regulating the effect of hydrocortisone injections on the proliferative population within neurogenic niches. I assumed that by injecting high levels of exogenous hydrocortisone into fish with low physiological levels of endogenous cortisol, I could more readily detect changes in the number of cycling cells within niches. Following three days of consecutive injections, the

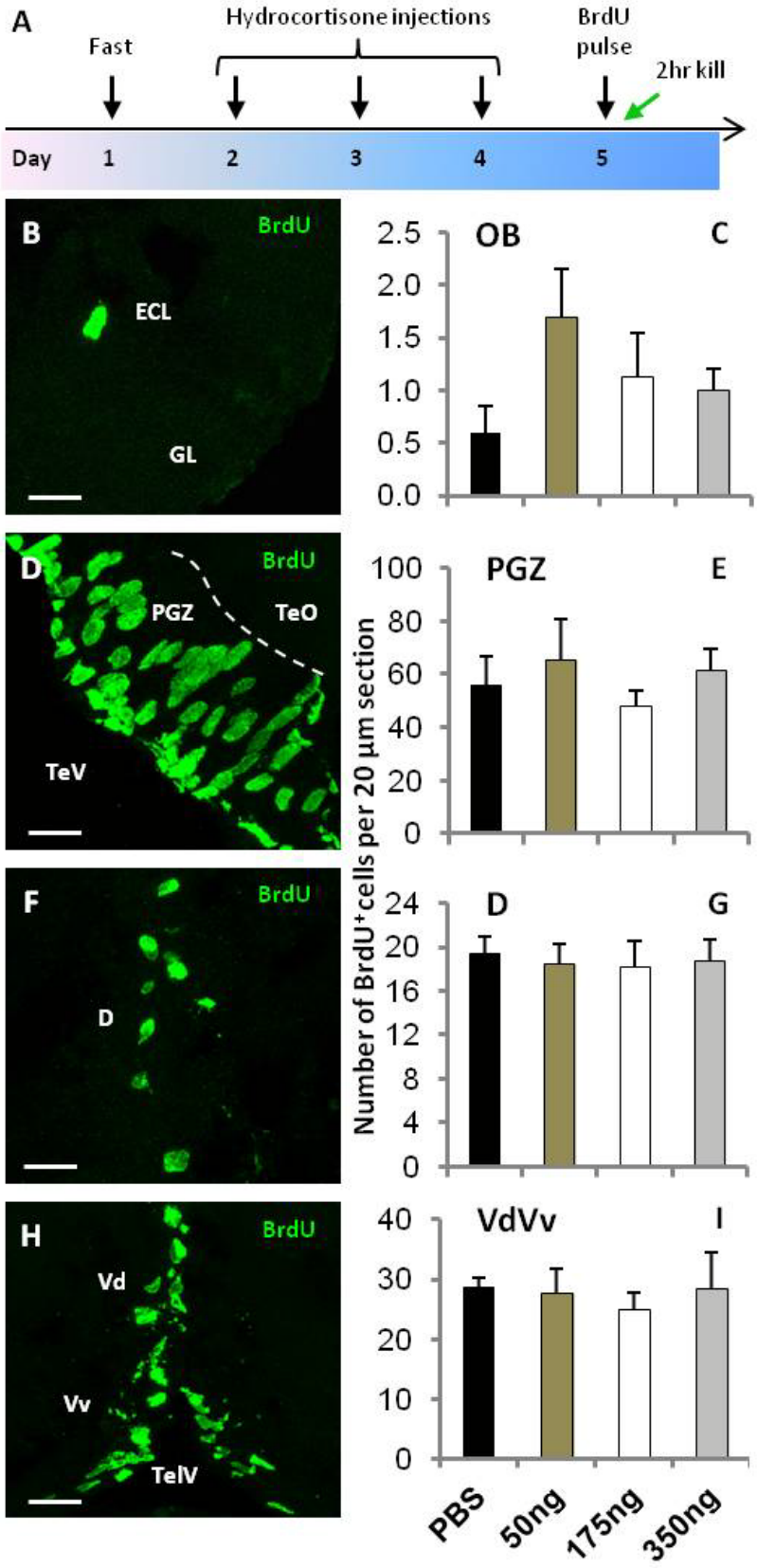
A
Fast
Hydrocortisone injections
BrdU pulse
2hr kill
Day 1 2 3 4 5
B
BrdU
ECL
GL
OB
C
D
PGZ
TeO
TeV
PGZ
E
F
D
D
G
H
Vd
Vv
TelV
VdVv
I
Number of BrdU+cells per 20 µm section
PBS
50ng
175ng
350ng

Figure 3-9. Effect of hydrocortisone injections in group-raised adult zebrafish on the number of BrdU$^+$ cells within sensory (OB, PGZ) and integrative telencephalic niches (D, VdVv). **A**,Timeline of experimental protocol performed over a 5-day period. Animals were injected with PBS control, or 50 ng, 175 ng, or 350 ng of hydrocortisone over 3 consecutive days and thereafter received a 2-hour pulse-chase with BrdU before being killed and processed for immunohistochemistry. **B-C**, Representative image of BrdU$^+$ cells in OB (**B**) and the corresponding number of BrdU$^+$ cells counted following injections of hydrocortisone compared with control (***C***). In **B**, ECL, external cellular layer; GL, glomerular layer. Hashed line represents the division between the GL and ECL. **D-E**, Representative image of BrdU$^+$ cells in PGZ (**D**) and the corresponding number of BrdU$^+$ cells counted following injections of hydrocortisone compared with control (**E**). In **D**, TeO, optic tectum proper; TeV, tectal ventricle. Hashed line represents the division between TeO and PGZ. **F-G**, Representative image of BrdU$^+$ cells in D (**F**) and the corresponding number of BrdU$^+$ cells counted following hydrocortisone injections compared with control (**G**). **H-I**, Representative image of BrdU$^+$ cells in VdVv (**H**) and the corresponding number of BrdU$^+$ cells counted following hydrocortisone injections compared with control (**I**). TelV, telencephalic ventricle. In **B, D, F, H** dorsal is up; scale bars = 10 µm. In **C, E, G, I**, statistical comparisons were performed between treatment groups using a one-way ANOVA (*$p < 0.05$).

resulting concentration of hydrocortisone per gram fish was ~62 ng/g (N = 8). Surprisingly, I found that 2-weeks of social isolation preceding cortisol injections at levels 4-fold greater than those reported for acute stress in zebrafish (Alderman and Vijahan, 2012) still gave rise to no significant difference in the number of $BrdU^+$ cells within the boundaries of OB (PBS: 0.97 ± 0.33; CORT: 0.99 ± 0.18; t-test; p = 0.955), PGZ (PBS: 76.8 ± 6.6; CORT: 78.9 ± 8.0; t-test; p = 0.852), LX (PBS: 4.6 ± 0.76; CORT: 3.4 ± 0.50; t-test; p = 0.208), D (PBS: 24.3 ± 3.2; CORT: 22.4 ± 1.8; t-test; p = 0.609), or VdVv (PBS: 31.6 ± 8.4; CORT: 32.0 ± 4.4; t-test; p = 0.960), and Dl (PBS: 15.13 ± 0.98; CORT: 14.0 ± 0.61; t-test; p = 0.34) compared with animals injection with vehicle control (*N* = 7). Taken together, these results imply that exogenous application of cortisol into zebrafish at concentrations known to be stressful in this species, and well above endogenous levels reported here, do not impact the rate of cell proliferation in sensory and integrative niches, unlike its inhibitory effect on hippocampal neurogenesis in mammals.

3.5 Discussion

A contemporary model of neurogenic plasticity in the adult vertebrate brain posits that environmental enrichment enhances neurogenesis, whereas environmental deprivation suppresses it. I tested this model by investigating the extent of neurogenic plasticity of six distinct neurogenic niches in response to social change in the adult zebrafish brain and whether these changes correlated with physiological levels of cortisol. By exposing animals to social isolation, social novelty, or a combination of the two, I show that neurogenic plasticity within the adult brain functions in a non-uniform, niche-specific manner, in which different niches adapt independently and distinct stages of neurogenesis can be differentially modulated (Fig. 3-10). Strikingly, I show that social isolation or social novelty are both capable of decreasing the number of proliferating cells while increasing the number of newborn neurons within a single niche, challenging the assumption that social deprivation and social enrichment have diametrically opposite effects on adult neurogenesis. This was most pronounced in sensory niches of the brain, supporting the notion that niches residing in primary sensory structures are more sensitive to changes in sensory cues compared to integrative niches of the telencephalon. Contrary to observations in rodents, I show that zebrafish isolated during development or adulthood do not display elevated cortisol levels compared with group-raised animals, and that this hormone correlates with the social context and acts independently from changes in adult neurogenesis.

3.5.1 Social Isolation and Novelty Dissociate Stages of Adult Neurogenesis in a Niche-Specific Manner in Primary Sensory Structures

What constitutes a stressful or enriching environment is largely determined by the life history of an animal. Environmental enrichment typically encompasses consistent multisensory/cognitive stimulation consisting of social stimulation, novel objects, and the opportunity for physical

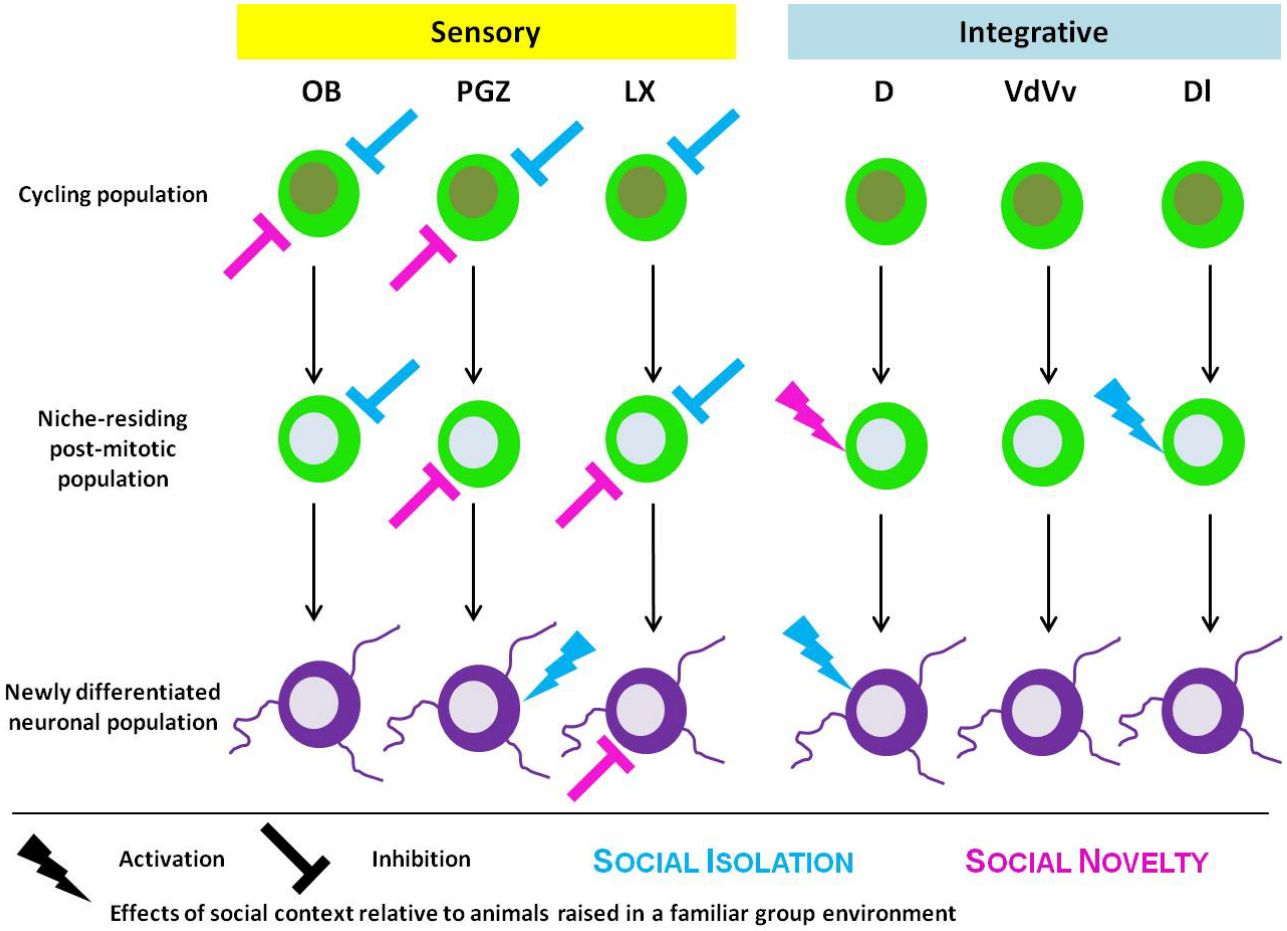
Sensory
Integrative
OB
PGZ
LX
D
VdVv
DI
Cycling population
Niche-residing post-mitotic population
Newly differentiated neuronal population
Activation
Inhibition
SOCIAL ISOLATION
SOCIAL NOVELTY
Effects of social context relative to animals raised in a familiar group environment

Figure 3-10. Model summarizing the effect of different social contexts (isolation; novelty) relative to group-raised animals within sensory (OB, PGZ, LX) and telencephalic (D, VdVv, Dl) neurogenic niches. Three distinct stages of adult neurogenesis are depicted: cycling stem/progenitor population 2-hours post BrdU injection; niche-residing post-mitotic population remaining 4-weeks post BrdU injection; newly differentiated neuronal population residing with the neurogenic niche 4-weeks post BrdU injection. Activation and inhibition refer to an increase or decrease, respectively, in the number of cells making up the population of interest at a given stage. OB, olfactory bulb; PGZ, periventricular grey zone; LX, vagal lobe; D, pallium; VdVv, subpallium; Dl, lateral zone of the dorsal telencephalon.

activity and exploration, with the objective of enrichment to enhance the well-being of animals (Baroncelli et al., 2010). In contrast, social deprivation often involves the removal of such stimuli, with animals restricted to an isolated and/or barren environment with little or no social contact. Both environmental enrichment and deprivation lead to structural changes at the level of neural networks and neuronal populations during sensitive periods of development, and it is clear that experience-driven environmental plasticity can also impinge on the composition and function of neurogenic niches in adulthood (Spolidoro et al., 2009). Recently, it has been proposed that the complex brains of vertebrates maintain greater levels of plasticity to allow adult stem/progenitor cells within the niche to adapt and thrive in response to changes in their natural environment (Kempermann, 2012). Outside of mammalian models of adult neurogenesis however, how these stem/progenitor populations within adult neurogenic niches adapt under conditions of environmental enrichment or deprivation still continue to be enigmatic (Zupanc, 2001A).

By comparing sensory and integrative neurogenic niches in the adult zebrafish brain, I provide evidence that a bias exists towards neurogenic plasticity in sensory niches, and that the preconceived notion that enrichment increases adult neurogenesis and deprivation decreases it, cannot be generalized across distinct niches, or stages of this process. Zebrafish rely heavily on visual, olfactory, and taste cues for numerous behaviors (Gerlach et al., 2008), and accordingly, my data suggest that sensory neurogenic niches more readily adapt to changes in the social context, resulting in a re-organization of the composition of cells making up the adult niche at different stages of adult neurogenesis. The limited neurogenic plasticity in telencephalic niches could be due to the fact that my experiments relied on manipulating the degree of sensory/social stimulation available to animals, and did not explicitly address any form of learning, which would be predicted to engage plasticity inherent in the telencephalon. To my surprise, neither isolation nor novelty conditions led to any change in the $BrdU^{+}$ population across integrative niches. However, consistent with reports in the mammalian hippocampus (Lieberwirth et al., 2012), I do show that developmental and adult social isolation in zebrafish generally produce a decrease in the stem/progenitor population in sensory niches.

A most fascinating finding of my study was that the size of the stem/progenitor pool could be regulated independently from the resulting number of newly differentiated neurons under

specific social contexts. Within PGZ, the population size of niche-residing $BrdU^+$ cells at 2-hours and 4-weeks both declined following isolation or novelty. From the remaining population however, a greater proportion of differentiated neurons were generated. This was most clearly demonstrated during conditions of adult social isolation compared with isolation plus novelty, revealing stage-specific differences in the direction of the neurogenic response. Thus, I illustrate that stages in the process of adult neurogenesis need not always occur in a linear fashion (i.e., each stage increasing or decreasing accordingly), but that under certain conditions and within some niches the social context can give rise to bi-directional changes within this process. One mechanism for the lower rate of cell division could be that the non-glial-like stem/progenitor cells residing in PGZ (Ito et al., 2010) are more susceptible to changes in environmental stimuli compared with glial-like stem/progenitor cells located in the pallial and subpallial niches of the zebrafish telencephalon (Ganz et al., 2010). This is further supported by my observations within the lateral zone of the dorsal telencephalon (Dl) of the zebrafish, believed to be homologous to the mammalian hippocampus (Salas et al, 2006; Lau et al., 2011), that also demonstrated little adaptive responses with exposure to isolation or novelty, and are composed of morphologically similar cell types as the pallium and dorsal subpallium (Lindsey et al., 2012).

Dissociation between the birth and survival of the stem/progenitor cell population was also evident in OB following developmental isolation and novelty. Congruent with olfactory sensory deprivation studies in mice using occlusion paradigms (Mandairon et al., 2006), developmental isolation in zebrafish resulted in a decreased number of $BrdU^+$ cells, while this effect was exacerbated by social novelty, a form of enrichment predicted to restore such decreases. This exemplifies how two seemingly opposing social contexts can impose the same directional change on a single neurogenic niche. Experiments in the adult zebrafish telencephalon have demonstrated that the ‘social isolation context’ also plays a role, and that zebrafish socially isolated in a barren environment compared with an enriched environment (rocks, flora) have lower levels of $PCNA^+$ cells (von Krogh et al., 2010). Though this report did not examine effects in the olfactory bulb, it suggests the possibility that the type of enrichment applied may have a significant impact on the odds of detecting neurogenic plasticity in corresponding niches. Work in the electric fish has more recently shown that fish paired with multiple different partners over a 14-day period is required to increase rates of proliferation (Dunlap and Chung, 2012). Therefore, I must consider that continuously housing isolates with a single social group may

have prevented the ability to restore proliferation rates due to habituation to the novel stimulus. By monitoring the surviving, post-mitotic, niche-residing population after 4-weeks, I did however observe a significant increase in the labeled OB population under group, isolate, and novelty conditions. These data suggest that proliferative cells reside within the niche of OB under various social contexts, and that over time these populations expand, possibly by emigration of cells from the subpallial niche along the putative rostral migratory stream (RMS) into the glomerular layer of OB (Kishimoto et al., 2011). The likelihood of this hypothesis is corroborated by my results revealing a significant decrease in the population of $BrdU^{+}$ post-mitotic population in the subpallium 4-weeks after labeling.

Finally, the pre-existing social environment of animals may additionally be implicated in how different neurogenic niches adapt to social change. For instance, animals raised in isolation lack the experience of sensory stimuli from social interactions, and upon exposure to social novelty new sensory neurons are born to process this information, regardless of the state of the progenitor population. By contrast, group-raised animals have increased competition for food, partners, and social status (Maruska et al., 2012), which increase anxiety and suppress neuronal differentiation (Diniz et al., 2012; Sah et al., 2012). With exposure to isolation, this may provide a reprieve from the challenges of the social context, resulting in increased neuronal differentiation. My data support the notion that stage-specific changes detected in adult neurogenesis following a shift to a new environmental context are relative to the preceding social context of the animal, as well as the duration of time spent exposed to these conditions.

3.5.2 Physiological Relationship of Cortisol Under Different Social Contexts and its Impact on Stem/progenitor Cell Proliferation During Adult Neurogenesis

Most forms of stress inhibit adult neurogenesis by lowering the rate of cell proliferation within neurogenic niches (Schoenfeld and Gould, 2011); however, we now know that even in mammals exceptions exist and that regulation of the stress axis and how it impinges on stages of adult neurogenesis is more complicated than once thought. Rewarding experiences such as running, sexual experience, and enrichment, some of which themselves are coupled with increased cortisol, can protect against the inhibitory effects of increased glucocorticoids on adult

neurogenesis (Schoenfeld and Gould, 2013). Running, for example, elevates stress hormone levels, while at the same time increases cell proliferation and induces neuronal differentiation in the dentate gyrus of mice (Snyder et al., 2009) and rats (Stranahan et al., 2006). However, in a separate study, mice housed in isolation or social groups and allowed access to a running wheel have shown similar increases in the number of $BrdU^+$ and $doublecortin^+$ cells in the hippocampus compared with their respective sedentary controls, with no corresponding increase in cortisol levels (Kannangara et al., 2009). Here, I predicted that zebrafish subjected to 6-months of developmental, or 2-week and 4-week adult social isolation would be under chronic stress (long-term, continuous exposure; Lupien and McEwen, 1997), while animals exposed to novelty in the form of an unfamiliar social group would be under a 'non-stressful' condition. My results show that changes in the complex social environment of zebrafish (i.e., isolation or novelty) are associated with distinct physiological changes in cortisol levels that occur independently of changes in proliferation rates within neurogenic niches.

By assaying endogenous cortisol levels in group-raised zebrafish subjected to social change via a shift to acute (1-hour) or long-term social isolation (2-week; 4-week) or novelty (2-week) beginning at 6-months, I show that these changes in social context are consistently associated with a significantly lower level of cortisol compared with grouped controls, refuting my prediction. These data reveal that the physiological response to cortisol can be triggered similarly under contexts perceived as deprived (i.e., isolation) or enriched (i.e., novelty), unlike the situation in mammals where social isolation is often correlated with elevated cortisol levels and reduced hippocampal neurogenesis (Rizzi et al., 2007; Perez et al., 2012). This supports the idea that environmental and social factors comprising a group setting can produce elevated endogenous cortisol levels compared with isolated fish or animals exposed to novelty during adulthood.

Studies examining social status in zebrafish (Filby et al., 2010; Dahlbom et al., 2011; Pavlidis et al., 2011) and African cichlids (Maruska et al., 2012; 2013) have proposed that elevated cortisol levels in grouped animals may be explained by social competition for food and mates, and dominant or subordinate status, all of which could increase anxiety-related or vigilance-related behaviours in fish. Nevertheless, conflicting data concerning the relationship between stress levels and social status currently exists between these species. Within populations of African cichlids, holding a dominant position is associated with elevated cortisol levels and proliferation

rates, while the inverse is true in subordinates (Maruska et al., 2012; 2013). By contrast, subordinate, not dominant status within zebrafish hierarchies have been correlated with elevated levels of plasma cortisol (Filby et al., 2010), implying that the environmental impact of social status on activation of the hypothalamus-pituitary-interrenal (HPI) axis may differ between taxonomically distinct Families. Although this was not directly examined in my study, it is likely that group-raised controls formed established social hierarchies over a 6-month period. Of groups consisting of six fish, most would be of subordinate status, and thus the likelihood of transferring a subordinate compared with a dominant into a social isolation or novelty context would be much greater. My data suggest that removal of stressors associated with social status in zebrafish during adulthood correlate, at least temporarily with decreases in cortisol, and either a decrease (sensory) or no change (integrative) in the stem/progenitor population across neurogenic niches.

The precocial nature of zebrafish led me to further question whether long-term social isolation beginning at 5 dpf and continuing until 6-months was similarly correlated with lower levels of circulating cortisol compared with short-term isolation during adulthood. Markedly, I found that long-term developmental social isolation had nearly identical elevated cortisol levels as group-raised controls, further substantiating that cortisol levels respond in accordance with the social context and are dissociated from the neurogenic response, as shown by significantly greater rates of cell proliferation in group-raised animals compared with isolates. This view is further supported by my hydrocortisone injection experiments that displayed no effect on the size of the proliferative population within neurogenic niches despite concentrations well above endogenous levels and those reported in zebrafish following a stressful event (Dhanasiri et al., 2013; Alderman and Vijahan, 2012). I note, however, that these results oppose earlier observations in the dentate gyrus of mammals showing decreases in rates of cell proliferation following direct injections of synthetic cortisol (Gould et al., 1992; Cameron and Gould, 1994). One physiological mechanism that may have blocked the effect of hydrocortisone on the stem/progenitor population in zebrafish is upregulation of type 2, 11β-hydroxysteroid dehydrogenase (Hsd11b2) that converts active glucocorticoids to their inactive derivatives (Alderman and Vijayan, 2012). Not only does the spatial distribution of *hsd11b2* mRNA overlap with adult neurogenic niches in the zebrafish brain, but acute stress is sufficient to upregulate Hsd11b2 activity, implying a role in negative feedback regulation of cortisol following activation

of the teleost HPI axis. At present, it remains unclear as to why such a disparity exists between cortisol levels following long-term developmental social isolation compared to isolation at adulthood. A possible explanation could be that long-term deprivation of stimuli is equally as stressful as the stress of long-term social interactions within a group environment as a subordinate. These findings bring to light that we cannot simply extrapolate interpretations of the changes in cortisol levels reported in animals exposed to isolation at adulthood to animals chronically exposed to long-term social isolation beginning at early development.

3.5.3 Conclusions

Using adult zebrafish, I have investigated how the social context can differentially shape neuronal production in sensory and telencephalic neurogenic niches and whether cortisol is involved in regulating these changes. This study leads to the following major observations: (1) there is a robust negative effect of social change on the proliferation of stem/progenitor cells, primarily in sensory regions. In contrast, social change can have a positive effect on survival and neuronal differentiation in both sensory and integrative regions of the brain; (2) within a single neurogenic niche, the same change in the social context can uncouple (i.e., increase or decrease) distinct stages of adult neurogenesis; (3) experience from a preceding social context is associated with how cortisol levels will respond under a new social environment; (4) opposite to mammals, cortisol levels correlate with changes in the social context independently of the neurogenic response and are not sufficient to drive changes in adult neurogenesis. Collectively, my findings highlight that interpretations of how a single neurogenic niche is modulated under different environmental contexts must be made with caution, and considered a niche-specific property rather than a universal tenet of adult neurogenesis, as I have shown that distinct niches are characterized by varying degrees of neurogenic plasticity at each stage of this process. Additionally, we must reconsider how we define a stressful environment and how the complexities of the social milieu can impinge on neurogenic plasticity within adult neurogenic niches. Future systematic niche-to-niche comparisons will be required to understand how different social environments can activate or inhibit stages of adult neurogenesis and whether, in fact, the resulting changes are of adaptive significance to the lifestyle of the animal.

CHAPTER 4

SENSORY-DEPENDENT NEUROGENIC PLASTICITY AND THE CELLULAR COMPOSITION OF ADULT SENSORY NEUROGENIC NICHES IN THE ZEBRAFISH BRAIN

4.1 Abstract

Teleost fishes are unique among vertebrates in that they retain populations of adult stem/progenitor cells within multiple primary sensory processing structures of the mature brain. This suggests that adult neurogenesis within these niches could be directly involved in encoding sensory information perceived from the external environment. Aside from a few recent studies examining the cell types composing the proliferative domain of the optic tectum, very little is known about the properties of sensory neurogenic niches. In the present study, by examining the cytoarchitectural organization, modality-specific neurogenic plasticity, and intrinsic regulation by Fibroblast Growth Factor (FGF) within chemosensory niches of the olfactory bulb (OB) and vagal lobe (LX) and visual processing niches of the periventricular grey zone (PGZ) of the optic tectum and torus longitudinal (TL) in the adult zebrafish brain, I illustrate three primary features of sensory neurogenic niches and provide comparisons with forebrain compartments previously studied. First, the ultrastructural organization between sensory niches is highly variable, but includes many of the same cellular morphologies described in forebrain niches of the adult zebrafish; some suggestive of a radial glial phenotype. Second, sensory niches adapt to modality-specific stimulation at distinct stages in the process of adult neurogenesis, displaying sensory-dependent neurogenic plasticity. Third, preliminary results suggest that FGF signalling may not be involved in regulating constitutive levels of stem/progenitor cell proliferation in contrast to previous studies in the subpallium of the zebrafish telencephalon. These data suggest that sensory neurogenic niches residing in primary sensory structures are likely governed by a subset of different stem/progenitor populations and molecular programs compared with forebrain niches, which collectively may function to regulate properties of sensory-dependent modulation.

4.2 Introduction

In all vertebrates, including humans, sensory information processing of the surrounding environment is continuously perceived and analyzed, with this input influencing behavior and higher cognitive decisions (Stein and Standford, 2008). Perception of the external world is carried out via multisensory integration of primary sensory modalities, and in the wild, species rely on this sensory information for survival and the ability to adapt to environmental change. Across the animal kingdom, relevant sensory information may take the form of olfactory, visual, gustatory, mechanosensory, auditory, or tactile stimuli, which may be processed as separate or compound stimuli. With the discovery of adult neurogenesis and its ability to undergo plasticity in response to environmental stimuli, one question that arises is how different forms of sensory stimuli may modulate physiological rates of neurogenesis.

Common to all forms of environmental stimuli is that they contain modality-specific or multimodal sensory information. Both vertebrate and invertebrate models alike have shown shifts from physiological levels of adult neurogenesis following exposure to olfactory enrichment or deprivation (Alverez-Buylla and Lois, 1995; Hansen and Schmidt, 2001; Tanapat et al., 2001; Rochefort et al., 2002; Bovetti et al., 2009; Feierstein, 2012), seasonality (Barnea and Nottebohm, 1994; Dawley et al., 2000; Lavenex et al., 2000; Hansen and Schmidt, 2004; Hoshooley and Sherry, 2004; Hamdani et al., 2008; Delgado-Gonzalez et al., 2011), social interactions (Maruska et al., 2012; Song et al., 2007; Mak and Weiss, 2010; Dunlap and Chung, 2013; Lieberwirth et al., 2012; Lindsey and Tropepe, submitted), and mating pheromones (Mak et al., 2007; Oboti et al., 2009; Wu et al., 2013). In many of the above examples however, the resulting effect on cell proliferation, differentiation, or neuronal survival occur in niches whose function are not dedicated to processing information from primary sensory stimuli from the environment.

It remains unclear how neurogenic niches present in adulthood within primary sensory structures of the brain are remodelled by activation or inhibition of cellular populations with sensory stimuli. With few exceptions (Gritti et al., 2002; Alunni et al., 2010; Ito et al., 2010; de Oliveira-Carlos et al., 2013), even the fundamental properties of sensory neurogenic niches are poorly understood, including the cellular composition and intrinsic regulatory mechanisms. Interestingly, an earlier *in vitro* study by Gritti et al. (2002) in adult rodents did show that

multipotent precursors with stem cell characteristics could be isolated from the distal portion of the rostral extension of the SVZ located within the core of the olfactory bulb, demonstrating evidence that a small number of resident ANSCs are maintained in adulthood in the olfactory bulb proper. However, since this report, no subsequent studies have followed up this claim *in vivo*, leaving it unknown how this population of cells may respond to sensory stimulation, compared with the more intensely studied populations of ANSCs arising from the SEZ. In light of the above, what we know about neurogenic plasticity in the olfactory bulb of mammals holds few clues, since the origin of ANSCs examined do not reside in the olfactory bulb but rather in the supependymal zone (SEZ; Gheusi et al., 2013). Based on the current literature, it would appear that mammals, birds, nor reptiles retain stem/progenitor pools in any primary processing centers of the adult brain (reviewed in Garcia-Verdugo et al., 2002), or at least to any extent worthy of investigation. Therefore, our state of knowledge of neurogenic plasticity has relied largely on modulation of actively dividing populations of cells lining the ventricular zones or within the hippocampal structures of these species. Moreover, how different sets of growth factors, signalling pathway, and hormones control the microenvironment of the niche arises primarily from mammalian studies (Doetsch, 2003B; Mudo et al., 2009; Imayoshi and Kageyama, 2011; Schoenfeld and Gould, 2011). One vertebrate group that remains an exception is teleost fishes.

Modality-specific stimuli can impinge directly upon the size of primary processing structures. For instance, natural populations of African cichlids within the freshwater lakes of East Africa have demonstrated that the optic tectum is smallest in animals from deep water microhabitats and largest in pelagic species (Huber et al., 1997; Kotrschal et al., 1998). More recently, detailed mapping studies have shown that adult zebrafish maintain populations of actively dividing stem/progenitor cells in a number of primary sensory processing structures, capable of producing adult-born neurons (Zupanc et al., 2005; reviewed in Lindsey and Tropepe, 2006; Grandel et al., 2006; Kaslin et al., 2008). Work in the neurogenic niche of the adult optic tectum of zebrafish over the last few years has begun to advance our understanding of the phenotype of stem/progenitor cells in the local environment, their differentiated neuronal phenotype (Ito et al., 2010), and endogenous signalling pathways proposed to be involved in regulating the niche (de Oliveira-Carlos et al, 2013). Additionally, adult zebrafish have been shown to undergo olfactory conditioning in response to L-type amino acids (Braubach et al., 2009) and color-dependent

visual discriminatory learning (Coldwill et al., 2005), suggesting that the presence of stem/progenitor cells residing within sensory niches may have a functional role. Finally, it has been shown that neurogenic niches residing in adult olfactory bulbs, optic tecta and vagal lobe of zebrafish respond more readily to changes in the social environment which contain complex sensory stimuli, compared with integrative regions of the telencephalon (Chapter 3; Lindsey and Tropepe, submitted).

In the present study, I set out to address three specific questions using the zebrafish model (*Danio rerio*) to begin to characterize fundamental properties of adult sensory neurogenic niches localized to chemosensory or visual processing structures. First, are the cell types composing sensory niches conserved with those previously described in forebrain niches of the adult zebrafish brain (Lindsey et al., 2012)? Second, does exposure to modality-specific stimuli act explicitly on the corresponding primary sensory processing niche, and what stage in the process of adult neurogenesis does it affect? Third, is FGF Receptor-1 (FGFR-1) signalling required to regulate constitutive levels of adult neurogenesis in sensory niches similar to the ventral glial domain of the adult subpallium (Ganz et al., 2010; Topp et al., 2008)? With adult neurogenesis persistent under physiological conditions within the olfactory bulbs, vagal lobe, optic tectum, and torus longitudinalis, and many social behaviours in this species guided strongly by chemosensory or visual cues (Wullimann et al., 1996), this model allows me to investigate the composition, plasticity and regulation of the niche and hypothesize how resident populations of stem/progenitor cells in primary sensory processing centers are influenced by exposure to modality-specific stimuli. Moreover, available transgenic lines allow to further catalogue additional molecular programs controlling sensory neurogenic niches. Findings from this study will expand our current thinking of adult neurogenesis and stem cell biology beyond forebrain niches and establish the zebrafish as an effective vertebrate model of adult sensory neurogenesis.

4.3 Methodology

4.3.1 Animals

Wildtype zebrafish of both sexes (AB background) or the dominant-negative heatshock transgenic zebrafish line Tg(hsp70l:dnFgfr1-eGFP) raised on an AB background (Zebrafish International Resource Center; ZIRC) were used for all experiments and maintained on a 14h light:10h dark photoperiod at 28°C in our fish facility (Aquaneering Inc., San Diego, U.S.A.). Fish were fed a diet of granular food (ZM, Winchester, U.K.) and brine shrimp thrice daily. All zebrafish used for experiments were between 8-months to 1-year of age. Animals were killed using an overdose of 0.4% Tricaine methanesulfonate diluted in tank water. Thereafter, the total body length (mm), weight (g), and sex of the fish were recorded. Handling procedures were done in accordance with the policies set forth by the University of Toronto and the Canadian Council for Animal Care (CCAC).

4.3.2 Chemosensory Stimulant Screening

To determine chemosensory stimulants (smell/taste) to which adult zebrafish responded an assay was designed to screen a variety of L-type amino acid combinations, bile salts, and food extracts, previously suggested to elicit a response in zebrafish (Hara, 1994; Yaksi et al., 2009). Mixtures of like-amino acids consisting of the same side chain were tested, including neutral amino acids (Cys, Gln, Met, Ser; 100 µM), basic amino acids (Arg, Lys, His; 300 µM), acidic amino acids (Asp, Glu; 100 µM), and hydrophobic aromatic amino acids (Phe, Trp, Tyr; 100 µM). Bile salts tested included Sodium taurocholate hydrate (TCA) and its derivative, Sodium taurodeoxycholate hydrate (TDCA), both at final concentrations of 100 µM. Food extracts consisted of dried Bloodworms, made by dissolving 50 g of crushed extract in 1 L of tank water and filtered to yield a final 0.02% solution. All concentrations given are for stimulants dissolved in 2 L tank water.

One day prior to chemosensory screening, fish were acclimated in individual 3 L testing tanks with a water volume of 2 L, and fasted for 24 hrs. Photoperiod and water temperature was maintained as above throughout the acclimation and testing period. The morning of testing, 10

mL aliquots of concentrated stimulants or vehicle control (tank water) were prepared fresh and warmed to 28º C with testing commencing at 10:00. During stimulant screening single adult zebrafish were tested sequentially using 4.5-min long trials and recorded from above using a JVC camcorder for downstream analysis of swimming-evoked movement. The first 2-min of each trial was recorded to obtain a baseline of zebrafish swimming activity. Thereafter, 10 mL of chemosensory stimulant or vehicle was infused over a period of 20-30 sec, and the response of zebrafish recorded for an additional 2-min. For each stimulant, a total of N =6 -10 fish of mixed sex were tested, while N = 12 control trials were run.

Swimming-evoked movement was assessed using Ethovision 3.1, with the total distance travelled by zebrafish within the tank used to evaluate a response to chemosensory exposure. This method of assessment is one of a number of commonly used quantification methods to analyze swimming patterns in zebrafish under laboratory conditions (Blaser and Gerlai, 2006). I assumed that zebrafish would increase their swimming activity if a stimulant was detected, regardless of whether it was aversive or favorable, and as a result would increase the total path length travelled during the post-infusion trial period. To determine whether a significant difference was present before and after infusion of each stimulant, the total distance travelled (cm) was calculated by analyzing the last minute pre-infusion and the first minute post-infusion and compared using a paired samples t-test. Those stimulants producing a significant increase in swimming activity in zebrafish were then used to establish a chemosensory assay to test adult neurogenic plasticity.

4.3.3 Effect of Chemosensory Stimulants on Adult Neurogenesis

To investigate the effect of chemosensory stimulants on physiological levels of stem/progenitor cell proliferation, neuronal differentiation, and neuronal survival, adult zebrafish were exposed to a randomized design of five different stimulants or tank water (vehicle control) over a 7-day period. One day prior to exposure, animals were acclimated in testing tanks filled with tank water under standard housing conditions. Thereafter, over days 1-7 zebrafish received a randomized exposure of five different chemosensory stimulants (Fig. 4-6A; 100 µM taurocholate hydrate, 100 µM acidic amino acids, 100 µM neutral amino acids, 100 µM aromatic amino acids,

or 0.02% bloodworms). All stimulants were warmed to 28ºC prior to infusion; the same temperature at which tanks were maintained. The first stimulant was administered at a volume of 10 mL at 08:00, with a different stimulant added thereafter every 2-hours until 20:00. To avoid compounding of chemosensory stimulants, tanks were flushed daily with facility water for 30 min at 10:30, 13:30, and 20:30. This prevented poor water quality over the exposure period, as well, allowed 2-3 stimulants to interact over a 4-6 hour period and reduce the chances that fish habituated to similar combinations of stimulants.

The time period over which zebrafish were exposed to the 7-day chemosensory assay (or vehicle) varied according to the stage of adult neurogenesis under investigation. To examine changes in stem/progenitor cell proliferation and neuronal differentiation, animals were exposed to chemosensory stimulants over days 1-7. At 10:00 on day 8, specimens were injected with a 10 mM bolus of BrdU and transferred to housing tanks with fresh facility water until the time of sacrifice. Following a 2-hour (Fig. 4-6D; proliferation) or 2-week period (Fig. 4-7A; differentiation) post-BrdU injection, animals were killed and brain tissue processed for IHC. By contrast, zebrafish allocated for experiments examining survival of newly differentiated neurons were injected with BrdU as above on day 1 then left in housing tanks under standard conditions until day 14 (Fig. 4-7C). Thereafter, over days 15-21, animals were exposed to the 7-day randomized chemosensory stimulants, and sacrificed on day 22 for analysis. Exposure of zebrafish to chemostimulants 2-weeks post BrdU injection was based on earlier work in forebrain neurogenic niches (Lindsey et al., 2012), showing that the proportion of newborn neurons after 2-weeks began to decline across most niches. Thus by exposing animals to chemosensory enrichment over this time period I predicted that I would be able to either sustain or enhance the size of the *de novo* neuronal population.

4.3.4 Effect of Monochromatic Light on Adult Neurogenesis

To test the effect of a limited visual spectrum on physiological levels of cell stem/progenitor cell proliferation, neuronal differentiation, and neuronal survival, zebrafish were exposed to monochromatic light in the green (560 nm) and blue (480 nm) spectrum, in line with peak wavelengths reported for zebrafish cones (Fig. 4-8A; Fleisch and Neuhauss, 2006). Each

monochromatic light condition was counterbalanced with full spectrum light normalized to the same light intensity using a Fisher Brand Light Meter (Fisher, Scientific): green light = ~200 lux; blue light = ~ 15 lux. For these studies, the same fiber optic light source and bulbs (21 volt; 150 watt; Ushio Halogen projector lamp) was used for experimental and control conditions, with the assumption that bulbs provided animals with near full spectrum light. Monochromatic light within chambers was achieved by shining fiber optic lights through bandpass filters (Asahi Spectra Co., Ltd., Tokyo, Japan) positioned on the lids of testing chambers. One day prior to exposure, zebrafish were placed in 2.5 L of tank water in standard housing tanks, and tanks placed inside grey light-tight testing chambers. For the purposes of acclimation, lids were removed from chambers for 24-hours prior to exposure. Each housing tank was equipped with PVC tubing for inflow and outflow to allow for water changes, and digital thermometers to monitor that water temperature remained at 28°C. Room lights and fiber optic lights were set to 14h light (08:00-10:00):10h dark (10:00-08:00) photoperiod, and water temperature in tanks maintained at 28°C. Over days 1-7 of the exposure period, zebrafish were housed in light-tight chambers under experimental (monochromatic) or control (full spectrum) conditions, with lids opened twice at 08:00 and 17:00 for feeding, and a 1 L water change performed daily at 12:00. The timing of exposure to monochromatic light and BrdU injections were executed the same as for chemosensory experiments, and tissue processed accordingly for IHC.

4.3.5 Heatshock Experiments to Examine the Role of Fibroblast Growth Factor Receptor-1 (FGFR-1)

The transgenic zebrafish line Tg(hsp70l:dnFgfr1-eGFP) was used (Zebrafish International Resource Center; ZIRC) to examine the role of the Fibroblast Growth Factor Receptor-1 (FGFR-1) signalling pathway in regulating constitutive levels of adult neurogenesis in sensory niches (Fig. 4-9A). The same transgenic line has been previously used to examine FGFR-1 signalling in the pallial and subpallial zones of the adult zebrafish telencephalon (Ganz et al., 2010). Upon heatshock, the hsp70 promoter induces expression of a dominant-negative FGF receptor-1-eGFP fusion protein, which heterodimerizes with all endogenous Fgfr subtypes, and as a result, competitively blocks downstream signalling of all Fgfr subtypes (Lee et al., 2005). To downregulate FGF signalling, adult zebrafish were exposed to two 1-hour heatshocks (HS^{+}) at

38°C, with a 2-hour interval at standard tank temperatures of 28°C (Fig. 4-9B).

To first assert that FGF signalling was downregulated in neurogenic niches of interest, zebrafish were sacrificed 3-hours following the second HS^{+} and processed for GFP immunohistochemistry compared with control animals (HS^{-}). Thereafter, to examine the requirement of FGF signalling on cell proliferation, zebrafish were injected with BrdU 24-hours after the second HS^{+} and sacrificed 2-hours later. A separate set of transgenic animals underwent the same protocol, but were continuously maintained at standard tank temperatures of 28°C (HS^{-}). Wildtype control fish on an AB background were additionally exposed to the same experimental (AB^{+}) and control (AB^{-}) heatshock conditions. All animals were processed for IHC upon sacrifice.

4.3.6 Sensory Neurogenic Niches Examined

Cell counting was completed in four neurogenic niches localized within separate primary sensory structures of the adult zebrafish brain. Sensory neurogenic niches were defined as neurogenic niches displaying constitutive levels of adult neurogenesis and residing within a neuroanatomical subregion of adult primary sensory processing structures of known function (Figs. 4-6B-C; 4-8B-C; red portion of schematics). All neuroanatomical terminology and rostrocaudal boundaries are in accordance with Wullimann et al. (1996). Sensory neurogenic niches located within chemosensory processing structures were localized within the olfactory bulb (OB; olfaction; 23-50x; primarily the glomerular layer, GL; Fig. 4-6B) and the vagal lobe (LX; gustation; 279-303; Fig. 4-6C), while sensory niches within visual processing structures resided within the caudal periventricular grey zone (PGZ; movement, shape, color; 213-223x; Fig. 4-8B) of the optic tectum (TeO) and the torus longitudinalis (TL; light intensity; 153-190x; Fig. 4-8C).

4.3.7 BrdU Administration and Brain Processing

Bromodeoxyuridine (BrdU) administration was performed by injecting a single 10 mM pulse of BrdU (Sigma) intraperitoneally at a volume of 50 µL/g body weight into anaesthetized fish to detect proliferating cells in the S-phase of the cell cycle. Following chase periods, animals were sacrificed and either placed directly into 4% paraformaldehyde (PFA) or transcardially perfused with ice-cold 1X-phosphate buffered saline (PBS; pH 7.4) and 4% PFA, and brains excised.

Thereafter, brains were prepared for cryosectioning and tissue sections cut at 20 µm intervals through the rostrocaudal axis for IHC as described previously (Lindsey et al., 2012).

4.3.8 Immunohistochemistry

Immunohistochemistry (IHC) was used to detect $BrdU^+$ proliferative populations, populations of putative adult neural stem/progenitor cells having a glial phenotype, or cells that differentiated into a neuronal phenotype within neurogenic niches. Single-labeling of $BrdU^+$ cells and double-labeling of $BrdU^+$ cells with the neuronal marker HuCD or the glia marker Glutamine Synthetase (GS) were carried out accordingly to protocols described in Lindsey et al. (2012), with the modification that secondary antibodies were applied for 3-hours at room temperature. For BrdU labeling alone, brain sections were incubated in rat-anti-BrdU polyclonal primary antibody (1:1000; Serotec; MCA2060), followed by goat-anti-rat-Cy3 secondary antibody (1:400; Cederlane). For double-labeling, the above BrdU primary antibody was conjugated to a goat-anti-rat Cy2 secondary antibody (1:200; Cederlane), and tissue next labelled with monoclonal mouse-anti-HuCD (1:400; Molecular Probes; 16A11) or mouse-anti-GS (1:800; Millipore; MAB302) conjugated to goat-anti-mouse Cy3 secondary antibody (1:400; Cederlane).

To confirm downregulation of FGFR-1 signalling in Tg(hsp70l:dnFgfr1-eGFP) zebrafish, brain sections were labelled with anti-GFP rabbit polyclonal antibody conjugated to Alexa488 (1:1000; Invitrogen; A21311). Brain sections were blocked with 5% normal goat serum diluted in 1X-PBS prior to overnight incubation in the antibody. Following rinses in 1X-PBS, Hoechst 33258 nuclear counterstaining was performed. All brain sections were mounted in 100% glycerol for visualization and confocal imaging.

4.3.9 Transmission Electron Microscopy

Transmission electron microscopy (TEM) was used to examine the ultrastructural profile of cells composing sensory neurogenic niches of the olfactory bulb (OB; x50), periventricular grey zone (PGZ; x219-223) of the optic tectum, and vagal lobe of the hinbrain (LX; x290-303). Animals were perfused using ice-cold 1X-PBS followed by 3% gluteraldehyde primary fixative (GLUT),

and brains excised. Following overnight fixation of tissue in 3% GLUT, specimens were rinsed in 0.1 M Sorenson's phosphate buffer and postfixed for 2 hours with 1% osmium tetroxide. Thereafter, tissue was rinsed and dehydrated through an ascending ethanol series, and then infiltrated with an ascending series of 100% ethanol and Spurr's epoxy resin. The next day, tissue was infiltrated with fresh Spurr's resin twice over a 6-hour period and then flat-embedded and polymerized at 65C overnight.

Using a Leica EM UC6 ultramicrotome, 1 µm semithin sections and 100 nm ultrathin sections were taken at the corresponding rostrocaudal level of each niche at 5 µm intervals. At each interval, semithin sections collected onto glass slides were stained with 0.035% Toluidine Blue/Methylene Blue diluted in methanol, while ultrathin sections were collected onto copper grids for TEM. Ultrathin sections were stained with 3% uranyl acetate in 50% methanol for 45 minutes, followed by Reynold's lead citrate for 10 min, and then dried overnight. Imaging was done by using an HT7700 Hitachi Transmission Electron Microscope and images captures using EMIP VO522 Software. Brightfield images of semithin sections were taken on a Leica DMI 300B inverted microscope.

For analysis, the morphology of cells present in OB, PGZ, and LX were compared with the six distinct ultrastructural profiles (Type IIa, Type IIb, Type III, Type IVa, Type IVb, Type V) previously described in forebrain neurogenic niches in Lindsey et al., 2012 (see Chapter 2; Table 2-4).

4.3.10 Cell Counting and Imaging

Imaging was performed using a Leica TCS SP5 confocal microscope. Quantification of $BrdU^+$ cells was done by counting a minimum of every second section through the rostrocaudal range of each niche at 40x magnification (Figs. 4-6B-C; 4-8B-C; red region of each niche). For analysis in the PGZ, $BrdU^+$ cells in individual hemispheres were counted then summed together to represent numbers for the entire brain. To quantify the number of $BrdU^+/HuCD^+$ cells or assess the presence of $BrdU^+/GS^+$ cells only a subregion of each niche was analyzed from images taken at 100x magnification from two or more, non-adjacent, sections (Figs. 4-6B-C; 4-8B-C; black rectangles within red niches). For co-labeling of $BrdU^+/HuCD^+$, all $BrdU^+$ cells were counted

within subregions and those positively co-labeled confirmed using orthogonal view and represented as a percentage of the $BrdU^+$ population. Cell counting was completed by quantifying the number of cells present in 0.5 µm z-stacks using the optical disector principle (West, 1999; Geuna, 2005) with Leica Application Suite Advance Fluorescence Lite 2.3.0 proprietary software. Images shown are maximum projections or orthogonal views where appropriate and were adjusted for brightness and contrast using Adobe Photoshop 7.0 software.

4.3.11 Statistical Analysis

Values are expressed as mean ± standard error of the mean. Pairs of means were compared using independent samples or paired-samples t-tests. For multiple comparisons between treatment groups a one-way ANOVA was used. Where a between group effect was present, Tukey's post hoc tests were performed. Samples were considered significant at $p < 0.05$, and statistical analyses completed using SigmaPlot 11.0 and graphs made using Microsoft Excel 2003.

4.4 Results

4.4.1 Putative Radial Glia Type IIa Cells are Present in Chemosensory Niches of LX and OB but absent in the Visual Niche of PGZ

Transmission electron microscopy was used to examine the ultrastructural organization and cell types composing sensory niches residing in the olfactory bulbs (OB; *N* = 3), vagal lobe (LX; *N* = 2), and periventricular grey zone (PGZ; *N* = 3) of the optic tectum. Terminology used for cell types is based on descriptions from Chapter 2. Niches are described separately below.

4.4.1.1 Olfactory Bulbs

The niche of OB spanned the ventrolateral portion of the olfactory bulbs between rostrocaudal levels 23-50, and was located primarily within the glomerular layer (Fig. 4-1A). Cell morphologies could be seen interspersed between sets of glomeruli or laying ventral to glomeruli next to the outer lining of the bulb (Fig. 4-1B), though no clear cellular organization was observed. In rare instances, large aggregates of cells dominated by Type IVa and Type III cell morphologies were identified near adjacent vasculature (Fig. 4-1C-E). A small number of Type IIa with numerous vacuoles and mitochondria within the cytoplasm, and Type V cells characterized by chromatin located at the periphery of the nucleus also appeared within the boundaries of the niche (Fig. 4-1F-H). Evidence of a small number of cilia was also present in the niche, however, from the images analyzed it was not possible to correlate this structure with a specific cell type.

4.4.1.2 Vagal Lobe

The niche of LX was positioned around the periphery of the vagal lobe, and spanned rostrocaudal levels 283-303. The lateral boundary of the niche was located adjacent the vagal

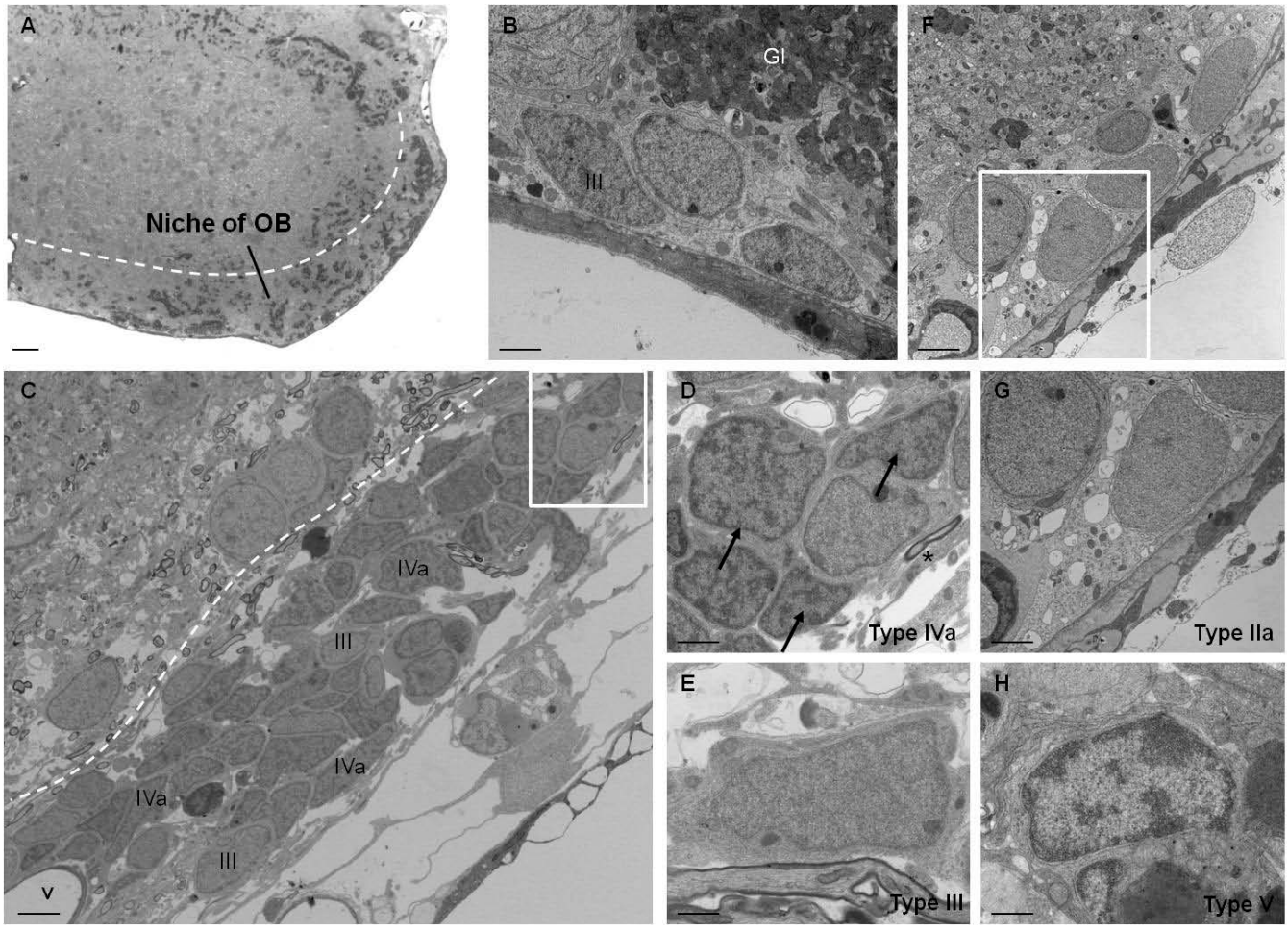

Figure 4-1. Ultrastructural organization and cell types of the sensory niche of the olfactory bulbs (OB). **A**, Brightfield semithin image of a single hemisphere of the olfactory bulb. The niche is demarcated to the ventrolateral aspect of the bulb (white hashed line), made up primarily of the glomerular layer of the bulb. Dark clusters within the niche are glomeruli. **B**, Cluster of cells in the ventral bulb, positioned below one ore more glomeruli (Gl). The morphological profile of a putative ***Type III*** cell can be seen. **C**, Example of a large heterogeneous cluster of cells in the ventral aspect of the niche, including profiles of mainly ***Type IV*** and ***Type III*** cells. The white hashed line demarcates the approximate dorsal extremity of the niche boundary. White box shown in **D**. **D**, Higher magnification image from C depicting the chromatin organization in ***Type IVa*** cells (black arrows). Evidence of a single cilium in longitudinal section is shown by the asterisk (*) **E**, High magnification image of ***Type III*** cell. **F**, Ventrolateral image of niche displaying a collection of three putative ***Type IIa*** cells, one showing characteristic features including numerous large vacuoles and mitochondria in the cytoplasm (white box). **G**, Higher magnification image from **F** (white box) showing ultrastructural details of a ***Type IIa*** cell in the OB. **H**, Image of an infrequently detected ***Type V*** cell with nuclear chromatin localized at the periphery. In all images dorsal is up. Scale bars: **A**, 10 µm; **B, D, G,** 2 µm; **C, F,** 3 µm; **E, H,** 1 µm.

nerve, with the niche continuing dorsally before extending ventromedially along the rhombencephalic ventricle (Fig. 4-2A). An epithelial lining consisting partially of squamous cells covered the niche dorsolaterally, but terminated at the ventricle. No ependymal cells were seen in this region. Dorsolaterally the niche consisted of 3-4 layers of mainly neurons, with a small number of non-neuronal phenotypes interspersed (Fig. 4-2B). At the dorsomedial aspect of the niche where the ventricular lumen began, the number of cell layers and cellular morphologies increased (Fig. 4-2C), some of which included Type III and Type V cells (Fig. 4-2G-H). Moving ventrally along the lateral wall few neurons were present, but a fairly continuous row of cells 1-2 layers deep, many having the ultrastructural profiles of Type IIa cells with microvilli extending into the lumen were present (Fig. 4-2D-E). In a few instances, cells having characteristics of Type IIa, but additionally displaying a single cilium extending from the cytoplasm were detected (Fig. 4-2F). This indicates that either this is a novel cell type other than the Type IIa previously defined, or during earlier studies I was unable to detect cilia on this cell type. A number of vessels could also be identified within the niche or in the adjacent parenchyma of the vagal lobe.

4.4.1.3 Periventricular Grey Zone

The niche of PGZ was located between rostrocaudal levels 219-223 deep to the superficial tectum opticum, adjacent the tectal ventricle (TeV), and opposite the eminentia granularis of the cerebellum (Fig. 4-3A). It was composed almost exclusively of a high density of both Type IVa and Type III cells that together spanned nearly 10 cell layers deep (Fig. 4-3B-D). Extending along much of the border of the niche, a physical division between irregularly shaped Type III cells, many of which were oriented perpendicular to the tectal ventricle, and more deep Type IVa cells was conspicuous (Fig. 4-3E). A high density of ribosomes could often be seen in the cytoplasm of Type III cells. Examination of this cell population at the margin of the niche showed that Type III cells were oriented parallel to the ventricle (Fig. 4-3F). Infrequently Type V cells were also noted in the niche (Fig. 4-3G). Collectively, ultrastructural analyses of sensory niches revealed that Type IIa cells, previously shown to have characteristics of radial glia (Chapter 2), resided in OB and LX, but were absent in PGZ.

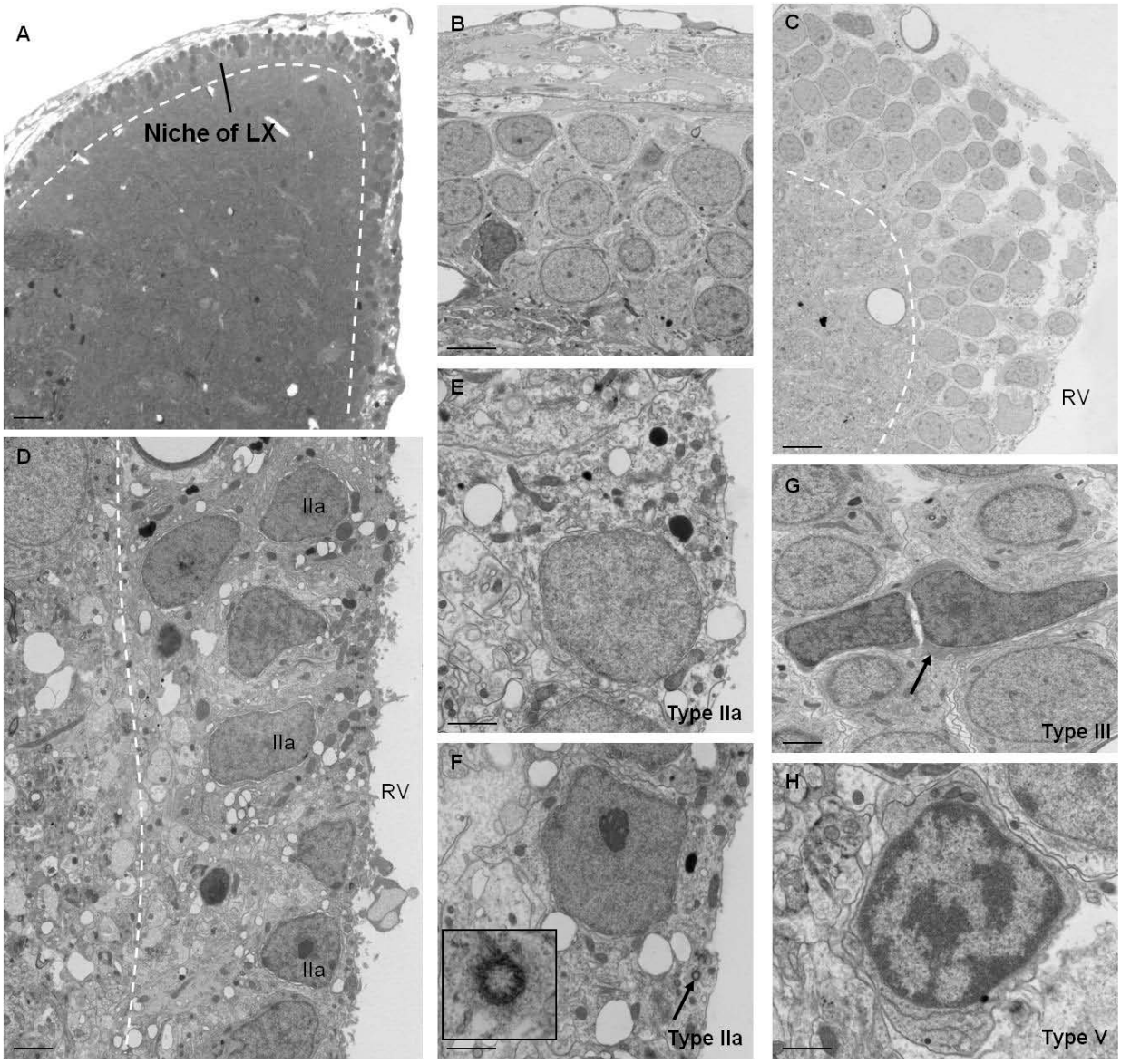
A
Niche of LX
B
C
RV
D
IIa
IIa
IIa
RV
E
Type IIa
F
Type IIa
G
Type III
H
Type V

Figure 4-2. Ultrastructural organization and cell types of the sensory niche of the vagal lobe (LX). **A**, Brightfield image of a single hemisphere of the vagal lobe showing its stereotypical 2-5 cell layered organization and heterogeneity of cell types located dorsally in LX and continuing medially along the rhombencephalic ventricle (white hashed line). **B**, Image depicting dorsal epithelial lining devoid of ependymal cells and niche of LX located ventrally and 3 cell layers deep. **C**, Dorsomedial corner of niche showing an increase in the number of layers and cell types, and a narrowing as the niche continues medially in the adjacent the ventricle. **D**, Image showing a number of ***Type IIa*** cell morphologies in the periventricular zone of the niche of LX. White hashed line demarcates the boundary of the niche adjacent the parenchyma. **E**, Higher magnification showing ultrastructural features of ***Type IIa*** cells. **F**, Example of a putative ***Type IIa*** cell with a single cilium (black arrow) present in the cytoplasm shown at higher magnification. Inset shows higher magnification of cilium in cross-section. **G**-**H**, Examples of ***Type III*** (**G**) and ***Type V*** (**H**) cellular morphologies observed within the niche. RV, rhombencephalic ventricle. In all images dorsal is up. Scale bars: **A**, 8 µm; **B**, 4 µm; **C**; 3 µm; **D, G,** 2 µm; **E, F, H,** 1 µm.

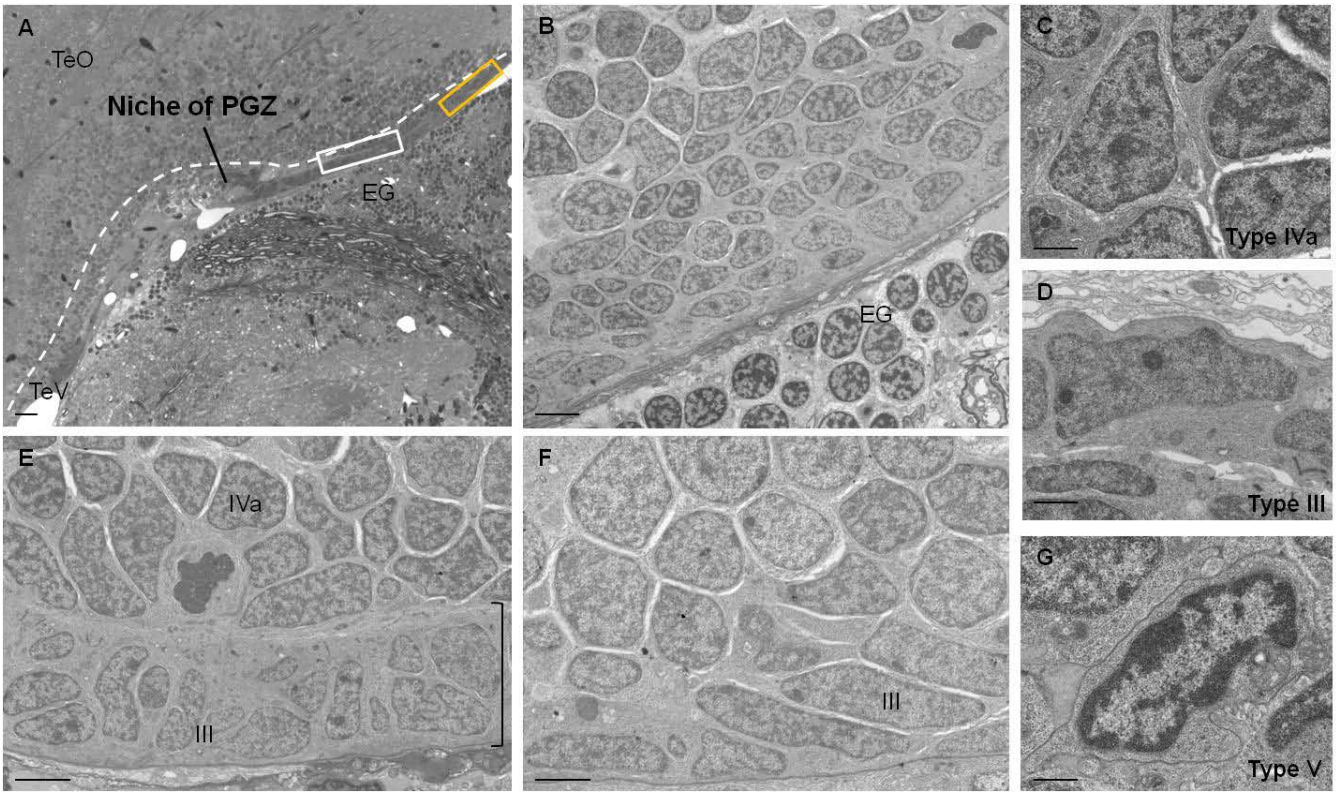
A
TeO
Niche of PGZ
EG
TeV
B
EG
C
Type IVa
D
Type III
E
IVa
III
F
III
G
Type V

Figure 4-3. Ultrastructural organization and cell types of the sensory niche of the periventricular grey zone (PGZ). **A**, Brightfield image showing the location of the niche of PGZ in the outer layers of this structure (white hashed lines) adjacent the midbrain tectal ventricle (TeV) and opposite the eminentia granularis (EG) of the cerebellum. White and yellow rectangles shown at higher magnification in **E** and **F**, respectively. **B**, Representative image of the niche composed of 8-10 layers deep, originating from the ventricular lining and consisting primarily of ***Type IVa*** and ***Type III*** cellular profiles. **C-D**, Higher magnification of the cellular morphologies of ***Type IVa*** (**C**) and ***Type III*** (**D**) cells. **E**, Higher magnification image of white box in **A** depicting physical division between outer layer of the niche of PGZ composed of irregular shaped ***Type III*** cells (black bracket) and deeper layers of niche where clusters of ***Type IVa*** cells reside. **F**, Higher magnification of yellow box in **A** showing ***Type III*** cells located at the margin of the niche where the number of cell layers decreases, and oriented parallel to the ventricle. **G**, Example of a ***Type V*** cell. TeO,optic tectum. In all images dorsal is up. Scale bars: **A**, 10 µm; **B**, 3 µm; **C, D, G**, 2 µm; **E, F,** 4 µm.

To further validate the possibility that Type IIa cells could be radial glial stem/progenitors, in a separate cohort of animals (N = 6) I provided a 2-hour chase of BrdU and then co-labeled cryosectioned tissue with BrdU and Glutamine Synthetase (GS), a marker for astrocytes/radial glia. Within the niche of OB (Fig. 4-4A-A') and LX (Fig. 4-4B-B'), co-labeling of $BrdU^+/GS^+$ cells was detected, supporting the ultrastructural phenotype of these cells. However, from the olfactory bulb tissue examined, the presence of $BrdU^+/GS^+$ cells was infrequent compared with LX, despite robust GS^+ staining within the boundaries of the niche. Conversely, co-labeling of $BrdU^+/GS^+$ proliferative cells was absent in PGZ, coroborating the notion that this niche likely does not contain $BrdU^+/GS^+$ Type IIa radial glial phenotypes (Fig. 4-4C-D). Examination of the BrdU/GS staining pattern at caudal (223x) versus more rostral (213x) cross-sectional levels of PGZ nonetheless revealed that although the caudal-most aspect of the PGZ investigated here showed no GS^+ labeling (Fig. 4-4C), more rostrally GS^+ labeling could be detected in the PGZ in the deeper layers of this structure separately from the location of $BrdU^+$ cells (Fig. 4-4D).

The ultrastructral analysis performed here reveals that the sensory niches of OB, LX, and PGZ display distinct heterogeneity in their cellular organization. In comparison with the cytoarchitecture of forebrain niches (Chapter 2; Lindsey et al., 2012), the organization and cell types of LX most closely paralleled that of pallial niches, while PGZ was characterized by Type III and Type IVa cells similar to the subpallial niches of Vv and Ppa. Moreover, by combining ultrastructural data with immunohistochemical labeling I show the likelihood of $BrdU^+/GS^+$ Type IIa radial glial stem/progenitor phenotypes in LX and OB, but their absence in PGZ, in line with earlier reports within pallial and subpallial niches, respectively.

4.4.2 Chemosensory Stimulation Enhances Neuronal Survival

To probe whether chemosensory specific stimuli had an effect on adult neurogenesis, zebrafish were exposed to 7-days of randomized chemosensory stimulation. Five chemo-stimulants that had a significant effect on the swimming-evoked movement of zebrafish were identified by screening a number of different compounds (Fig. 4-5A). These included acidic amino acids (Fig. 4-5B; N = 7; paired-samples t-test; p = 0.01), aromatic amino acids (Fig. 4-5C; N = 10; paired-

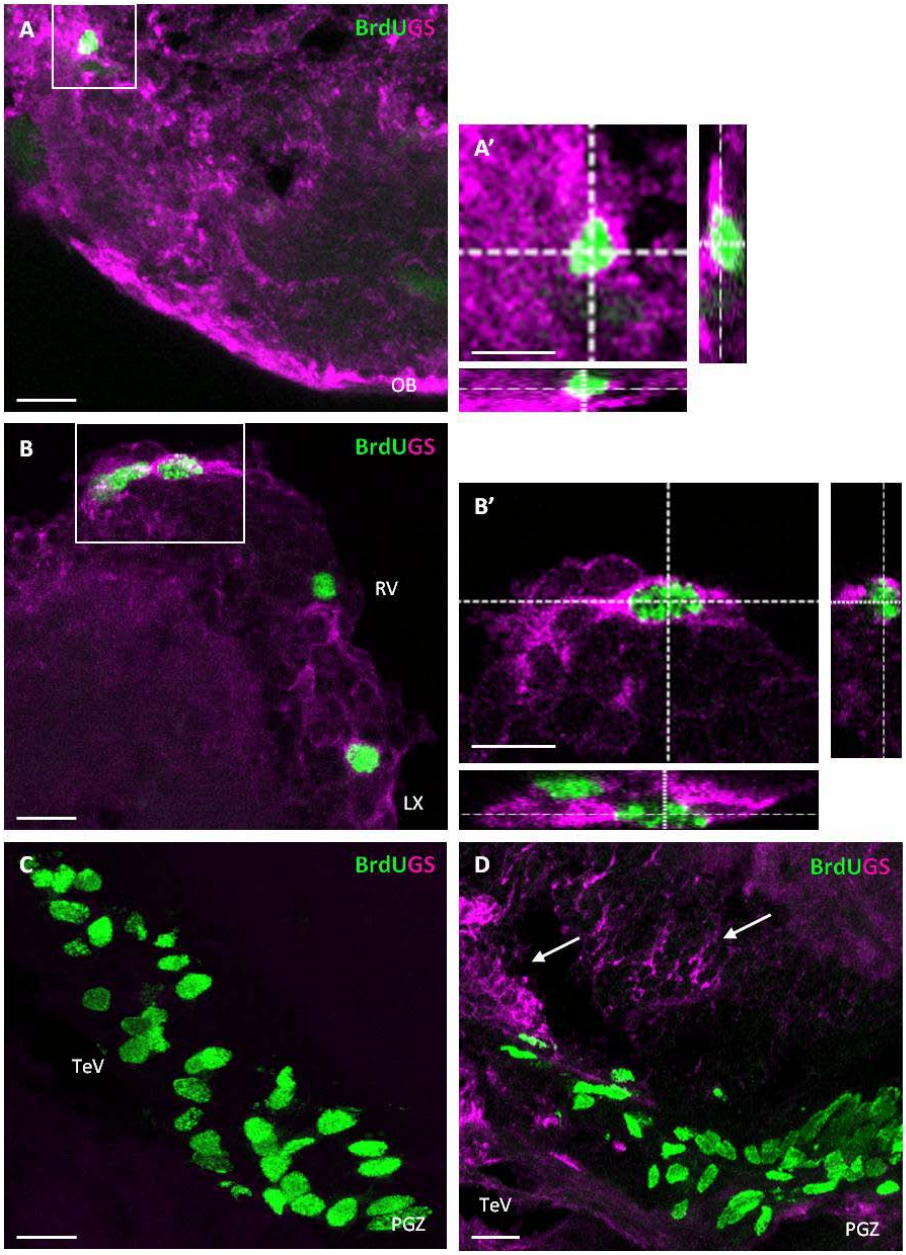
A
BrdUGS
OB
A'
B
BrdUGS
RV
LX
B'
C
BrdUGS
TeV
PGZ
D
BrdUGS
TeV
PGZ

Figure 4-4. Co-labeling of $BrdU^+/GS^+$ cells in sensory niches. A-A', Image showing co-labeling of $BrdU^+/GS^+$ in cells at ventromedial aspect of OB (**A**). White square depicts higher magnification shown in orthogonal view in **A'**. **B-B',** Image showing co-labeling of $BrdU^+/GS^+$ in cells at dorsomedial aspect of LX (**B**). White square depicts higher magnification shown in orthogonal view in **B'**. RV, rhombencephalic ventricle. **C**,$BrdU^+/GS^-$ labeling of cells in the medial aspect of PGZ bordering the ventricle at rostrocaudal level 223x. **D**, Population of $BrdU^+/GS^-$ cells observed at the ventral edge of the niche and the presence of GS^+ labeling appearing more medially within PGZ at rostrocaudal level 213x (white arrows). TeV, tectal ventricle. In all images dorsal is up; scale bars = 10 μm.

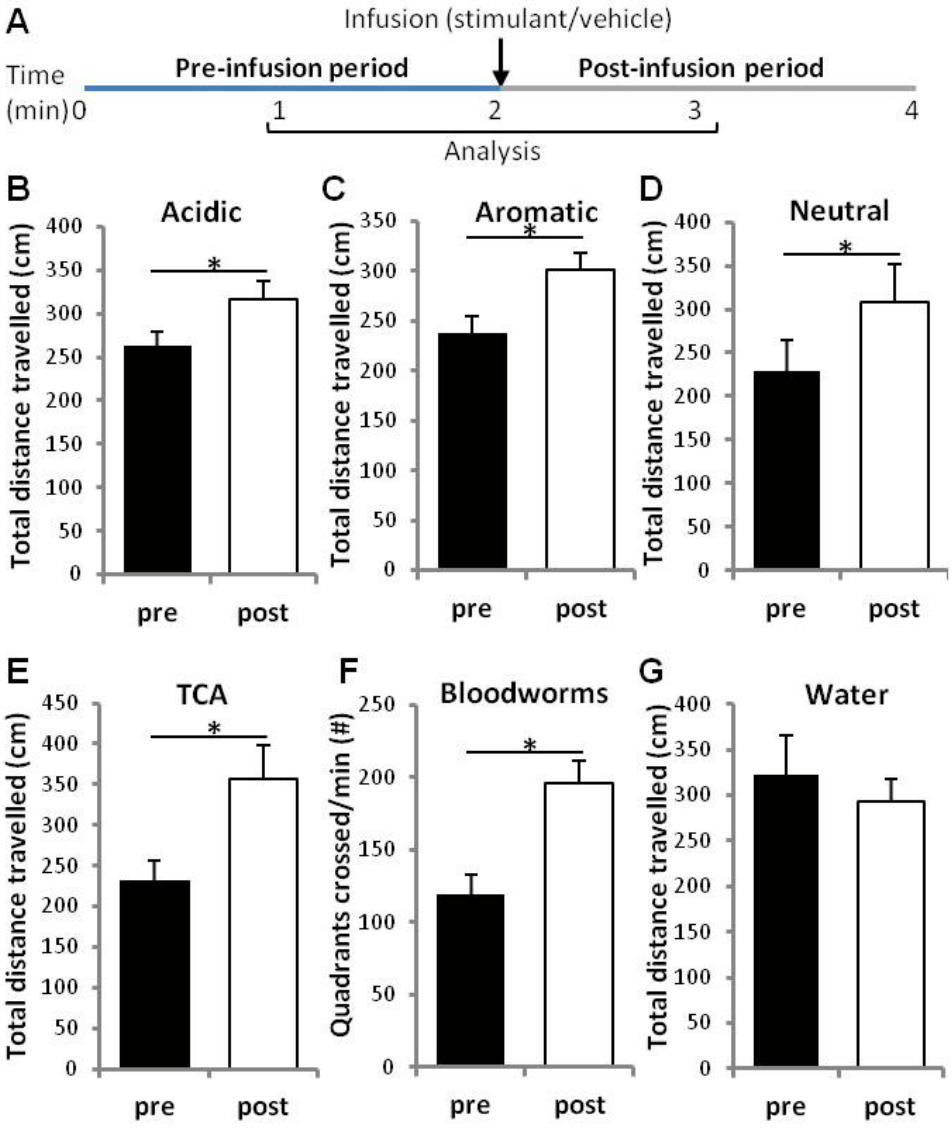
A
Infusion (stimulant/vehicle)
Time
(min) 0
Pre-infusion period
Post-infusion period
1
2
3
4
Analysis
B
Acidic
C
Aromatic
D
Neutral
E
TCA
F
Bloodworms
G
Water
Total distance travelled (cm)
Quadrants crossed/min (#)
pre
post
*

Figure 4-5. Chemo-stimulants tested to which adult zebrafish responded. **A**, Chemosensory assay designed to screen stimulants. Animals were exposed to a 2 min pre-infusion period of tank water and post-infusion period of the stimulant or vehicle control (water). Analysis of stimulus-evoked movement was performed between minute 1-2 of pre and 2-3 of post. **B-G**, Chemosensory stimulants displaying a significant change in the total distance travelled by zebrafish compared to vehicle alone (G, water). TCA, taurocholate hydrate. *$p < 0.05$ (paired-samples t-tests).

samples t-test; $p = 0.005$), neutral amino acids (Fig. 4-5D; $N = 6$; paired-samples t-test; $p = 0.049$), sodium taurocholate hydrate (TCA; Fig. 4-5E, $N = 8$; paired-samples t-test; $p = 0.012$), and Bloodworms (Fig. 4-5F; $N = 7$; paired-samples t-test; $p = 0.0002$). The behavioural response of zebrafish to stimulants exemplified by increased swimming-evoked movement indicated that animals could sense these compounds in their aqueous environment. No significant difference was noted in animals exposed to sodium taurodeoxycholate hydrate (TDCA; data not shown; $N = 10$; paired-samples t-test; $p = 0.084$) or vehicle control (Fig. 4-5G, $N = 12$; paired-samples t-test; $p = 0.396$). Using the five significant chemosensory stimulants above, a randomized chemosensory design was established (Fig. 4-6A).

I next investigated the specificity of chemosensory exposure on sensory neurogenic niches of the OB and LX (Fig. 4-6B-C) compared with PGZ at different stages of adult neurogenesis. Examination of the proliferative stem/progenitor population 2-hours post-BrdU injection following 7-day chemosensory exposure (Fig. 4-6D) showed no significant effect across any of the three niches (Fig. 4-6E-H; $N = 7$-11; independent samples t-test; OB: $p = 0.213$; LX: $p = 0.776$; PGZ: $p = 0.497$). Additionally, no significant difference in the proportion of $BrdU^+/HuCD^+$ cells 2-weeks after exposure was observed in any niche (Fig. 4-7A-B; $N = 5$-9; independent samples t-test; OB: $p = 0.932$; LX: $p = 0.542$; PGZ: $p = 0.907$). However, when I injected adult zebrafish with the S-phase marker BrdU and exposed them to 7-days of chemosensory stimuli over days 15-21 to assess neuronal survival (Fig. 4-7C), I observed a significant increase and niche-specific effect in chemosensory niches of OB and LX only, in the number of newborn neurons surviving after 3-weeks (Fig. 4-7D-F; $N = 4$-7; independent samples t-test; OB: $p = 0.028$; LX: $p = 0.018$; PGZ: $p = 0.440$). These data suggest that chemosensory exposure can function to enhance neuronal survival and that it acts in a modality-specific manner.

4.4.3 Monochromatic Light Induces Changes in Cell Proliferation in the Niche of PGZ and TL that Correlate with the Function of Sensory Structures

To examine whether exposure to ambient, full-spectrum, lighting conditions was required for constitutive levels of adult neurogenesis in the PGZ of zebrafish, I exposed animals to 7-days of

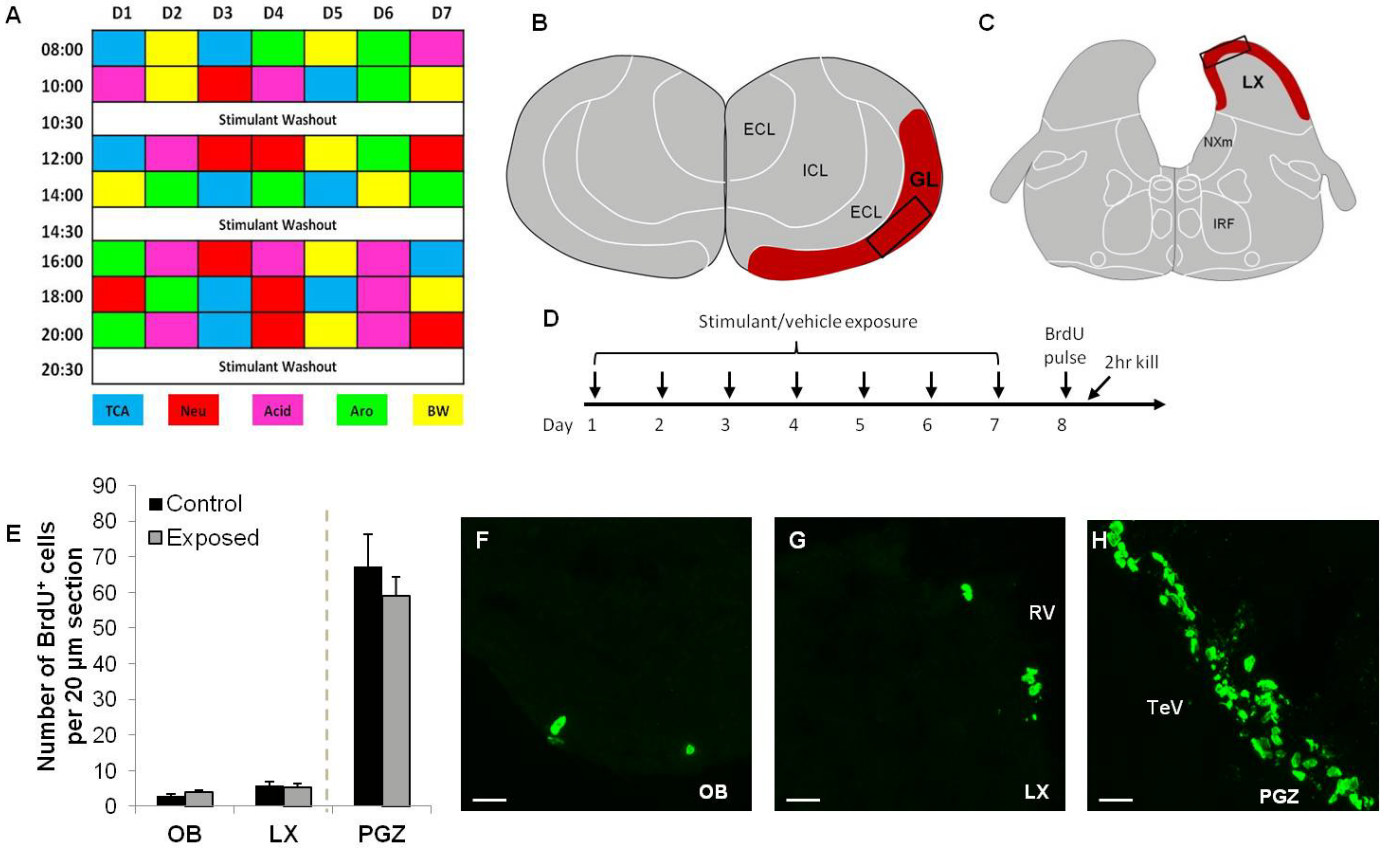
A
D1
D2
D3
D4
D5
D6
D7
08:00
10:00
10:30
12:00
14:00
14:30
16:00
18:00
20:00
20:30
Stimulant Washout
Stimulant Washout
Stimulant Washout
TCA
Neu
Acid
Aro
BW
B
ECL
ICL
GL
ECL
C
LX
NXm
IRF
D
Stimulant/vehicle exposure
BrdU pulse
2hr kill
Day 1 2 3 4 5 6 7 8
E
Control
Exposed
Number of BrdU+ cells per 20 µm section
90
80
70
60
50
40
30
20
10
0
OB
LX
PGZ
F
OB
G
RV
LX
H
TeV
PGZ

Figure 4-6. Experimental design and effects of chemosensory exposure on cell proliferation in OB, LX, and PGZ. **A**, 7-day randomized chemosensory design. TCA, taurocholate hydrate; Neu, neutral; Acid, acidic; Aro, aromatic amino acids; BW, blood worms. **B-C**, Schematic drawings showing the location of chemosensory niches in red within the primary sensory structures of the OB (**B**) and LX (**C**). $BrdU^+$ cells were analyzed in red region of niche, while co-labeling of $BrdU^+/HuCD^+$ cells was sub-sampled as indicated by black rectangles. **D**, Experimental protocol used to test the effects of chemosensory exposure on stem/progenitor proliferation. **E-H**, Results of $BrdU^+$ cell counts (**E**) and representative confocal images (**F-H**) within chemosensory neurogenic niches (OB, LX) and the visual processing niche of PGZ (negative control). ECL, external cellular layer; ICL, internal cellular layer; GL, glomerular layer; NXm, vagal motor nucleus; IRF, inferior reticular formation; RV, rhombencephalic ventricle; TeV, tectal ventricle. In all images dorsal is up; scale bars = 10 μm.

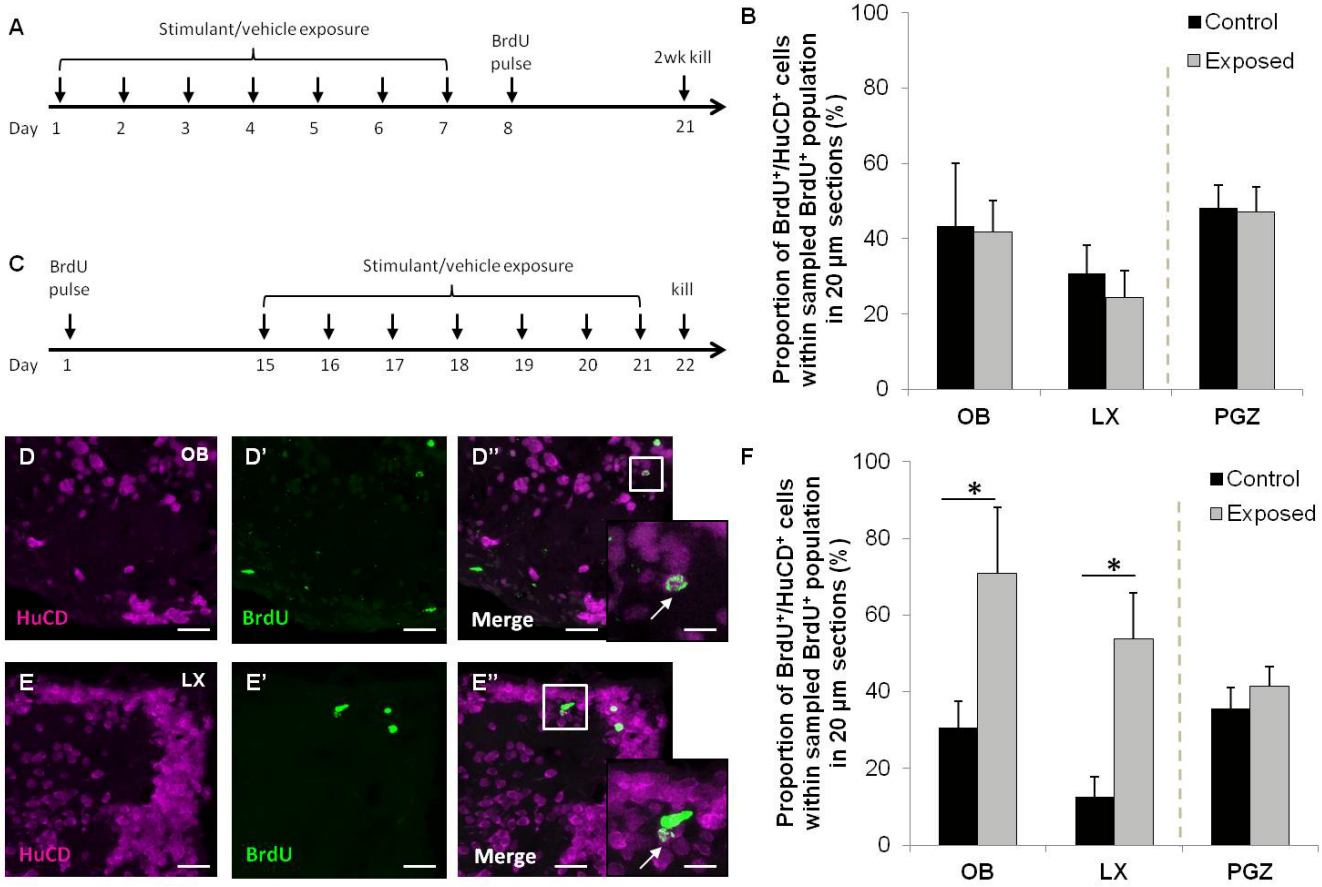
A
Stimulant/vehicle exposure
BrdU pulse
2wk kill
Day 1 2 3 4 5 6 7 8 21
C
BrdU pulse
Stimulant/vehicle exposure
kill
Day 1 15 16 17 18 19 20 21 22
B
Proportion of BrdU+/HuCD+ cells within sampled BrdU+ population in 20 µm sections (%)
Control
Exposed
OB LX PGZ
D OB
D'
D''
HuCD
BrdU
Merge
E LX
E'
E''
F
*
*

Figure 4-7. Effects of chemosensory exposure on neuronal differentiation and survival in OB, LX, and PGZ. **A**, Experimental protocol used to test the effects of chemosensory exposure on neuronal differentiation. **B**, Results of $BrdU^+/HuCD^+$ co-labeling in chemosensory niches of OB and LX and the visual processing niche of PGZ (negative control). **C**, Experimental protocol used to test the effect of chemosensory exposure on survival of newborn neurons. **D-E**, Representative confocal images showing $BrdU^+/HuCD^+$ cells in chemosensory niches of OB (**D**) and LX (**E**). White squares in **D"** and **E"** depicted at higher magnification in bottom, right corner. **F**,Results of $BrdU^+/HuCD^+$ co-labeling in sensory niches. In all images dorsal is up; scale bars = 10 µm. *$p < 0.05$ (one-way ANOVA).

monochromatic green or blue light alongside full spectrum light-intensity matched controls (Fig. 4-8A). Results demonstrated that exposure to monochromatic green light (but not blue light) is sufficient to significantly decrease the $BrdU^+$ stem/progenitor population within the niche of the PGZ (Fig. 4-8E-G; t-test; $p = 0.045$). However, as predicted I saw no significant difference within TL (Fig. 4-8H; t-test; $p = 0.529$) or LX (Fig. 4-8I; t-test; $p = 0.561$). Since these latter two niches displayed no change in the size of the $BrdU^+$ population between full spectrum and monochromatic light for green (200 lux) or blue (15 lux), I re-examined these data and asked whether differences in light intensity (200 vs. 15 lux) might affect the stem/progenitor pool of TL given its role in detecting differences in light intensity (Gibbs and Northmore, 1998). Indeed, my results revealed that in the TL (Fig. 4-8K-M; t-test; $p = 0.001$), but not LX (Fig. 4-8J; t-test; $p = 0.282$), a significant decrease in the size of the $BrdU^+$ proliferative population was observed. These findings support the notion that stem/progenitor proliferation in these niches change according to the function of the sensory processing structure: PGZ decreasing with reduced color stimuli; TL decreasing with reduced irradiance (Gibbs and Northmore, 1998).

4.4.4 FGFR-1 Signaling is Not Required to Maintain Constitutive Levels of Cell Proliferation in Sensory Neurogenic Niches

Fibroblast Growth Factor (FGF) signaling plays a critical role in tissue development and homeostasis during early ontogeny in vertebrates in the brain and retina (Campochiaro et al., 1996; Rousseau et al., 2000; Dono, 2003; Eckenstein et al., 2006), and more recently FGF and its receptor subtypes have been implicated in maintaining the adult neurogenic niche (Topp et al., 2008; Mudo et al., 2009; Ganz et al., 2010). Previous studies in zebrafish have successfully utilized the dominant-negative transgenic zebrafish line Tg(hsp70l:dnFgfr1-eGFP) to downregulate FGF signaling and investigate the requirement of FGFR-1 in regulating stem/progenitor cell proliferation during fin regeneration (Lee et al., 2005) and within forebrain neurogenic zones (Ganz et al., 2010).

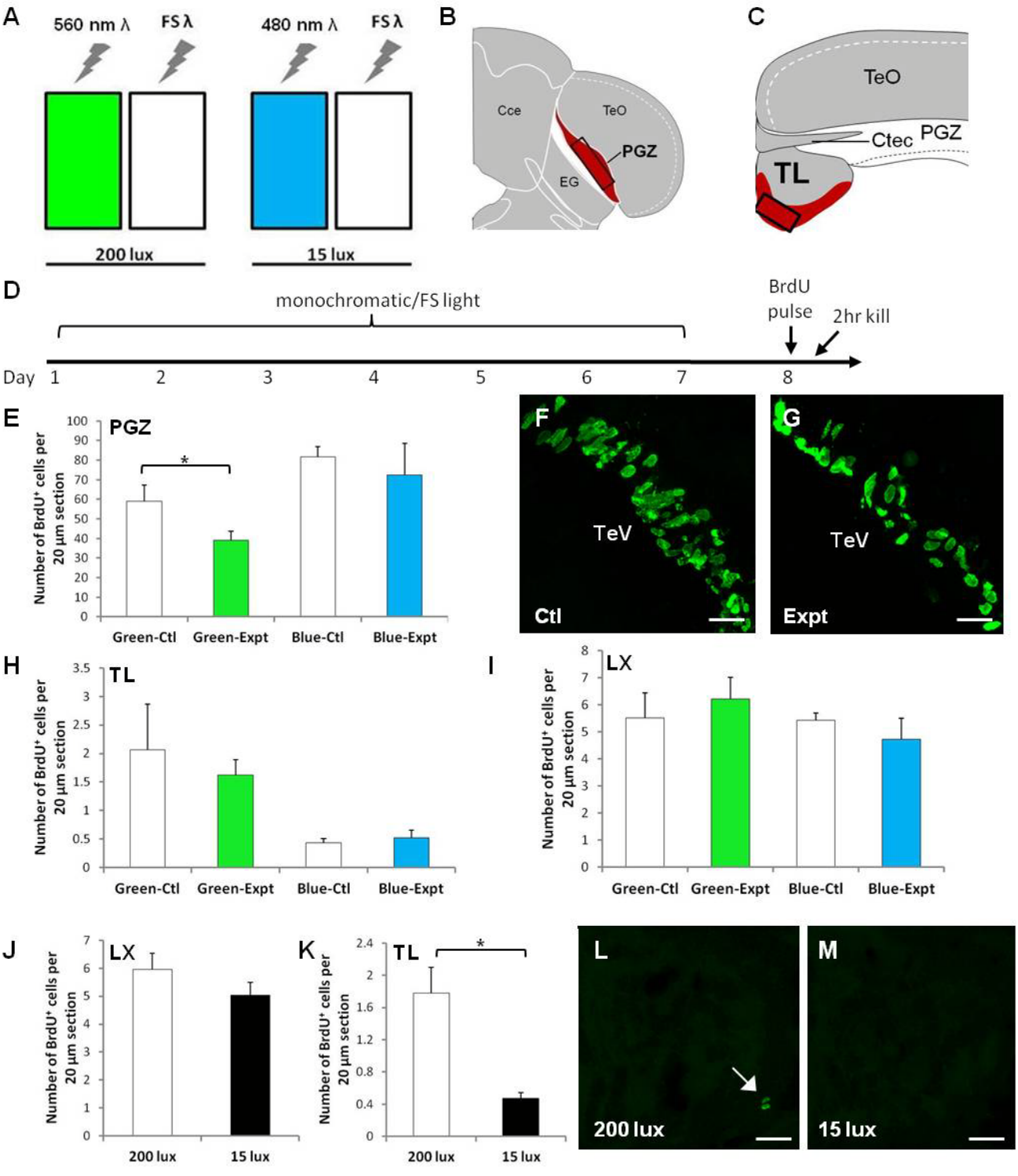
A
560 nm λ
FS λ
480 nm λ
FS λ
200 lux
15 lux
B
Cce
TeO
PGZ
EG
C
TeO
Ctec
PGZ
TL
D
monochromatic/FS light
BrdU pulse
2hr kill
Day 1 2 3 4 5 6 7 8
E
PGZ
Number of BrdU+ cells per 20 µm section
Green-Ctl
Green-Expt
Blue-Ctl
Blue-Expt
F
TeV
Ctl
G
TeV
Expt
H
TL
Number of BrdU+ cells per 20 µm section
Green-Ctl
Green-Expt
Blue-Ctl
Blue-Expt
I
LX
Number of BrdU+ cells per 20 µm section
Green-Ctl
Green-Expt
Blue-Ctl
Blue-Expt
J
LX
Number of BrdU+ cells per 20 µm section
200 lux
15 lux
K
TL
Number of BrdU+ cells per 20 µm section
200 lux
15 lux
L
200 lux
M
15 lux

Figure 4-8. Experimental design and effects of monochromatic light exposure on cell proliferation in PGZ, TL, and LX. **A**, Schematic of monochromatic light and intensity-matched full spectrum (FS) light stimuli to which zebrafish were exposed over 7-days. **B-C**, Schematic drawings showing the location of visual processing niches in red within the primary sensory structures of the PGZ (**B**) and TL (**C**). $BrdU^+$ cells were analyzed in red region of niche, while co-labeling of $BrdU^+/HuCD^+$ cells was sub-sampled as indicated by black rectangles. **D**, Experimental protocol used to test the effect of monochromatic light exposure on cell proliferation. **E-I**, Results of monochromatic light exposure on the number of $BrdU^+$ cells in the PGZ, TL, and LX (negative control), compared with their full spectrum, intensity-matched control. Confocal images in **F** and **G** represent differences in number of proliferative cells detected in the niche of PGZ where a significant effect of green light was present. **J-K**, Results of light intensity analysis in LX and TL, showing a significant effect in TL under low light (15 lux) conditions. **L-M**, Representative confocal images of TL under high (200 lux) and low (15 lux) light conditions. TeV, tectal ventricle; TeO, tectum opticum; CCe, corpus cerebella; EG, eminentia granularis; Ctec, commissural tecti. In all images dorsal is up; scale bars = 10 µm. $*p < 0.05$ (independent samples t-tests).

In the present study, to first confirm that my heatshock protocol induced transgene expression in sensory niches of OB, LX, PGZ, and TL using the Tg[hsp70l:dnFGFr1-eGFP] line (Fig. 4-9A-B), I assessed the presence of eGFP expression using GFP immunohistochemistry. I showed that eGFP expression is indeed expressed within all four sensory neurogenic niches compared with non-heatshocked controls (Fig. 4-9C-J), though expression was most pronounced in PGZ and LX (Fig. 4-9E; G). However, a limitation of these experiments is that I did not directly assess the levels of FGF signaling after heatshock to confirm that it faithfully correlates with the pattern of eGFP expression I observed in sensory niches. Additional experiments will address this by using either Western Blots to examine protein levels of FGF or the downstream target of FGF, phosphorelated extracellular signal-regulated kinase-1/2 (p-ERK-1/2), following heatshock using region-specific protein extracts, or by using p-ERK-1/2 immunohistochemistry on cryosections from sensory niches.

To examine the necessity of endogenous FGFR-1 signaling within the sensory niche to maintain constitutive levels of stem/progenitor proliferation, following my heatshock protocol animals were injected with BrdU at 10:00 the next morning, and sacrificed 2-hour thereafter (Fig. 4-10A). Preliminary results showed that compared to non-heatshocked fish (HS-), there was no change in the size of the $BrdU^+$ population within chemosensory niches of OB (Fig. 4-10B-C; $N = 4$; t-test; $p = 0.793$) and LX (Fig. 4-10D-E; $N = 4$; t-test; $p = 0.770$), and visual processing niches of PGZ (Fig. 4-10F-G; $N = 5$; t-test; $p = 0.973$) and TL (Fig. 4-10H-I; $N = 5$; $p = 0.222$) in animal that received heatshock (HS+). The small sample size of control wildtype AB fish analyzed to date with and without exposure to heatshock did not permit statistical comparisons with the preliminary results of the transgenic line (data not shown).

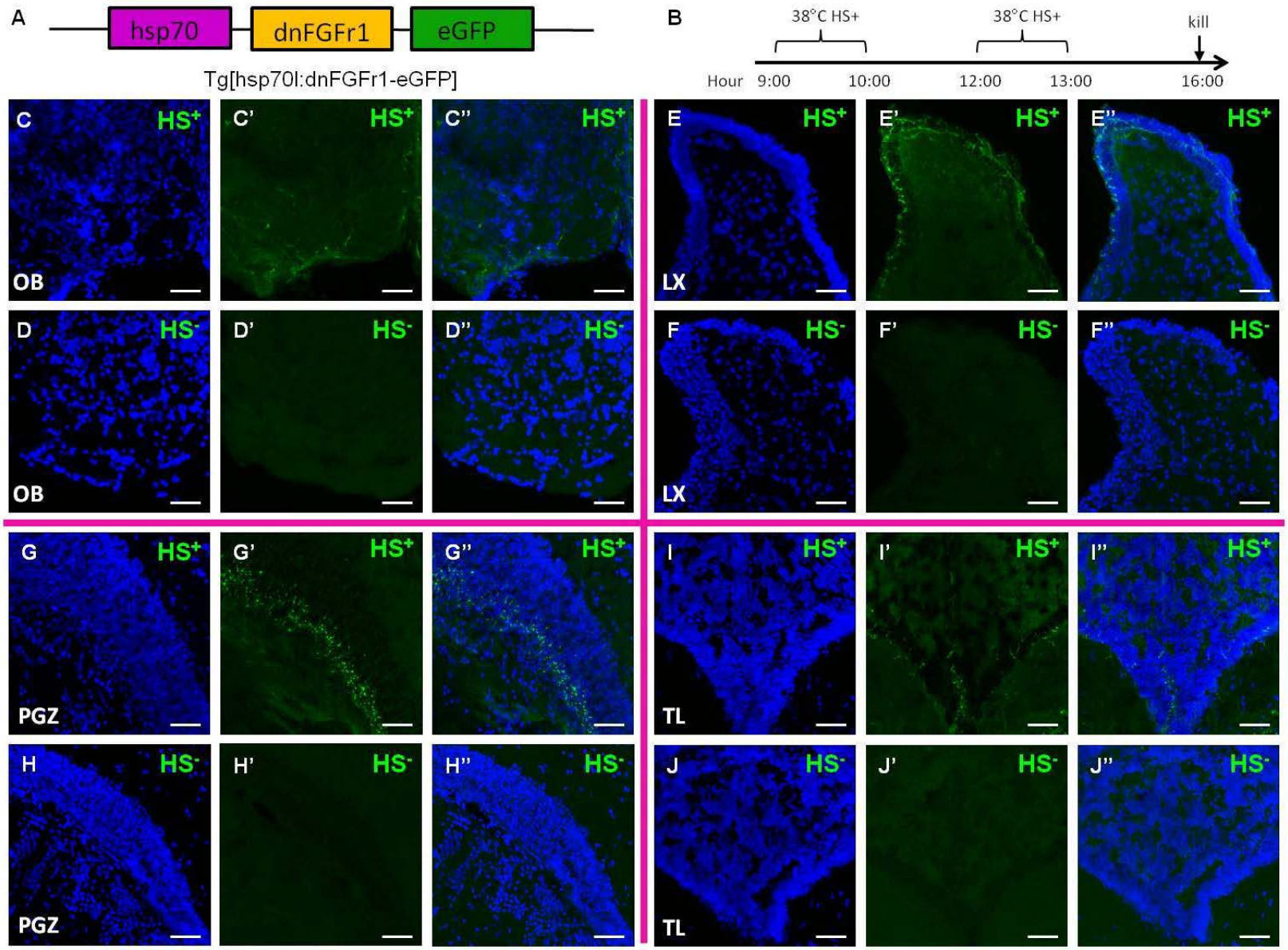
A
hsp70
dnFGFr1
eGFP
Tg[hsp70l:dnFGFr1-eGFP]
B
38°C HS+
38°C HS+
kill
Hour 9:00 10:00 12:00 13:00 16:00
C HS+
C' HS+
C'' HS+
D HS-
D' HS-
D'' HS-
OB
E HS+
E' HS+
E'' HS+
F HS-
F' HS-
F'' HS-
LX
G HS+
G' HS+
G'' HS+
H HS-
H' HS-
H'' HS-
PGZ
I HS+
I' HS+
I'' HS+
J HS-
J' HS-
J'' HS-
TL

Figure 4-9. eGFP expression across sensory neurogenic niches following heatshock paradigm using the transgenic line Tg[hsp70l:dnFgfr1-eGFP]. **A-B**, Dominant-negative fibroblast growth factor receptor-1 (FGFR-1) transgenic line (**A**) and heatshock (HS) protocol used to downregulate FGFR-1 (**B**). **C-F**, GFP expression in chemosensory niches of OB and LX with (HS^+) and without (HS^-) heatshock. **G-J**, GFP expression in visual processing niches of PGZ and TL with (HS^+) and without (HS^-) heatshock. In all images dorsal is up; scale bars = 10 µm.

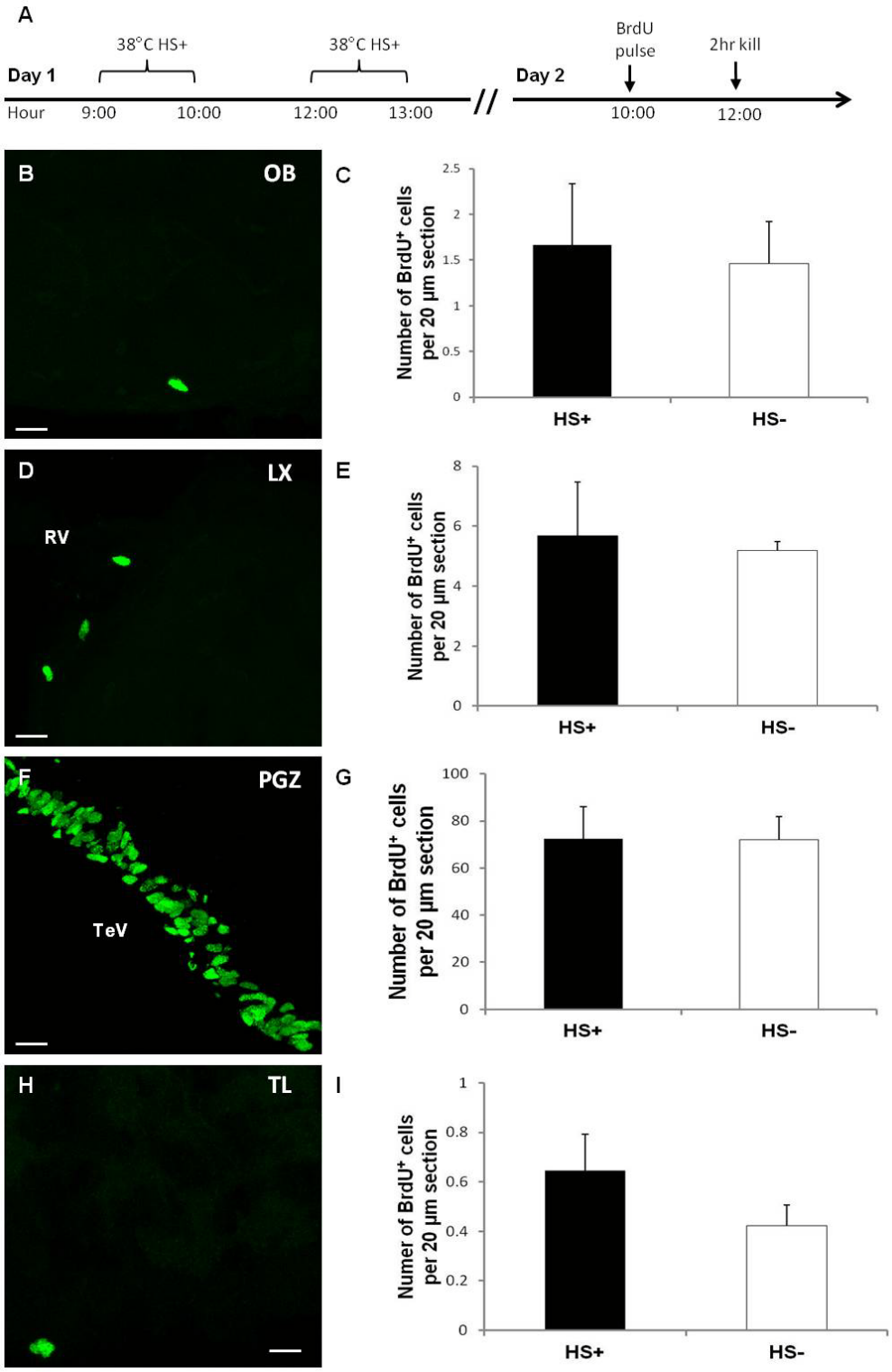
A
38°C HS+
38°C HS+
BrdU pulse
2hr kill
Day 1
Day 2
Hour
9:00
10:00
12:00
13:00
10:00
12:00
B
OB
C
Number of BrdU+ cells per 20 µm section
HS+
HS-
D
LX
RV
E
F
PGZ
TeV
G
H
TL
I
Numer of BrdU+ cells per 20 µm section

Figure 4-10. Effect of downregulation of Fibroblast Growth Factor Receptor-1 (FGFR-1) signaling on cell proliferation in sensory niches. A, Heatshock (HS) protocol used to examine the effects of downregulation of FGFR-1 on stem/progenitor cell proliferation. **B-H**, Results of HS on chemosensory niches of OB and LX (**B-E**) and visual processing niches of PGZ and TL (**F-I**). RV, rhombencephalic ventricle; TeV, tectal ventricle. In all images dorsal is up; scale bars = 10 µm. $*p < 0.05$ (Independent samples t-tests).

4.5 Discussion

The findings presented here contribute new insight into how four adult neurogenic niches residing within primary sensory structures of the CNS are composed at the ultrastructural level and modulated by modality-specific stimuli, and provide preliminary data concerning the role of Fibroblast Growth Factor signaling. Despite a small number of previous studies examining the composition of the adult optic tectum in the zebrafish (Ito et al., 2010), goldfish (Raymond and Easter, 1983), and medaka (Nguyen et al., 1999), an understanding of adult neurogenic plasticity and signals required to maintain these niches continue to be lacking. The results of the current experiments showcase two seminal properties of vertebrate sensory neurogenic niches. First, the cytoarchitecture of sensory niches is extremely heterogeneous, but appears to include many of the same cellular morphologies that compose forebrain niches of the adult zebrafish. Here, the niche of LX most resembles the organization of pallial niches and most clearly demonstrates the existence of putative radial glial stem/progenitors adjacent the rhomencephalic ventricle of the hindbrain. Conversely, the organization and cell types in the niche of PGZ most closely aligns with subpallial niches of Vv and Ppa, including the absence of GS^{+} staining and radial glial morphological profiles. Second, sensory niches respond to external stimulation in a modality-specific manner, albeit at different stages in the process of adult neurogenesis. This implies a sensory-dependent role in how neurogenic plasticity can modulate the stem/progenitor population, their neuronal progeny, and the chances that they survive to serve a functional role in the adult brain. Moreover, I have shown preliminary evidence that Fibroblast Growth Factor Receptor-1 signaling may not be involved in maintaining endogenous levels of stem/progenitor proliferation within sensory niches, opposite to reports in the subpallial niche of the zebrafish (Ganz et al., 2010). However, future experiments are required to confirm reductions in FGF signaling, and whether this growth factor acts at later stages of adult neuorogeneis in sensory niches, including neuronal differentiation and survival. These data, and the use of the zebrafish model, open new and exciting avenues of inquiry into vertebrate adult sensory neurogenesis, a branch of the adult neurogenesis field that remains largely unexplored.

4.5.1 Investigating Adult Neurogenesis in Primary Sensory Structures of the Vertebrate Brain

A major difference in studying neurogenic niches located in sensory structures compared with forebrain niches is that they are responsible for processing a specific type of sensory input. Thus by exposing animals to modality-specific stimuli associated with the primary processing structure, one can clearly evaluate the effect of that modality on various properties of adult neurogenesis. This includes how the stem/progenitor population behaves within the confines of the niche, without having to take into account how sensory cues impinge upon long-distance neural stem cell migration and differentiation, such as in the case of mammalian olfactory bulb neurogenesis (Lois et al., 1996). In designing experiments to test the effect of modality-specific stimuli on adult neurogenesis in sensory structures, two points must be considered however. First, what form of stimuli does the study model respond to? Second, what is known about the proliferative behaviour of the niche?

Zebrafish are endemic to shallow streams and slow moving water of the flood-plains of India (Spence et al., 2008), and have a wide repertoire of social behaviours, many which are related to conspecific recognition and shoaling (Saverino and Gerlai, 2008). Additionally, mating is triggered by the photoperiod as well as pheromones released into the water, and generally occurs at dawn. In the aqueous environment, odorants and tastants are transmitted rapidly, and teleosts are known to be highly receptive to a wide range of natural and synthetic stimulants (Hara, 1994). In all cases, these behaviours rely heavily on chemosensory and visual information, making the associated sensory processing structures of the OB, LX, PGZ and TL relevant candidate niches to investigate (Wullimann et al., 1996).

Literature on cell proliferation and/or neuronal differentiation in sensory structures of the adult central nervous system across vertebrates and invertebrates alike is nearly non-existent. The cause for this is that the models investigated to date do not harbor adult neurogenesis in sensory structures, but process multimodal sensory stimuli in integrative niches (Cayre et al., 1996, 2002; Strausfeld et al., 1998; Malaterre et al., 2002); making it challenging to interpret the findings here in a broader sense. Outside of teleosts, constitutively active cell proliferation within a primary sensory niche *in vivo* has only been reported in the optic tectum of the bullfrog, where these cells undergo both gliogenesis and neurogenesis (Simmons et al., 2008). Within teleosts,

studies examining adult neurogenesis in sensory structures have been most common in the zebrafish (Byrd and Brunjes, 1995; Zupanc et al., 2005; Marcus et al., 1999; de Oliveira-Carlos et al., 2013), and medaka (Nguyen et al., 1999; Alunni et al., 2010; Kuroyanagi et al., 2010), with experiments mainly focusing on characterization of cells within the olfactory bulb and optic tectum. However, earlier studies characterizing the tectum of adult goldfish also contributes important comparative data with the results found here (Raymond and Easter, 1983; Raymond et al., 1983). Conversely, aside from reporting the presence of cell proliferation in the torus longitudinalis and vagal lobe (Zupanc et al., 2005; Alunni et al., 2010), we have no understanding of how adult neurogenesis proceeds in these niches.

At first glance, the olfactory bulb appears to be an ideal candidate sensory niche to pursue in the context of adult neurogenesis. It offers both a small, localized populations of $BrdU^{+}$ cells within the external layers of the bulb, and receives first-order input via the first cranial nerve directly from the olfactory receptor neurons situated in neuroepithelia (i.e. rosettes). Evidence has surmounted however, that a second population of stem/progenitor cells residing within the subpallial niche of the telencephalon migrate into the olfactory bulbs (Byrd and Brunjes, 2001; Grandel et al., 2006; Kishimoto et al., 2011). This finding, which parallels the trajectory of ANSCs from the SEZ to the OB in mammals, has significant consequences for the interpretation of results arising from this niche. With short pulse-chase periods of 2-4 hours the existence of two populations is not problematic. However, with longer chase periods to assess the post-mitotic populations or newly differentiated neuronal progeny, one can no longer discriminate between the contributions of each population. In the present study, this means that the significant increase in neuronal survival displayed in the OB following chemosensory exposure cannot be definitively attributed to the local stem/progenitor population. Still, the consistent effect within the LX indicates that chemosensory exposure does play a role in promoting survival of newly differentiated neurons. The general lack of a well-defined neurogenic niche at the ultrastructural level as a result of the position of cells between glomeruli, as shown here, further hinders future investigations compared to neurogenesis in other sensory structures. Until the proper experiments are run to test the contribution of both populations of stem/progenitor cells, it will remain challenging to draw conclusions regarding how sensory stimuli modulate later stages of this process exclusively within the bulb.

Unlike the olfactory bulbs of zebrafish, which have received some level of attention over the years in relation to adult neurogenesis, the vagal lobe of the hindbrain responsible for processing taste stimuli has received none. Considering the drawbacks associated with studying neurogenic plasticity in the olfactory bulb, investigating neurogenesis in this chemosensory structure may be a refreshing alternative. At the ultrastructural level, the niche of LX is in many ways homologous to the organization of pallial niches of the zebrafish forebrain. In particular, $GS^{+}/BrdU^{+}$ cells appear to label Type IIa cellular profiles, suggesting the presence of a radial glia stem/progenitor population. This raises the question of whether similarities in the cytoarchitectural organization of different niches are indicative of homologies in molecular regulation. Additionally the small cycling population of $BrdU^{+}$ cells observed after short chase periods is well circumscribed mainly at the dorsomedial corner of the niche, at the mouth of the rhombencephalic ventricle. In zebrafish, taste buds are located on the oropharynx and gill arches (intraoral system), and are innervated by the glossopharyngeal and vagal nerves, leading to a more developed vagal lobe for taste processing in cyprinids (e.g. carp, goldfish, zebrafish) compared with silurids (e.g. catfish) that process taste information predominantly in the facial lobe (Morita and Finger, 1985; Hayama and Caprio, 1989). In both vagal and facial lobes of the hindbrain, gustatory information is topographically mapped. Though zebrafish depend primarily on the vagal lobe for processing taste stimuli within their environment, constitutive rates of cell proliferation and differentiation are regularly observed in the facial lobe as well (B.W.L, unpublished data), and may additionally display properties of neurogenic plasticity.

The optic tectum of the zebrafish is the largest structure in the brain, making it highly accessible to study. Its stereotypical organization consists of multiple outer layers dominated by tangentially directed axons, and a deeper periventricular grey zone (PGZ) housing densely packed neural soma. Visual input from four different cone types, as well as rods in the retina (Cameron, 2002; Fleisch and Neuhauss, 2006) receive this information and relay it via axons of the retinal ganglion cells to the outer layers of the tectum. Though sparse labeling of $BrdU^{+}$ cells are scattered in superficial layers (B.W.L. unpublished data), a well-defined sensory neurogenic niche resides in the PGZ, adjacent the tectal ventricle. The PGZ spans nearly the entire rostrocaudal axis of the tectum, and thus depending on the level analyzed the size of the cycling population will vary. By dividing the rostrocaudal axis of the PGZ into a rostral and caudal zone, I previously found that the greatest density of cells was confined to caudal-most region of this

structure, between neuroanatomical levels 219-223 (Wullimann et al., 1996; B.W.L., data not shown), in agreement with earlier studies in the goldfish tectum (Raymond and Easter, 1983). Here, labeled cells were generally identified along the entire periventricular zone, with the densest region situated medially. Previous work in zebrafish (Ito et al., 2010) and medaka (Alunni et al., 2010) has analyzed regions of the PGZ more rostral than in the present study. In these situations proliferative populations are located at the margins of this structure, and are generally absent medially.

Detailed analysis of the cellular populations making up the dorsomedial niche of PGZ has proposed that the phenotype of stem/progenitor cells lining the ventricle is $PCNA^{+}/Sox2^{+}/Msi1^{+}$, but devoid of glial characteristics (Ito et al., 2010). A similar finding has been reported in the medaka (Alunni et al., 2010). This agrees in part with ultrastructural data in the present study. Here, I found that the niche of PGZ was composed primarily of Type III and Type IVa cells, the same dominant cellular prolifes forming the niche of Vv and Ppa in the ventral aspect of the adult zebrafish forebrain (Chapter 2). The location of these cell types directly correlated with the location of $BrdU^{+}$ staining following IHC and which have previously been shown to label with BrdU and S100β, but not GS at the ultrastructural level (Chapter 2). Moreover, no GS^{+} labeling in cryosectioned tissue was detected in PGZ at the caudalmost domain, similar to Vv and Ppa. Earlier work examining the ultrastructural features of tectal cells lining the border of the periventricular zone in the adult goldfish further show strikingly similar morphology to the Type III cells shown here in the PGZ of zebrafish (Raymond and Easter, 1983). In both cases, cellular profiles were highly irregular, located adjacent the tectal ventricle, and included scant cytoplasm with a high density of ribosomes.

Evidence of a second, slowly cycling, $PCNA^{-}/Sox2^{+}/Msi1^{+}$ putative stem/progenitor population having classical radial glial features located at the dorsal margin of PGZ has also been proposed by Ito et al. (2010). The absence of GS^{+} labeling seen at the margin of this niche described here does not support this finding however. Two explanations may account for this difference. First, the more rostral position of the PGZ analyzed by these authors may house different populations of stem/progenitor cells, some immunopositive for GFAP. Second, the gluthamine synthetase antibody used during my experiments as a marker of radial glia/astrocytes may give rise to a different pattern of labeling than the Tg(gfap:GFP) used by Ito et al. (2010). Without directly performing IHC-TEM labeling of BrdU and GS, as well as examining additional markers in the

niche however, it cannot be dismissed that the $BrdU^+$ labeling in the PGZ (medially and marginally) consists entirely of Type III cells. Future marker analyses will be needed to match proposed stem/progenitor cells characterized at the IHC level, with the ultrastructural phenotypes of cells composing the niche of PGZ. These findings indicate that in line with earlier studies of three teleost models (Raymond and Easter, 1983; Alunni et al., 2010; Ito et al., 2010), proliferating stem/progenitor cells located in the PGZ at the tectal ventricle are not radial glial in nature, but rather may have features of neuroepithelial cells, with the specific ultrastructural profile of Type III cells.

4.5.2 Evidence of Sensory-Dependent Neurogenic Plasticity in Adult Sensory Neurogenic Niches

One of the most fascinating findings of this study was that adult neurogenesis was modulated in a sensory modality-specific manner. This evidence is the first of its kind to demonstrate this relationship within a neurogenic compartment localized to a primary sensory center. I have shown that modality-specific stimuli is both niche-specific; affecting only relevant sensory niches, and stage-specific; altering the population size of cells at a single stage in the process of adult neurogenesis, leading to the conclusion that sensory niches are governed by sensory-dependent neurogenic plasticity. Within OB and LX, exposing animals to continuously changing chemosensory stimuli produced an increase in the number of surviving newborn neurons, while no effect was detected in the stem/progenitor population. Likewise, examination of the PGZ, as well as select forebrain niches (B.W.L., unpublished data), showed no change with stimuli at any stage of adult neurogenesis, indicating the specificity of the effect to processing structures where this sensory information is biological relevant. By contrast, limiting the visual spectrum or intensity of light, I found that the rate of stem/progenitor proliferation was altered in accordance with increases or decreases in level of stimuli received by PGZ and TL. For instance, providing animals with monochromatic light in the green wavelength over 7-days produced a decrease in the stem/progenitor population localized within the PGZ, but not the TL. Conversely, when data was analyzed to examine the contribution of light intensity on niches, TL displayed a significant difference while PGZ remained unchanged. In all cases LX neurogenesis was unaltered across visual experiments.

The visual experiments performed here illustrate how the neurogenic response of sensory niches appears to segregate functionally. Although all layers of the PGZ are involved in encoding visual stimuli related to movement, shape, and color, this information is foremost processed by the collection of neurons within the deep layer of the PGZ (Meek, 1983). Rather, the torus longitudinalis (TL), which is distinct from the optic tectum, has long been implicated in processing changes in light intensity. Studies in the goldfish, a close relative of the zebrafish sharing homologies in brain structures, has shown at the electrophysiological level that the PGZ and TL do indeed respond to different forms of visual input (Gibbs and Northmore, 1998). Where the TL displayed spiking activity in response to changes in monochromatic stimulus radiance, spiking activity in the tectum showed increases at different rates across the spectrum, indicating sensitivity and functionality related to color dependence. In line with the function of these structures, a recent study examining sleep in zebrafish showed no significant difference in cell proliferation in the optic tectum with exposure to either extended dark or light photoperiods compared to control animals (Sigurgeirsson et al., 2013). Neuroanatomical tract-tracing methods using lipophilic dye in the rainbow trout has also shown that connections exist between the TL and PGZ in the rainbow trout, indicating that crosstalk between these structures is likely to occur (Folgueira et al., 2007). However, whether stimuli specific to one structure can evoke a neurogenic response in the other is unclear. This study also characterized two neuronal subtypes within the TL: medium-sized GABAergic neurons and small GABA-negative granule cells, with this structure subdivided into two ventrolateral and central domains. Though detailed characterization of the niche of TL in the zebrafish is still pending, the location of the neurogenic niche demarcated in the present work would most closely correspond with the ventrolateral domain described in trout.

The zebrafish visual system is functional at 4 days postfertilization (Clark, 1981). Already at this early stage of ontogeny these animals contain four different cone types, as well as rods, that are morphologically distinct, and capable of responding to peak wavelengths for green, red, blue, and UV (Nowrocki et al., 1985; Fleisch and Neuhauss, 2006). In the present study, fish were exposed to either green or blue monochromatic light, but only an effect of green lights on stem/progenitor cell proliferation was observed. It is unclear why only green light elicited an effect on the proliferative population in the PGZ, however, it’s possible that this wavelength has some biological relevance. Earlier studies have suggested that the strongest input arises from

green and red cones (Orger and Baier, 2005), and such differences may account for the current results. The requirement for normal visual input to sustain constitutive populations of proliferating cells within the PGZ has previously been illustrated in goldfish (Raymond et al., 1983). These authors showed that permanent removal of optic input (by enucleation) or temporary denervation (by optic nerve crush) both resulted in a reduction in the number of thymidine-labelled cells in the germinal zone of the PGZ, but upon reinervation of the tectum by regenerating optic fibers, proliferation was not only restored but enhanced compared to baseline levels. An interesting future experiment to perform would be to examine the effect of monochromatic light exposure during adulthood or over development on the properties of cones, or more generally, retinogenesis at the ciliary marginal zone (Stenkamp, 2007), in combination with the tectum. Moreover, it is possible that changes in the visual spectrum as well as changes in radiance could equally modulate neurogenesis in the retina since all forms of visual information enter via the retina. Performing these experiments could test the notion of neurogenic plasticity at both the level of input (i.e. retina) and downstream processing (i.e. tectum) and whether like-stimuli could simultaneously modulate both structures, at similar or different stages of neurogenesis. Given the convincing evidence shown here depicting a putative functional role of the stem/progenitor niche in line with that of the sensory structure, subsequent studies should examine whether the same holds true at stages of neuronal differentiation and survival.

4.5.3 Intrinsic Regulation of Sensory Niches by Fibroblast Growth Factor

Elucidating the molecular mechanisms regulating the neurogenic niche continues to be a major initiative in the adult neurogenesis field. Fibroblast Growth Factor (FGF) is one signaling pathways that has recently been implicated in controlling the behaviour of cells within the niche, though its functional role at stages of adult neurogenesis and under different contexts still remains poorly characterized. Numerous studies have shown that FGF signaling plays an important role in tissue development, homeostasis, and during the process of regeneration in vertebrates, in particular in the brain, retina, and fins (Campochiaro et al., 1996; Poss et al., 2000; Rousseau et al., 2000; Lee et al., 2005; Whitehead et al., 2005; Eckenstein et al., 2006). In mammals, FGF acts to expand the progenitor cell population in the SEZ, but exerts little effect in

the SGZ (Kuhn et al., 1997). In the SEZ, FGF-2 is expressed in GFAP-positive ANSCs but has gone undetected in daughter cells expressing FGFR-1 and FGFR-2 mRNA (Mudo et al., 2009). In adult zebrafish, FGFR-1 signalling has been shown to be involved in maintaining proliferation rates of $BrdU^+$ cells in the ventral glial-domain of the telencephalic subpallium but imposing little effect on the dorsal pallial niche (Ganz et al., 2010). Examination of FGFR1-4/p-ERK expression additionally showed that although present in the ventricular niche, FGF-signalling does not correlate specifically with proliferative progenitors (Topp et al., 2008). Interestingly, at the behavioural level, mutations in the gene encoding fibroblast growth factor receptor 1a (fgfr1a) lead to increases in aggression, boldness, and exploratory behaviour in adult zebrafish, and that this correlates with reductions in brain histamine levels (Norton et al., 2011).

The function of FGF signalling in adult sensory neurogenic niches has yet to be investigated. Here, using a dominant-negative heatshock line capable of downregulating endogenous FGFR-1 (Lee et al., 2005), I show preliminary evidence that FGF signalling does not appear to be required to maintain physiological rates of stem/progenitor proliferation in chemosensory (OB, LX) and visual processing niches (PGZ, TL) of the adult zebrafish brain. Whether this is indicative of endogenously low levels of FGF signalling in the niche or a result of a restricted number of receptors to bind FGF necessitate further investigation. However, it is possible that FGF signalling is simply not involved at earlier stages of adult neurogenesis in these niches, as has been revealed in the ventricular pallium (Ganz et al., 2010), but rather canonical FGF signalling may be necessary for neuronal differentiation or survival. Future studies will be needed to confirm whether this is the case.

Work in the adult zebrafish retina has confirmed the requirement of FGF signalling for photoreceptor maintenance (Hochmann et al., 2012). This is different from the situation observed here in the adult niche of PGZ where blockade of FGFR-1 signaling does not appear to disrupt normal rates of stem/progenitor cell proliferation. Conditionally blocking FGFR-1 using the same transgenic line as here produced photoreceptor degeneration and the loss of stereotypical organization of retinal layers. These data imply an innate heterogeneity in the molecular control of adult neurogenic niches that is likely to differ at the level of the niche as well as within individual cellular phenotypes. In line with this, studies of the Notch signalling pathways show opposing roles in the maintenance of the active or quiescent state of ANSCs in mammals compared to zebrafish in specific neurogenic compartments. In the SEZ of mammals, Notch

signalling is required to maintain ANSCs in an active, rather than quiescent state (Basak et al., 2012). Conversely, in adult zebrafish periventricular neurogenic zones of the telencephalon, Notch induction drives progenitors into a quiescent state whereas reductions in Notch transition progenitors back into an active state (Chapouton et al., 2010). Most recently, is has been shown that Notch receptor expression is heterogeneous among different neurogenic zones in the adult zebrafish brain, including the telencephalon, optic tectum, and cerebellum (de Oliveira-Carlos et al., 2013). Specifically in the optic tectum, notch 1a/1b/3 are expressed in the majority of proliferating cells, including putative stem/progenitor cells characterized by neuroepithelial properties in the PGZ. Taken together, these studies imply that considerable work is needed in order to understand the molecular programs governing classically studied niches of the forebrain, and particularly, those whose properties are only beginning to be understood in sensory neurogenic compartments.

4.5.4 Conclusions

The objective of the present study has been to expand our knowledge of adult neurogenesis beyond conventionally studied forebrain niches, and consider the properties and potential function of neurogenic zones residing within primary sensory processing structures. Here, using detailed cellular analyses, modality-specific paradigms, and a transgenic heatshock line, I describe cellular features and adult neurogenic plasticity inherent to chemosensory and visual processing related niches, including the torus longitudinalis and vagal lobe which have yet to be investigated in this context. A major finding of this work was that sensory niches commonly displayed sensory-dependent neurogenic plasticity, exhibiting a cellular response to sensory stimuli in line with the functional role of the sensory structure. Further testing this sensory-depending neurogenic plasticity hypothesis within select sensory niches will significantly contribute to our thinking of the adaptive role of neurogenic niches as a whole. Future studies combining the response of sensory niches to modality-specific stimuli and the requirement of signalling pathways such as FGF will prove useful to build upon our existing understanding of the molecular control of the niche under physiological conditions and to elucidate mechanisms governing the neurogenic niche with exposure to external environmental factors.

CHAPTER 5
GENERAL DISCUSSION

5.1 Principle Findings

The body of work presented here has contributed new insight into the cellular composition and modulation of forebrain and sensory neurogenic niches in the adult zebrafish. My research has given rise to five principle findings: (1) up to six morphologically distinct cell types are present in forebrain and sensory niches, having either a direct or supportive role in the process of adult neurogenesis. Unlike the situation in all other vertebrates studied to date, ependymal cells are not a component of the niche; (2) heterogeniety in the phenotype of the putative stem/progenitor cell exists across niches, some of which have characteristics of radial glia. UItrastructural and immunohistochemical evidence indicates that constitutively active radial glial progenitors are present in niches of D, Dl, Dm, Vd, OB, and LX, but absent in Vv, PPa, and PGZ, and that this correlates with the overall ultrastructral organization of the niche; (3) active populations of proliferating stem/progenitor cells reside directly within primary sensory processing structures of the adult brain, forming a “sensory neurogenic niche”, unlike the situation in other vertebrate and invertebrate models of adult neurogenesis studied to date; (4) changes in the social environment modulate adult neurogenesis in sensory neurogenic niches greater than integrative forebrain niches, and occur independently of changes in cortisol levels. Moreover, within sensory niches, neurogenic plasticity can give rise to bi-directional changes in the population size of cells at different stages of adult neurogenesis; (5) modality-specific sensory stimulation influences stages of adult neurogenesis exclusively in corresponding primary sensory niches and exhibits structure-dependent neurogenic plasticity in line with the functional role of sensory structures. Additionally, preliminary experiments indicate that primary sensory neurogenic niches might not require Fibroblast Growth Factor signalling to maintain constitutive levels of stem/progenitor proliferation. The results of these studies emphasize the diversity of neurogenic compartments within a single adult vertebrate species, and their unique properties of cellular plasticity. In synthesising these findings, and attempting to bridge our understanding of integrative niches with sensory niches, many new questions emerge. Below I discuss those questions I believe require most immediate inquiry, and which may have the largest impact on shaping our view of why adult neurogenesis has been so widely conserved.

5.2 Uncharted Waters: Towards an Understanding of Sensory Neurogenesis in the Olfactory Bulb and Optic Tectum

One of the central findings of my research is that neurogenic niches residing in primary sensory structures are modulated in response to changes in the social environment and by sensory modality-specific stimulation. Teleost fishes appear to be the only vertebrate group where adult stem cell pools are localized within multiple sensory structures, and despite suggestive evidence that mammals may harbor multipotent stem/progenitor cells within the olfactory bulb (Gritti et al., 2002), and a small number of studies investigating the composition of the optic tectum of zebrafish, goldfish, and medaka (Raymond and Easter, 1983; Nguyen et al., 1999; Alunni et al., 2010; Ito et al., 2010), the present experiments are the first to test the neurogenic plasticity of different sensory systems. Being able to investigate how the process of adult neurogenesis is maintained and regulated in a neuroanatomical structures that has a specialized function, and which is constantly processing cues from its environment, yields a new wave of exciting and challenging comparative questions. First, between sensory structures, are there homologies among the cells of the niche? Second, how does the phenotype of ANSCs compare with those in forebrain integrative niches of the zebrafish and other models of adult neurogenesis? Third, how are sensory niches controlled at the molecular level and in this regard, what is the role of the primary sensory receptors in providing signals to the niche? Fourth, do ANSCs within sensory niches respond more readily to environmental enrichment compared with higher-order integrative centers, since much of the information is sensory-based? Fifth, can sensory learning induce neurogenic plasticity in the appropriate sensory niche and equally modulate hippocampal-like structures necessary to retain these memories, as has been elegantly shown during paternal recognition of adult offspring (Mak and Weiss, 2010). Finally, can a functional or adaptive role be ascribed to forms of adult sensory neurogenesis?

Among sensory niches, those localized within the olfactory bulbs and optic tectum offer good starting points to address many of the above questions. In particular, the olfactory bulbs of mammals, reptiles, and birds along with the central olfactory pathway of crustaceans have been best investigated in terms of sensory neurogenesis. Sensory deprivation leading to declines in constitutive levels of adult neurogenesis at one or more stages has be achieved in these species

via naris occlusion in mice (Corotto et al., 1994), peripheral sensory deafferentation in zebrafish (Villanueva and Byrd-Jacobs, 2009), and amputation of the antennules in the adult shore crab (Hanson and Schmidt, 2001). However, the limitation of these models has been that the source of neural stem cells is not endemic to the sensory structure itself, but is located within the ventricular zone in vertebrates (Garcia-Verdugo et. al., 2002) or arises externally from the hematopoeitic system in the case of crustacean models (Chaves da Silva et al., 2013). A possible exception to the above may be the olfactory bulbs of mice, although conclusive *in vivo* evidence of this is lacking. In one of the only studies investigating the presence of multipotent precursor cells at different levels of the rostral migratory stream (RMS), it was found that precursor cells endowed with stem cell features could be isolated from the distal portion of the rostral extension located within the olfactory bulb core (Gritti et al., 2002). Unlike SEZ precursors, these cells proliferated more slowly, but *in vitro* were capable of producing the entire complement of neurons, astroglia, and oligodendrocytes. Nevertheless, without additional studies following up this claim, it still remains unclear whether this finding has simply been overlooked due to the larger, more plastic population of stem/progenitor cells residing in the SEZ, or that it is a species-specific exception. This means that by and large changes in adult neurogenesis in the primary olfactory structures of vertebrate and invertebrate animals is occurring as a by-product of the effects of environmental change on stem/progenitor pools located distally. So how are the properties of stem/progenitor populations within a sensory structure influenced under these same conditions?

In adult zebrafish and cichlids, a small population of $BrdU^+$ cells is observed in the glomerular and external cellular layers of the olfactory bulbs after short chase periods (Chapter 3; 4; Zupanc et al., 2005; Kishimoto et al., 2011; Maruska et al., 2012). We know little about the nature of these cells in the context of neurogenic plasticity however and whether they are even involved in adult neurogenesis or can be perturbed by environmental change. In the zebrafish, accumulating evidence of an RMS arising from the telencephalic subpallium, similar to that of mammals, further complicates the picture (Chapter 3; Byrd and Brunjes, 2001; Grandel et al., 2006; Kishimoto et al., 2011). This implies the likelihood of a second population of cells, and as a consequence distinguishing how resident stem/progenitor cells (versus migratory cells) and their differentiated progeny are modulated directly within this sensory structure is made more difficult. In agreement with earlier studies (Byrd and Brunjes, 1998), in Chapter 3 I show

evidence that under multiple social contexts the population of $BrdU^+$ cells at 2-hours compared with 4-weeks is significantly smaller. Accordingly, the number of $BrdU^+$ post-mitotic cells decreases over 4-weeks in the subpallium as they presumably populate the olfactory bulbs. Nevertheless, following a 2-hour pulse-chase with BrdU, an effect in the proliferative population within the olfactory bulb is elicited under the context of developmental social isolation and novelty, indicating that direct modulation of this local population of cells is possible. This is under the assumption that cells within the subpallium or rostral extent of the RMS, do not migrate into the bulb over a 2-hour window. One method of assessing the contribution of each of these cycling populations would be to selectively ablate the $BrdU^+$ subpallial cells in order to exclusively examine the effects of resident stem/progenitor cells over time. Alternatively, characterization of resident $BrdU^+$ cells in the olfactory bulb using marker analysis may aid to first decipher this population from the phenotype of radial glia stem/progenitor cells of the subpallium (Ganz et al., 2010; Marz et al., 2010; Grandel and Brand, 2012). In performing these experiments however, the possibility that cycling stem/progenitor cells may be present along the entire RMS as seen in mammals (Gritti et al., 2002), and have migrated into the bulb but maintained their proliferative capacity must also be considered. These studies will be insightful to assert whether the characteristics of the stem/progenitor cells of mammals and zebrafish within the RMS are more closely conserved than originally thought under homeostasis and with response to sensory stimulation.

Given the presence of populations of proliferating cells within the olfactory bulb of zebrafish, one cannot help but think that these play some functional role within the structure. Anatomically, zebrafish and mammals share a number of homologies concerning the olfactory system and output pathways to higher order structures (Wulliman, 2009). Olfactory receptor neurons that first receive olfactory cues from the environment reside in rosettes and nares of zebrafish and mammals, respectively (Byrd and Brunjes, 1995; Isaacson, 2010). Information is then relayed via the olfactory nerve (i.e. first cranial nerve) to the olfactory bulbs, where collections of glomeruli serve as the first processing station of olfactory input. In mammals, efferent pathways exit the bulb and innervate the olfactory cortex (lateral pallium) at the telencephalic ventricles, as well as the hippocampus (Leinwand and Chalasani, 2011; Sequerra et al., 2013). In zebrafish, the primary target structures that receive downstream olfactory input via the lateral and medial olfactory tracts (LOT; MOT) include the ventral telencephalon (Vv) and

posterior portion of the dorsal telencephalon (Dp; Friedrich, 2013). Mammalian studies show that changes in the olfactory environment can lead to recruitment of neuroblasts originating from the SEZ that populate the olfactory bulbs. In one of the only studies examining the effect of olfactory input on neurogenesis in the zebrafish, it was reported that peripheral sensory deafferentation in the adult zebrafish does not perturb the number of resident cycling cells in the olfactory bulb 4-hours post-surgery but 3-weeks later an effect can be observed (Villanueva and Byrd-Jacobs, 2009). Problematic is that the design of the BrdU pulse-chase experiments does not negate the possible contribution of incoming proliferating cells from the subpallium with longer chase periods. Therefore, as it stands, no study has yet to dissociate the contribution of these two proliferative populations, despite the usefulness of this in elucidating the role of each. What is puzzling is that under the context of developmental social isolation and/or novelty a change in the $BrdU^+$ population ensues, while with deafferentiation of the olfactory nerve no effect is observed following short BrdU pulses.

Multiple lines of reasoning may account for why local stem/progenitor cell proliferation does not occur as readily as one might expect with seemingly relevant forms of olfactory stimulation. First, this population of putative stem/progenitor cells may have an extremely slow cell cycle rate, limiting the number of $BrdU^+$ cells in the OB at any given time regardless of stimulation. Second, this population of cells may be mainly quiescent and only with the proper form of olfactory-mediated stimuli are more cells induced to enter the cell cycle and potentially give rise to newborn neurons locally. Third, it is possible that different forms of olfactory enrichment (or deprivation) differentially elicit adult neurogenic plasticity in the bulb compared to the subpallium or activate different subpopulations of stem/progenitor cells. In Chapter 3, I provide evidence that this could be the case as resident $BrdU^+$ cells within the olfactory bulb are reduced with developmental social isolation after a 2-hour pulse, while no effect is observed in the integrative niche of the subpallium, which receives secondary olfactory input. Conversely, 7-day exposure to randomized chemosensory stimuli shows no effect in the bulb 2-hours post-BrdU injection, but enhances neuronal survival after 2-weeks (Chapter 4). The caveat though is the inability to decipher *de novo* neurogenesis arising from within the bulb, or from distal cells migrating into this structure. Fourth, physical constraints may be implicated. Here, the notion is that the olfactory bulb proper cannot accommodate the process of adult neurogenesis, possibly due to interference with resident neurons or odor-encoding glomeruli, and thus relies primarily

on a pool of stem/progenitors supplied by the subpallium for the addition of new neurons. This could explain the largely absent populations of resident stem/progenitor cells in the mammalian or reptilian olfactory bulbs. Likewise, molecular programs or limited vascularisation to support a "permissive environment" conducive to environmental plasticity in the olfactory bulb may be involved. These hypotheses require considerable work to separate the cellular behaviour of local cycling cells within the bulb verses those immigrating from the telencephalon, and whether each population serves a different biological function, if any, for zebrafish and related teleost species.

A less well-understood sensory neurogenic niche, but one that offers new avenues of sensory neurogenesis to be explored, is the optic tectum. Unlike the niche of the OB, the multi-layered optic tectum of the midbrain of teleosts is one of the largest structures in the CNS, and is positioned adjacent the tectal ventricle. In the adult zebrafish all four layers of the optic tectum display constitutive rates of cell proliferation, including the deep periventricular grey, deep white, central, and superficial grey and white zones (Zupanc et al., 2005). Though extensive work on retinal neurogenesis and regeneration continues to progress rapidly using the zebrafish model (Bernardos et al., 2007; Stenkamp, 2007; Wong et al., 2010; Huang et al., 2012; Meyers et al., 2012; Lenkowski et al., 2013), probing questions concerning the composition, regulation, and modulation of neurogenesis in its midbrain target, the adult optic tectum, are sparse (Ito et al., 2010; de Oliveira-Carlos et al., 2013; Chapter 3; 4). Among teleosts, studies have generally examined retinotectal projections or the cellular composition of the niche (Raymond and Easter, 1983; Arochena et al., 2004; Kinoshita and Ito, 2006; Kinoshita et al., 2006; Ito et al., 2010; Tozzini et al., 2012; Chapter 4). In fact, up until now, with few exceptions (Raymond et al., 1983), studies addressing adult neurogenic plasticity in this structure are absent. The advantage of this is that the field is wide open for investigating neurogenic properties of the optic tectum and posing questions related to the biological function of neurogenesis. Even more exciting is the prospect of bridging retinal neurogenesis with canonical neurogenesis occurring in the optic tectum of the adult brain. Understanding the interplay between the cellular and molecular programs regulating both structures could provide significant advancements in combating visual disorders that present in one or both of these structures. However, before doing so we must develop our knowledge of the network connections that exist between cell layers of the optic tectum and associated structures that make use of visual input for behaviour processing, and how they relate to the phenotype of stem/progenitor cells residing locally in the niche.

In many ways the optic tectum acts both as a primary sensory structure as well as a relay station. Earlier mapping studies across a number of teleosts have demonstrated that the morphology of tectal neurons is made up of periform cells residing within the PGZ with radially oriented dendrites extending through most superficial tectal layers (Venegas et al., 1974). Topographically this arrangement permits incoming tangential axons of the visual system or different sensory systems to make contact with these neurons within distinct layers. Studies in the goldfish have revealed up to 15 morphologically distinct subtypes of neurons populating the PGZ, all of which possess unique branching patterns extending into the more superficial layers of the tectum (Meek, 1983). More recently, intracellular staining of periventricular neurons in the rainbow trout revealed two morphologically distinct cell types emanating from the PGZ: periventricular neurons having a large cell body and extending processes to the most superficial layers of the tectum; and, periventricular neurons with smaller cell bodies and less branching, and extending a lesser distance (Kinoshita and Ito, 2006). Aside from these studies, additional mature neuronal phenotypes likely exist and vary between groups of teleosts. First-order afferent connections from the retinal ganglion cells enter the superficial most layer of the tectum, synapsing on dendritic branches. Following processing of visual information from the retina by periventricular neurons in the tectum, one of the major target structures of tectal efferents conserved across teleosts is the lateral zone of the dorsal telencephalon (Dl), which in zebrafish shows constitutively active neurogenesis and is involved in learning and memory (i.e. hippocampal homologue; Broglio et al., 2005; Salas et al., 2006). Additionally, reciprocal connections between the tectum and the torus semicircularis (i.e. inferior colliculus homologue) and torus longitudinalis have been identified, this latter structure involved in sensing changes in light intensity (Gibbs and Northmore, 1998). So the question is how does the presence of adult stem/progenitor cells along with their neuronal progeny within the PGZ fit into this scheme of visual network connections?

It is a reasonable supposition that visual stimulus from the external environment exerts the greatest effect of neurogenic plasticity at the level of synaptic connectivity and adult neurogenesis. Pioneering work by Weisel and Hubel showed the former to be true for the proper development of connections and visual processing from the retina to higher-order cortical structures in mammals (Weisel and Hubel, 1963; Hubel and Weisel, 1964). Studies in goldfish have similarly shown that temporary unilateral optic nerve crush or removal of the eye can both

lead to decreased levels of cell proliferation in the PGZ (Raymond et al., 1983). Here, at the level of adult neurogenic plasticity, I have demonstrated that under complex social environments (or social isolation) and with monochromatic light exposure, stage-specific effects on the cellular population within the stem cell niche of the PGZ can be elicited (Chapter 3; 4). If in fact the phenotype of newborn neurons that are modulated with changing visual stimuli are related to periventricular neuronal morphologies described above, and which project to superficial layers of the optic tectum, *de novo* neurogenesis could be intimately linked with the rate of information processing from retinal ganglion cells and output pathways to associated visual structures. The underlying hypothesis would be that with greater production of these neurons, more processes are available to receive, encode, and transmit visual information in superficial layers of the tectum. Likewise, this could have implications on how quickly relevant visual information from an animal's environment is learned and preserved, since secondary connections from the tectum project to the hippocampal homologue of zebrafish located within the lateral zone of the dorsal telencephalon. In line with the requirement of new neurons for olfactory learning and memory in rodents (Lazarini and Lledo, 2011), it is foreseeable that within zebrafish adult-born neurons may contribute to visual learning and memory of these events.

In testing the above notion, a number of fundamental questions must first be addressed. First would be to create a detailed map of where the efferent connections arising from the retina synapse within the outer layers of the optic tectum in the zebrafish. This could be accomplished using classical tracing methods incorporating vital dyes, the use of fluorescent lipophilic tracers, or horseradish peroxidase (Solek and Ekker, 2012). Next, the phenotype of newborn neurons arising from the neurogenic niche of PGZ, and the ultrastructural characteristics of these cells, in particular the trajectory of their dendrites to superficial layers of the optic tectum would need to be elucidated. The close phylogenetic relationship between goldfish and zebrafish would suggest that some of these neurons should fit the morphological profiles of neuronal subtypes described previously by Meek (1983) in the goldfish PGZ. Immunohistochemical analysis in the adult zebrafish PGZ thus far have shown that one month after BrdU administration, a number of mature newly generated neurons have committed glutamatergic and gabaergic phenotypes, and have migrated into the deeper layers of the PGZ (Ito et al., 2010). Additionally, my results in Chapter 4 reveal the ultrastructural profiles of putative stem/progenitor cells. By applying immuno-TEM staining techniques developed in Chapter 2 in the niche of PGZ, one could track

the cellular morphology of $BrdU^+$ proliferating stem/progenitor cells as they progress to a neuronal fate, by sacrificing animals at multiple time points and assessing the ultrastructural profile of cells retaining the proliferative marker. Transgenic lines may serve best however, to uncover the branching properties of mature neurons and their target layers. With a better understanding of the neuroanatomy of visual pathways and cell types, one could then utilize transgenic lines to conditionally and selectively eliminate stem/progenitor populations in the PGZ and assess visual-related tasks in zebrafish devoid of adult neurogenesis compared with control animals. Since zebrafish display a number of complex social behaviours (Saverino and Gerlai, 2008), many of which rely on visual cues, this model is well suited to test future questions related to the functional significance of adult neurogenesis and plasticity in the optic tectum.

5.3 Comparing Structure-Dependent Neurogenic Plasticity Between Adult Sensory and Integrative Neurogenic Niches

Having now a vertebrate model with local populations of adult stem cells residing in major sensory processing structures of the nervous system, we may begin to probe how these cellular populations respond to environmental enrichment or deprivation compared with more commonly studied integrative niches. In doing so, it is useful to first make clear the definition of both. Adult neurogenic niches located within a primary sensory structure are assumed to respond most readily to the sensory modality associated with the sensory structure itself, with the underlying notion that elevated or diminished levels of sensory stimulation above baseline levels should produce a shift in the neurogenic population. Examples of these include the central olfactory pathway of crustaceans and the sensory systems of zebrafish investigated here. By contrast, integrative neurogenic niches generally encode multiple forms of information from the outside world that is more complex in nature. These may consist of multimodal sensory stimuli, learned behaviours, or relevant contextual events requiring long-term retention. Moreover, the trajectory of this information to the niche can require multiple nodes of processing in some cases before reaching the neuroanatomical location of the niche, unlike the situation in sensory niches. It

would seem that the majority of niches studied to date fall into this latter category, including the vertebrate ventricular zone, hippocampus, insect mushroom bodies, and crustacean hemi-ellipsoid bodies. The diverse forms of external information processed within integrative niches continues to make these niches more challenging to understand, but perhaps by comparing their response with that of sensory niches, clarity concerning their properties of neurogenic plasticity may emerge.

The social environment of an animal offers an intricate tapestry of sensory and non-sensory stimuli, and a fitting starting point to consider the responsiveness of sensory and integrative neurogenic niches. Multiple vertebrate (and some invertebrate) studies have demonstrated that in gregarious species, the social environment, or at least components of it, function to enhance neurogenesis (Segovia et al., 2006; Bovetti et al., 2009; Ayub et al., 2011; Dunlop and Chung, 2013; Veena et al., 2009), while social impoverishment serves to suppress it (Barnea et al., 2006; Mandairon et al., 2006; Stranahan et al., 2006; Leasure and Decker, 2009; Diniz et al., 2013; Sah et al., 2012; Lieberwirth et al., 2012). The social environment is in many ways synonymous with environmental enrichment. The objective of environmental enrichment is to improve the overall quality of life of an individual by providing them with multi-sensory and higher-cognitive stimuli with opportunities for learning, increased physical activity, continuous social interactions with a number of animals, and exploratory behaviour (Baroncelli et al., 2010). Social isolation/deprivation rather, lacks nearly all of these components. Thus, if we correlate these individual components with the functional role of sensory and integrative niches, we should be able to predict how physiological rates of adult neurogenesis will respond. Indeed, in many neurogenic niches this structure-function relationship is observed.

Within the hippocampus of mammals, multiple learning/memory paradigms rely on the presence of newborn neurons (Gould et al., 1999A; Hernandes-Rabaza et al., 2008; Deng et al., 2009; Thuret et al., 2009; Martinez-Canabal et al., 2012), while similarly migratory or food caching behaviour in birds depends on the recruitment of adult neurons from the ventricular niche to the hippocampal complex (Sherry and Vaccarino, 1989; Sherry et al., 1989; Smulders et al., 1995; Clayton, 1998; Smulders et al., 2000; Hoshooley and Sherry, 2004; 2007; Hoshooley et al., 2007; Sherry and Hoshooley, 2009; LaDage et al, 2010; 2011; Barnea and Pravosudov, 2011). The same can be said for the HVC, with its function of song production fulfilled by elevated levels of adult neurogenesis (Paton and Nottebohm, 1984; Nottebohm, 2002B; Nottebohm, 2005;

Andalman and Fee, 2009). Acute exposure to male chemosensory cues also increased cell proliferation in the SEZ of prairie voles (Smith et al., 2001). In Chapter 4, I demonstrate that sensory niches of the olfactory bulb and vagal lobe, but not the tectum, process chemosensory stimuli in the environment leading to enhanced survival of newborn neurons. Even more intriguing was the functional segregation of visual information in the niche of the PGZ compared with TL. Here, limited color input in the form of monochromatic light decreased cell proliferation in PGZ, while not color, but changes in irradiance correlated with proliferation rates in TL. Thus, in sensory neurogenic niches of the zebrafish, sensory-dependent neurogenic plasticity appears to be responsible for modulating stages of adult neurogenesis. More broadly, the examples presented above support the notion that structure-dependent neurogenic plasticity correlates directly with the functional role of sensory and integrative structures under contexts where there is a goal-oriented behaviour or single sensory stimuli. However, not all environmental conditions have shown to be as straightforward.

One of the most puzzling findings across the mammalian literature has been that social isolation modulates hippocampal rather than olfactory bulb neurogenesis. This does not agree with the structure-dependent neurogenic plasticity hypothesis. Foremost, we would expect that social isolation should have little effect on the SGZ, while significantly reducing the stem/progenitor population in the SEZ. So why is this not the case? In line with the function of the hippocampus, one explanation for this could be that a process of “unlearning” is occurring with the removal of stimuli. For instance, the number of stem/progenitor cells available to give rise to newborn neurons may diminish in order to save resources since no novel stimuli is present to be learned or encoded. An interesting experiment would be to test whether a subpopulation of normally active stem/progenitor cells becomes quiescent or reduce their cycling rate under conditions of social isolation, or whether they undergo cell death. Thus, the response of hippocampal neurogenesis to social isolation could be rationalized with its functional role if it is equally sensitive to changes in the degree of external information (sensory or other) to be learned. Here, the hypothesis would be that under standard housing conditions an animal undergoes some baseline level of learning/memory in response to its familiar environment leading to control rates of adult neurogenesis, and that with additional learning/memory tasks or novel stimuli neurogenesis is enhanced, whereas when placed in a barren environment with a paucity of stimuli or social interactions neurogenesis is reduced.

A large body of evidence has revealed that decreases in adult hippocampal neurogenesis associated with social isolation are a result of stress (reviewed in Schoenfeld and Gould, 2013). Given this, investigating the above hypothesis becomes more difficult. Stress receptors are widely expressed throughout the hippocampus, and social isolation is a stressful event in mammals. Thus as a byproduct of the stress response, hippocampal neurogenesis is diminished, or at least this is the current notion. But does this mean that any stressful stimulus will reduce hippocampal neurogenesis? Could populations of ANSCs simply undergo structure-dependent neurogenic plasticity in the absence of an enriched environment such as social isolation? Testing the effect of social isolation on the SGZ while simultaneously blocking the hypothalamic-pituitary-adrenal axis would be one method of addressing this question and to additionally examine whether the above hypothesis is upheld. If blockade of stress receptors eliminate decreases in hippocampal neurogenesis, this would agree with my recent findings in the adult zebrafish. In zebrafish the effects of the stress axis are independent of changes in cell proliferation in neurogenic niches, and accordingly, both developmental and adult social isolation do not lead to changes in the hippocampal homologue of the lateral zone of the dorsal telencephalon (Chapter 3).

If we next consider the behaviour of the SEZ with social isolation, a reasonable prediction would be that the stem cell pool within this environment might be slowed under conditions of social isolation since normal olfactory cues are lacking. But this does not happen; there is no change in ANSCs or subsequent populations. If environmental enrichment that typically includes multiple social interactions, many of which undoubtedly have strong odor components, is able to increase SEZ neurogenesis (Fowler et al., 2002), why is the opposite not true in the context of social isolation? Odor deprivation experiments in mice have shown that proliferation of SEZ stem cells, differentiation and survival of granule cells in the olfactory bulbs are reduced (Corotto et al., 1994; Maindarin et al., 2006). In the adult zebrafish, long-term developmental social isolation decreases the size of the proliferative population following a 2-hour BrdU pulse, but similar to the situation in mammals, this structure shows no change with adult social isolation (Chapter 3). This implies that the timing of exposure to social isolation may be an important factor to consider when designing these experiments. Proliferation in the zebrafish optic tectum and vagal lobe also decrease with social isolation, correlating with the removal of sensory stimuli, and presumably a decreased need for stem/progenitor cells to produce new neurons to process stimuli

in the environment. Rather, chemosensory stimuli do not appear to have any effect on cell proliferation in higher-order niches of the zebrafish telencephalon (B.W.L., unpublished data). Therefore, in the situation of zebrafish, the notion of structure-dependent neurogenic plasticity in sensory structures generally holds true, but seems at odds in the case of mammals.

The source of stem/progenitor cells and their properties may provide additional clues as to why SEZ/OB neurogenesis does not respond to social isolation, as well as other contexts where structure-depending neurogenic plasticity does not immediately correlate with function. In zebrafish a local population of putative stem/progenitor cells reside in the olfactory bulb (Byrd and Brunjes, 1995), while in mammals the large majority of differentiating neuroblasts migrate a considerable distance along the RMS into the bulb (Lois et al., 1996). In this respect, the threshold of change in olfactory stimuli with social isolation may be too low to trigger a change in the more distant ANSC population, whereas odorants and tastants are transmitted and detected much quicker by olfactory receptor neurons that relay sensory information only a short distance to the olfactory bulbs. This brings to light two intriguing questions. First, is there a relationship between the rate of migration of neuroblasts and the type or intensity of experimental stimuli? Second, how do external stimuli influence the migratory cues directing developing neurons to their target layer in the olfactory bulb? Evidence that multipotent progenitor cells are present along the entire axis of the RMS of rodents (Gritti et al., 2002) additionally raises the question of whether different populations of ANSCs can be differentially activated by stimuli, and posess different properties of cellular migration. Since across all major radiations of vertebrates, stem cell populations residing along the telencephalic ventricles supply one or more brain regions to carry out a specialized and often species-specific function, addressing these questions from a comparative standpoint could be fruitful.

Most central to how niches respond to changes in social or environmental stimuli are the unique properties of the stem/progenitor cell population itself. Not all stem/progenitor cells are made equal despite the common glial characteristics of these populations across animals studied and within the majority of niches. In fact, the ultrastructural profiles of putative stem/progenitor cells described between forebrain and sensory niches in the zebrafish reveals interesting trends. Across niches where Type IIa radial glial cells were absent (Vv, Ppa, PGZ), 2-hour BrdU-pulse chase experiments produced the largest population of $BrdU^+$ cycling cells (Chapter 2, 4). Likewise, among sensory niches, the PGZ was most consistently responsive to changes in the

social context (Chapter 3). An earlier study has shown that $PCNA^+$ cells residing in the PGZ have neuroepithelial characteristics, a fast cycling rate, and are devoid of glial properties, while a second slow-cycling, glial population is also present (Ito et al., 2010). Accordingly, common to the niches of Vv, Ppa, and PGZ is that they consisted of a large population of Type III cells, the putative ultrastructural profile of neuroepithelial stem/progenitor cells. By contrast, niches housing Type IIa radial-glial type stem/progenitor cells (D, Vd, Dl, Dm, OB, LX), often produced a smaller cohort of $BrdU^+$ cells, and in many case appeared to be less responsive to changes in the social environment (Chapter 3). These data imply that different stem/progenitor populations (glial or non-glial) among subsets of forebrain and sensory niches are endowed with different molecular programs, which could determine the neurogenic response to stimuli.

In mammals, ANSCs consistently maintain a glial phenotype, but morphological differences exist between astrocytes and radial-astrocytes in the SEZ and SGZ, respectively (Kriegstein and Alverez-Buylla, 2009). Likewise, although relationships between the lineage descendents of putative ANSCs of mammals, birds, and reptiles are present at the ultrastructural level in the adult ventricular zone (Garcia-Verdugo et al., 2002), it is largely unknown how the genes controlling the properties of these stem cells are involved in regulating these cells under homeostasis, and especially with environmental change. Recently, transcriptome analysis of the genes present in the hippocampal SGZ of rodents revealed 363 candidates enriched in this niche (Miller et al., 2013). Future studies allocating these genes to ANSCs and lineage descendents and investigating their expression patterns in the niche under constitutive conditions and with stimulation is likely to have a significant impact from both a biological and therapeutic perspective. Furthermore, comparative analyses at the molecular level across the diversity of contemporary neurogenic niches known to exist today would be a powerful approach to contribute to our functional and evolutionary understanding of adult neurogenesis.

5.4 Concluding Remarks

The adult neurogenesis field has progressed immensely since its inception nearly two decades ago. Today, five different models are prominent in the field, including rodents, songbirds, zebrafish, crickets, and crustaceans. Each one of these model organisms continues to offer different ways of thinking about this biological process at all levels of analysis, from its functional significance in the wild to the set of genes controlling the stem cell niche. With the properties of new niches being uncovered, we must mature our thinking of the role of the niche from a functional and evolutionary standpoint. In moving forward, it is often useful to reflect back and re-visit what past studies may tell us today. In developing an appreciation for sensory neurogenesis, returning to the original studies of natural populations of African cichlids where structure-function relationships in sensory systems were prevalent could be invaluable in testing the notion of structure-dependent neurogenic plasticity. Moreover, the sheer diversity of teleost fishes with specialized sense organs correlating with their microhabitat offer an untapped group of animals, that more than any other vertebrate class, may resolve many questions regarding the presence of adult neurogenesis within sensory structures. The years to come are sure to hold many exciting revelations that will shape our view of adult neurogenesis, and it’s conceivable, that this new way of thinking we embrace may be a direct consequence of adult-born neurons themselves.

References

Abdi, H. (2010). Holm's Sequential Bonferroni Procedure. In Encyclopedia of Research Design, Neil Salkind, ed. (Thousand Oaks, CA; Sage Press), pp. 1-8.

Ables, J.L., Breunig, J.J., Eisch, A., and Rakic, P. (2011). Not(ch) just development: Notch signaling in the adult brain. Nature Rev. Neurosci. *12*, 269-283.

Abrous, D.N., Koehl, M., and Le Moal, M. (2005). Adult neurogenesis: From precursors to network and physiology. Physiol. Rev. *85*, 523-569.

Adolf, B., Chapouton, P., Lam, C.S., Topp, S., Tanhauser, B., Strahle, U., Gotz, M., and Bally-Cuif, L. (2006). Conserved and acquired features of adult neurogenesis in the zebrafish telencephalon. Dev. Biol. *295*, 278-293.

Alderman, S.L., and Vijayan, M.M. (2012). 11β-Hydroxysteroid dehydrogenase type 2 in zebrafish brain: a functional role in hypothalamus-pituitary-interrenal axis regulation. J. Endocrinol. *215*, 393-402.

Allen, K.M., Fung, S.J., Rothmond, D.A., Noble, P.L., and Weickert, C.S. (2013). Gonadectomy increases neurogenesis in the male adolescent rhesus monkey. Hippocampus *In Press*

Almli, L.M., and Wilczynski, W. (2012). Socially modulated cell proliferation is independent of gonadal steroid hormones in the brain of the adult green treefrog (*Hyla cinerea*). Brain Behav. Evol. *79*, 170-180.

Alonso, M., Viollet, C., Gabellec, M.-M., Meas-Yedid, V., Olivo-Martin, J.-C., Lledo, P.-M. (2006). Olfactory discrimination learning increases the survival of adult-born neurons in the olfactory bulb. J. Neurosci. *264*, 10508-10513.

Altman, J. (1962). Are new neurons formed in the brains of adult mammals? Science *135*, 1127-1128.

Altman, J. (1963). Autoradiographic investigation of cell proliferation in the brains of rats and cats. Postnatal growth and differentiation of the mammalian brain, with implications for a morphological theory of memory. Anat. Rec. *145*, 573-591.

Altman, J. (1966). Autoradiographic and histological studies of postnatal neurogenesis II. A longitudinal investigation of the kinetics, migration and transformation of cells incorporating tritiated thymidine in infant rats, with special reference to postnatal neurogenesis in some brain regions. J. Comp. Neurol. *128*, 431-474.

Altman, J. (1969). Autoradiographic and histological studies of postnatal neurogenesis. IV. Cell proliferation and migration in the anterior forebrain, with special reference to persisting neurogenesis in the olfactory bulb. J. Comp. Neurol. *137*, 433-457.

Altman, J., and Das, G.D. (1965). Autoradiographic and histological evidence of postnatal hippocampal neurogenesis in rats. J. Comp. Neurol. *124*, 319-336.

Altman, J., and Das, G.D. (1966). Autoradiographic and histological studies of postnatal neurogenesis I. A longitudinal investigation of the kinetics, migration and transformation of cells incorporating tritiated thymidine in neonate rats, with special reference to postnatal neurogenesis in some brain regions. J. Comp. Neurol. *126*, 337-390.

Alunni, A., Hermel, J.-M., Neuze, A., Bourrat, F., Jamen, F., and Joly, J.-S. (2010). Evidence for neural stem cells in the Medaka optic tectum proliferation zone. Dev. Neurobiol. *70*, 693-713.

Alvarez-Buylla, A. and Nottebohm, F. (1988). Migration of young neurons in adult avian brain. Nature *335*, 353-354.

Alvarez-Buylla, A., Theelen, M, and Nottebohm, F. (1990). Proliferation "Hot spots" in adult avian ventricular zone reveal radial cell division. Neuron *5*, 101-109.

Alvarez-Buylla, A. and Lois, C. (1995). Neuronal stem cells in the brain of adult vertebrates. Stem Cells *13*, 263-272.

Alvarez-Buylla, A., Garcia-Verdugo, J.M., and Tramontin, A.D. (2001). A unified hypothesis on the lineage of neural stem cells. Nature Rev. Neurosci. *2*, 287-293.

Alvarez-Buylla, A., Seri, B., and Doetsch, F. (2002). Identificaiton of neural stem cells in the adult vertebrate brain. Brain Res. Bull. *57*, 751-758.

Alvarez-Buylla, A., and Lim, D.A. (2004). For the long run: Maintaining germinal niches in the adult brain. Neuron *41*, 683-686.

Amador-Arjona, A., Elliott, J., Miller, A., Ginbey, A., Pazour, G.J., Enikolopov, G., Roberts, A.J., and Terskikh, A.V. (2011). Primary cilia regulate proliferation of amplifying progenitors in adult hippocampus: Implications for learning and memory. J. Neurosci. *31*, 9933-9944.

Ampatzis, K., and Dermon, C.R. (2007). Sex differences in adult cell proliferation with the zebrafish (Danio rerio) cerebellum. Euro. J. Neurosci. *25*, 1030-1040.

Ampatzis, K., Makantasi, P., and Dermon, C.R. (2012). Cell proliferation pattern in adult forebrain is sexually dimorphic. Neuroscience *226*, 367-381.

Amrein, I., Slomianka, L, and Lipp, H.-P. (2004A). Granule cell number, cell death and cell proliferation in the dentate gyrus of wild-living rodents. Eur. J. Neurosci. *20*, 3342-3350.

Amrein, I, Slomianka, L., Poleteava, I.I., Bologov, N.V., and Lipp, H.-P. (2004B). Marked species and age-dependent differences in cell proliferation and neurogenesis in the hippocampus of wild-living rodents. Hippocampus *14*, 1000-1010.

Andalman, A.S., and Fee, M.S. (2009). A basal ganlia-forebrain circuit in the songbird biases motor output to avoid vocal errors. Pro. Natl. Acad. Sci. U.S.A. *106*, 12518-12523.

Ayub, N., Benton, J.L., Zhang, Y., and Bletz, B. (2011). Environmental enrichment influences neuronal stem cells in the adult crayfish brain. Dev. Neurobiol. *71*, 351-361.

Bain, M.J., Dwyer, S.M., and Rusak, B. (2004). Restraint stress affects hippocampal cell proliferation differently in rats and mice. Neurosci. Lett. *368*, 7-10.

Barker, J.M., Wojtowicz, J.M., and Boonstra, R. (2005). Where's my dinner? Adult neurogenesis in free-living food-storing rodents. Genes Brain Behav. *4*, 89-98.

Barnea, A. (2009). Interactions between environmental changes and brain plasticity in birds. Gen. Comp. Endocrinol. *163*, 128-134.

Barnea, A. and Nottebohm, F. (1994). Seasonal recruitment of hippocampal neurons in adult free-ranging black-capped chickadees. Proc. Natl. Acad. Sci. U.S.A. *8*, 11217-11221.

Barnea, A., Mishal, A., and Nottebohm, F. (2006). Social and spatial changes induce multiple survival regimes for new neurons in two regions of the adult brain: An anatomical representation of time? Beh. Brain Res. *167*, 63-74.

Barnea, A., and Pravosudov, V. (2011). Birds as a model to study adult neurogenesis: Bridging evolutionary, comparative and neuroethological approaches. Eur. J. Neurosci. *34*, 884-907.

Baroncelli, L., Braschi, C., Spolidoro, M., Begenisic, T., Sale, A., and Maffei, L. (2010). Nurturing brain plasticity. Impact of environmental enrichment. Cell Death Differ. *17*, 1092-1103.

Basak. O., Giachino, C., Fiorini, E., Robson MacDonald, H., and Taylor, V. (2012). Neurogenic subventricular zone stem/progenitor cells are notch1-dependent in their active but not quiescent state. J. Neurosci. *32*, 5654-5666.

Bayer, S.A., Yackel, J.W., and Puri, P.S. (1982). Neurons in the rat dentate gyrus granular layer substantially increase during juvenile and adult life. Science *216*, 890-892.

Bédard, A. and Parent, A. (2004). Evidence of newly generated neurons in the human olfactory bulb. Brain Res. Dev. Brain Res. *151*, 159-168.

Bednarczyk, M.R., Hacker, L.C., Fortin-Nunez, S., Aumont, A., Bergeron, R., and Fernandes, K.J.L. (2011). Distinct stages of adult hippocampal neurogenesis are regulated by running and the running environment. Hippocampus 21, 1334-1347.

Beltz, B.S., Zhang, Y., Benton, J.L., and Sandeman, D.C. (2011). Adult neurogenesis in the decapods crustacean brain: A hematopoietic connection? Eur. J. Neurosci. *34*, 870-883.

Berardi, N., Pizzorusso, T., and Maffei, L. (2000). Critical periods during sensory development. Curr. Opin. Neurobiol. *10*, 138-145.

Berg, D.A., Kirkham, M., Wang, H., Frisen, J., and Simon, A. (2011). Dopamine controls neurogenesis in the adult salamander midbrain in homeostatis and during regeneration of dopamine neurons. Cell Stem Cell *8*, 426-433.

Berg, D.A., Belnoue, L., Song, H., and Simon, A. (2013). Neurotransmitter-mediated control of neurogenesis in the adult vertebrate brain. Development *140*, 2548-2561.

Bernardos, R.I., Barthel, L.K., Meyers, J.R., and Raymond, P.A. (2007). Late-stage neuronal progenitors in the retina are radial muller glia that function as retinal stem cells. J. Neurosci. *27*, 7028-7040.

Bernier, P.J., Bedard, A., Vinet, J., Levesque, M., and Parent, A. (2002). Newly generated neurons in the amygdale and adjoining cortex of adult primates. Proc. Natl. Acad. Sci. U.S.A. *99*, 11464-11469.

Bernocchi, G., Scherini, E., Giacometti, S., and Mares, V. (1990). Premitotic DNA synthesis in the brain of the adult frog (*Rana esculenta* L.): An autoradiographic 3H-thymidine study. Anat. Rec. *228*, 461-470.

Beukelaers, P., Vandenbosch, R., Caron, N., Nguyen, L., Moonen, G., and Malgrange, B. (2011). Cycling or not cycling: Cell cycle regulatory molecules and adult neurogenesis. Cell. Mol. Life Sci. *69*, 1493-1503.

Biga, P. R., and Goetz, F. W. (2006). Zebrafish and giant danio as models for muscle growth: determinate vs. indeterminate growth as determined by morphometric analysis. Am. J. Physiol. Regul. Integr. Comp. Physiol. *291*, R1327-R1337.

Blaser, R., and Gerlai, R. (2006). Behavioral phenotyping in zebrafish: Comparison of three behavioral quantification methods. Beh. Res. Methods *38*, 456-469.

Booker, R., Babashak, J., and Bum Kim, J. (1996). Postembryonic neurogenesis in the central nervous system of the tobacco hornworm, *Manduca sexta*. III. Spatial and temporal patterns of proliferation. J. Neurobiol. *29*, 233-248.

Boonstra, R., Galea, L., Matthews, S., and Wojtowicz, J.M. (2001). Adult neurogenesis in natural populations. Can. J. Physiol. Pharmacol. *79*, 297-302.

Border, A. (2006). Adult neurogenesis: Basic concepts of signaling. Cell Cycle *5*, 722-728.

Bovetti, S., Veyrac, A., Peretto, P., Fasolo, A., De Marchis, S. (2009). Olfactory enrichment influences adult neurogenesis modulating GAD67 and plasticity0related molecules expression in newborn cells of the olfactory bulb. PLoS ONE *4*, e6359.

Brand, A.H., and Livesey, F.J. (2011). Neural stem cell biology in vertebrates and invertebrates: More alike than different? Neuron *70*, 719-729.

Braubach, O.R., Wood, H.-D., Gadbois, S., Fine, A., and Croll, R.P. (2009). Olfactory conditioning in the zebrafish (*Danio rerio*). Beh. Brain Res. 198, 190-198.

Brazel, C.Y., Nunez, J.L., Yang, Z., and Levison, S.W. (2005). Glutamate enhances survival and proliferation of neural progenitors derived from the subventricular zone. Neuroscience *131*, 55-65.

Broglio, C., Gomez, A., Duran, E., Ocana, F.M., Jimenez-Moya, F., Rodriguez, F., and Salas, C. (2005). Hallmarks of a common forebrain vertebrate plan: Specialized pallial areas for spatial, temporal and emotional memory in actinopterygian fish. Brain Res. Bull. *66*, 277-281.

Brown, J., Cooper-Kuhn, C., Kempermann, G., van praag, H., Winkler, J., Gage, F.H., and Kuhn, H.G. (2003). Enriched environment and physical activity stimulate hippocampal but not olfactory bulb neurogenesis. Eur. J. Neurosci. *17*, 2042-2046.

Bruel-Jungerman, E., Veyrac, A., Dufour, F., Horwood, J., Laroche, S., and Davis, S. (2009). Inhibition of PI3K-Akt signaling blocks exercise-mediated enhancement of adult neurogenesis and synaptic plasticity in the dentate gyrus. PLoS ONE *4*, e7901.

Brus, M., Keller, M., and Levy, F. (2013). Temporal features of adult neurogenesis: Differences and similarties across mammalian species. Front. Neurosci. *7*, 1-9.

Buckwalter, M.S., Yamane, M. Coleman, B.S., Ormerod, B.K., Chin, J.T., Palmer, T, and Wyss-Coray, T. (2006). Chronically increased transforming growth factor-β1 strongly inhibits hippocampal neurogenesis in aged mice. Am. J. Pathol. *169*, 154-164.

Brummelte, S., and Galea, L.A.M. (2010). Chronic corticosterone during pregnancy and postpartum affects maternal care, cell proliferation and depressive-like behavior in the dam. Horm. Behav. *58*, 769-779.

Buddensiek, J., Dressel, A., Kowalski, M., Runge, U., Schroeder, H., Hermann, A., Kirsch, Storch A, and Sabolek, M. (2010). Cerebrospinal fluid promotes survival and astroglial differentiation of adult human neural progenitor cells but inhibits proliferation and neuronal differentiation. BMC Neurosci. *11*, 1-11.

Burnie, D., and Wilson, D.E. (Editors-in-Chief) (2001). Animal. (Smithsonian Institution; Dorling Kindersley; New York Press).

Byrd, C.A., and Brunjes, P.C. (1998). Addition of new cells to the olfactory bulb of adult zebrafish. Ann. N.Y. Acad. Sci. *855*, 274-276.

Byrd, C.A., and Brunjes, P.C. (1995). Organization of the olfactory system in the adult zebrafish: Hisotlogical, immunohistochemical, and quantitative analysis. J. Comp. Neurol. *358*, 247-259.

Byrd, C.A., and Brunjes, P.C. (2001). Neurogenesis in the olfactory bulb of adult zebrafish. Neuroscience *105*, 793-801.

Cachat, .J, Stewart, A., Grossman, L., Gaikwad, S., Kadri, F., Chung, K.M., Wu, N., Wong, K., Roy, S., Suciu, C., Goodspeed, J., Elegante, M., Bartels, B., Elkhayat, S., Tien, D., Tan, J., Denmark, A., Gilder, T., Kyzar, E., DiLeo, J., Frank, K., Chang, K., Utterback, E., Hart, P., and Kalueff, A.V. (2010). Measuring behavioral and endocrine responses to novelty stress in adult zebrafish. Nature Protoc. *5*, 1786-1799.

Cameron, D.A. (2002). Mapping absorbance spectra, cone fractions, and neuronal mechanisms to photopic spectral sensitivity in the zebrafish. Vis. Neurosci. *19*, 365-372.

Cameron, H.A., and Gould, E. (1994). Adult neurogenesis is regulated by adrenal steroids in the dentate gyrus. Neuroscience *61*, 203-209.

Campochiaro, P.A., Chang, M, Ohsato, M., Vinores, S.A., Nie, Z., Hjelmeland, L., Mansukhani, A., Basilico, C., and Zack, D.J. (1996). Retinal degeneration in transgenic mice with photoreceptor-specific expression of a dominant-negative fibroblast growth factor receptor. J. Neurosci. *16*, 1679-1688.

Castro, A., Becerra, M., Manso, M.J., and Anadon, R. (2006). Calretinin immunoreactivity in the brain of the zebrafish, *Danio rerio*: Distribution and comparison with some neuropeptides and neurotransmitter-synthesizing enzymes. II. Midbrain, hindbrain, and rostral spinal cord. J. Comp. Neurol. *494*, 792-814.

Cavegn, N., Maarten van Kijk, R., Menges, K., Brettschneider, H., Phalanndwa, M., Chimimba, C.T., Isler, K., Lipp, H.-P., Slomianka, L., and Amreain, I. (2013). Habitat-specific shaping of proliferation and neuronal differentiation in adult hippocampal neurogenesis of wild rodents. Front. Neurosci. *7*, 1-11.

Cayre, M., Strambi, C., and Strambi, A. (1994). Neurogenesis in an adult insect brain and its hormonal control. Nature *368*, 57-59.

Cayre, M., Strambi, C., Charpin, P., Augier, R., Meyer, M.R., Edwards, J.S., and Strambi, A. (1996). Neurogenesis in adult insect mushroom bodies. J. Comp. Neurol. *371*, 300-310.

Cayre, M., et al., 2002. The common properties of neurogenesis in the adult brain: From invertebrates to vertebrates. Comp. Biochem. Physiol. Part B 132, 1-15.

Cayre, M, Malaterre, J., Scotto-Lomassese, S., Aouane, A., Strambi, C., and Strambi, A. (2005). J. Neurosci. Res. *82*, 659-664.

Cayre, M., Scotto-Lomassese, S., Malaterre, J., Strambi, C., and Strambi, A. (2007). Understading the regulation and function of adult neurogenesis: Contribution from an insect model, the house cricket. Chem. Senses *32*, 385-395.

Chadashvili, T., and Peterson, D.A. (2006). Cytoarchitecture of fribroblast growth factor receptor 2 (FGFR-2) immunoreactivity in astrocytes of neurogenic and non-neurogenic regions of the young adult and aged rat brain. J. Comp. Neurol. *498*, 1-15.

Chapouton, P., Jagasia, R., and Bally-Cuif, L. (2007). Adult neurogenesis in non-mammalian vertebrates. BioEssays *29*, 745-757.

Chapouton, P., Skupien, P., Hesl, B., Coolen, M., Moore, J.C., Madelaine. R., Kremmer, E., Faus-Kessler, T., Blader, P., Lawson, N.D., and Bally-Cuif, L. (2010). Notch activity levels control the balance between quiescence and recruitment of adult neural stem cells. J. Neurosci. *30*, 7961-7974.

Chapouton, P., Webb, K.J., Stigloher, C., Alunni, A., Adolf, B., Hesl, B., Topp, S., Kremmer, E., and Bally-Cuif, L. (2011). Expression of Hairy/enhancer of split genes in neural progenitors and neurogenesis domains of the adult zebrafish brain. J. Comp. Neurol. *519*, 1748-1769.

Chaves da Silva, P.G., Benton, J.L., Beltz, B.S., and Allodi, S. (2012). Adult neurogenesis: Ultrastructure of a neurogenic niche and neurovascular relationships. PLoS ONE *7*, e39267

Chaves da Silva, P.G., Benton, J.L., Sandeman, D.C., and Beltz, B.S. (2013). Adult neurogenesis in the crayfish brain: The hematopoietic anterior proliferation center has direct access to the brain and stem cell niche. Stem Cells Dev. *22*, 1027-1041.

Chen, Z., Ye, R., and Goldman, S.A. (2013). Testosterone modulation of angiogenesis and neurogenesis in the adult songbird. Neuroscience *239*, 139-148.

Clark, D. (1981). Visual responses in developing zebrafish. Ph.D. dissertation. Univ. of Oregon.

Clark, P.J., Kohman, R.A., Miller, D.S., Bhattacharya, T.K., Haferkamp, E.H., Rhodes, J.S. (2010). Adult hippocampal neurogenesis and c-Fos induction during escalation of voluntary wheel running in C57BL/6J mice. Behav. Brain Res. *213*, 246-252.

Clayton, N.S. (1998). Memory and the hippocampus in food-storing birds: A comparative approach. Neuropharmacology *37*, 441-452.

Coldwill, R.M., Raymond, M.P., Ferreira, L., and Escudero, H. (2005). Visual discrimination learning in zebrafish (Danior rerio). Behav. Process. *70*, 19-31.

Corroto, F.S., Henegar, J.A., and Maruniak, J.A. (1993). Neurogenesis persists in the subependymal layer of the adult mouse brain. Neurosci. Lett. *149*, 111-114.

Corotto, F.S., Henegar, J.R., and Maruniak, J.A. (1994). Odor deprivation lead to reduced neurogenesis and reduced neuronal survival in the olfactory bulb of the adult mouse. Neuroscience *61*, 739-744.

Craig, C.G., Tropepe, V., Morshead, C.M., Reyholds, B.A., Weiss, S., and van der Kooy, D. (1996). In vivo growth factor expansion of endogenous subependymal neural precursor cell populations in the adult mouse brain. J. Neurosci. *16*, 2649-2658.

Crosnier, C., Vargesson, N., Gschmeisser, S., Ariza-McNaughton, L., Morrison, A., and Lewis, J. (2005). Delta-Notch signalling controls commitment to a secretory fate in the zebrafish intestine. Development *132*, 1093-1104.

Curtis, M.A., Kam, M., Nannmark, U., Anderson, M.F., Axell, M.Z., Wikkelso, C., Holtas, S., van Roon-Mom, W.M.C., Bjork-Eriksson, T., Nordborg, C., Frisen, J., Dragunow, M., Faull, R.L.M., and Eriksson, P.S. (2007). Human neuroblasts migrate to the olfactory bulb via a lateral ventricular extension. *315*, 1243-1248.

Curtis, M.A., Low, V.F., and Faull, R.L.M. (2012). Neurogenesis and progenitor cells in the adult human brain: A comparison between hippocampal and subventricular progenitor proliferation. Dev. Neurobiol. *72*, 990-1005.

Dahlbom, S.J., Lagman, D., Lundstedt-Enkel, K., Sundstrom, L.F., and Winberg, S. (2011). Boldness predicts social status in Zebrafish (*Danio rerio*). PLoS ONE *6*, e23565.

Dawley, E.M., Fingerlin, A., Hwang, D., John, S.S., and Stankiewicz, C.A. (2000). Seasonal cell proliferation in the chemosensory epithelium and brain of red-backed salamanders, *Plethodon cinereus*. Brain Behav. Evol. *56*, 1-13.

Dawley, E.M., Nelsen, M., Lopata, A., Schwartz, J., and Bierly, A. (2006). Cell birth and survival following seasonal periods of cell proliferation in the chemosensory epithelia of red-backed salamanders, *Plethodon cinereus*. Brain Behav. Evol. *68*, 26-36.

Delgado-Gonzalez, F.J., Gonzalez-Granero, S., Trujillo-Trujillo, C.M., Carcia-Verdugo, J.M., and Domas-Hernandez, M.C. (2011). Study of adult neurogenesis in the *gallotia galloti* lizard during different seasons. Brain Res. *1390*, 50-58.

Deng, W., Saxe, M.D., Gallina, I.S., and Gage, F.H. (2009). Adult-born hippocampal dentate granule cells undergoing maturation modulate learning and memory in the brain. J. Neurosci. *29*, 13532-13542.

de Oliveira-Carlos, V., Ganz, J., Hans, S., Kaslin, J., and Brand, M. (2013). Notch receptor expression in neurogenic regions of the adult zebrafishb brain. PLoS ONE *8*, e73384.

Dhanasiri, A.K.S., Fernandes, J.M.O., and Kiron, V. (2013). Acclimation of zebrafish to transport stress. Zebrafish *10*, 87-98.

Dieni, C.V., Chancy, J.H., and Overstreet-Wadiche, L.S. (2013). Dynamic functions of GABA signalling during granule cell maturation. Front. Neural Circuits *6*, 1-11.

Dimitrov, E., and Usdin, T.B. (2010). Tuberoinfundibular peptide of 39 residues modulates the mouse hypothalamic-pituitary-adrenal axis via paraventricular glutamatergic neurons. J. Comp. Neurol. *518*, 4375-4394.

Diniz, L., dos Santos, T.B., Britto, L.R.G., Cespedes, I.C., Garcia, M.C., Spadari-Bratfisch, R.C., Medalha, C.C., de Castro, G.M., Montesano, F.T., and Viana, M.B. (2013). Effects of chronic treatment with corticosterone and imipramine on fox immunoreactivity and adult hippocampal neurogenesis. Beh. Brain Res. *238*, 170-177.

Doetsch, F. (2003A). The glial identity of neural stem cells. Nature Neurosci. *6*, 1127-1134.

Doetsch, F. (2003B). A niche for adult neural stem cells. Curr. Opin. Genet. Dev. *13*, 543-550.

Doetsch, F., Garcia-Verdugo, J.M., and Alverez-Buylla, A. (1997). Cellular composition and three-diemensional organization of the subventricular germinal zone in the adult mammalian brain. J. Neurosci. *17*, 5046-5061.

Doetsch, F., Caille, I., Lim, D.A., Garcia-Verdugo, J.M., and Alverez-Buylla, A. (1999). Suventricular zone astrocytes are neural stem cells in the adult mammalian brain. Cell *97*, 703-716.

Doetsch, F., and Scharff, C. (2001). Challenges for brain repair: Insights from adult neurogenesis in birds and mammals. Brain Behav. Evol *58*, 306-322.

Dono, R. (2003). Fibroblast growth factors as regulators of central nervous system development and function. Am. J. Physiol. Regul. Integr. Comp. Physiol. *284*, R867-R881.

Doupe, A.J. (1994). Songbirds and adult neurogenesis: a new role for hormones. Proc. Natl. Acad. Sci. U.S.A. *91*, 7836-7838.

Driscoll, I., Howard, S.R., Stone, J.C., Monfils, M.H., Tomanek, B., Brooks, W.M., and Sutherland, R.J. (2006). The aging hippocampus: A multi-level analysis in the rat. Neuroscience *139*, 1173-1185.

Dufour, M.-C., and Gadenne, C. (2006). Adult neurogenesis in a moth brain. J. Comp. Neurol. *495*, 635-643.

Dunlap, K.D., and Chung, M. (2013). Social novelty enhances brain cell proliferation, cell survival and chirp production in an electric fish, *Apteronotus leptorhynchus*. Dev. Neurobiol. *73*, 324-332.

Eckenstein, F.P., McGovern, T., Kern, D., Deignan, J. (2006). Neuronal vulnerability in transgenic mice expressing an inducible dominant-negative FGF receptor. Exp. Neurol. *198*, 338-349.

Ekström, P., Johnsson, C.-M., and Ohlin, L.-M. (2001). Ventricular proliferation zones in the brain of an adult telost fish and their relation to neuromeres and migration (secondary matrix) zones. J. Comp. Neurol. *436*, 92-110.

Emsley, J., Mitchell, B.D., Kempermann, G., and Macklis, J.D. (2005). Adult neurogenesis and repair of the adult CNS with neural progenitors, precursors, and stem cells. Prog. Neurobiol. *75*, 321-341.

Enwere, E., Shingo, T., Gregg, C., Fujikawa, J., Ohta, S., Weiss, S. (2004). Aging results in reduced epidermal growth factor receptor signaling, diminished olfactory neurogenesis, and deficits in fine olfactory discrimination. J. Neurosci. *24*, 8354-8365.

Epp, J.R., Chow, C., Galea, L.A.M. (2013). Nippocampus-dependent learning influences hippocampal neurogenesis. Front. Neurosci. *7*, 1-9.

Eriksson, P.S., Perfilieva, E., Bjork-Eriksson, T., Alborn, A.-M., Nordborg, C., Peterson, D.A., and Gage, F.H. (1998). Neurogenesis in the adult human hippocampus. Nature Med. *4*, 1313-1317.

Fahrbach, S.E., Strande, J.L., and Robinson, G.E. (1995). Neurogenesis is absent in the brains of adult honey bees and does not explain behavioral neuroplasticity. Neurosci. Lett. *197*, 145-148.

Feierstein, C.E. (2012). Linking adult olfactory neurogenesis to social behavior. Front. Neurosci. *6*, 1-13.

Feldman, D.E., and Brecht, M. (2005). Map plasticity in somatosensory cortex. Science *310*, 810-815.

Filby, A.L., Paull, G.C., Bartlett, E.J., Van Look, K.J.W., and Tyler, C.R. (2010). Physiological and health consequences of social status in zebrafish (*Danio rerio*). Physiol. Behav. *101*, 576-587.

Finch, C.E. (1990). Longevity, senescence, and the genome. (Chicago, IL; University of Chicago Press).

Finch, C.E., and Austad, S.N. (2012). Primate aging in the mammalian scheme: The puzzle of extreme variation in brain aging. Age *34*, 1075-1091.

Fleisch, V.C., and Neuhauss, S.C.F. (2006). Visual behavior in zebrafish. Zebrafish *3*, 191-201.

Folgueira, M., Sueiro, C., Rodriguez-Moldes, I., Yanez, J., and Anadon, R. (2007). Organization of the torus longitudinalis in the rainbow trout (Oncorhynchus mykiss): An immunohistochemical study of the GABAergic system and a DiI trac-tracing study. J. Comp. Neurol. *503*, 348-370.

Font, E., Desfilis, E., Perez-Canellas, M.M., and Garcia-Verdugo, J.M. (2001). Neurogenesis and neuronal regeneration in the adult reptilian brain. Brain Beh. Evol. *58*, 276-295.

Font, E., Barbosa, D., Sampedro, C., and Carazo, P. (2012). Social behavior, chemical communication, and adult neurogenesis: Studies of scent mark function in *Podarcis* wall lizards. Gen. Comp. Endocrinol. *177*, 9-17.

Fowler, C.D., Liu, Y., Ouimet, C., and Wang, Z. (2002). The effects of social environment on adult neurogenesis in the female prairie vole. J. Neurobiol. *51*, 115-128.

Frankland, P.W., Kohler, S., and Josselyn, S.A. (2013). Hippocampal neurogenesis and forgetting. Trends Neurosci. *36*, 497-503.

Friedrich, R.W. (2013). Neuronal computations in the olfactory system of zebrafish. Annu. Rev. Neurosci. *36*, 383-402.

Fuentealba, L.C., Obernier, K., and Alvarez-Buylla, A. (2012). Adult neural stem cells bridge their niche. Cell Stem Cell *10*, 698-708.

Galea, L.A.M. (2008). Gonadal hormone modulation of neurogenesis in the dentate gyrus of adult male and female rodents. Brain Res. Rev. *57*, 332-341.

Galea, L.A.M., Wainwright, S.R., Roes, M.M., Duarte-Guterman, P., Chow, C., and Hamson, D.K. (2013). Sex, hormones and neurogenesis in the hippocampus: Hormonal modulation of neurogenesis and potential functional implications. J. Neuroendocrinol. *25*, 1039-1061.

Ganz, J., Kaslin, J., Hochmann, S., Fredenreich, D., and Brand, M. (2010). Heterogeneity and Fgf dependence of adult neural progenitors in the zebrafish telencephalon. Glia *58*, 1345-1363.

Garcia-Verdugo, J.M., Ferron, S., Flames, N., Collado, L., Desfilis, E., and Font, E. (2002). The proliferative ventricular zone in adult vertebrates: A comparative study using reptiles, birds, and mammals. Brain Res. Bull. *57*, 765-775.

Garthe, A., Behr, J., and Kempermann, G. (2009). Adult-generated hippocampal neurons allow the flexible use of spatially precise learning strategies. PLoS ONE *4*, e5464.

Gerlach, G., Hodgins-Davis, A., Avolio, C., and Schunter, C. (2008). Kin recognition in zebrafish: A 24-hour window for olfactory imprinting. Proc. R. Soc. Biol. Sci. *275*, 2165-2170.

Geuna S. (2005). The revolution of counting "tops": two decades of the disector principle in morphological research. Micros. Res. Tech. *66*, 270-274.

Gheusi, G., Ortega-Perez, I. Murray, K., and Lledo, P.-M. (2009). A niche for adult neurogenesis in social behavior. Beh. Brain Res. *200*, 315-322.

Gheusi, G., Lepousez, G., and Lledo, P.-M.. (2013). Adult-born neurons in the olfactory bulb: Integration and functional consequences. Curr. Topics Behav. Neurosci. *15*, 49-72.

Ghosal, K., Gupta, M, and Killian, K.A. (2009). Agonistic behavior enhances adult neurogenesis in male *Acheta domesticus* crickets. J. Exp. Biol. *212*, 2045-2056.

Gibbs, M.A., and Northmore, D.P.M. (1998). Spectral sensitivity of the goldfish Torus longitudinalis. Vis. Neurosci. *15*, 859-865.

Gibson, E.M., Wang, C., Tjho, S., Khattar, N., and Kriegsfeld, L.J. (2010). Experimental 'Jet Lag' inhibits adult neurogenesis and produces long-term cognitive deficits in female hamsters. PLoS ONE *5*, e15267.

Gil-Perotin, S., Duran-Moreno, M., Belzunegui, S., Luquin, M.R., and Garcia-Verdugo, J.M. (2009). Ultrastructure of the subventricular zone in *Macaca fascicularis* and evidence of a mouse-like migratory stream. J. Comp. Neurol. *514*, 533-554.

Glasper, E.R., and Gould, E. (2012). Sexual experience restores age-related decline in adult neurogenesis and hippocampal function. Hippocampus *23*, 303-312.

Goldman, S.A. (1998). Adult neurogenesis: From canaries to the clinic. J. Neurobiol. *36*, 267-286.

Goldman, S.A., Nottebohm, F. (1983). Neuronal production, migration and differentiation in a vocal control nucleus of the adult female canary brain. Proc. Natl. Acad. Sci. U.S.A. *80*, 2390-2394.

Gotz, M., Hartfuss, E., and Malatesta, P. (2002). Radial glial cells as neuronal precursors: A new perspective on the correlation f morphology and lineage restriction in the developing cerebral cortex of mice. Brain Res. Bull. *57*, 777-788.

Gould, E. (1999). Serotonin and hippocampal neurogenesis. Neuropsychopharmacology *21*, 46S-51S.

Gould, E., Cameron, H.A., Daniels, D.C., Woolley, C.S., and McEwen, B.S. (1992). Adrenal hormones suppress cell division in the adult rate dentate gyrus. J. Neurosci. 12, 3642-3650.

Gould, E., McEwen, B.S., Tanapt, P., Galea, L.A.M., and Fuchs, E. (1997). Neurogenesis in the dentate gyrus of the adult tree shrew is regulated by psychosocial stress and NMDA receptor activation. J. Neurosci. *17*, 2492-2498.

Gould, E., Tanapat, P., McEwen, B., Flugge, G., and Fuchs, E. (1998). Proliferation of granule cell precursors in the dentate gyrus of adult monkeys is diminished by stress. Proc. Natl. Acad. Sci. USA. *95*, 3168-3171.

Gould, E., Beylin, A., Tanapat, P., Reeves, A.J., and Shors, T.J. (1999A). Learning enhances adult neurogenesis in the hippocampal formation. Nature Neurosci. *2*, 260-265.

Gould, E., Reeves, A.J., Fallah, M., Tanapat, P., Gross, C.G., and Fuchs, E. (1999B). Hippocampal neurogenesis in adult Old World primates. Proc. Natl. Acad. Sci. U.S.A. *96*, 5263-5267.

Gould, E., Tanapat, P., Rydel, T., and Hastings, N. (2000). Regulation of hippocampal neurogenesis in adulthood. Biol. Psychiatry *48*, 715-720.

Gould, E., and Gross, C.G. (2002). Neurogenesis in adult mammals: Some progress and problems. J. Neurosci. *3*, 619-623.

Grandel, H., Kaslin, J., Ganz, J., Wenzel, I., and Brand, M. (2006). Neural stem cells and neurogenesis in the adult zebrafish brain: Origin, proliferation dynamics, migration and cell fate. Dev. Biol. *295*, 263-277.

Grandel, H., and Brand, M. (2013). Comparative aspects of adult neural stem cell activity in vertebrates. Dev. Genes Evol. *223*, 131-147.

Graziadei, P.P.C, and Metcalf, J.F. (1971). Autoradiographic and ultrastructural observations on the frog's olfactory mucosa. Z. Zellforsch. *116*, 305-318.

Gritti, A., Bonfanti, L., Doetsch, F., Caille, I., Alvarez-Buylla, A., Lim, D.A., Galli, R., Garcia-Verdugo, J.M., Herrera, D.G., and Vescovi, A.L. (2002). Multipotent neural stem cells reside into the rostral extension and olfactory bulb of adult rodents. J. Neurosci. *22*, 437-445.

Gross, C.G. (2000). Neurogenesis in the adult brain: Death of a dogma. Nature Rev. Neurosci. *1*, 67-73.

Grupp, L., Wolburg, H., and Mack, A.F. (2010). Astroglial structures in the zebrafish brain. J. Comp. Neurol. *518*, 4277-4287.

Guzman-Marin, R., Bashir, T., Suntsova, N., Szymusiak, R., and McGinty, D. (2007). Hippocampal neurogenesis is reduced by sleep fragmentation in the adult rat. Neuroscience *148*, 325-333.

Hagg, T. (2005). Molecular regulation of adult CNS neurogenesis: An integrated view. Trends Neurosci. *28*, 589-595.

Halpern, M., and Martinez-Marcos, A. (2003). Structure and function of the vomeronasal system: An update. Prog. Neurobiol. *70*, 245-318.

Hamdani, E.H., Lastein, S., Gregersen, F., and Doving, K.B. (2008). Seasonal variations in olfactory sensory neurons – fish sensitivity to sex pheromones explained? Chem. Senses *33*, 119-123.

Hamilton, A. (1901). The division of differentiated cells in the central nervous system of the white rat. J. Comp. Neurol. *11*, 297-320.

Hamilton, L.K., Aumont, A., Julien, C., Vadnais, A., Calon, F., and Fernandes, K.J.L. (2010). Widespread deficits in adult neurogenesis precede plaque and tangle formation in the 3xTg mouse model of Alzheimer's disease. Eur. J. Neurosci. *32*, 905-920.

Hamilton, L.K., Joppe, S.E., Cochard, L.M., and Fernandes, K.J.L. (2013). Aging and neurogenesis in the adult forebrain: What we have learned and where we should go from here. Eur. J. Neurosci. *37*, 1978-1986.

Hamson, K.K., Wainwright, S.R., Taylor, J.R., Jones, B.A., Watson, N.V., and Galea, L.A.M. (2013). Androgens increase survival of adult-born neurons in the dentate gyrus by and androgen receptor-dependent mechanism in male rats. Endocrinology *154*, 3294-3304.

Hans, S, Kaslin, J., Freudenreich, D., and Brand, M. (2009). Temporally-controlled site-specific recombination in zebrafish. PLoS ONE *4*, e4640.

Hans, S., Freudenreich, D., Geffarth, M., Kaslin, J., Machate, A., and Brand, M. (2011). Generation of a non-leaky heat shock-inducible Cre line for conditional Cre/lox strategies in zebrafish. Dev. Dyn. *240*, 108-115.

Hansen, A., and Schmidt, M. (2001). Neurogenesis in the central olfactory pathway of the adult shore crab, *Carcinus maenas* is controlled by sensory afferents. J. Comp. Neurol. *441*, 223-233.

Hansen, A., and Schmidt, M. (2004). Influence of season and environment on adult neurogenesis in the central olfactory pathway of the shore crab, *Carcinus maenas*. Brain Res. *1025*, 85-97.

Hara, T.J. (1994). The diversity of chemical stimulation in fish olfaction and gestation. Rev. Fish Biol. Fish. *4*, 1-35.

Harzsch, S., and Dawirs, R.R. (1996). Neurogenesis in the developing crab brain: Postembryonic generation of neurons persists beyond metamorphosis. J. Neurobiol. *29*, 384-398.

Hayama, T., and Caprio, J. (1989). Lobule structure and somatotopic organization of the medullary facial lobe in the channel catfish *Ictalurus punctatus*. J. Comp. Neurol. *285*, 9-17.

Hensch, T.K. (2004). Critical period regulation. Annu. Rev. Neurosci. 27, 549-579.

Hensch, T.K. (2005). Critical period plasticity in local cortical circuits. Nature Rev. Neurosci. *6*, 877-888.

Hernandes-Rabaza, V., Llorens-Martin, M., Valazquez-Sanchez, C., Ferragud, A., Arcusa, A., Gumus, H.G., Gomez-Pinedo, U., Perez-Villalba, A., Rosello, J., Trejo, J.L., Barcia, J.A., and Canales, J.J. (2008). Inhibition of adult hippocampal neurogenesis disrupts contextual learning but spares spatial working memory, long-term conditional rule retention and spatial reversal. Neuroscience *159*, 59-68.

Hinsch, K., and Zupanc, G.K.H. (2007). Generation and long-term persistence of new neurons in the adult zebrafish brain: A quantitative analysis. Neuroscience *146*, 679-696.

Hochmann, S., Kaslin , J., Hans, S., Weber, A., Machate, A., Geffarth, M., Funk, R.H.W., and Brand, M. (2012). Fgf signaling is required for photoreceptor maintenance in the adult zebrafish retina. PLoS ONE *7*, e30365.

Holland, N.D. (2003). Early central nervous system evolution: An era of skin brains? Nature Rev. Neurosci. *4*, 1-11.

Hoshooley, J.S., and Sherry, D.F. (2004). Neuron production, neuron number, and structure size are seasonally stable in the hippocampus of the food-storing black-capped chickadee (*Poecile atricapillus*). Beh. Neurosci. 1*18*, 345-355.

Hoshooley, J.S., and Sherry, D.F. (2007). Greater hippocampal neuronal recruitment in food-storing than in non-food storing birds. Dev. Neurobiol. *67*, 406-414.

Hoshooley, J.S., Phillmore, L.S., Sherry, D.F., and MacDougall-Shackeleton, S.A. (2007). Annual cycle of the black-capped chickadee: Seaonality of food-storing and the hippocampus. Brain Behav. Evol. *69*, 161-168.

Huang, T., Cui, J., Hitchcok, P.F., and Li, Y. (2012). The role of microglia in the neurogenesis of zebrafish retina. Biochem. Biophys. Res. Commun. *421*, 214-220.

Hubel, D.H., and Wiesel, T.N. (1964). Effects of monocular deprivation in kittens. Naunyn Schmiedebergs Arch. Exp. Pathol. Pharmakol. *248*, 492-497.

Huber, R., van Staaden, M.J., Kaufman, L.S., and Liem, K.F. (1997). Microhabitat use, trophic patterns, and the evolution of brain structure in African Cichlids. Brain Behav. Evol. *50*, 167-182.

Ibi, D. Takuma, K., Koke, H., Mizoguichi, H., Tsuritani, K., Kuwahara, Y., Kamei, H., Nagai, Y., Yonedo, Y., Nabeshima, T., and Yamada, K. (2008). Social isolation rearing-induced impairment of the hippocampal neurogenesis is associated with deficits in spatial memory and emotion-related behaviors in juvenile mice. J. Neurochem. *105*, 921-932.

Imayoshi, I., and Kageyama, R. (2011). The role of notch signaling in adult neurogenesis. Mol. Neurobiol. *44*, 7-12.

Inestrosa, N.C., and Arenas, E. (2010). Emerging role of Wnts in the adult nervous system. Nature Rev. Neuro. *11*, 77-86.

Isaacson, J.S. (2010). Odor representations in mammalian cortical circuits. Curr. Opin. Neurobiol. *20*, 328-331.

Ito, K., Hotta, Y. (1992). Proliferation pattern of postembryonic neuroblasts in the brain of *Drosophila melanogaster*. Dev. Biol. *149*, 134-148.

Ito, Y., Tanaka, H., Okamoto, H., and Ohshima, T. (2010). Characterization of neural stem cells and their progeny in the adult zebrafish optic tectum. Dev. Biol. *342*, 26-38.

Jin, K., Peel, A.L., Mao, X.O., Cottrell, B.A., Henshall, D.C., and Greenberg, D.A. (2003). Increased hippocampal neurogenesis in Alzheimer's disease. Proc. Natl. Acad. Sci. U.S.A. *101*, 343-347.

Junek, A., Rusak, B., and Semba, K. (2010). Short-term sleep deprivation may alter the dynamics of hippocampal cell proliferation in adult rats. Neuroscience *170*, 1140-1152.

Kam, M., Curtis, M.A., McGlasha, S.R., Connor, B., Nannmark, U., and Faull, R.L. (2009). The cellular composition and morphological organization of the rostral migratory stream in the adult human brain. J. Chem. Neuroanat. *37*, 196-205.

Kaneko, N., Marin, O., Koike, M., Hirota, Y., Uchiyama, Y., Wu, J.Y., Lu, Q., Tessier-Lavigne, M., Alvarez-Buylla, A., Okano, H., Rubenstein, J.L.R., and Sawamoto, K. (2010). Neuron *67*, 213-223.

Kannangara, T.S., Webber, A., Gil-Mohapel, J., and Christie, B.R. (2009). Stress differentially regulates the effect of voluntary exercise on cell proliferation in the dentate gyrus of mice. Hippocampus *19*, 889-897.

Kaplan, M.S., and Hinds, J.W. (1977). Neurogenesis in the adult rat: Electron microscopic analysis of light radioautographs. Science *197*, 1092-1094.

Kaplan, M.S. (1984). Mitotic neuroblasts in the 9-day-old and 11-month-old rodent hippocampus. J. Neurosci. *4*, 1439-1441.

Kaplan, M.S. (1983). Proliferation and subependymal cells in the adult primate CNS: Differential uptake of DNA labeled precursors. J. Hirnforsch. *23*, 23-33.

Kaplan, M.S. (1985). Formation and turnover of neurons in young and senescent animals: An electron microscopic and morphometric analysis. Ann. N.Y. Acad. Sci. *457*, 173-192.

Kaplan, M.S., McNelly, N.A., and Hinds, J.W. (1985). Population dynamics of adult-formed granule neurons of the rat olfactory bulb. J. Comp. Neurol. *239*, 117-125.

Kara, T.C. (1994). Ageing in amphibians. Gerontology *40*, 161-173.

Kaslin, J., Ganz, J., and Brand, M. (2008). Proliferation, neurogenesis and regeneration in the non-mammalian vertebrate brain. Phil. Trans. R. Soc. B *363*, 101-122.

Kaslin, J., Ganz, J., Geffarth, M., Grandel, H., Hans, S., and Brand, M. (2009). Stem cells in the adult zebrafish cerebellum: Initiation and maintenance of a novel stem cell niche. J. Neurosci. *29*, 6142-6153.

Kaslin, J., Kroehne, V., Benato, F., Argenton, F., and Brand, M. (2013). Development and specification of cerebellar stem and progenitor cells in zebrafish: From embryo to adult. Neural. Dev. *8*, 1-15.

Kee, N., Sivalingam, S., Boonstra, R., and Wojtowicz, J.M. (2002). The utility of Ki-67 and BrdU as proliferative markers of adult neurogenesis. J. Neurosci. Methods *115*, 97-105.

Kee, N., Teixeira, C.M., Wang, A.H., and Frankland, P.W. (2007). Preferential incorporation of adult-generated granule cells into spatial memory networks in the dentate gyrus. Nature Neurosci. *10*, 355-362.

Kempermann, G. (2011). Seven principles in the regulation of adult neurogenesis. Eur. J. Neurosci. *33*, 1018-1024.

Kempermann, G. (2012). New neurons for 'survival of the fittest'. Nature Rev. Neurosci. *13*, 727-736.

Kempermann, G., Kuhn, H.G., and Gage, F.H. (1997). More hippocampal neurons in adult mice living in an enriched environment. Nature *386*, 493-495.

Kempermann, G., Kuhn, H.G., and Gage, F.H. (1998). Experience-induced neurogenesis in the senescent dentate gyrus. J. Neurosci. *18*, 3206-3212.

Kim, W.-Y., and Shen, J. (2008). Presenilins are required for maintenance of neural stem cells in the developing brain. Mol. Neurodegener. *3*, 1-13.

Kinoshita, M., and Ito, E. (2006). Roles of periventricular neurons in retinotectal transmission in the optic tectum. Prog. Neurobiol. *79*, 112-121.

Kinoshita, M., Ito, E., Urano, A., Ito, H., and Yamamoto, N. (2006). Periventricular efferent neurons in the optic tectum of rainbow trout. J. Comp. Neurol. *499*, 546-564.

Kirsche, W. (1967). On postembryonic matrix zones in the brain of various vertebrates and their relationship to the study of the brain structure. Z. Mikrosk. Anat. Forsch. *77*, 313-406.

Kishimoto, N., Alfaro-Cervello, C., Shimizu, K., Asakawa, K., Urasaki, A., Nonaka, .S, Kawakami, K., Garcia-Verdugo, J.M., and Sawamoto, K. (2011). Migration of neuronal precursors from the telencephalic ventricular zone into the olfactory bulb in adult zebrafish. J. Comp. Neurol. *519*, 3549–3565.

Kishimoto, N., Shimizu, K, and Sawamoto, K. (2012). Neuronal regeneration in a zebrafish model of adult brain injury. Dis. Model Mech. *5*, 200-209.

Kizil, C., and Brand, M. (2011). Cerebroventricular microinjection (CVMI) into adult zebrafish brain is an efficient misexpression method for forebrain ventricular cells. PLoS ONE *6*, e27395.

Kizil, C., Kaslin, J., Kroehne, V., and Brand, M. (2012A). Adult neurogenesis and brain regeneration in zebrafish. Dev. Neurobiol. *72*, 429-461.

Kizil, C., Kyritsis, N., Dudczig, S., Kroehne, V., Freudenreich, D., Kaslin, J., and Brand, M. (2012B). Regenerative neurogenesis from neural progenitor cells requires injury-induced expression of Gata3. Dev. Cell *23*, 1230-1237.

Klempin, F., Beis, D., Mosienko, V., Kempermann, G., Bader, M., and Alenina, N. (2013). Serotonin is required for exercise-induced adult hippocampal neurogenesis. J. Neurosci. *33*, 8270-8275.

Koehl, M, and Abrous, D.N. (2011). A new chapter in the field of memory: Adult hippocampal neurogenesis. Eur. J. Neurosci. *33*, 1101-1114.

Koketsu, D., Mikami, A., Miyamoto, Y, and Hisatsune, T. (2003). Nonrenewal of neurons in the cerebral neocortex of adult macaque monkeys. J. Neurosci. *23*, 937-942.

Kornack, D.R., and Rakic, P. (1999). Continuation of neurogenesis in the hippocampus of the adult macaque monkey. Proc. Natl. Acad. Sci. U.S.A. *96*, 5768-5773.

Kornack, D.R., and Rakic, P. (2001). The generation, migration, and differentiation of olfactory neurons in the adult primate brain. Proc. Natl. Acad. Sci. U.S.A. *98*, 4752-4757.

Kotrschal, R., Van Staaden, M.J., and Huber, R. (1998). Fish brains: Evolution and environmental relationships. Rev. Fish Biol. Fish *8*, 373-408.

Kozorovitskiy, Y., and Gould, E. (2004). Dominance hierarchy influences adult neurogenesis in the dentate gyrus. J. Neurosci. *24*, 6755-6759.

Korsching, S.I., Argo, S., Campenhausen, H., Freidrich, R.W., Rummrich, A., and Weth, F. (1997). Cell Develop. Biol. *8*, 181-187.

Kriegstein, A., and Alvarez-Buylla, A. (2009). The glial nature of embryonic and adult neural stem cells. Annu. Rev. Neurosci. *32*, 149-184.

Kroehne, V., Freudenreich, D., Hans, Kaslin, J., and Brand, M. (2011). Regeneration of the adult zebrafish brain from neurogenic radial glial-type progenitors. Development *138*, 4831-4841.

Kuhn, H.G., Dickinson-Anson, H., and Gage, F.H. (1996). Neurogenesis in the dentate gyrus of the adult rat: Age-related decrease of neuronal progenitor proliferation. J. Neurosci. *16*, 2027-2033.

Kuhn, H.G., Winkler, J., Kempermann, G., Thal, L.J., and Gage, F.H. (1997). Epidermal growth factor and fibroblast growth factor-2 have different effects on neural progenitors in the adult rat brain. J. Neurosci. *17*, 5820-5829.

Kukekov, V.G., Laywell, E.D., Suslove, O., Davies, K., Scheffler, B., Thomas, L.B., O'Brien, T.F., Kisakabe, M., and Steindler, D.A. (1999). Multipotent stem/progenitor cells with similar properties arise from two neurogenic regions of adult human brain. Exp. Neurol. *156*, 333-344.

Kuroyanagi, Y., Okuyama, T., Suehiro, Y., Imada, H., Shimada, A., Naruse, K., Takeda, H., Kubo, T., and Takeuchi, H. (2010). Proliferation zones in the adult medaka (*Oryzias latipes*) brain. Brain Res. *1323*, 33-40.

LaDage, L.D., Roth, T.C., II, Fox, R.A., and Pravosudov, V.V. (2010). Ecologically relevant spatial memory use modulates hippocampal neurogenesis. Proc. R.Soc. B. *365*, 859-867.

LaDage, L.D., Roth, T.C., and Pravosudov, V.V. (2011). Hippocampal neurogenesis is associated with migratory behavior in adult but not juvenile white-crowned sparrows (Zonotrichia leucophrys ssp.) Proc. R. Soc. B. *278*, 138-143.

Lam, C.S., Marz, M, and Strahle, U. (2009). Gfap and nestin reporter lines reveal characteristics of neural progenitors in the adult zebrafish brain. Dev. Dyn. *238*, 475-486.

Lau, B.Y.B., Mathur, P., Gould, G.G., and Guo, S. (2011). Identification of a brain center whose activity discriminates a choice behavior in zebrafish. Proc. Natl. Acad. Sci. U.S.A. *108*, 2581-2586.

Lazarini, F., and Lledo, P.-M. (2011). Is adult neurogenesis essential for olfaction? Trends Neurosci. *34*, 20-30

Lavenex, P., Steele, M.A., and Jacobs, L.F. (2000). The seasonal pattern of cell proliferation and neuron number in the dentate gyrus of wild adult eastern grey squirrels. Eur. J. Neurosci. *12*, 643-648.

Lawrence, C. (2007). The husbandry of zebrafish (*Danio rerio*): A review. Aquaculture *269*, 1-20.

Leasure, J.L., and Decker, L. (2009). Social isolation prevent exercise-induced proliferation of hippocampal progenitor cells in female rats. Hippocampus *19*, 907-912.

Lee, Y., Grill, S., Sanchez, A., Murphy-Ryan, M., and Poss, K.D. (2005). Fgf signaling instructs position-dependent growth rate during zebrafish fin regeneration. Development *132*, 5173-5183.

Leinwand, S.G., and Chalasani, S.H. (2011). Olfactory networks: From sensation to perception. Curr. Opin. Gen. Dev. *21*, 806-811.

LeMaster, M., Moore, I.T., and Mason, R.T. (2001). Conspecific trailing behavior of red-sided garter snakes, *Thamnophis sirtalis parietalis*, in the natural environment. Anim. Behav. *61*, 827-833.

Lenkowski, J.R., Qin, Z., Sifuentes, C.J., Thummel, R., Soto, C.M., Moens, C.B., and Raymond, P.A. (2013). Retinal regeneration in adult zebrafish requeis regulation of TGFβ signaling. Glia *61*, 1687-1697.

Levi, G. (1898). Sulla cariocinesi delle cellule nervose. Riv. Patol. Nerv. Ment. *3*, 97-113.

Lie, D.C., Song, H., Colamarino, S.A., Ming, G.-l., and Gage, F.H. (2004). Neurogenesis in the adult brain: New strategies for central nervous system diseases. Annu. Rev. Pharmacol. Toxicol. *44*, 399-421.

Lie, D.-C., Colamarino, S.A., Song, H.-J., Desire, L., Mira, H., Consiglio, A., Lein, E.S., Jessberger, S., Lansford, H., Dearie, A.R., and Gage, F.H. (2005). Wnt signaling regulates adult hippocampal neurogenesis. Nature *437*, 1370-1375.

Lieberwirth, C., and Wang, Z. (2012). The social environment and neurogenesis in the adult mammalian brain. Front. Hum. Neurosci. *6*, 1-19.

Lieberwirth, C., Liu, Y., Jia, X., and Wang, Z. (2012). Social isolation impairs adult neurogenesis in the limbic system and alters behaviors in female prairie voles. Horm. Behav. *62*, 357-366.

Lin, S., Marin, E.C., Yang, C.-P., Kao, C.-F., Apenteng, B.A., Huang, Y., O-Connor, M.B., Truman, J.W., and Lee, T. (2013). Extremes of lineage plasticity in the *Drosophila* brain. Curr. Biol. *23*, 1-6.

Lindsey, B.W., and Tropepe, V. (2006). A comparative framework for understanding the biological principals of adult neurogenesis. Prog. Neurobiol. *80*, 281-307.

Lindsey, B.W., Darabie, A., and Tropepe V. (2012). The cellular composition of neurogenic periventricular zones in the adult zebrafish forebrain. J. Comp. Neurol. *502*, 2275-2316.

Lindsey, B.W., and Tropepe, V. (2013). Changes in the social environment induce neurogenic plasticity predominantly in primary sensory niches of the zebrafish brain independently of cortisol levels. Dev. Neurobiol. *Submitted.*

Lipkind, D., Nottebhom, F., Rado, R., and Barnea, A. (2002). Social change affects the survival of new neurons in the forebrain of adult songbirds. Behav. Brain Res. *133*, 31-43.

Liu, Z., and Martin, L.J. (2003). Olfactory bulb core is a rich source of neural progenitor and stem cells in adult rodent and human. J. Comp Neurol. *459*, 368-391.

Lois, C., and Alvarez-Buylla, A. (1994). Long-distance neuronal migration in the adult mammalian brain. Science *264*, 1145-1148.

Lois, C., Garcia-Verduo, J.-M., and Alvarez-Buylla, A. (1996). Chain migration of neuronal precursors. Science *271*, 978-981.

Louissaint, A.Jr., Rao, S., Leventhal, C., and Goldman, S.A. (2002). Coordinated interaction of neurogenesis and angiogenesis in the adult songbird brain. Neuron *34*, 945-60.

Lu, L., Bao, G., Chen, H., Xia, P., Fan, X., Zhang, J., Pei, G., and Ma, L. (2003). Modification of hippocampal neurogenesis and neuroplasticity by social environments. Exp. Neurol. *183*, 600-609.

Luo, J., Daniels, S.B., Lennington, J.B., Notti, R.Q., and Conover, J.C. (2006). The aging neurogenic subventricular zone. Aging Cell *5*, 139-152.

Lupien, S.J., and McEwen, B.S. (1997). The acute effects of corticosteroids on cognition: integration of animal and human model studies. Brain Res. Rev. *24*, 1-27.

MacDonald, R.B., Debiais-Thibaud, M., Talbot, J.C., and Ekker, M. (2010). The relationship between dlx and gad1 expression indicates highly conserved genetic pathways in the zebrafish forebrain. Dev. Dyn. *239*, 2298-2306.

Mackay-Sim, A., and Patel, U. (1984). Regional differences in cell density and cell genesis in the olfactory epithelium of the salamander, *Ambystoma tigrinum*. Exp. Brain. Res. *57*, 99-106.

Mackowiak, M., Chocyk, A., Markowicz-Kula, K., and Wedzony, K. (2004). Neurogenesis in the adult brain. Pol. J. Pharmacol. *56*, 673-687.

Maeyama, K., and Nakayasu, H. (2000). Postembryonic neurogenesis in zebrafish (*Danio rerio*) brain: Prsence of two different systems. Zool. Science *17*, 959-966.

Malaterre, J., Strambi, C., Chiang, A.-S., Aouane, A., Strambi, A., and Cayre, M. (2002). Development of cricket mushroom bodies. J. Comp. Neurol. *452*, 215-227.

Malaterre, J., Strambi, C., Aouane, A., Strambi, A., Rougon, G. and Cayre, M. (2003). Effect of hormones and growth factors on the proliferation of adult cricket neural progenitor cells *in vitro*. J. Neurobiol. *56*, 387-397.

Mak, G.K., Enwere, E.K., Gregg, C., Pakarainen, T., Poutanen, M., Huhtaniemi, I., and Weiss, S. (2007). Male pheromones - stimulate neurogenesis in the adult female brain: Possible role in mating behavior. Nature Neurosci. *10*, 1003-1011.

Mak, G.K., and Weiss, S. (2010). Paternal recognition of adult offspring mediated by newly generated CNS neurons. Nature Neurosci. *13*, 753-760.

Makinodan, M., Rosen, K.M., Ito, S., and Corfas, G. (2012). A critical period for social experience-dependent oligodendrocyte maturation and myelination. Science *337*, 1357-1360.

Mandairon, N., Sacquet, J., Jourdan, F., and Didier, A. (2006). Long-term fate and distribution of newborn cells in the adult mouse olfactory bulb: Influences of olfactory deprivation. Neuroscience. *141*, 443-451.

Mandairon, N., Sultan, S., Nouvian, M., Sacquet, J., and Didier, A. (2011). Involvement of newborn neurons in olfactory associative learning? The operant or non-operant component of the task makes all the difference. J. Neurosci. *31*, 12455-12460.

Marchioro, M., de Azevedo Mota Nunes, J.-M., Rabelo Ramalho, A.M., Molowny, A., Perez-Martinez, E., Ponsoda, X., and Lopez-Garcia, C. (2005). Postnatal neurogenesis in the medial cortex of the tropical lizard. Neuroscience *134*, 407-413.

Marcus, R.C., Delaney, C.L., and Easter, Jr., S.S. (1999). Neurogenesis in the visual system of embryonic and adult zebrafish (*Danio rerio*). Vis. Neurosci. *16*, 417-424.

Margotta, V., and Caronti, B. (2005). PCNA-negativity in the telencephalon of adult female songbirds (*Serinus serinus*): Absence of signs of normal proliferation. Italian J. Anat. Embryol. *110*, 237-245.

Marquardt, T., Ashery-Padan, R., Andrejewski, N., Scardigli, R., Guillemot, F., and Gruss, P. (2001). Pax6 is required for the multipotent state of retinal progenitor cells. Cell *105*, 43-55.

Martinez-Canabal, A., Akers, K.G., Josselyn, S.A., and Frankland, P.W. (2012). Age-dependent effets of hippocampal neurogenesis suppression on spatial learning. Hippocampus *23*, 66-74.

Marusich, M.F., Furneaux, H.M., Henion, P.D., and Weston, J.A. 1994. Hu neuronal proteins are expressed in proliferating neurogenic cells. J. Neurobiol. *25*, 143:155.

Maruska, K.P., Carpenter, R.E., and Fernald, R.D. (2012). Characterization of cell proliferation throughout the brain of the African cichlid fish *Astatotilapia burtoni* and its regulation by social status. J. Comp. Neurol. *520*, 3471-3491.

Maruska, K.P., Zhang, A., Neboori, A., and Fernald, R.D. (2013). Social opportunity causes rapid transcriptional changes in behaviour network of the brain in an African cichlid fish. J. Neuroendocrinol. *25*, 145-157.

Marxreiter, F., Regensburger, M., and Winkler, J. (2013). Adult neurogenesis in Parkinson's disease. Cell Mol. Life Sci. *70*, 459-473.

Marz, M., Chapouton, P., Diotel, N., Vaillant, C., Hesl, B., Takamiya, M., Lam, C.S., Kah, O., Bally-Cuif, L., and Strahle, U. (2010). Heterogeneity in progenitor cell subtypes in the ventricular zone of the zebrafish adult telencephalon. Glia *58*, 870-888.

Marz, M., Schmidt, R., Rastegar, S., Strahle, U. (2011). Regenerative reponse following stab injury in the adult zebrafish telencephalon. Dev. Dyn. *240*, 2221-2231.

Maslov, A.Y., Barone, T.A., Plunkett, R.J., and Pruitt, S.C. (2004). Neural stem cell detection, characterization, and age-related changes in the subventricular zone of mice. J. Neurosci. *24*, 1726-1733.

McCormick, C.M., Thomas, C.M., Sheridan, C.S., Nixon, F., Flyn, J.A., and Mathews, I.Z. (2011). Social instability stress in adolescent male rats alters hippocampal neurogenesis and produces deficits in spatial location memory in adulthood. Hippocampus *22*, 1300-1312.

McDermott, K.W.G., and Lantos, P.L. (1990). Cell proliferation in the subependymal layer of the postnatal marmoset, *Callithrix jacchus*. Dev. Brain Res. *57*, 269-277.

Meek, J. (1983). Functional anatomy of the tectum mesencephali of goldfish. An explorative analysis of the functional implications of the laminar structural organization of the tectum. Brain Res. Rev. *6*, 247-297.

Meerlo, P., Mistlberger, R.E., Jacobs, B.L., Heller, H.C., and McGinty, D. (2009). New neurons in the adult brain: The role of sleep and consequences of sleep loss. Sleep Med. Rev. *13*, 187-194.

Metin, C., Valle, R.B., Rakic, P., and Bhide, P.G. (2008). Modes and mishaps of neuronal migration in the mammalian brain. J. Neurosci. *28*, 11746-11752.

Meyers, J.R., Hu, L., Moses, A., Kaboli, K., Papandrea, A., and Raymond, P.A. (2012). B-catenin/Wnt signaling controsl progenitor fate in the developing and regenereating zebrafish retina. Neural Dev. *7*, 1-17.

Miljkovic-Licina, M., Gauchat, D., and Galliot, B. (2004). Neuronal evolution: analysis of regulatory genes in a first-evolved nervous system, the hydra nervous system. BioSystems *76*, 75-87.

Miller, N.Y., and Gerlai, R. (2011). Shoaling in zebrafish: What we don't know. Rev. Neurosci. *22*, 17-25.

Miller, J.A., Nathanson, J., Franjic, D., Shim, S., Dalley, R.A., Shapouri, S., Smith, K.A., Sunkin, S.M., Bernard, A., Bennett, J.L., Lee, C.-K., Hawrylycz, M.J., Jones, A.R., Amaral, D.G., Sestan, N., Gage, F.H., and Lein E.S. (2013). Conserved molecular signatures of neurogenesis in the hippocampal subgranular zone of rodents and primates. Development *140*, 4633-4644.

Minelli, G., and Quaglia, A. (1968). I rapporti nervosi nel tetto mesencefalico di Triturus cristatus. Arch. Ital. Anat. Embriol. *73*, 203-218.

Ming, G.-I., and Song, H. (2005). Adult neurogenesis in the mammalian central nervous system. Annu. Rev. Neurosci. *28*, 223-250.

Ming, G.-I., and Song, H. (2011). Adult neurogenesis in the mammalian brain: Significant answers and significant questions. Neuron *70*, 687-702.

Mirescu, C., Peters, J.D., Noiman, L., and Gould, E. (2006). Sleep deprivation inhibits adult neurogenesis in the hippocampus by elevating glucocorticoids. Proc. Natl. Aca. Sci. U.S.A. *103*, 19170-19175.

Mirescu, C., and Gould, E. (2006). Stress and adult neurogenesis. Hippocampus *16*, 233-238.

Mirzadeh, Z., Merkle, F.T., Soriano-Navarro, M., Garcia-Verdugo, J.M., and Alvarez-Buylla, A. (2008). Neural stem cells confer unique pinwheel architecture to the ventricular surface in neurogenic regions of the adult brain. Cell Stem Cell *3*, 265-278.

Mirzadeh, Z., Han, Y.-G., Soriano-Navarro, M., Garcia-Verdugo, J.M., and Alvarez-Buylla, A. (2010). Cilia organize ependymal planar polarity. J. Neurosci. *30*, 2600-2610.

Monje, M.L., Mizumatsu, S., Fike, J.R., and Palmer, T.D. (2002). Irradiation induces neural precursor-cell dysfunction. Nature Med. *8*, 955-962.

Morimoto, M., Norita, N., Ozawa, H., Yokoyama, K, and Kawata, M. (1996). Distribution of glucocorticoid receptor immunoreactivity and mRNA in the rate brain: An immunohistochemcial and in situ hybridization study. Neurosci. Res. *26*, 235-269.

Morita, Y., and Finger, T.E. (1985). Topographic and laminar organization of the vagal gustatory system in the goldfish, *Carassius auratus*. J. Comp. Neurol. *238*, 187-201.

Morrison, S.J., and Spradling, A.C. (2008). Stem cells and niches: Mechanisms that promotestem cell maintenance throughout life. Cell *132*, 598-611.

Morshead, C.M., and van der Kooy, D. (1992). Postmitotic death is the fate of constitutively proliferating cells in the subependymal layer of the adult mouse brain. J. Neurosci. *12*, 249-256.

Morshead, C.M., Garcia, D., Sofroniew, M.V., and van der Kooy, D. (2003). The ablation of glial fibrillary acidic protein-positive cells from the adult central nervous system results in the loss of forebrain neural stem cells but not retinal stem cells. Eur. J. Neurosci. *18*, 76-84.

Mouret, A., Lepousez, G., Gras, J., Gabellec, M.-M., and Lledo, P.-M. (2009). Turnover of newborn olfactory bulb neurons optimizes olfaction. J. Neurosci. *29*, 12302-12314.

Moyle, P.B., and Cech, J.J. Jr. (2004). Fishes: An Introduction to Ichthyology. Fifth Edition (New Jersey; Prentice-Hall Press).

Mudo, G., Bonomo, A., Di Liberto, V., Frinchi, M, Fuxe, K., and Belluardo, N. (2009). The FGF-2/FGFRs neurotrophic system promotes neurogenesis in the adult brain. J. Neural Transm. *116*, 995-1005.

Nacher, J., Soriano, S., Varea, E., Molowny, A., Ponsoda, X., Lopez-Garcia, C. (2002). CRMP-4 expression in the adult cerebral cortex and other telencephalic areas of the lizard *Podarcis hispanica*. Dev. Brain Res. *139*, 285-294.

Nasiadka, A., and Clark, M.D. (2012). Zebrafish breeding in the laboratory environment. ILAR J. *53*, 161-168.

Nawrocki, L., BreMiller, R., Streisinger, G., and Kaplan, M. (1985). Larval and adult visual pigments of the zebrafish, *Brachydanio rerio*. Vision Res. *25*, 1569-1576.

Nguyen, V., Deschet, K., Henrich, T., Godet, E., Joly, J.-S., Wittbrodt, J., Chourrout, D., Bourrat, F. (1999). Morphogenesis of the optic tectum in the Medaka (Oryzias latipes): A morphological and molecular study, with special emphasis on cell proliferation. J. Comp. Neurol. *413*, 385-404.

Ngwenya, L.B., Peters, A., and Rosene, D.L. (2006). Maturation sequence of newly generated neurons in the dentate gyrus of the young adult rhesus monkey. J. Comp. Neurol. *498*, 204-216.

Noonin, C., Lin, X., Jiravanichpaisal, P., Doderhaill, K., and Soderhall, I. (2012). Invertebrate hematopoiesis: An anterior proliferation center as a link between the hematopoietic tissue and the brain. Stem Cells Dev. *21*, 3173-3186.

Norlander, R.H., and Edwards, J.S. (1970). Postembryonic brain development in the monarch butterfly, *Danaus plexippus plexippus* L. Wilhem. Roux'Archiv. *164*, 247-260.

Norton, W.H.J., Stumpenhorst, K., Faus-Kessler, T., Folchert, A., Rohner, N., Harris, M.P. Callebert, J., and Bally-Cuif, L. (2011). Modulation of Fgfr1a signaling in zebrafish reveals a genetic basis for aggression-boldness syndrome. J. Neurosci. *31*, 13796-13807.

Nottebohm, F. (1985). Neuronal replacement in adulthood. In: Hope for a new neurology. Ann. N.Y. Acad. Sci. *457*, 143-161.

Nottebohm, F. (2002A). Neuronal replacement in adult brain. Brain Res. Bull. *57*, 737-749.

Nottebohm, F. (2002B). Why are some neurons replaced in adult brain? J. Neurosci. *22*, 624-628.

Nottebohm. F. (2005). The neural basis of birdsong. PLoS Biology *3*, e164.

Nottebohm, F., and Arnold, A.P. (1976). Sexual dimorphism in vocal control areas of the songbird brain. Science *194*, 211-213.

Nottebohm, F., Kelley, D.B., and Paton, J.A. (1982). Connections of vocal control nuclei in the canary telencephalon. J. Comp. Neurol. *207*, 344-357.

Nottebohm, F., and Alvarez-Buylla, A. (1993). Neurogenesis and neuronal replacement in adult birds. Restorative Neurol. *6*, 227-236.

Nottebohm, F., and Liu, W.-C. (2010). The origins of vocal learning: New sounds, new circuits, new cells. Brain Lang. *115*, 3-17.

Nowakowski, R.S., Lewin, S.B., and Miller, M.W. (1989). Bromodeoxyuridine immunohistochemical determination of the lengths of the cell cycle and the DNA-synthetic phase for an anatomically defined population. J. Neurocytol. *18*, 311-318.

Nowakowski, R.S., and Hayes, N.L. (2001). Stem cells: the promises and pitfalls. Neuropsychopharmacology *25*, 799-804.

Nusse, R. (2008). Wnt signaling and stem cell control. Cell Res. *18*, 523-527.

Oboti, L., Savalli, G., Giachino, C., De Marshis, S., Panzica, G.C., Fasolo, A., and Peretto, P. (2009). Integration of sensory experience-dependent survival of newly-generated neurons in the accessory olfactory bulb of female mice. Eur. J. Neurosci. *29*, 679-692.

Oomen, C.A., Girardi, C.E.N., Cahyadi, R., Verbeek, E.C., Krugers, H., Joels, M., and Lucassen, P.J. (2009). Opposite effects of early maternal deprivation on neurogenesis in male versus female rats. PLoS ONE *4*, e3675.

Orger, M.B., and Baier, H. (2005). Channeling of red and green cone inputs to the zebrafish optomotor response. Vis. Neurosci. *22*, 275-281.

Overall, R.W., Paszkowski-Rogacz, M, and Kempermann, G. (2012). The mammalian adult neurogenesis gene ontology (MANGO) provides a structural framework for published information on genes regulating adult hippocampal neurogenesis. PLoS ONE, *7*, e48527.

Overli, O., Sorensen, C. Pulman, K.G.T., Pottinger, T.G., Korzan, W., Summers, C.H., and Nilsson, G.E. (2007). Evolutionary background for stress-coping styles: Relationships between physiological, behavioral, and cognitive traits in non-mammalian vertebrates. Neurosci. Biobehav. Rev. *31*, 396-412.

Patnaik, B.K. (1994). Ageing in reptiles. Gerontology *40*, 200-220.

Paton, J.A., and Nottebohm, F.N. (1984). Neurons generated in the adult brain are recruited into functional circuits. Science *225*, 1046-1048.

Patzke, N., Spocter, M. A., Karlsson, K.E., Bertelsen, M.F., Haagensen, M., Chawana, R., Streicher, S., Kaswera, C., Gilissen, E., Alagaili, A.N., Mohammed, O.B., Reep, R.L., Bennett, N.C., Siegel, J.M., Ihunwo, A.O., and Manger, P.R. (2013). In contrast to many other mammals, ceteceans have relatively small hippocampi that appear to lack adult neurogenesis. Brain Struc. Funct. *In Press*.

Pavlidis, M., Sundvik, M., Chen, Y.-C., Panula, P. (2011). Adaptive changes in zebrafish brain in dominant-subordinate behavioral context. Beh. Brain Res. *225*, 529-537.

Pawluski, J.L., van den Hov, D.L.A., Rayen, I., Prickaerts, J., and Steinbusch, H.W.M. (2011). Stresa dn the pgrenant female: Impact on hippocampal cell proliferation, but not affective-like behaviors. Horm. Behav. *59*, 572-580.

Pawluski, J.L., and Galea, L.A.M. (2007). Reproductive experience alters hippocampal neurogenesis during the postpartum period in the dam. Neuroscience *149*, 53-67.

Pechenik, J.A. (2005). Biology of the Invertebrates. Fifth Edition. (New York; McGraw-Hill Press).

Pellegrini, E., Mouriec, K., Anglade, I., Menuet, A., Le Page, Y., Gueguen, M.-M., Marmignon. M.-H., Brion, F., Pakdel, F., and Kah, O. (2007). Identification of aromatase-positive radial glial cells as progenitor cells in the ventricular layer of the forebrain in zebrafish. J. Comp. Neurol. *501*, 150-167.

Peñafiel, A., Rivera, A., Cutierrez, A., Trias, S., and De la calle, A. (2001). Temperature affects adult neurogenesis in the lizard brain. Int. J. Dev. Biol. *45*, S83-S84.

Perera, T.D., Dwork, A.J., Keegan, K.A., Thirumangalakudi, L., Lipira, C.M., Joyce, N., Lange, C., Higly, J.D., Rosoklija, G., Hen, R., Sackeim, H.A., and Coplan, J.D. (2012). Necessity of hippocampal neurogenesis for the therapeutic action of antidepressants in adult nonhuman primates. PLoS ONE *6*, e17600.

Perez, E.C., Elie, J.E., Soulage, C.O., Soula, H.A., Mathevon, N., and Vignal, C. (2012). The acoustic expression of stress in a songbird: Does corticosterone drive isolation-induced modifications of zebra finch calls? Horm. Behav. *61*, 573-581.

Perez-Canellas, M.M., and Garcia-Verdugo, J.M. (1996). Adult neurogenesis in the telencephalon of a lizard: a [3H]thymidine autoradiographic and bromodeoxyuridine immunocytochemical analysis. Dev. Brain Res. *93*, 49-61.

Pérez-Cañellas, M.M., Font, E., and Garcia-Verdugo, J.M. (1997). Postnatal neurogenesis in the telencephalon of turtles: Evidence for nonradial migration of new neurons from distant proliferative ventricular zones to the olfactory bulbs. Dev. Brain Res. *101*, 125-137.

Perez-Sanchez, F., Molowny, A., Garcia-Verdugo, J.M., and Lopez-Garcia, C. (1989). Postnatal neurogenesis in the nucleus sphericus of the lizard, Podarcis hispanica. Neurosci. Lett. *106,* 71-75.

Platel, J.-C., Heintz, T., Young, S., Gordon, V., and Bordey, A. (2008). Tonic activation of GLU_{K5} kainate receptors decreases neuroblast migration in whole-mounts of the subventricular zone. J. Physiol. *586*, 3783-3793.

Polenov, A.L., and Chetverukhin, V.K. (1993). Ultrastructural radioautographic analysis of neurogenesis in the hypothalamus of the adult frog, *Rana temporaria,* with special reference to physiological regeneration of the proeptic nucleus. Cell Tissue Res. *271*, 351-362.

Ponti, G., Obernier, K., and Alvarez-Buylla, A. (2013). Lineage progression from stem cells to new neurons in the adult brain ventricular-subventricular zone. Cell Cycle *12*, 1649-1650.

Portillo, W., Unda, N., Camacho, F.J., Sanchez, M, Corona, R., Arzate, D.M., Diaz, N.F., and Paredes, R.G. (2012). Sexual activity increases the number of newborn cells in the accessory olfactory bulb of male rats. Front. Neuroanat. *6,* 1-9.

Poss, K.D., Shen, J., Nechiporuk, A., McMahon, G., Thisse, B., Thisse, C., and Keating, M.T. (2000). Roles for Fgf signaling during zebrafish fin regeneration. Dev. Biol. *222*, 347-358.

Rakic, P. (1985). Limits of neurogenesis in primates. Science *227*, 1054-1056.

Rakic, P. (2002). Adult neurogenesis in mammals: An identity crisis. J. Neurosci. *22*, 614-618.

Ramirez, C., Nacher, J., Molowny, A., Sanchez-Sanchez, F., Irurzun, A., and Lopez-Garcia, C. (1997). Photoperiod-temperature and neuroblast proliferation-migration in the adult lizard cortex. Neuroreport *8*, 2337-2342.

Raymond, P.A., and Easter, S.S. Jr. (1983). Postembryonic growth of the optic tectum in goldfish. I. Location of germinal cells and number of neurons produced. J. Neurosci. *3*, 1077-1091.

Raymond, P.A., Easter, S.S. Jr., Burnham, J.A., and Powers, M.K. (1983). Postembryonic growth of the optic tectum in goldfish. II. Modulation of cell proliferation by retinal fiber input. J. Neurosci. *3*, 1092-1099.

Reynolds, B.A., and Weiss, S. (1992). Generation of neurons and astrocytes from isolated cells of the adult mammalian central nervous system. Science 255, 1707-1710.

Richter, W., Kranz, D. (1981). Autoradiographic investigations on postnatal proliferative activity of the telencephalic and diencephalic matrix-zones in the axolotl (*Ambystoma mexicanum*), with special references to the olfactory organ. Z. Mikrosk. Anat. Forsch. *95*, 883-904.

Ricklefs, R.E. (2006). Embryo development and ageing in birds and mammals. Proc. Royal. Soc. Lon. Series B. *273*, 2077-2082.

Rietze, R., Poulin, P., and Weiss, S. (2000). Mitotically active cells that generate neurons ans astrocytes are present in multiple regions of the adult mouse hippocampus. J. Comp. Neurol. *424*, 397-408.

Rizzi, S., Bianchi, P., Guidi, S., Ciani, E., and Bartesaghi, R. (2007). Neonatal isolation impairs neurogenesis in the dentate gyrus of the Guinea Pig. Hippocampus *17*, 78-91.

Rochefort, C., Gheusi, G., Vincent, J.-D., and Leedo, P.-M. (2002). Enriched odor exposure increases the number of newborn neurons in the adult olfactory bulb and improves odor memory. J. Neurosci. *22*, 2679-2689.

Roesch, K., Jadhav, A.P., Trimarchi, J.M., Stadler, M.B., Roska, B., Sun, B.B., and Cepko, C.L. (2008). The transcriptome of retinal muller glial cells. J. Comp. Neurol. *509*, 225-238.

Rothenaigner, I., Krecsmarik, M., Hayes, J.A., Bahn, B., Lepier, A., Fortin, G., Gotz, M., Jagasia, R., and Bally-Cuif, L. (2011). Clonal analysis by distinct viral vectors identifies bona fide neural stem cells in the adult zebrafish telencephalon and characterizes their division properties and fate. Dev. Stem Cell *138,* 1459-1469.

Rougon, G., Dubois, C., Buckley, N., Magnani, J.L., and Zollinger, W. (1986). A monoclonal antibody against meningococcus group B polysaccharides distinguishes embryonic from adult N-CAM. J. Cell. Biol. *103*, 242924-232937.

Rousselot, P., Heintz, N, and Nottebohm, F. (1997). Expression of brain lipid binding protein in the brain of the adult canary and its implications for adult neurogenesis. J. Comp. Neurol. *385*, 415-426.

Rousseau, B., Dubayle, D., Sennlaub, F., Jeanny, J.C., Costet, P., Bikfalvi, A., and Javerzat, S. (2000). Neural and angiogenic defects in eyes of transgenic mice expressing a dominant-negative FGF receptor in the pigmented cells. Exp. Eye Res. *71*, 395-404.

Ruppert, E.E., and Barnes, R.D. (1996). Invertebrate Zoology. Sixth Edition. (New York; Harcourt College Publishers).

Sah, A., Schmuckermair, C., Sartori, S.B., Gaburro, S., Kandasamy, M., Irschick, R., Klimaschewski, L., Landgraf, R., Aigner, L., and Singewald, N. (2012). Anxiety- rather than depression-like behavior is associated with adult neurogenesis in a female mouse model of higher trait anxiety- and comorbid depression-like behavior. Transl. Psychiatry. *2*, e171.

Sakaguchi, M., Mizusina, M., and Kobayakawa, Y. (1996). Structure, development, and maintenance of the nerve net of the body column in hydra. J. Comp. Neurol. *373*, 41-54.

Sakurai, K., and Osumi, N. (2008). The neurogenesis-controlling factor, Pax6, inhibits proliferation and promotes maturation in murine astroctyes. J. Neurosci. 28, 4604-4612.

Salas, C., Broglio, C., Duran, E., Gomez, A., Ocana, F.M., Jimenez-Moya, F., and Rodriguez, F. (2006). Neurospsychology of learning and memory in teleost fish. Zebrafish *3*, 157-171.

Sanai, N., Tramontin, A.D., Quinones-Hinojosa, A., Barboro, N.M., Gupta, N., Kunwar, S., Lawton, M.T., McDermott, M.W., Parsa, A.T., Garcia-Verdugo, J.M., Berger, M.S., and Alvarez-Buylla, A. (2004). Unique astrocyte ribbon in adult human brain contains neural stem cells bu lacks chain migration. *427*, 740-744.

Sanai, N., Nguyen, T., Ihrie, R.A., Mirzadeh, Z., Tsai, H.-H., Wong, M., Gupta, N., Berger, M.S., Huang, E., Garcia-Verdugo, J.M., Rowitch, D.H., and Alvarez-Buylla, A. (2011). Nature *478*, 382-387.

Sandeman, R., and Sandeman, D. (1996). Pre- and postembryonic development, growth and turnover of olfactory receptor neurones in crayfish antennules. J. Exp. Biol. *199*, 2409-2418.

Sandeman, R., Clarke, D., Sandeman, D., and Manly, M. (1998). Growth-related and antennular amputation-induced changes in the olfactory centers of crayfish brain. J. Neurosci. *18*, 6195-6206.

Sandeman, R., and Sandeman, D. (2000). Impoverished and enriched living conditions influence the proliferation and survival of neurons in crayfish brain. J. Neurobiol. *45*, 215-226.

Sandeman, D.C., Bazin, F., and Beltz, B.S. (2011). Adult neurogenesis: Examples from the decapods crustaceans and comparisons with mammals. Arthropod Struct. Dev. *40*, 258-275.

Saverino, C., and Gerlai, R. (2008). The social zebrafish: Behavioral responses to conspecific, heterospecific, and computer animated fish. Beh. Brain Res. *191*, 77-87.

Sawamoto, K., Hirota, Y., Alfaro-Cervello, C., Soriano-Navarro, M., He, X., Hayakawa-Yano, Y., Yamada, M., Hikishima, K., Tabata, H., Iwanami, A., Alvarez-Buylla, A., Garcia-Verdugo, J.M., and Okano, H. (2011). Cellular composition and organization of the subventricular zone and rostral migratory stream in the adult and neonatal common marmoset brain. J. Comp. Neurol. *519*, 690-713.

Sawamoto, K., Wichterle, H., Gonzalez-Perez, O., Cholfin, J.A., Yamada, M., Spassky, N., Murcia, N.S., Garcia-Verdugo, J.M., Marion, O., Rubenstein, J.L., Tessier-Lavigne, M., Okano, H., and Alvarez-Buylla, A. (2006). New neurons follow the flow of cerebrospinal fluid in the adult brain. Science *311, 629*-632.

Schaper, A. (1897). Die fruhesten differenzierungsvorgange im centralnervensystems. Arch. F Entw-Mech. Organ. *5*, 81-132.

Scharff, C. (2000). Chasing the fate and function of new neurons in adult brains. Curr. Opin. Neurobiol. *10*, 774-783.

Scharff, C., and Nottebohm (1991). A comparative study of the behavioral deficits following lesions of various parts of the zebraf finch song system: Implications for vocal learning. J. Neurosci. *11*, 2896-2913.

Scharff, C., Kim, J.R., Grossman, M., Macklis, J.D., and Nottebohm, F. (2000). Targeted neuronal death affects neuronal replacement and vocal behavior in adult songbirds. Neuron *25*, 481-492.

Schmidt, M. (1997). Continuous neurogenesis in the olfactory brain of adult shore crabs, *Carcinus maenas*. Brain Res. *762*, 131-143.

Schmidt, M. (2001). Neuronal differentiation and long-term survival of newly generated cells in the olfactory midbrain of the adult spiny lobster, *Panulirus argus*. J. Neurobiol. *48*, 181-203.

Schmidt, M. (2007A). Identification of putative neuroblasts at the base of adult neurogenesis in the olfactory midbrain of the spiny lobster, *Panulirus argus*. J. Comp. Neurol. *503*, 64-84.

Schmidt, M. (2007B). The olfactory pathway of decapods crustaceans – An invertebrate model for life-long neurogenesis. Chem. Senses *32*, 365-384.

Schmidt, M., and Harzsch, S. (1999). Comparative analysis of neurogenesis in the central olfactory pathway of adult decapod crustaceans by *in vivo* BrdU labeling. Biol. Bull. *196*, 127-136.

Schmidt, M., and Derby, C.D. (2011). Cytoarchitecture and ultrastructure of neural stem cell niches and neurogenic complexes maintaining adult neurogenesis in the olfactory midbrain of Spiny Lobsters, *Panulirus argus*. J. Comp. Neurol. *519*, 2283-2319.

Schmidt, R., Strahle, U., and Scholpp, S. (2013). Neurogenesis in zebrafish – from embryo to adult. Neural Dev. *8*, 1-13.

Schoenfeld, T.J., and Gould, E. (2011). Stress, stress hormones, and adult neurogenesis. Exp. Neurol. *233*, 12-21.

Schoenfeld, T.J., and Gould, E. (2012). Stress, stress hormones, and adult neurogenesis. Exp. Neurol. *233*, 12-21.

Schoenfeld, T.J., and Gould, E. (2013). Differential effects of stress and glucocorticoids on adult neurogenesis. Curr. Topics Behav. Neurosci. *15*, 139-164.

Scotto-Lomassese, S., Strambi, C., Strambi, A., Charpin, P., Augier, R., Aouane, A., and Cayre, M. (2000). Influence of environmental stimulation on neurogenesis in the adult insect brain. J. Neurobiol. *45*, 161-171.

Scotto-Lomassese, S., Strambi, C., Aouane, A., Strambi, A., and Cayre, M. (2002). Sensory inputs stimulate progenitor cell proliferation in an adult insect brain. Curr. Biol. *12*, 1001-1005.

Scotto-Lomassese, S., Strambi, C., Strambi, A., Aouane, A., Augier, R., Rougon, G., and Cayre, M. (2003). Suppression of adult neurogenesis impairs olfactory learning and memory in an adult insect. J. Neurosci. *23*, 9289-9296.

Segovia, G., Yague, A.G., Garcia-Verdugo, J.M., and Mora, F. (2006). Environmental enrichment promotes neurogenesis and changes the extracellular concentrations of glutamate and GABA in the hippocampus of aged rats. Brain Res. Bull. *70*, 8-14.

Seib, D.R.M., Corsini, N.S., Ellwanger, K., Plass, C. Mateos, A., Pitzer, C., Niehrs, C., Celikel, T., and Martin-Villalba, A. (2013). Loss of Dickkopf-1 restores neurogenesis in old age and counteracts cognitive decline. Cell Stem Cell *12*, 204-214.

Seki, T., and Arai, Y. (1995). Age-related production of new granule cells in the adult dentate gyrus. NeuroReport *6*, 2479-2482.

Sequerra, E.B., Costa, M.R., Menezes, J.R.L., and Hedin-Pereira, C. (2013). Adult neural stem cells: Plastic or restricted neuronal fates? Development 140, 3303-3309.

Seri, B., Garcia-Verdugo, J.M., McEwen, B., and Alvarez-Buylla, A. (2001). Astrocytes give rise to new neurons in the adult mammalian hippocampus. J. Neurosci. *21*, 7153-7160.

Seri, B., Garcia-Verdugo, J.-M., Collado-Morente, L., McEwen, B.S., and Alvarez-Buylla, A. (2004). Cell types, lineage, and architecture of the germinal zone in the adult dentate gyrus. J. Comp. Neurol. *478*, 359-378.

Shen, Q., Wang, Y., Kokovay, E., Lin, G., Chuang, S.-M., Goderie, S.K., Roysam, B., and Temple, S. (2008). Adult SVZ stem cells lie in a vascular niche: A quantitative analysis of niche cell-cell interactions. Cell Stem Cell *3*, 289-300.

Sherry, D.E., and Vaccarino, A.L. (1989). Hippocampus and memory for food caches in the black-capped chickadee. Behav. Neurosci. *103*, 308-318.

Sherry, D.F., Vaccarino, A.L., Buckenham, K., and Hertz, R.S. (1989). The hippocampal complex of food-storing birds. Brain Behav. Evol. *34*, 308-317.

Sherry, D.E., and Hoshooley, J.S. (2009). The seasonal hippocampus of food-storing birds. Behav. Process *80*, 334-338.

Shors, T.J. (2008). From stem cells to grandmother cells: How neurogenesis relates to learning and memory. Cell Stem Cell *3*, 253-258.

Sierra, A., Encinas, J.M., and Maletic-Savatic, M. (2011). Adult human neurogenesis: From microscopy to magnetic resonance imaging. Front. Neurosci. *5*, 1-18.

Sigurgeirsson, B., Porsteinsson, H., Sigmundsdottir, S., Lieder, R., Sveinsdottir, H.S., Sigurjonsson, O.E., Halldorsson, B., and Karlsson, K. (2013). Sleep-wake dynamics under extended light and extended dark conditions in adult zebrafish. Beh. Brain Res. *256*, 377-390.

Silvestroff, L., Bartucci, S., Soto, E., Gollo, V., Pasquini, J., and Franco, P. (2010). Cuprizone-induced demyelination in CNP:GFP transgenic mice. J. Comp. Neurol. *518*, 2261-2283.

Simmons, A.M., Horowitz, S.S., and Brown, R.A. (2008). Cell proliferation in the forebrain and midbrain of the adult bullfrog, *Rana catesbeiana*. Brain Behav. Evol. *71*, 41-53.

Sintoni, S. Benton, J.L., Beltz, B.S., Hansson, B.S., and Harzsch, S. (2012). Neurogenesis in the central olfactory pathway of adult decapods crustaceans: Development of the neurogenic niche in the brains of procambarid crayfish. Neural Dev. *7*, 1-25.

Slomianka, L., Drenth, T., Cavegn, N., Menges, D., Lazic, S.E., Phalanndwa, M., Chimimba, C.T., and Amrein, I. (2013). The hippocampus of the eastern rock sengi: Cytoarchitecture, markers of neuronal function, principal cell numbers, and adult neurogenesis. Front. Neurosci. *7*, 1-20.

Smith, M.T., Pencea, V., Want, Z., Luskin, M.B., and Insel TR. (2001). Increased number of BrdU-labelled neurons in the rostral migratory stream of the estrous prairie vole. Horm. Behav. *39*, 11-21.

Smulders, T.V., Sasson, A.D., and DeVoogd, T.J. (1995). Seasonal variation in hippocampal volume in a food-storing bird, the black-capped chickadee. J. Neurobiol. *27*, 15-25.

Smulders, T.V., Shiflett, M.W., Sperling, A.J., and DeVoogd, T.J. (2000). Seasonal changes in neuron numbers in the hippocampal formation of a food-hoarding bird, the black-capped chickadee. J. Neurobiol. *44*, 414-422.

Snyder, J.S., Kee, N., and Wojtowicz, J.M. (2001). Effects of adult neurogenesis on synaptic plasticity in the rate dentate gyrus. J. Neurophysiol. *85*, 2423-2431.

Snyder, J.S., Hong, N.S., McDonald, R.J., and Wojtowicz, J.M. (2005). A role for adult neurogenesis in spatial long-term memory. Neuroscience *130*, 843-852.

Snyder, J.S., Glover, L.R., Sanzone, K.M., Kamhi, J.F., and Cameron, H.A. (2009). The effects of exercise and stress on the survival and maturation of adult-generated granule cells. Hippocampus *19*, 898-906.

Sofroniew, M.V., and Vinters, H.V. (2010). Astrocytes: Biology and pathology. Acta. Neuropathol. *119*, 7-35.

Solek, M.C., and Ekker, M. (2012). Cell lineage tracing techniques for the study of brain development and regeneration. Int. J. Dev. Neurosci. *30*, 560-569.

Song, C.-K., Herberholz, J., and Edwards, D.H. (2006). The effects of social experience on the behavioural response to unexpected touch in crayfish. J. Exp. Biol. *209*, 1355-1363.

Song, C.-K., Johnstone, L.M., Schmidt, M., Derby, C.D., and Edwards, D.H. (2007). Social domination increases neuronal survival in the brain of juvenile crayfish *Procambarus clarkii*. J. Exp. Biol. *201*, 1311-1324.

Song, C.-K., Johnstone, L.M., Edwards, D.H., Derby, C.D., and Schmidt, M. (2009). Cellular basis of neurogenesis in the brain of crayfish, Procambarus clarkia: Neurogenic complex in the olfactory midbrain from hatchlings to adults. Arthropod Struct. Dev. *38*, 339-360.

Souza, B.R., Romano-Silva, M.A., and Tropepe, V. (2011). Dopamine D_2 receptor activity modulates Akt signalling and alters GABAergic neuron development and motor behaviour in zebrafish larvae. J. Neurosci. *31*, 5512-5525.

Spence, R., Gerlach, G., Lawrence, C., and Smith, C. (2008). The behaviour and ecology of the zebrafish. *Danio rerio*. Biol. Rev. *83*, 13-34

Spolidoro, M., Sale, A., Berardi, N., and Maffei, L. (2009). Plasticity in the adult brain: lessons from the visual system. Exp. Brain. Res. *192*, 335-341.

Sportiche, N., Suntsova, N., Methippara, M., Bashir, T., Mitrani, B., Szymusiak, R., and McGinty, D. (2010). Sustained sleep fragmentation results in delayed changes in hippocampal-dependent cognitive function associated with reduced dentate gyrus neurogenesis. Neuroscience *170*, 247-258.

Spritzer, M.D., Ibler, E., Inglis, W., and Curtis, M.G. (2011). Testosterone and social isolation influence adult neurogenesis in the dentate gyrus of male rats. Neuroscience *195*, 180-190.

Stein, B.E., and Stanford, T.R. (2008) Multisensory integration: Current issues from the perspective of the single neuron. Nature Rev. Neurosci. *9*, 255-266.

Steiner, B., Klempin, F., Wang, L., Kott, M., Kettenmann, H., and Kempermann, G. (2006). Type-2 cells as link between glial and neuronal lineage in adult hippocampal neurogenesis. Glia *54*, 805-814.

Stenkamp, D.L. (2007). Neurogenesis in the fish retina. Inter. Rev. Cytol. *259*, 173-224.

Stone, S.S.D., Teixeira, C.M., Zaslavsky, K., Wheeler, A.L., Martinez-Canabal, A., Wang, A.H., Sakaguchi, M., Lozano, A.M., and Frankland, P.W. (2010). Hippocampus *21*, 1348-62.

Stranahan, A.M., Khalil, D., and Gould, E. (2006). Social isolation delays the positive effects of running on adult neurogenesis. Nature Neurosci. *9*, 526-533.

Strausfeld, J.J., Hansen, L., Li, Y., Gomez, R.S., and Ito, K. (1998). Evolution, discovery, and interpretations of arthropod mushroom bodies. Learn. Mem. *5*, 11-37.

Srobl-Mazzulla, P.H., Nunez, A., Pellegrini, E., Gueguen, M.-M., Kah, O., and Somoza, G.M. (2010). Progenitor radial cells and neurogenesis in Pejerrey fish forebrain. Brain Beh. Evol. *76*, 20-31.

Sullivan, J.M., and Beltz, B.S. (2005). Adult neurogenesis in the central olfactory pathway in the absence of receptor neuron turnover in *Libinia emarginata*. Eur. J. Neurosci. *22*, 2397-2402.

Sullivan, J.M., Benton, J.L., Sandeman, D.C., and Beltz, B.S. (2007). Adult neurogenesis across diverse species. J. Comp. Neurol. *500*, 574-584.

Takahashi, H., and Sakamoto, T. (2013). The role of ‘mineralocorticoids’ in teleost fish: Relative importance of glucocorticoid signaling in the osmoregulation and ‘central’ actions of mineralocorticoid receptor. Gen. Comp. Endocrinol. *181*, 223-228.

Tanapat, P., Hastings, N.B., Rydel, T.A., Galea, L.A.M., Gould, E. (2001). Exposure to fox odor inhibits cell proliferation in the hippocampus of adult rats via an adrenal hormone-dependant mechanism. J. Comp Neurol. *437*, 496-504.

Taupin, P. (2007A). BrdU immunohistochemistry for studying adult neurogenesis: Paradigms, pitfalls, limitations, and validation. Brain Res. Rev. *53*, 198-214.

Taupin, P. (2007B). Protocols for studying adult neurogenesis: Insights and recent developments. Reg. Med. *2*, 51-62.

Taupin, P., and Gage, F.H. (2002). Adult neurogenesis and neural stem cells of the central nervous system in mammals. J. Neurosci. Res. *69*, 745-749.

Tavazoie, M., Van der Veken, L., Silva-Vargas, V., Loussaint, M., Colonna, L., Zaida, B., Garcia-Verdugo, J.M., and Doetsch, F. (2008). A specialized vascular niche for adult neural stem cells. Cell Stem Cell *3*, 279-288.

Technau, G.M. (1984). Fiber number in the mushroom bodies of adult *Drosophila melanogaster* depends on age, sex, and experience. J. Neurogenet. *1*, 113-126.

Thompson, C.K., and Brenowitz, E.A. (2009). Neurogenesis in an adult avian song nucleus is reduced by decreasing caspase-mediated apoptosis. J. Neurosci. *29*, 4586-4591.

Thompson, C.K., Meitzen, J., Replogle, K., Drnevich, J., Lent, K.L., Wissman, A.M., Farin, F.M., Bammler, T.K., Beyer, R.P., Clayton, D.F., Perkel, D.J., and Brenowitz, E.A. (2012). Seasonal changes in patterns of gene expression in avian song control brain regions. PLoS ONE *7*, e35119.

Thuret, S., Toni, N., Aigner, S., Yeo, G.W., and Gage, F.H. (2009). Hippocampus-dependent learning is associated with adult neurogenesis in MRL/MpJ mice. Hippocampus. *19*, 658-669.

Topp, S., Stigloher, C., Kormisarczuk, A.Z., Adolf, B., Becker, T.S., and Bally-Cuif, L. (2008). Fgf signalling in the zebrafish adult brain: Association of Fgf activity with ventricular zones but not cell proliferation. J. Comp. Neurol. *510*, 422-439.

Tozzini, E.T., Baumgart, M, Battistoni, G., and Cellerino, A. (2012). Adult neurogenesis in the short-lived teleost Nothobranchius furzeri: Localization of neurogenic niches, molecular characterization and effects of aging. Aging Cell *11*, 241-251.

Tropepe, V., Craig, C.G., Morshead, C.M., and van der Kooy, D. (1997). Transforming growth factor-α null and senescent mice show decreased neural progenitor cell proliferation in the forebrain subependyma. J. Neurosci. *17*, 7850-7859.

Tseng, Y.-Y., Gruzdeva, N., Li, A., Chuang, J.-Z., and Sung, C.-H. (2010). Identification of the Tctex-1 regulatory element that directs expression to neural stem/progenitor cells in developing and adult brain. J. Comp. Neurol. *518*, 3327-3342.

Uyttebroek, L., Shepherd, I.T., Harrisson, F., Hubens, G., Blust, R., Timmermans, J.-P., and Van Nassauw, L. (2010). Neurochemical coding of enteric neurons in adult and embryonic zebrafish (*Danio rerio*). J. Comp. Neurol. *518*, 4419-4438.

van Praag, H., Kempermann, G., and Gage, F.H. (1999A). Running increases cell proliferation and neurogenesis in the adult mouse dentate gyrus. Nature Neurosci. *2*, 266-270.

van Praag, H., Christie, B.R., Sejnowski, T.J., and Gage, F.H. (1999B). Running enhances neurogenesis, learning, and long-term potentiation in mice. Proc. Natl. Acad. Sci. U.S.A. *96*, 13427-13431.

Veena, J., Srikumar, N.B., Mahati, K., Bhagya, V., Raju, T.R., and Rao B.S.S. (2009). Enriched environment restores hippocamal cell proliferation and ameliorates cognitive deficits in chronically stressed rats. J. Neurosci. Res. *87*, 831-843.

Venegas, H., Laufer, M, and Amat., J. (1974). The optic tectum of a perciform teleost. I. General configuration and cytoarchitecture. J. Comp. Neurol. *154*, 43-60.

Villanueva, R., and Byrd-Jacobs, C.A. (2009). Peripheral sensory deafferentation affects olfactory bulb neurogenesis in zebrafish. Brain. Res. 1269, 31-39.

von Krogh, K., Sorensen, C., Nilsson, G.E., and Overli, O. (2010). Forebrain cell proliferation, behavior, and physiology of zebrafish, *Danio rerio*, kept in enriched or barren environments. Physiol. Behav. *101*, 32-39.

Wainwright, M.S., Craft, J.M., Griffin, W.S., Marks, A., Pineda, J., Padgett, K.R., and Van Eldik, L.J. (2004). Increased susceptibility of S100β transgenic mice to perinatal hypoxia-ischemia. Ann. Neurol. *56*, 61-67.

Walton, J.C., Pyter, L.M., Weil, Z.M, and Nelson, R.J. (2012). Photperiod mediated changes in olfactory bubl neurogenesis and olfactory behavior in male White-foodted mice (Peromyscus leucopus). PLoS ONE *7*, e42743.

Wang, R.T., and Halpern, M. (1988). Neurogenesis in the vomeronasal epithelium of adult garter snakes: 3. Use of H-Thymidine autoradiography to trace the genesis and migration of bipolar neurons. Am. J. Anat. *183*, 178-185.

Wang, T.-W., Stromberg, G.P., Whitney, J.T., Brower, N.W., Klymkowsky, M.W., and Parent, J.M. (2006). Sox3 expression identified neural progenitors in persistent neonatal and adult mouse forebrain germinative zones. J. Comp. Neurol. *496*, 88-100.

Wang, C., Liu, F., Liu, Y.-Y., Zhao, C.-H., You, Y., wang, L., Zhang, J., Wei, B., Ma, T., Zhang, Q., Zhang, Y., Chen, R., Song, H., Yang, Z. (2011). Identification and characterization of neuroblasts in the subventricular zone and rostral migratory stream of the adult human brain. Cell Res. *21*, 1534-1550.

Want, S., Okun, M.S., Suslov, O., Zheng, T., McFarland, N.R., Vedam-Mai, V., Foote, K.D., Roper, S.N., Yachnis, A.T., Siebzehnrubl, F.A., and Steindler, D.A. (2012). Neurogenic potential of progenitor cells isolated from post-mortem hyman Parkinsonian brains. Brain Res. *1464*, 61-72.

Waterhouse, E.G., An, J.J., Orefice, L.L., Baydyuk, M., Liao, G.-Y., Zheng, K., Lu, Bai, and Xu, B. (2012). BDNF promotes differentiation and maturation of adult-born neurons through GABAergic transmission. J. Neurosci. *32*, 14318-14330.

Weisel, T.N., and Hubel, D.H. (1963). Effects of visual deprivation on morphology and physiology of cells in the cats lateral geniculate body. J. Neurophysiol. *26*, 978-993.

West, M.J. (1999). Stereological methods for estimating the total number of neurons and synapses: Issues of precision and bias. Trends Neurosci. *22*, 51-61.

Westenbroek, C. Den Boer, J.A., Veenhuis, M., and Ter Horst, G.J. (2004). Chronic stress and social housing differentially affect neurogenesis in male and female rats. Brain Res. Bull. *64*, 303-308.

Whitehead, G.G., Makino, S., Lien, C.L., and Keating, M.T. (2005). Fgf20 is essential for initiating zebrafish fin regeneration. Science *301*, 1957-1960.

Wong, L., Weadick, C.J., Kuo, C., Chang, B.S.W., and Tropepe, V. (2010). Duplicate dmbx1 genes regulate progenitor cell cycle and differentiation during zebrafish midbrain and retinal development. BMC Dev. Biol. *10*, 100.

Wu, M.V., and Hen, R. (2013). The young and the restless: Regulation of adult neurogenesis by Wnt Signaling. Cell Stem Cell *12*, 139-140.

Wullimann, M.F. (1998) The central nervous system. In The Physiology of Fishes (Second edition), Evans, D.H. (ed) (New York, NY; CRC Press LLC), pp. 245-281.

Wullimann, M.F., Rupp, B., and Reichert, H. (1996). Neuroanatomy of the zebrafish brain: A topological atlas. (Basal, Switzerland; Birkhauser Verlag Press).

Wullimann, M.F., and Rink, E. (2002). The teleostean forebrain: A comparative and developomental view based on early proliferation, *Pax6* activity and catecholaminergic organization. Brain Res. Bull. *57*, 363-370.

Wullimann, M.F. (2009). Secondary neurogenesis and telencephalic organization in zebrafish and mice: a brief review. Integ. Zool. *4*, 123-133.

Yaksi, E., von Saint Paul, F., Niessing, J., Bundschub, S.T., and Friedrich, R.W. (2009). Transformation of odor representations in target areas of the olfactory bulb. Nature Neurosci. *12*, 474-482.

Yang, M., Cagle, M.C., and Honig, M.G. (2010). Identification of cerebellin2 in chick and its preferential expression by subsets of developing sensory neurons and their targets in the dorsal horn. J. Comp. Neurol. *518*, 2818-2840.

Zhang, Y., Allodi, S., Sandeman, D.C., and Beltz, B.S. (2009). Adult neurogenesis in the crayfish brain: Proliferation, migration, and possible origin of precursor cells. Dev. Neurobiol. *69*, 415-436.

Zhao, C., Deng, W., and Gage, F.H. (2008). Mechanisms and functional implications of adult neurogenesis. Cell *132*, 645-660.

Zikopoulos, B., Kentouri, M., and Dermon, C.R. (2000). Proliferation zones in the adult brain of a sequential hermaphrodite teleost species (*Sparus aurata*). Brain Behav. Evol. *56*, 310-322.

Zupanc, G.K.H., and Zupanc, M.M. (1992). Birth and migration of neurons in the central posterior/prepacemaker nucleus during adulthood in weakly electric knifefish (*Eigenmannia* sp.). Proc. Natl. Acad. Sci. U.S.A. *89*, 9539-9543.

Zupanc, G.K.H., and Horschke, I. (1995). Proliferation zones in the brain of adult gymnotiform fish: A quantitative mapping study J. Comp. Neurol. *353*, 213-233.

Zupanc, G.K.H., Horschke, I., Ott, R., and Rascher, G.B. (1996). Postembryonic development of the cerebellum in gymnotiform fish. J. Comp. Neurol. *370*, 443-464.

Zupanc, G.K.H. (1999). Neurogenesis, cell death and regeneration in the adult gymnotiform brain. J. Exp. Biol. *202*, 1435-1446 .

Zupanc, G.K.H., and Ott, R. (1999). Cell proliferation after lesions in the cerebellum of adult teleost fish: Time course, origin, and type of new cells produced. Exp. Neurol. *160*, 78-87.

Zupanc, G.K.H. (2001A). A comparative approach towards the understanding of adult neurogenesis. Brain Behav. Evol. *58*, 246-249.

Zupanc, G.K.H. (2001B). Adult neurogenesis and neuronal regeneration in the central nervous system of teleost fish. Brain Behav. Evol. *58*, 250-275.

Zupanc, G.K.H, Hinsch, K., and Gage, F.H. (2005). Proliferation, migration, and neuronal differentiation, and long-term survival of new cells in the adult zebrafish brain. J. Comp. Neurol. *488*, 290-319.

Zupanc, G.K.H. (2006). Neurogenesis and neuronal regeneration in the adult fish brain. J. Comp. Physiol. A. *192*, 649-670.

Zupanc, G.K.H., Wellbrock, U.M., Sirbulescu, R.F., and Rajendran, R.S. (2009). Generation, long-term persistence, and neuronal differentiation of cells with nuclear aberrations in the adult zebrafish brain. Neuroscience *159*, 1338-1348.